4-17-2012 12:00 AM

Molecular Mechanisms of Cell Migration Inhibition by Synthetic Triterpenoids

Ciric Chi Wing To
The University of Western Ontario

Supervisor
John DiGuglielmo
The University of Western Ontario

Graduate Program in Pharmacology and Toxicology
A thesis submitted in partial fulfillment of the requirements for the degree in Doctor of Philosophy
© Ciric Chi Wing To 2012

MOLECULAR MECHANISMS OF CELL MIGRATION INHIBITION BY SYNTHETIC TRITERPENOIDS

(Spine title: Cell Migration Inhibition by Synthetic Triterpenoids)

(Thesis format: Integrated Article)

by

Ciric Chi Wing <u>To</u>

Graduate Program in Physiology and Pharmacology

A thesis submitted in partial fulfillment
of the requirements for the degree of
Doctor of Philosophy

The School of Graduate and Postdoctoral Studies
The University of Western Ontario
London, Ontario, Canada

© Ciric Chi Wing To, 2012

THE UNIVERSITY OF WESTERN ONTARIO
School of Graduate and Postdoctoral Studies

CERTIFICATE OF EXAMINATION

<u>Supervisor</u>   <u>Examiners</u>

_____   _____
Dr. Gianni M. Di Guglielmo   Dr. Eric Ball

<u>Supervisory Committee</u>

                                          _____
                                          Dr. Nica Borradaile

_____
Dr. Lina Dagnino

                                          _____
                                          Dr. Jeff Dixon

_____
Dr. Andy Babwah

                                          _____
                                          Dr. Paola Marignani

The thesis by

Ciric Chi Wing <u>To</u>

entitled:

Molecular Mechanisms of Cell Migration Inhibition by Synthetic Triterpenoids

is accepted in partial fulfillment of the
requirements for the degree of
Doctor of Philosophy

_____   _____

Date   Chair of the Thesis Examination Board

ABSTRACT

Cell migration is an important mediator of cancer metastasis and invasion, which is responsible for 90% of cancer-related premature deaths in Canada. Synthetic triterpenoids are a class of promising anti-cancer compounds that have shown considerable efficacy in targeting various cellular functions including apoptosis, growth, inflammation and cytoprotection in both cell culture and animal tumor models. However, their effect on cell migration, an important event in metastasis, remains poorly understood. This thesis focuses on deciphering the molecular mechanisms whereby the synthetic triterpenoids affect cell migration. I observed that the imidazolide and methyl ester derivatives of the synthetic triterpenoid, 2-cyano-3,12-dioxooleana-1,9-dien-28-oic aic acid (CDDO-Im and CDDO-Me), inhibit cell migration by disrupting microtubule dynamics. In addition, I found that these triterpenoids disrupt cell polarity by displacing proteins at the leading edge of migrating cells. Furthermore, using a two-pronged proteomic approach involving protein arrays and mass spectrometry, I identified numerous triterpenoid-binding targets involved in actin polymerization and focal adhesion maintenance. My data further revealed that triterpenoids inhibit branched actin polymerization by targeting Arp3 in the Arp2/3 complex and target GSK3β activity to alter focal adhesion sizes. Collectively, my studies provided novel insights on the underlying molecular mechanisms by which triterpenoids act to affect cell migration. This knowledge will be important for developing a more efficacious and specific therapeutic triterpenoid compound that targets cancer metastasis.

KEYWORDS

Cell migration

Synthetic triterpenoids

Microtubule and actin cytoskeletal network

 Cell polarity

Focal adhesion dynamics

CO-AUTHORSHIP

All synthetic triterpenoid compounds used in Chapter 2, 3 and 4 were synthesized by Drs. T. Honda, and G.W. Gribble, and generously provided by M.B. Sporn from Dartmouth Medical School in Hanover, USA.

Chapter 2 of the thesis is previously published in the Journal of Biological Chemistry on April 25th, 2008 under 283(17): 11700-11713. The peer-reviewed paper is titled 'The Synthetic Triterpenoid 2-Cyano-3, 12-dioxooleana-1,9-dien-28-oic Acid-Imidazolide Alters Transforming Growth Factor β-dependent Signaling and Cell Migration by Affecting the Cytoskeleton and the Polarity Complex'. The sources of all plasmids and antibodies that were used in the studies are noted in the Materials and Methods section of the chapter. We especially thank Drs. K. Kaibuchi (Nagoya University, Nagoya, Japan), J.J.M. Bergeron and P.H. Cameron (McGill University, Montreal, Canada), F. Perez (CNRS, Paris, France) for their generous contributions of these reagents and plasmids. All the experiments except for the Figure 2.9C and supplementary movies 1-3 were performed by Ciric Chi Wing To. For the figure and movie, the microinjection of the GFP-CLIP170 plasmid was done by Sarang Kulkarni from Dr. T. Pawson's laboratory and imaged by Dr. G.M. Di Guglielmo in Dr. J. Wrana's laboratory.

Chapter 3 of the thesis is previously published in the Journal of Biological Chemistry on September 3rd, 2010 under 285(36): 27944-27957. The peer-reviewed paper is titled 'Synthetic Triterpenoids Target the Arp2/3 Complex and Inhibit Branched Actin Polymerization'. All the experiments, except for those in Figure 8 A-C, were performed

by Ciric Chi Wing To. The experiment involving the docking of CDDO-Me to the Arp2/3 complex was performed by Dr. Brian Shilton (University of Western Ontario, London, Canada).

All other experiments including those conducted in Chapter 4 of the thesis were done by Ciric Chi Wing To under the supervision and in the laboratory of Dr. John Di Guglielmo at the University of Western Ontario in the Department of Physiology and Pharmacology.

ACKNOWLEDGMENTS

It has been a challenging but nonetheless, a remarkable journey completing my Ph.D. here at Western. I would like to take this opportunity to express my greatest appreciation to the many people who helped make this possible.

First and foremost, my deepest gratitude goes to my thesis supervisor, Dr. John Di Guglielmo. Thank you for taking me into your lab, over all the more experienced graduate students you could have chosen, and always believing in me (and my data). Your patience, understanding, guidance and wisdom have not only made me a better scientist but have made me a better person than when I first walked into your lab five years ago. Without your enthusiasm that inspired me to move forward against what I deemed to be impossible challenges at times, finishing my thesis would have been out of question. Much more than a thesis supervisor, you are a great life mentor and an outstanding role model whom I have tremendous respect for. Thank you for teaching me everything that I know in the lab, in life, and encouraging me to always strive for excellence. I could not have asked for a better supervisor.

I would also like to sincerely thank my advisory committee members, Drs. Andy Babwah, Lina Dagnino, and my GSRs, Drs. Lique Coolen and Graham Wagner. Thank you for all the insightful comments, guidance and constructive criticisms throughout the years. Your support is truly appreciated. In addition, I would like to thank Dr. Peter Chidiac for all the encouragement that he has given me over the years - your passion and enthusiasm for research have inspired me throughout my Ph.D. studies.

To the many friends (and family) that I made at Western. Thank you, Di Guglielmo Lab. I am so blessed to have such an awesome *lab family* that I can share all my frustrating and exciting bits of life with. Thank you for your understanding, encouragement, and all the fun and laughter throughout the years. Special thanks to the first friends whom I met in London - Boun, Tim, Han, Ben and Viv – thank you for making my first year in London away from home bearable; more importantly, thank you for all the love you have generously given to make London feel like home. Who would have thought that I would ever learn how to cook? Thank you, Boun – for always taking care of me like a little sister. I am so lucky to have you always looking out for me and I am going to miss our coffee breaks and all the great times we had together. To my friends in the Dagnino, Hammond, Bhattacharya and Chidiac labs, thank you for never saying no when I needed something and listening to me rant, not to mention all the fun we had when science didn't quite work out as well as we expected. Special thanks to Timothy (Tames) Irvine and Cynthia Pape – the awesome research technicians 'next door'. Without you two, many of my experiments could not have been completed with such ease. To my friends at Robarts, thank you for all the laughter that we shared during barbeques, hotpots and sushi nights. Words can't begin to describe how effective these nights were in helping me 'de-stress'. Thank you, Ash, for all the things you do for me – from the littlest and most insignificant things to the biggest and most important things that you do always with me in mind - especially during the last few months of my Ph.D. studies. Without you, I would have undoubtedly had many more meltdowns than I could count.

To the most ambitious and passionate researcher friend I know - Dr. Kelvin K.W. Hui. You have been instrumental to my career as a scientist since the day I stepped into the Henderson Lab as a summer volunteer at the University of Toronto. Thank you for all the advice and encouragement over the years. Your not-so-ambitious Ph.D. friend is finally done!

Finally, to my friends all over the world and my family, who always wondered when I would ever finish school - thank you for the constant support you have given me throughout the years from miles away even though you were clueless as to what I was doing but still believe that one day, I would finish and/or succeed. Your love really helped me see the light at the end of the tunnel.

TABLE OF CONTENTS

LIST OF TABLES

LIST OF FIGURES

LIST OF ABBREVIATIONS

Abbreviation	Full name
+TIP	Microtubule plus end-tracking proteins
ADP	Adenosine 5' diphosphate
Akt	Protein kinase B
ANOVA	Analysis of variance
APC	Adenomatous polyposis coli
aPKCι/ζ	Atypical protein kinase C iota or zeta
Arf	ADP-ribosylation factor
Arp	Actin-related protein
ARPC	Actin-related protein complex subunit
ATP	Adenosine 5' triphosphate
BSA	Bovine serum albumin
C2C12	Murine myoblast (cell line)
$CaCl_2$	Calcium chloride

CDC42	Cell division cycle 42
CDDO	2-cyano-3, 2-dioxooleana-1,9-dien-28-oic acid
CDDO-Im	CDDO-Imidazolide
CDDO-Me	CDDO-Methyl ester
cDNA	Complementary deoxyribonucleic acid
CLASP	Cytoplasmic linker- associated protein
CLIP170	Cytoplasmic linker protein 170
Cos7	African green monkey SV40-transfected kidney fibroblasts (cell line)
CRIB	Cdc42/Rac1 interacting binding
DAPI	4', 6 diamidino-2-phenylindole
DIC	Differential interference contrast
DMEM	Dulbecco's modified Eagle's medium
DMSO	Dimethyl sulfoxide
EB	End binding protein
ECM	Extracellular matrix

EDTA	Ethylenediaminetetraacetic acid
EEA1	Early endosomal antigen 1
EGTA	Ethylene glycol tetraacetic acid
EMT	Epithelial to mesenchymal transition
ER	Endoplasmic reticulum
ERK2	Extracellular signal-regulated kinase 2
ESI-MS	Electrospray ionization mass spectrometry
F-actin	Filamentous-actin
FAK	Focal adhesion kinase
FBS	Fetal bovine serum
G-actin	Globular-actin
GAP	GTPase activating protein
GAPDH	Glyceraldehyde 3-phosphate dehydrogenase
GDI	Guanosine nucleotide dissociation inhibitor
GDP	Guanosine diphosphate

GEF	Guanine nucleotide exchange factor
GFP	Green fluorescent protein
GSH	Glutathione
GSK3	Glycogen synthase kinase 3
GST	Glutathione S-transferase
GTP	Guanosine triphosphate
HeLa	Henrietta Lacks cervix carcinoma cancer cells
HepG2	Human hepatoma cells
HO-1	Heme-oxygenase 1
IFN-γ	Interferon gamma
IgG	Immune globulin G
IκB	Inhibitor of kappa beta
IKK	Inhibitor of κB (IκB) kinase
IL	Interleukin
iNOS	Inducible nitric oxide synthase

IQGAP1	IQ motif containing GTPase activating protein 1
JNK	c-jun NH_2-terminal kinase
KEAP1	Kelch-like ECH-associated protein 1
KH_2PO_4	Mono potassium phosphate
KRH	Krebs–Ringer-Hepes
LAMP-1	Lysosomal associated membrane glycoprotein-1
LiCl	Lithium chloride
LPS	Lipopolysaccharides
MAP	Microtubule-associated protein
MAPK	Mitogen-activated protein kinase
MEM	Minimal essential medium
Mes	2-(N-morpholino) ethanesulfonic acid
$MgCl_2$	Magnesium chloride
MMP	Matrix metalloproteinases
MSB	Microtubule stabilization buffer

MTOC	Microtubule organizing center
mTOR	Mammalian target of rapamycin
NaCl	Sodium chloride
$NaHCO_3$	Sodium biocarbonate
NEAA	Non-essential amino acids
NPF	Nucleation promoting factor
Nrf2	Nuclear factor erythroid 2-related factor 2
n-WASp	Neural wiskott aldrich syndrome protein
PI3K	Phosphatidylinositol 3-kinase
PAK	P21 activating kinase
Par6	Partitioning-defective
PB1	Phox and Bem 1
PBS	Phosphate-buffered saline
PDZ	PSD-95/Dlg1/ZO-1 homology
PMSF	Phenylmethanesulphonylfluoride

PPARγ	Peroxisome proliferator-activated receptor gamma
PT	Permeability transition
Rac	Rho-related C3 botulinum toxin substrate
Rat2	Rat fibroblasts (cell line)
REDOX	Reduction oxidation
Rho GTPase	Rho guanine trisphosphatase
RhoA	Ras homolog gene family, member A
ROS	Reactive oxygen species
SD	Standard deviation
SDS-PAGE	Sodium dodecyl sulfate polyacrylamide gel electrophoresis
SH	Src homology
siRNA	Small interfering RNA
Smad	Mothers against decapentaplegic, drosophilia homolog
SMURF1	SMAD Ubiquitination Regulatory Factor 1
STAT3	Signal transducer and activator of transcription 3

TGFβ or TGFβR	Transforming growth factor beta (receptor I/II)
TNF or TNFα or TNFR	Tumor necrosis factor alpha (receptor)
TNTE	Tris-NaCl-Tween-EDTA
Tris-HCl	Tris-hydrochloric acid
VCA	Verprolin-cofilin-acidic
WAVE	WASP-family verprolin homologous protein

CHAPTER 1

INTRODUCTION

1   INTRODUCTION

1.1   CELL MIGRATION

Cell migration is a process in which cells move in response to stimuli in the cellular environment. This process plays an essential role in many different physiological processes such as growth and development, immune responses, and wound healing.

1.2   CELL MIGRATION IN PHYSIOLOGICAL PROCESSES

1.2.1   Cell migration in growth and development

Cell migration is crucial in gastrulation, a process during early embryonic development in which germ cell layers are formed and the basic blueprint of the organism is established. Gastrulation arises from the reorganization of a single-layered blastula into a three-germline-layered gastrula. These three layers are composed of the endoderm, mesoderm and the ectoderm and they eventually give rise to different organs and tissues. In order for these cells to form specific tissues and organs and perform their functions, they must move to specific locations in a timely manner. The distance over which the cells migrate and the number and type of cells that do so vary widely and are regulated by different guidance signals.

Cells have been shown to migrate as either epithelial sheets or individual cells. In the first case, sheet-like epithelial cell movement is evident during massive tissue deformation where epithelial cells ingress and eventually surrounds the entire embryo. In

the latter case, cell movement requires the cells to undergo either a partial or near-complete process called epithelial to mesenchymal transition (EMT). EMT is a program of development where cells characterized to have a non-migratory phenotype with cell adhesions acquire changes that allow them to become more elongated in morphology and adopt a highly migratory phenotype. As a result, these cells detach from the epithelial sheet layer, form extensive protrusions and establish polarity in order to move towards a chemical gradient or stimulus. An example of this process is found in the adult animal in the form of wound healing.

1.2.2   *Cell migration and wound healing*

In response to tissue injury, cells initiate the wound healing process in order to protect the body from infection and undergo tissue repair. There are three phases in wound healing: inflammation, new tissue formation, and tissue remodeling, all of which are heavily regulated by cell migration. In response to an injury, tissues undergo an inflammatory phase where neutrophils, monocytes and lymphocytes arrive at the site of injury and release growth factors, cytokines, and hormones as part of the immune response. The factors attract endothelial cells and fibroblasts in order for the formation of new blood vessels and the deposition of extracellular matrix needed for blood clot formation to occur.

During the formation of new tissue, keratinocytes from the edge of the wound dedifferentiate, move towards the site of injury and proliferate to aid with the wound healing process. After re-epithelialization, these cells re-differentiate to restore the barrier

function of the skin, which protects the skin from water loss, bacteria or infection. Simultaneously, the connective tissue layer of the skin is repaired by the migration and proliferation of fibroblasts, which differentiate into myfibroblasts and promote wound contraction. Vascular, lymphatic and nerve networks are also restored by the migration and proliferation of respective cells into the wound. Overall, cell migration is a process that requires the highly orchestrated efforts of different components of the cell.

1.3 CELL MIGRATION: A MULTISTEP PROCESS

The process of cell migration is a complex multi-step phenomenon, which may differ between different organisms or even between cell types within an organism. For instance, cells can migrate as single cells where their morphologies are dependent on the expression of adhesion receptors and the surrounding microenvironment. Cells can also migrate *via* a chain-linked manner where a leading edge directs the migration of cells that are physically linked to one another. Cell migration has also been shown to occur with the assistance of heterotypic cell-cell contacts where they migrate in a manner that is guided by specific proteins (Figure 1.1).

Regardless of the mode of migration, most migrating cells form lamellipodia and filopodia (1). Lamellipodia consist of a meshwork of branched actin beneath the plasma membrane that forms a persistent protrusion over a surface, resulting in a 'leading edge'. Filopodia are fingerlike protrusions made up of actin bundles that extend beyond the lamellipodia and play an important sensory and exploratory role in steering the cell towards a stimulus (1). In turn, the cell starts establishing polarity where it undergoes

Figure 1.1 Cell migration is regulated by numerous signaling molecules and the cytoskeletal network.

In response to a stimulus, polarity proteins, including Rac1, CDC42, CLIP170, Par6, aPKCζ/ι, GSK3β, IQGAP1, Arp2/3 complex and n-WASp redistribute within the cell body and localize to the leading edge. Furthermore, the cytoskeletal network including actin filaments and microtubules rearranges to prepare for movement. Focal adhesions serve as traction points for cells to move forward on the ECM. The TGFβ receptor complex is located at the leading edge and plays an important role in Par6-dependent cell motility.

Rac1: Rho-related C3 botulinum toxin substrate; CDC42: cell division cycle 42; CLIP170: cytoplasmic linker protein of 170 kda; Par6: Partitioning defective 6; GSK3β: glycogen synthase kinase 3 beta; IQGAP1: IQ-motif containing GAP1; Arp2/3: actin-related protein 2/3; n-WASp: neural Wiskott Aldrich Syndrome protein; TGFβ: transforming growth factor beta; TGFβRI/II: transforming growth factor beta receptor I/II; ECM: extracellular matrix.

Figure 1-1

Leading Edge

Actin bundles

Lamellipodia

Membrane ruffles

Focal complex

Focal adhesion

CELL MOVEMENT

Microtubule

Filopodia

Stress fiber

Actin meshwork

IQGAP1

Rac1/Cdc42

Focal adhesion proteins (paxillin/FAK)

Par6

TGFβ Receptor I/II complex

aPKCζ/ι

Arp2/3 complex

+TIP (CLIP170)

nWASp

GSK3β
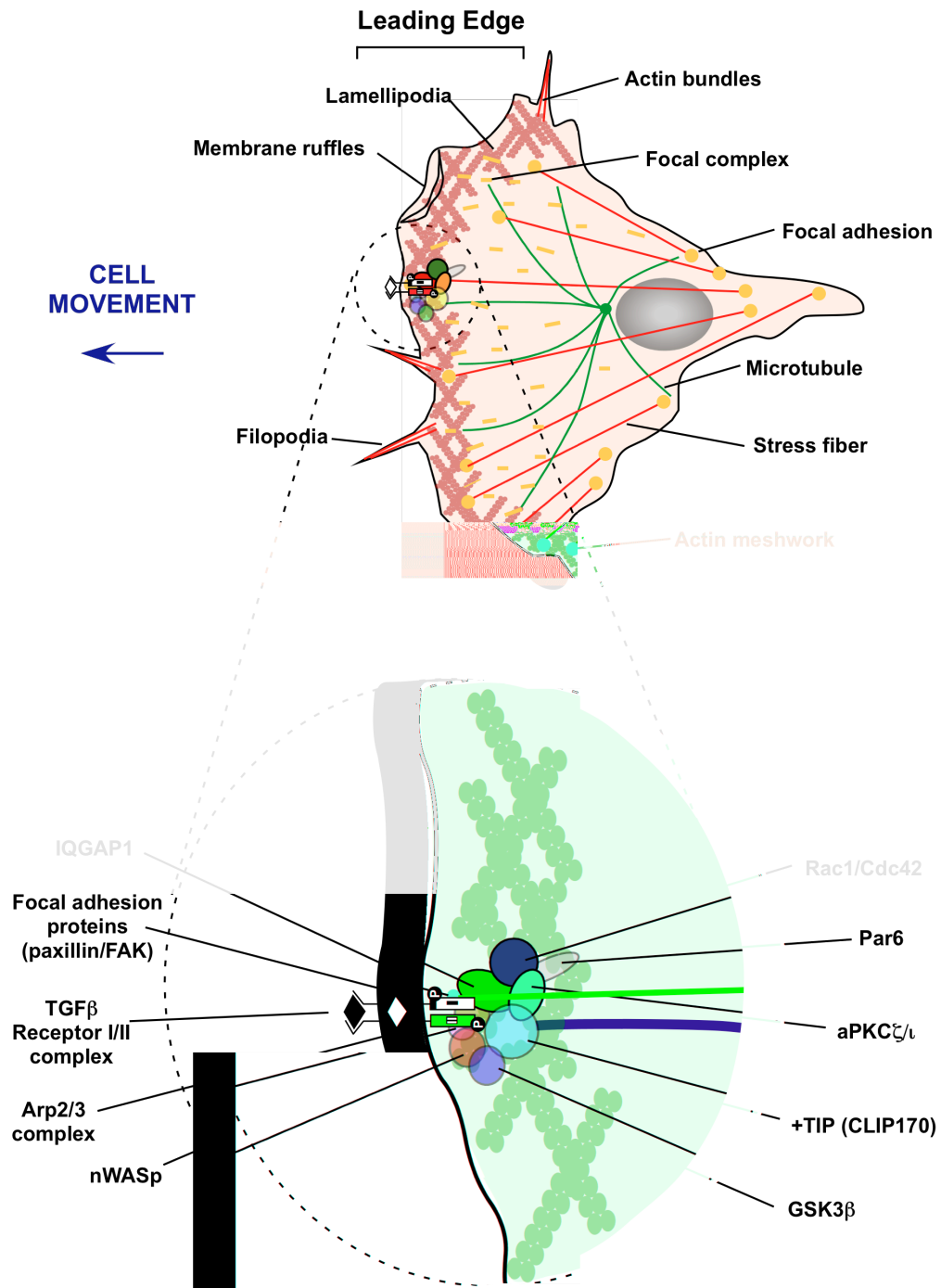
asymmetrical distribution of proteins and the rearrangement of cytoskeleton in order to prepare for directional movement. Simultaneously, the cell also begins to anchor itself to a new area *via* focal adhesion formation and the lagging end of the cell then experiences contraction and cell adhesion turnover in order for the cell to detach itself and move forward. There are many proteins that initiate and sustain directional cell movement and are described in further detail below.

1.4   CELLULAR COMPONENTS IMPORTANT FOR CELL MIGRATION

1.4.1   *The microtubule cytoskeleton*

Microtubules are an integral part of the cytoskeletal network, which are involved in physiological processes such as cell division, vesicle trafficking, cell polarization and migration. Microtubules are made up of thirteen laterally associated protofilaments, which form stiff but dynamic tubular structures. The protofilaments are made up of stable alpha/beta (α/β) tubulin heterodimers. Tubulin heterodimers are oriented in the same direction, generating a polarity with distinctive minus and plus ends (2).

The minus end of the microtubule is often anchored to the microtubule-organizing center (MTOC) while the alpha/beta (α/β) heterodimers are added to the plus end of the protofilament, generating a guanosine triphosphate (GTP) cap, which stabilizes the growing microtubule. Eventually, steady state is reached when the rate of microtubule disassembly is balanced by the rate of microtubule assembly. However, as the tubulin heterodimer binds, the GTP bound by the β–tubulin monomer undergoes hydrolysis, causing the loss of the GTP cap. Hence, depending on the rate of addition of subunits to

the growing microtubule and the rate of hydrolysis of GTP, the protofilament can undergo either growth or shrinkage, a process known as dynamic instability (3).

Dynamic instability helps microtubules distribute throughout the cell during cytoskeletal reorganization as microtubules undergo the 'search and capture' process where the plus end of the microtubule grows and explores the intracellular space before it is captured by organelles or microtubule-associated proteins that stabilize its structure. For instance, microtubules are stabilized by different binding proteins such as the Tau family of proteins, microtubule-associated protein (MAP)2 and MAP4 and microtubule plus-end tracking proteins (+TIPs) such as cytoplasmic linker protein of 170 kDa (CLIP170), cytoplasmic linker-associated proteins (CLASPs), and end-binding protein (EB) 1. Similarly, microtubules can be destabilized by different end binding or microtubule severing proteins such as kinesin 13, stathmin/Op18 and katanin. These positive end proteins are also involved in interaction of microtubules with other cytoskeletal structures such as actin filaments.

1.4.2   The actin cytoskeleton

Actin is a protein of abundance in the cytosol with concentration that can range as high as 5 mM in the eukaryotic cell. It is often observed to extend across the interior of the cell and is crucial in regulating polarity and migration. Actin exists in a monomeric (globular or G-actin) form or in a polymeric (filamentous or F-actin) form.

The actin cyotskeleton is dynamic and cycles between G-actin and F-actin. The hydrolysis of adenosine triphosphate (ATP) to adenosine diphosphate (ADP) is an

important regulatory step in actin polymerization. F-actin is initially formed by the spontaneous and unstable nucleation of G-actin monomers. When three monomers associate, they form a stable seed or nucleus for effective actin elongation. In vitro, the subunits in an actin filament point towards one direction, creating a polarity in the filament. The steady state mechanism whereby actin undergoes polymerization and depolymerization at the same rate is known as actin filament treadmilling. As a result of treadmilling, rigid actin filaments move forward and help form the lamellipodia in the leading edge of migrating cells (4).

Actin filaments adopt different morphologies depending on their function and localization within a cell. The four main types of actin structures that are found within the cell are filopodia, lamellipodia, stress fibers, and actin arcs. Actin structures in filopodia and lamellipodia are regulated by the Ras homolog gene family (Rho) of small GTPases (Figure 1.2). Stress fibers are bundles of anti-parallel actin filaments, which interact with myosin II, a member of the ATP-dependent motor protein family that possesses contractile properties; hence, giving the cell the flexibility to move. These stress fibers are often found in the basal portion of the cell and are tethered to the ECM by adhesive structures. In addition, to provide transverse structural support for the cell, actin arcs, which are large actin filament bundles, are localized to the dorsal and side portions of cells (4).

All actin structures are the result of one of two modes of actin nucleation assembly: branched or unbranched. These two modes of actin assembly are similar in that the fundamental building block is G-actin and the formation of both types of F-actin

Figure 1.2 The formation of different actin cytoskeletal structures is regulated by the Rho small GTPase superfamily.

CDC42, Rac1 and RhoA are Rho small GTPases that play an important role in the formation of filopodia, lamellipodia and stress fibers. Lamellipodia are formed by the Arp2/3 complex through branched actin nucleation, whereas filopodia and stress fibers are formed by formin through progressive unbranched actin nucleation. Specifically, CDC42 activates n-WASp, which in turn promotes nucleation and branched actin polymerization. Alternatively, the activation of RhoA leads to the activation of myosin II and ROCK and induces formin-dependent unbranched actin polymerization. Interestingly, Rac1 has been shown to be involved both indirectly and directly in branched and unbranched actin polymerization through n-WASp, WAVE and formin.

Rho small GTPase: Ras homolog gene family small guanine triphosphatase; CDC42: cell dividing cycle 42; Rac1: Rho-related C3 botulinum toxin substrate; Arp2/3: actin-related protein 2/3; n-WASp: neural Wiskott Aldrich Syndrome protein; RhoA: Ras homolog gene family member A; ROCK: Rho-associated kinase; WAVE: WASP-family verprolin homologous protein.

Figure 1-2

Rho superfamily

CDC42   Rac1   RhoA

WASp   WAVE   mDia (formin)   Myosin II ROCK

Arp2/3

A. Filopodia

B. Lamellipodia   C. Stress fibers
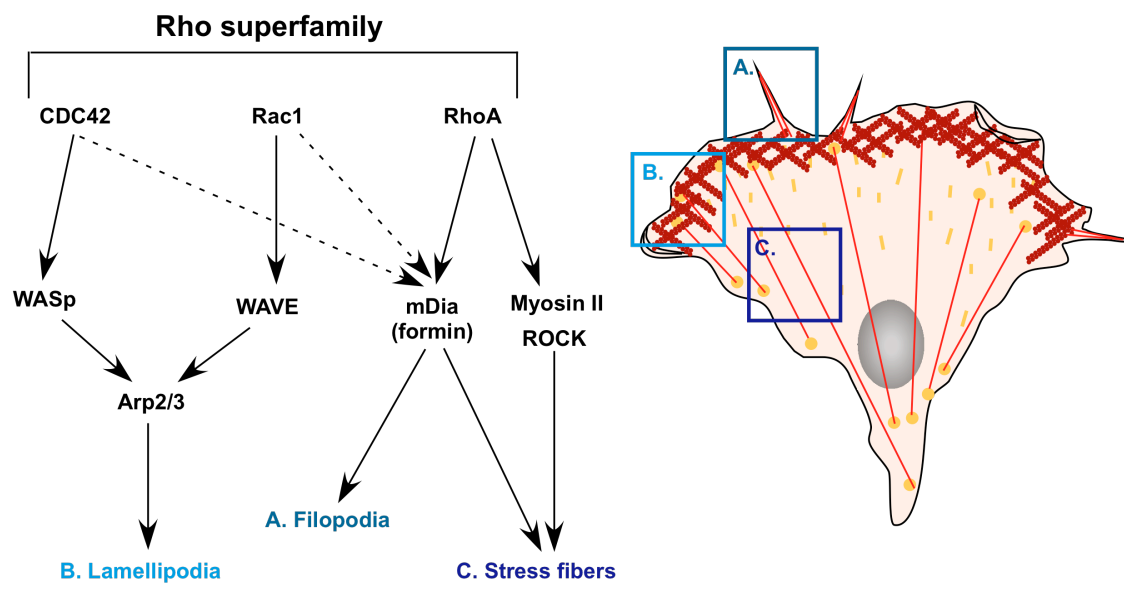
requires the activation of a nucleation promoting factor (NPF) and the protein that activates the NPF.

1.4.2.1 *Branched Actin Polymerization*

Nucleation of branched actin results in a dense meshwork of actin filaments that forms the lamellipodia. This initiation of branched actin is *via* the activation of the Actin-related protein (Arp) 2/3 complex. The Arp2/3 complex is a stable complex of seven conserved subunits that is composed of two actin-related proteins, Arp2 and Arp3, and five Arp-related protein subunits (ARPC): ARPC1, ARPC2, ARCPC3, ARPC4, and ARPC5 (4). Several studies have characterized the Arp2/3 complex and have found that Arp3 is involved in the nucleation process of actin, while ARPC2 and ARPC4 form the structural core of the complex. In addition, ARPC1, ARPC3 and ARPC5 have been shown to play a role in the activation of the complex by signaling proteins (5). The activation of Arp2/3 is regulated by the Wiskott-Aldrich Syndrome proteins (WASp) family of proteins which includes the hematopoietic WASp, the ubiquitous nWASp (neural WASp) and SCAR (suppressor of camp receptor) / WAVE (WASP-family verprolin homology protein) isoform 1, 2, and 3. These proteins are involved in the regulation of actin dynamics in different cellular processes including endocytosis, phagocytosis, cell migration, intracellular trafficking and internalization as well as the propulsion of pathogens. Thus far, two models have been proposed for the mechanism whereby branched actin is assembled via Arp2/3 and nWASP. In the first model, studies have shown that Arp2/3 serves as the nucleator. In fact, when activated by the verprolin-

cofilin-acidic (VCA) domain of WASP, the Arp2/3 complex has been shown to bind to the side of an existing actin filament and form a new branching actin filament (6-8).

In the second model, studies have indicated that the Arp2/3, WASP and G-actin complex bind to the barbed end of the mother filament and the hydrolysis of the GTP on the GTP-bound-actin dissociates the filament from the membrane bound activator, WASP. As a result, Arp2/3 then nucleates a lateral branch, that is now the daughter filament, and both the growth of the mother and daughter filaments drive membrane protrusion (9-11).

1.4.2.2   *Processive actin polymerization*

The second mode of actin assembly is known as the processive or unbranched actin assembly, which makes up the actin structures found in filopodia, stress fibers and actin arcs. This type of actin structure is formed by the activation of formin, which is a family of proteins that is involved in many physiological processes such as cytokinesis, endocytosis, filopodia formation, cell polarity, cell-cell adhesions and cell matrix adhesion (12). Specifically, the diaphanous-related formin, mDia, has been shown to induce the formation of processive actin assembly as a dimer with the actin-binding protein, profilin.

The rate of actin polymerization is regulated by different proteins that bind to G-actin monomers and/or the actin filament. These proteins can either enhance the rate of actin assembly or slow down actin polymerization. For instance, profilin and cofilin are actin-binding proteins that have been shown to stimulate the rate of treadmilling *in vivo*

by increasing the pool of ATP-bound actin, while gelsolin acts to sever actin filaments and stimulate depolymerization.

1.4.3 Polarity complex proteins and other proteins at the leading edge of migrating cells

Cell polarization is the process in which the cell undergoes cytoskeletal reorganization and directs its intracellular components and specific signaling proteins to form an internal axis of asymmetry. This process is evident in many physiological processes such as morphogenesis and cell migration.

The molecular machineries that are responsible for creating and maintaining cell polarity are the Scribble, Crumbs and the Par (Partitioning defective) complexes. These complexes define the basolateral domain, apical domain and the apical-lateral border respectively, by interacting with a wide array of signaling proteins in the cell (13). Specifically, the Par complex was the first polarity complex to be discovered (14) with the broadest functions (15) and is composed of the two *par* proteins, Par6 and Par3 and members of the atypical protein kinase C (aPKC) family.

Three Par6 proteins, Par6A/C, Par6B and Par6D/G, have been identified in mammals. Despite the fact that different genes encode these proteins, they are all of similar molecular weights and have three important conserved domains. These three domains include: the Phox/Bem1 (PB1) domain, which binds to other PB1 domain-containing proteins, the Cdc42/Rac1 interacting binding (CRIB) motif, which binds to activated Rho small GTPases (16,17), and the PSD95/Dlg1/ZO-1 (PDZ) domain

(18,19), which binds to other PDZ domain-containing proteins. Although Par6 lacks enzymatic function, it is able to scaffold several signaling proteins. In the context of cell migration, Par6 forms a complex with both aPKC (via its PB1 domain) and Par3 (via its PDZ domain) at the leading edge.

Two aPKC proteins, aPKCλ/ι and aPKCζ, are encoded by two different genes in mammals. These atypical PKCs are part of a much larger PKC family, which also includes classical PKCs and conventional PKCs. Although all PKCs possess a kinase domain at the C-terminus, atypical PKCs are different from the conventional PKCs and classical PKCs in that they have a PB1 domain that interacts with proteins such as Par6 but they lack a complete C1 domain which is necessary for calcium, diacylglyercol and phorbol ester-dependent activation (14). Studies have shown that in epithelial cells, aPKCs localize with the other members of the Par complex to tight junctions or the leading edge of migrating cells (20). In addition, aPKCs have an important role as activators of the downstream signaling cascades leading to the establishment of cell polarity. This was evident in a study where the overexpression of kinase-deficient aPKC mutants resulted in the blockage of tight junction formation as well as the disruption of cell polarity (21).

Studies in *C. elegans* and *D. melanogaster* have shown that Par3-Par6-PKC complex plays a critical role in anterior-posterior polarity (22). Subsequent studies in mammalian cells have confirmed that complex formation is important in regulating cell polarity (17,23). However, it is important to note that in some cases, aPKC-Par6 complex but not Par3 plays an indispensable role in polarized migration (24). Hence, although

Par3 is undoubtedly important in ensuring the function of the Par complex as a unit in some cell types, its interaction with Par6-aPKC may be transient and dynamic (24).

1.4.4   The Rho superfamily

Regulation of the Par complex is dependent on its interactions with a family of important proteins known as the Rho small GTPases. The mammalian Rho small GTPase superfamily is composed of about 20 intracellular signaling molecules. These Rho small GTPases are essential molecular switches that regulate different signaling networks by cycling between a guanosine diphosphate (GDP)-bound inactive form and a guanosine triphosphate (GTP)-bound active form (3).

The states of Rho small GTPases are controlled by three different types of regulators. In resting cells, Rho small GTPase often exists in the GDP-bound form in a complex with Rho GDP-dissociation inhibitor (GDI). GDI, when bound to GDP-Rho GTPase, inhibits the exchange of GDP for GTP.   In response to extracellular signals, GDP-Rho GTPase dissociates from GDI to allow the guanine-nucleotide-exchange factor (GEF) to promote the exchange of GDP for GTP. In its active GTP-Rho GTPase form, it can then bind to downstream effectors and elicit various signaling responses. To revert back to its inactive form, GTPase activating proteins (GAPs) act to enhance the intrinsic activity of Rho GTPase by hydrolysis and as a result, GDP-Rho GTPase associates with GDI.

Rho-related C3 botulinum toxin substrate 1 (Rac1) and cell divison cycle 42 (CDC42) are two Rho GTPases that localize to the leading edge of migrating cells and

have been shown to play important roles in cell polarization. Indeed, work by Etienne-Manneville and colleagues has shown that CDC42 localizes and binds to Par6, which in turn, activates the Par6-PKCζ complex by phosphorylating PKCζ in migrating astrocytes. As a result of this activation, PKCζ can then phosphorylate downstream substrates such as Glycogen Synthase Kinase 3 β (GSK3β) (25).

GSK3β is a constitutively active serine/threonine kinase that is known to have an inhibitory effect on the tumor suppressor protein, adenomatous polyposis coli (APC) by preventing it from binding to the microtubules. Thus, the phosphorylation and inactivation of GSK3β by activated PKCζ dissociates APC from GSK3β so that it can bind to and stabilize microtubules. The association of APC with microtubules and another protein, Dislarge1 (Dlg1), allows for reorientation of the centrosome, Golgi apparatus and nuclei and induces targeted vesicle transport to the leading edge, all of which are important for cell polarization (15,25). Interestingly, studies have shown that aPKC-mediated inactivation of GSK3β can also suppress Ras homolog gene family member A (RhoA) activity at the front of the cell by inhibiting p190ARhoGAP (26). Consistent with this study, RhoA has been shown to mostly localize at the lagging edge of migrating cells and is largely involved in the degradation of the Par complex and the induction of EMT through the Transforming Growth Factor Beta (TGFβ)-dependent pathway.

The TGFβ pathway is an extensively studied pathway that is known for its role in numerous physiological processes such as tissue morphogenesis, wound healing and migration as well as its roles as both a tumor suppressor and promoter in carcinogenesis. It signals through the canonical Mothers against decapentaplegic drosophilia, homolog (Smad) pathway in which the TGFβ ligand binds to the constitutively active transforming

growth factor beta receptor (TGFβR) II, which in turn, comes into close proximity with TGFβRI and transphosphorylates TGFβRI (27,28). The activated receptor complex is then internalized *via* clathrin-coated pits where it phosphorylates Smad2/3 and together with Smad4, the Smad2/4 complex translocates to the nucleus to propagate signal transduction (Figure 1.3). Alternatively, the activated receptor complex can enter the caveolae and bind to inhibitory-Smad7 and E3 ubiquitin ligases, Smad ubiquitination regulatory factor (SMURF) 1 and 2, which targets the complex for degradation and signal termination (29). In the context of cell polarity, the Par-aPKC complex associates with the TGFβ receptors (Figure 1.3). As a result of TGFβ binding, ligand-activated TGFβRII phosphorylates Par6, which in turn, activates the E3 ubiquitin ligase SMURF1 and induces the proteasomal degradation of RhoA (30,31). The degradation of RhoA contributes to the loss of apico-basal polarity and allows the cells to become more migratory. In addition, the activation of the Par-aPKC complex by CDC42 has been shown to be coupled to Rac1 activation through the Rac-specific GAP, T-cell lymphoma invasion and metastasis-1 (TIAM1). This results in actin polymerization, microtubule stabilization, and front-rear polarity (32). Therefore, studies have provided important insights on not only how Rho small GTPases work cooperatively but antagonistically to establish and regulate cell polarity in a migrating cell.

Beside Rho small GTPases, other leading edge proteins have also been shown to have essential roles in modulating the actin and microtubule cytoskeletons, which in turn, contribute to the establishment and maintenance of cell polarity. For instance, IQGAP1 is a 190-kDA protein found ubiquitously expressed in most, if not all organisms ranging from yeast to mammals. It has two other isoforms, IQGAP2 and IQGAP3, which exhibit

Figure 1.3 TGFβ signaling plays an important role in numerous physiological processes.

TGFβ signaling is initiated when TGFβ binds to TGFβRII at the cell surface, which in turns, transphosphorylates TGFβRI and induces receptor internalization. Activated receptor complexes on the early endosome associate and phosphorylate Smad2/3 proteins. Phosphorylated Smad2/3 then binds to Smad4, and together, these proteins translocate into the nucleus and affect gene transcription. Alternatively, TGFβ can also induce EMT and stimulate cell migration. Specifically, TGFβRII is redistributed to tight junctions where it activates TGFβRI and phosphorylates Par6. Phosphorylation of Par6 leads to the recruitment of SMURF1, which directs the ubiquitination of RhoA. Degradation of RhoA promotes EMT and cell migration.

TGFβ: transforming growth factor beta; TGFβR I/II: transforming growth factor beta receptor I/II; Smad: mammalian homolog of mothers against decapentaplegic; EMT: epithelial-to-mesenchymcal transition; Par6: Partitioning defective 6; SMURF1: Smad ubiquitination regulatory factor 1; Rho A: Ras homolog gene family, member A.

Figure 1-3
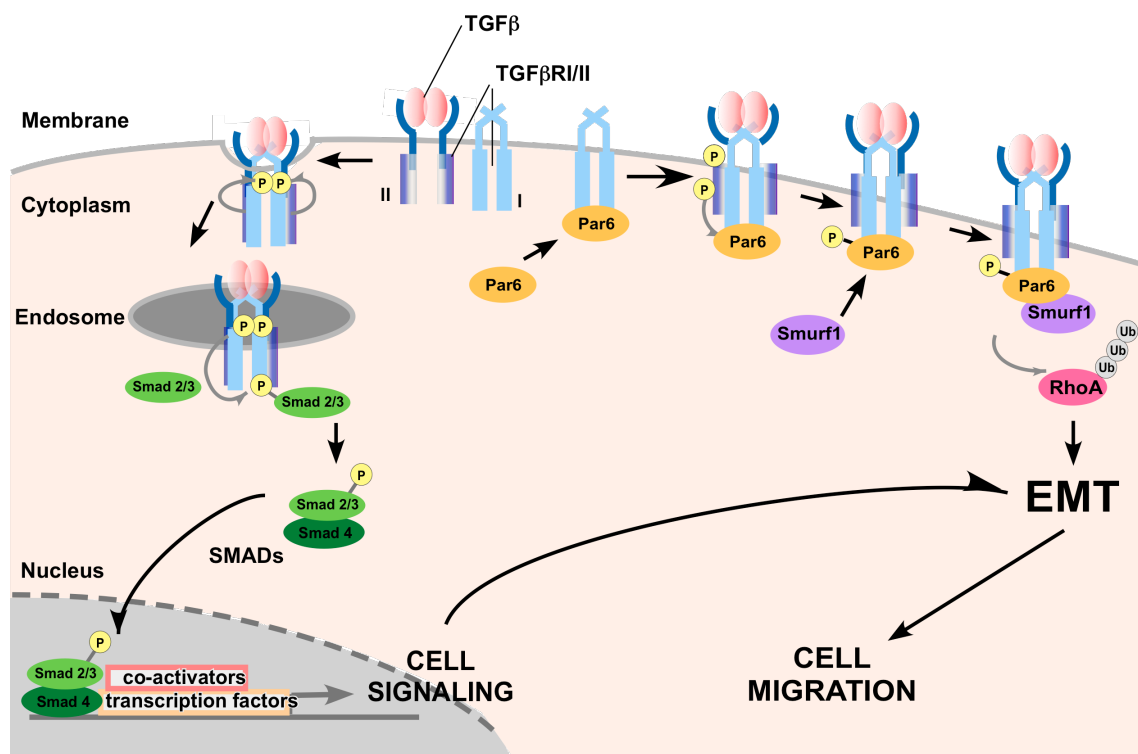
some common characteristics including considerable sequence overlap; however, they differ vastly in their functions, tissue distribution and subcellular localization. Of the three known isoforms, IQGAP1 is the most extensively studied. It was first identified as a Rac/Cdc42 binding protein that localized at the leading edge of migrating cells (33). Since then, over 90 proteins have been identified as IQGAP1 binding partners (34). These binding partners include adaptor/scaffold proteins, calcium-binding proteins, cytoskeleton-associated proteins, Rho small GTPases and their regulators, kinases, members of the mitogen-activated protein kinase (MAPK) family, microbial proteins, neuronal proteins, nuclear proteins, members of the phosphatidylinositol 3-kinase/protein kinase B (PI3K/Akt) survival pathway, receptors, and trafficking proteins (34). As a result, the ability to interact with these proteins makes IQGAP1 a protein with remarkably diverse biological functions.

The role of IQGAP1 in regulating the cytoskeleton and cell polarity is of particular interest and has been extensively studied. IQGAP1 was first found to bind directly to actin and induce the cross-linking of actin filaments in the cell (33). Further studies then showed that IQGAP1 can also bind to n-WASP, and stimulate Arp2/3-dependent branched actin assembly and is a barbed end actin capper for actin filaments (35,36), both of which are important in the formation of leading edge and cell polarity. In addition, activated Rac1 and CDC42 can form a complex with numerous microtubule plus end binding proteins such as CLIP170, CLASP2, EB1 and APC through IQGAP1 (37-39). These complexes all contribute to the underlying mechanism whereby microtubule dynamics and stability are modulated during cell polarization and cell migration. Specifically, IQGAP1 and CLIP170 have first been shown to mediate the

transient capturing of microtubules to the leading edge (37). Later studies then indicated that APC was part of this complex and helped with stabilizing the interaction of IQGAP1 and CLIP170 at the plus ends of microtubules (39). Recently, CLASP2 has also been identified as a novel binding partner of IQGAP1 and GSK3β is found to modulate the phosphorylation of CLASP2, which can then affect its binding ability to IQGAP1, EB1 and microtubules, and ultimately, cell polarization and cell migration (38). Since IQGAP1 can bind to both F-actin and microtubules, it is often observed to be a critical linker protein that bridges and organizes the cytoskeleton during cell migration.

Collectively, the proteins discussed above make up a small but important subset of proteins at the leading edge that, with their complementary and antagonistic regulatory roles, help establish and maintain cell polarity in order to form a focal point for directional cell movement.

1.4.5   Focal adhesions

As a cell initiates migration by polarizing and extending protrusions towards a stimulus, the protrusions are stabilized by cell adhesions in order to anchor the cell onto the extracellular matrix (ECM) (40) (Figure 1.4).

Structurally, adhesions can be characterized into morphologically distinct adhesion complexes, focal adhesions, or fibrillar adhesions, depending on their subcellular localization, size, shape, molecular composition or dynamics (40). Focal complexes are made up of small nascent adhesions that rapidly assemble and disassemble at the leading edge or at the periphery of migrating cells. They often consist of areas rich

Figure 1.4 The role of focal adhesions in cell migration.

At the leading edge of a migrating cell, focal adhesion proteins form a complex at the cell membrane. In response to stimuli, integrins are induced to form clusters, which in turn recruit different proteins including FAK, paxillin, tensin, vinculin, actinin and talin. These proteins play a key role as traction points in order for the cell to move forward.

FAK: focal adhesion kinase.

Figure 1-4

Stress fiber

Focal adhesion proteins

Actinin

vinculin

Tensin

Talin

FAK Paxillin

Cell membrane

Extracellular matrix

β α
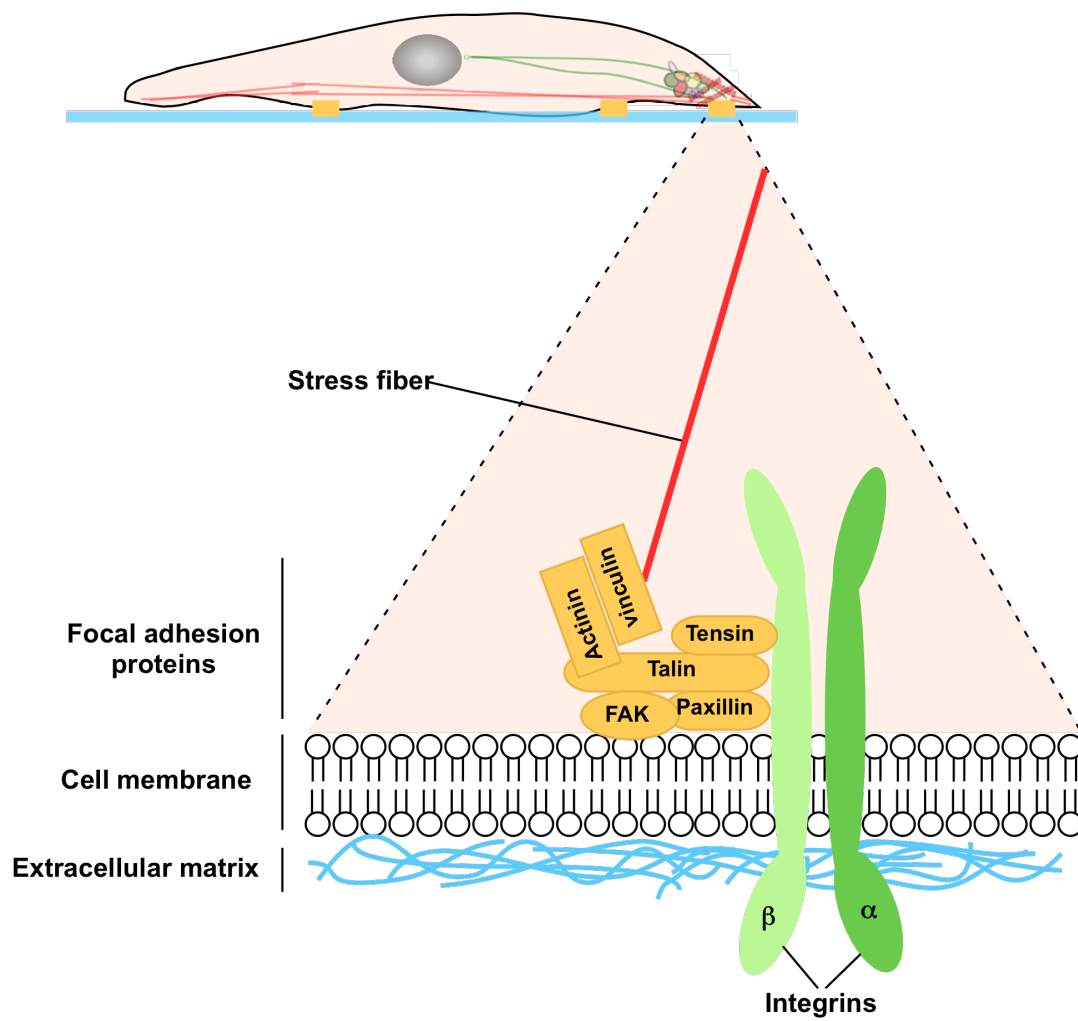
Integrins

in β3-integrin, talin, paxillin and appear as dot-like structures of 1 μm^2. Focal adhesions or focal contacts grow to about 2-5 μm oblongs and are observed in slower moving cells. These structures are more stable and are localized to the periphery and in the central area of the cell where there is less motility. In contrast to focal complexes, focal adhesions contain a much larger range of proteins including vinculin, talin, paxillin, zyxin, α-actinin, VASP, FAK, phosphotyrosine proteins and αvβ3 integrin. Fibrillar adhesions are elongated structures associated with fibronectin fibrils. These structures do not adhere to stress fibers and consist of high levels of tensin and α5β1 integrin. It is important to note that different types of adhesive structures can co-exist in a single cell at any one time (41). In fact, fibrillar adhesion structures often evolve from focal adhesions, which originate from nascent adhesion structures that have matured. However, although the molecular compositions of these adhesions share similarities, there are also subtle differences that distinguish them. For instance, zyxin is not found in focal complexes. In addition, a small amount of paxillin and no β3 integrin nor vinculin are found in fibrillar adhesions (4,40). Finally, besides the classical adhesion structures mentioned above, two other classes of cell-ECM adhesion structures known. They are podosomes and invadopodia which are adhesion structures that can recruit matrix metalloproteinases (MMPs) and facilitate matrix degradation (1).

The formation of focal adhesions are thought to be first initiated in response to the microclustering of more than ten integrin molecules at the ECM, which in turn, leads to the activation of integrin signaling. Activated integrins then recruit the adaptor protein, paxillin, to promote nascent adhesion formation and further integrin clustering. In addition, nascent focal adhesion growth also induces the recruitment of α-actinin, which

together with the actin-binding protein talin, helps stabilize the link between ECM-bound integrin and the actin cytoskeleton. These nascent adhesions normally undergo rapid turnover within minutes. Tension has been shown to cause the recruitment, phosphorylation and activation of FAK. In addition, tension can also induce the phosphorylation of other focal adhesion proteins such as paxillin and p130Cas and establish scaffolding platforms for numerous phosphotyrosine-binding, Src homology (SH)2 domain-containing proteins in order to promote adhesion growth. Similar to nascent focal complexes, focal adhesions often undergo adhesion turnover within 10-20 minutes; however, a subset of these mature further into fibrillar adhesions by the dephosphorylation of paxillin at tyrosine 31 or 118. Interestingly, these fibrillar adhesions do not promote cell migration but are involved in ECM remodeling (42).

The assembly and disassembly of focal adhesions depends on the conformation, the exposed binding motifs, and the signaling domains that are contained within each of the proteins that are recruited (40). More importantly, the turnover of focal adhesions is largely associated with the signal transduction that occurs as a result of the binding of these proteins. Focal adhesion-associated proteins often initiate downstream signaling cascades that ultimately determine the maturation and the lifespan of focal adhesions. Thus far, at least 150 different proteins have been shown to be involved in regulating the formation, maintenance and disassembly of adhesion structures (43). Of interest, FAK is one of the many proteins that play a critical role in focal adhesion dynamics and is known to be a master regulator of focal adhesion turnover. In fact, fibroblasts from *Fak$^{-/-}$* mice have reduced cell spreading and migration as well as an increase in the number and size of cell adhesions on the periphery of the cells (44).

FAK is a cytoplasmic non-receptor protein-tyrosine kinase, which was first identified as a substrate of the viral Src oncogene product and was found to localize to integrin-enriched cell adhesion sites in normal cells (45). FAK itself is a multi-domain protein which is maintained in an autoinhibitory position; however, when it is stimulated by integrin clustering, actin cytoskeleton-induced tension or by the binding of proteins and phospholipids, it can unfold and expose the tyrosine 397 site for phosphorylation (46). Specifically, the phosphorylation of tyrosine 397 creates a binding site for various SH2-containing proteins, which leads to downstream signaling cascades that regulate different cellular processes. In the context of cell migration, the phosphorylation of PI3K and Growth factor receptor-bound protein (GRB) 7 by FAK have been shown to promote cell motility in a cooperative manner (47). In addition, the phosphorylation and binding of these proteins to tyrosine 397 can lead to the phosphorylation of other tyrosine residues in the kinase domain, which are necessary for maximal FAK catalytic activity. Finally, the proline-rich repeats (PRRs) in FAK associate with SH3 domain-containing proteins such as p130Cas, GTPase regulator associated with FAK (GRAF) or the Arf-GTPase-activating proteins (ASAP), all of which regulate the activities of Rho small GTPases.

Interestingly, FAK possesses many more phosphorylation sites other than those mentioned above, most of which are not within the kinase region. To date, at least four serine phosphoryaltion sites (serine 722, 840, 843, 910) and a few other tyrosine phosphorylation sites (tyrosine 407, 861 and 925) were found (48). In particular, studies have shown that tyrosine 925 and serine 722 are important regulators of cell adhesions.

Indeed, FAK phosphorylation at serine 722 by GSK3β has been shown by Bianchi and colleagues to regulate cell spreading and cell migration (51).

GSK3 is a serine/threonine kinase family that was originally identified as an important mediator of glycogen metabolism and insulin signaling. The two isoforms, GSK3α and GSK3β, which are encoded by two different genes, share approximately 85% identity, with up to 98% homology between their kinase domains. The major differences between the two isoforms are the last 76 amino acids in the C-terminus and a glycine-rich extension on the N-terminus of GSK3α (52). However, despite their similarities, they are not functionally identical nor redundant. In fact, even though there are many overlapping properties between GSK3α and GSK3β, they play quite distinct roles in different cell types and in different physiological processes (53-64). For instance, *Gsk3β*$^{-/-}$ mice undergo hepatocyte apoptosis that leads to embryonic lethality (54) while *Gsk3α*$^{-/-}$ mice survive and only display enhanced glucose and insulin sensitivity as well as reduced fat mass (65).

Unlike many protein kinases, GSK3β is constitutively active in resting cells and it undergoes rapid and transient inhibition in response to different external signals. It is unique both in its regulation and its preference for substrates. Studies using the crystal structure of GSK3β have shown that there are two phosphorylation sites that can affect the catalytic activity of the protein (66,67). Specifically, the phosphorylation of tyrosine 216 in its activation loop is a pre-requisite for maximal catalytic activity. In addition, in its unphosphorylated form, it serves to block access of substrate from the binding groove (67). The other phosphorylation site, serine 9, is a site that, when phosphorylated, can lead to the inhibition of GSK3β activity. Interestingly, GSK3β has the unique preference

of targeting proteins that are pre-phosphorylated at a 'priming' residue located on the C-terminal three amino acids from the site of GSK3β phosphorylation. Although not absolutely required, priming phosphorylation increases the efficiency of phosphorylation by GSK3β by 100-1000 fold (68).

To date, GSK3β has been shown to be a multi-functional kinase that not only regulates glycogen metabolism but also affects signaling pathways involved in the regulation of cell fate, protein synthesis, proliferation, and survival. Thus, GSK3β has become an appealing protein target for treatment in diabetes, inflammation, neurological disorders, as well as cardiovascular diseases. Recently, the role of GSK3s has been extended to the field of cell migration, a precursor event of cancer metastasis. Studies have shown that GSK3β is an important player in cytoskeletal and adhesion dynamics. For instance, evidence suggests that GSK3β phosphorylates microtubule-associated proteins and interacts with microtubule motor proteins to regulate microtubule dynamics and microtubule-dependent vesicle transport (69). Moreover, inactive GSK3β is found to localize at the leading edge of migrating cells, which enables APC to localize at the plus end of microtubules and stimulate microtubule growth and stability during migration. In addition, GSK3β has also been shown to regulate several small Rho GTPases including Rac1, RhoA and Arf6, which in turn, control membrane ruffling, cell spreading and lamellipodia formation. GSK3β also plays an important role in regulating cell adhesions molecules such as FAK and paxillin. As mentioned above, GSK3β stimulates the maturation of nascent adhesions and inhibits adhesion disassembly (51). However, Kobayashi and colleagues showed that when GSK3β formed a complex with the cyclic adenosine monophosphate (cAMP) phosphodiesterase, h-prune, it facilitated focal

adhesion disassembly (70). In addition, paxillin, which has been previously shown to be an important target for FAK and c-Src is also a GSK3β substrate. Finally, it has been proposed that the phosphorylation of paxillin at serine 126 and 130 by GSK3β and extracellular signal-regulated kinase (ERK)2 respectively is required for cell spreading (71).

1.5   CELL MIGRATION IN PATHOLOGICAL PROCESSES

As previously shown, cell migration is a process that requires the efforts of numerous proteins. The dysregulation of any one of these molecules and hence, cell migration often leads to pathological diseases such as birth defects, auto-immune diseases, chronic inflammation and cancer. Tumor cell migration plays a critical role in the progression of cancer and tumor invasion as it is intricately connected to the ability of a tumor to metastasize. Studies have shown that 90% of cancer-related death is due to metastasis. The cause of dysfunction in tumor cell migration can be attributed to many different factors, which together, amplify the power of the process itself. Therefore, the development of chemotherapeutic compounds that can effectively target tumor cell migration, or at least aspects of it, could play a critical role in cancer therapy and improve the survival of cancer patients.

1.6   SYNTHETIC OLEANANE TRITERPENOIDS AND THEIR DEVELOPMENT

Triterpenoids are the largest group of natural plant products, composed of more than 20 000 known members. They are synthesized by the cyclization of squalene. The resulting carbon framework from the cyclization process is one or more cyclic triterpene alcohols with up to six carbocyclic rings (72). Oleanolic acid (3/3-hydrox-olea-12-en2-oic acid) (Figure 1.5A) is a pentacyclic triterpenoid compound that has been traditionally used in folk medicine for its anti-inflammatory and hepatoprotective activities. Later studies on oleanolic acid confirmed that this triterpenoid compound indeed has a positive effect in numerous diseases such as chemical-induced liver injuries and cancer (73,74). However, since the water solubility of oleanolic acid is limited and its biological activity is relatively weak (75), modification of the oleanolic acid into synthetic oleanane triterpenoids was initiated in an attempt to make the compound more bioavailable.

The work on synthetic oleanane triterpenoids started in the early 1990s in the Gribble laboratory where more than 80 synthetic triterpenoids derived from oleanolic acid were generated and screened for their ability to protect against inducible nitric oxide synthase (iNOS) production induced by interferon gamma (IFN-γ) in mouse macrophages (76). The rationale behind using this type of screening stems from the fact that inflammation is intricately linked with carcinogenesis; hence, designing unique agents that target inflammation represents a potential means for chemoprevention and chemotherapy. Of all the triterpenoid candidates, TP46 was identified as an active suppressor of nitric oxide production. The combined modification on both ring A and ring C on the original triterpenoid resulted in 2-cyano-3, 12-dioxooleana-1,9-dien-28-oic

acid (CDDO) (Figure 1.5B), a triterpenoid compound that is about 10 000 times more potent than the original lead compound and 400 000 times more potent than oleanolic acid (77). Furthermore, by modifying the C-28 site on 2-cyano-3, 12-dioxooleana-1,9-dien-28-oic acid (CDDO) and replacing it with different functional groups, (i.e. nitrile, ester, glycosides, and amides), more potent triterpenoid derivatives were developed, two of which are CDDO-Imidazolide (CDDO-Im) and CDDO-Methyl ester (CDDO-Me) (Figure 1.5C) (78). Recently, other C-28 amide derivatives including CDDO-ethyl amide, CDDO-diethyl amide, CDDO-trifluoroethyl amide and CDDO-methyl amide were also synthesized (79).

1.7   THE BIOLOGICAL ACTIVITY AND MECHANISM OF ACTION OF THE TRITERPENOIDS

Numerous studies have shown that this class of compounds has anti-inflammatory and cytoprotective properties. In addition, triterpenoids can induce the differentiation and apoptosis of cancer cells. The triterpenoids are such effective agents in targeting cancer cells because they are able to target regulatory proteins and/or transcriptional factors, which in turn modulate the activities of different regulatory networks and signaling pathways. This differs from many conventional chemotherapeutic agents, which target only individual proteins or kinases. However, cancer is a complex disease composed of different mutations that originated from different environmental causes and genetic mutations. As a result, gain-of-function, amplifications, and/or overexpression of oncogenes and loss-of-function mutations, and deletions and/or epigenetic silencing of

Figure 1.5 The molecular structure of oleanolic acid and synthetic triterpenoids.

A) The structure of oleanolic acid shows three areas of modification, which include the hydroxyl group at carbon 3, the double bond between carbon 12 and carbon 13, and the carbon 28 carboxyl group (red).

B) The structure of CDDO (TP151), a synthetic triterpenoid that is 400 000 times more potent than oleanolic acid when tested for iNOS production induced by IFN-γ in mouse macrophages . To make the synthetic triterpenoids more potent, further modifications are made (red).

C) The structure of two derivatives of synthetic triterpenoids, CDDO-Im (TP235) and CDDO-Me (TP155) are formed by replacing the reaction group (R; red dotted circle) with an imdiazolide group or a methyl ester group at carbon 28 respectively. These derivatives have been shown to have greater potencies compared to its parental compound, CDDO.

CDDO: 2-cyano-3,12-dioxooleana-1,9-dien-28-oic acid; Im, imidazolide; Me, methyl ester; iNOS, inducible nitric oxide; IFN-γ : interferon gamma.

Figure 1-5

A

Oleanolic acid

B

CDDO (TP151)

C

CDDO-Im (TP235)

CDDO-Me (TP155)
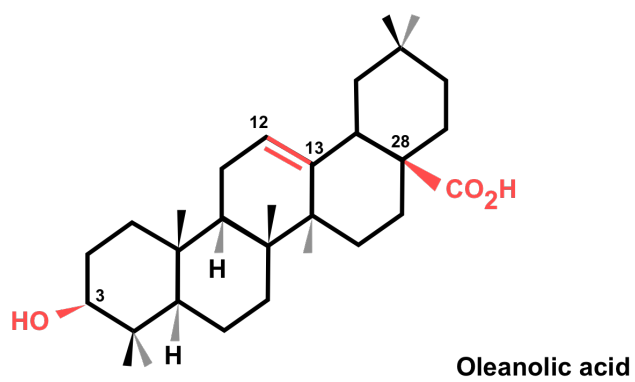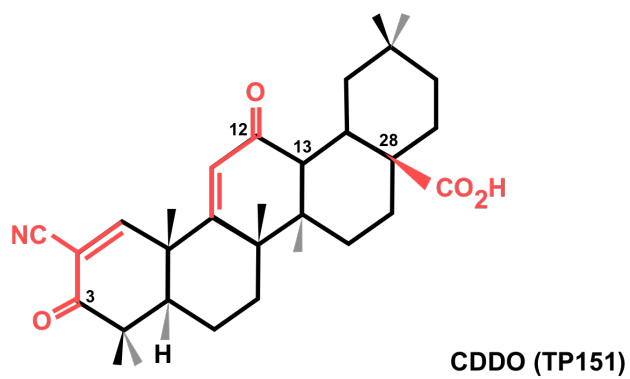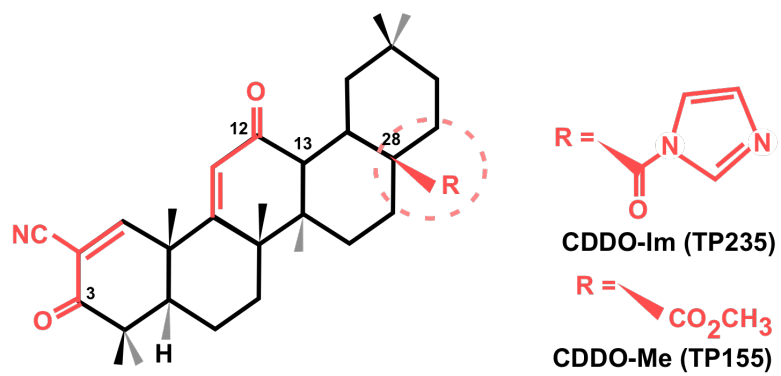
tumor suppressor genes can all lead to changes in the programming of a cell that affects the overall homeostasis of the body at multiple regulatory levels. Therefore, by targeting the regulatory network and the genes that regulate cellular activities, triterpenoids have the potential to effectively control a much larger range of dysfunctional pathways, which are common features of pre-malignant or malignant cells and tissues, compared to mono-functional targeted drugs (80).

The molecular mechanism of action of the triterpenoids is believed to involve the nucleophilic attack (thio-or aza-Michael addition) of a thiol or other nucleophile to the C1 and C9 position. Triterpenoids form reversible adducts with reagents containing thiol residues and directly interact with protein targets that contain specific reactive cysteine residues. So far, the known triterpenoid-binding targets include peroxisome proliferator-activated receptor-γ (PPARγ) (81), kelch-like ECH-associated protein 1 (KEAP1) (82), tubulin (83), I-kappaB kinase beta (IKKβ) (84,85), Arp3 (86), and mammalian target of rapamycin (mTOR) (87). It is interesting to note that although in most cases, more than one cysteine exists in these proteins, triterpenoids do not bind to all of these cysteine residues at random. Rather, the binding of the triterpenoids to a specific cysteine depends largely on the reduction oxidation (REDOX) potential of the cell and the accessibility of the cysteine residues as a folded protein structure. Although most of the targets identified so far contain reactive cysteines, the possibility that triterpenoids could also interact with other nucleophilic groups such as lysine, arginine, or histidine on target proteins should not be eliminated (79).

1.8 TRITERPENOIDS AND DISEASES

Since the triterpenoids target multiple pathways by modulating the activity of regulators and transcription factors, it is expected that this class of compounds will also affect neurodegenerative diseases including Parkinson's (88,89), Huntington's (88,90) and Alzheimer's diseases (89,91), inflammatory lung conditions from chronic granulomatous disease (92) or diseases such as cystic fibrosis (93), pulmonary fibrosis (94-96), acute lung injuries (97), retina-related injuries (98,99), emphysema (100), inflammatory cardiovascular diseases (100,101), acute liver injury (102-104), kidney diseases (105,106), diabetes (107) and obesogenesis (107,108). For the scope of the thesis, the effects of triterpenoids on cancer will be reviewed in detail.

1.9 SYNTHETIC TRITERPENOIDS AND THEIR ANTI-CANCER PROPERTIES

1.9.1 *Triterpenoids and tumor cell differentiation*

Cell differentiation is an important process that occurs in embryonic development or during normal cell turnover or tissue repair. All cells originate from stem cells where they mature and fully differentiate into specialized cell types to form different organs and parts of the organism. When a cell is fully differentiated, it loses its ability to divide. In the case of cancer, tumor cells are thought to have bypassed or arrested at a less mature or less differentiated state where they can rapidly divide. As a result, one of the hallmarks of

cancer cells is uncontrolled cell division. Therefore, much effort have been put towards differentiation therapy, which is based on the concept that treatment will force cells to undergo differentiation where they can mature and no longer divide.

Triterpenoids play a critical role in stimulating cell differentiation in numerous cancer cell cultures studies. For instance, one of the earliest studies on CDDO indicated that the compound could induce monocytic differentiation of human myeloid leukemia and adipogenic differentiation of mouse 3T3-L1 adipocyte-derived fibroblasts (109,110). In addition, it has been shown to enhance neuronal differentiation of rat pheochromocytoma cells (109). Further studies then proved that the induction of differentiation in human myeloid leukemia cells and osteosarcoma by CDDO and its derivatives CDDO-Im and CDDO-Me was *via* a caspase 8-dependent mechanism (111,112). The induction of monocytic differentiation of leukemia cell has been associated with the activation of the ERK and the TGFβ/Smad signaling pathways, as well as the upregulation of the CCAAT/enhancer-binding protein (CEBP) Beta ((113).

1.9.2 *Triterpenoids and growth inhibition*

Cell division is highly regulated by many cell cycle checkpoints including p53, p21, p27, and cyclin D. In the case of tumor cells, many of these cell cycle regulators are altered, hence allowing tumor cells to bypass these checkpoints and undergo uncontrolled cell division.

Nanomolar concentrations of CDDO and its derivatives have been shown to inhibit cell proliferation in tumor cells and the anti-proliferative effect of the triterpenoids has since been tested on numerous solid tumor cells from almost every organ as well as leukemia (79). Although most human cancers are biologically and pathologically different, the alteration of the p53 pathway occurs in many human cancers (115). Interestingly, the mechanism whereby triterpenoids inhibit tumor cell growth is independent of the status of p53 while the recruitment and expression of key cell cycle proteins such as cyclin D1, p21, p27, proliferating cell nuclear antigen (PCNA), caveolin and myc seem be affected in triterepenoid-treated cells (116,117,118). In addition, triterpenoids have been shown to associate and transactivate PPARγ, an important transcription factor that controls key differentiation genes, to inhibit cell proliferation (116,117). However, later studies have shown that the triterpenoids can actually affect growth inhibition *via* both PPARγ-dependent and independent mechanisms (119).

1.9.3   *Triterpenoids and anti-inflammation*

Inflammation is a biological response that is triggered by the body as a defense mechanism when faced with foreign and/or harmful stimuli, the stimulation of cytokine release, an increase in oxidative stress, or tissue injury. In response to these stimuli, the nuclear factor kappa B (NF-κB) signaling pathway is activated. In resting cells, NF-κB, a transcription factor that is important in regulating cell survival and immune responses, is sequestered by the IkappaB alpha (IκBα) inhibitory protein, which prevents NF-κB from translocating to the nucleus. However, when the signaling pathway is activated by

upstream enzymes, IκBα is phosphorylated by Ikappa Kinase (IκKα/β) and is targeted

for ubiquitination, leading to its release from NF-κB, thereby rendering the transcription

factor active. The free NF-κB dimer can then be phosphorylated and be translocated into

the nucleus to induce the transcription of pro-inflammatory genes such as iNOS,

cyclooxygenase (COX2) and tumor necrosis factor alpha (TNFα), in order to trigger the

immune response and initiate tissue repair (121). Although inflammation is a critical

process in wound healing and infection, chronic inflammation can be associated with

numerous diseases including cancer. In fact, it is estimated that underlying infections and

inflammatory reactions are linked to 15-20% of all cancer deaths. It is also evident in

numerous studies that inflammation helps with the initiation and progression of cancers

and is an important facilitator of the tumor microenvironment (122).

Synthetic triterpenoids have been shown to effectively suppress the induction of

iNOS and COX2 in primary macrophages when stimulated with different pro-

inflammatory molecules including IFNγ, TNFα, interleukin (IL)-1β and

lipopolysaccharides (LPS), block the *de novo* synthesis of COX2 in colon myofibroblasts

stimulated with IL-1β and inhibit the inflammatory and anti-apoptotic cytokine, IL6.

(109). In addition, triterpenoids have also been shown to suppress the production of these

pro-inflammatory molecules, which are often expressed in excess in tumor cells (89).

The anti-inflammatory properties of the triterpenoids are evident in both *in vivo* models

and in clinical trials (120,123). For instance, CDDO-Me elicits its anti-inflammatory

properties in response to lipopolysaccharides (LPS) challenge *in vivo* (123) and

suppresses the expression of vascular endothelial growth factor (VEGF), matrix metalloproteinase (MMP)9, tumor necrosis factor (TNF), IL-8 and IL-10 (124).

1.9.4   Triterpenoids and cytoprotection

In the event of oxidative stress and/or exposure to stress-related stimuli, cells can also activate the Nuclear factor erythrocyte 2-related factor 2 (Nrf2) signaling pathway as a cytoprotective mechanism. The Nrf2 signaling pathway functions very similarly to the NF-κβ signaling pathway in that Nrf2 is also held in its inhibitory position by KEAP1, a protein that have been shown to be an oxidative stress sensor and, when bound to Nrf2, targets it for ubiquitination and proteasomal degradation. However, under oxidative stress, KEAP1 releases Nrf2, enabling it to translocate into the nucleus and form heterodimers with small musculoaponeurotic fibosarcoma (Maf) proteins. The formation of this complex then recognizes and binds to the anti-oxidant responsive element (ARE) sequences and induce the transcription of phase-2 detoxifying enzymes or anti-oxidant genes (132). Since the triterpenoids have a profound effect on inflammation in tumor cells by affecting the NF-κβ pathway (which is linked to the Nrf2) (133), it is expected that the triterpenoids may also elicit some positive effect on tumor cells by modulating Nrf2 activity. Consistent with this hypothesis, numerous research studies have shown that the triterpenoids induce the Nrf2 pathway. Specifically, Liby and colleagues have shown that CDDO-Im is a potent inducer of heme-oxygenase-1 (HO-1) Nrf2/ARE signaling by increasing Nrf2 expression in monocytic U937 leukemia cells (134). Subsequent studies went on to show that CDDO-Im could increase nuclear accumulation

of Nrf2 proteins in peripheral blood mononuclear cells and in neutrophils (135). The potent cytoprotective activities mediated by the triterpenoids are shown in different cells originated from different tissues including liver, lung, small intestine mucosa, and cerebral cortex (137).

1.9.5   Triterpenoids and apoptosis

Apoptosis is the process in which cells undergo programmed cell death in response to different stimuli in order to control for cellular damage or allow for overall cellular homeostasis. The extrinsic apoptotic pathway involves the binding of death receptor (DR) ligands to death receptors at the membrane surface while the intrinsic pathway involves targeting the mitochrondria and inducing the release of pro-apopototic factors to the cytosol in response to intracellular stress signals (138).   Despite the different means of activation, the downstream effects of these two pathways eventually converge into the activation of caspases, which are cysteinyl aspartate-specific proteases that play a key role in executing the apoptosis process.

In the intrinsic pathway, apoptosis is commonly triggered within the cells by different stimuli ranging from UV radiation, DNA damage, hypoxia, cytoskeleton disruption, loss of adhesion or growth factor withdrawal, loss of survival signals, or endoplasmic reticulum stress (138,139).   As a result of these stress stimuli, the permeability of the outer mitochondrial membrane is increased, leading to the release of pro-apoptotic factors such as cytochrome C into the cytoplasm. The release of these pro-

apoptotic factors leads to the formation of an apoptosome, which works similarly to the death-inducing signaling complex (DISC) in the extrinsic pathway to recruit and facilitate the activation of pro-caspase 9. It is interesting to note that crosstalk does exist between the intrinsic and extrinsic pathway. For example, caspase 8 from the extrinsic pathway can cleave BH3 interacting-domain agonist (Bid), a pro-apoptotic Bcl-2 family protein and activate the intrinsic mitochrondrial apoptosis pathway (138).

At concentrations of 1-5 μM, CDDO and its derivatives have been shown to induce apoptosis in numerous cancer cells including human acute myeloid leukemia (112,142), multiple myeloma (143), chronic lymphocytic leukemia (144), lung cancer (145,146), breast cancer (147), prostate cancer (148), ovarian cancer (149), and osteosarcoma (112). Specifically, studies have shown that triterpenoids are effective in inducing apoptosis *via* both the intrinsic and extrinsic apoptotic pathways. Triterpenoids have been shown to induce TRAIL-dependent apoptosis by upregulating DRs, TRAIL receptor 1 and TRAIL receptor 2 (142,145-150), inhibiting cFLIP, (144-147,149) and activating caspase 3, caspase 8, and caspase 9 (148,151,152,153). Although caspases are critical players in apoptosis, it is important to note that the triterpenoids do not only act on caspases to induce apoptosis.

In addition, other studies have shown that the triterpenoids can play an important role on different pro-apoptotic factors to trigger apoptosis. For example, the cleavage of Bid and the translocation of Bcl-2-associated X protein (Bax) to the mitochrondria (148,151) as well as the release of cytochrome-c and apoptosis-inducing factor (AIF) from the mitochrondria (148,149,152,153) are induced by triterpenoids.

CDDO has also been shown to reduce glutathione (GSH) and in some cases, increase ROS levels (156). GSH is an important peptide that, in its reduced state, can neutralize ROS by donating an electron to other unstable molecules in the system. Therefore, it may seem counter-intuitive that triterpenoids reduce the amount of glutathione, a protective antioxidant in the body. However, studies have shown that synthetic triterpenoids are not toxic to normal cells such as lymphocytes harvested from the same patient or from healthy volunteers (143,144,157,158). This selective apoptosis in cancer cells may result from higher endogenous levels of oxidative stress that exists in transformed cells. In these tumor cells that are already under oxidative stress, triterpenoids provide the additional production of ROS required to destroy the tumor cells by apoptosis (79).

Since the triterpenoids are multi-functional compounds, CDDO and its derivatives are inevitably also going to induce the apoptosis cascade by targeting other signaling pathways, which also ultimately result in programmed cell death. For instance, CDDO-Me have been shown to activate the c-Jun-NH_2-terminal kinase (JNK) *via* coupling with endoplasmic reticulum (ER) stress and depleting intracellular GSH as well as increasing ROS levels. As a result, activated JNK causes the upregulation of DR expression, which triggers apoptosis in leukemia cells (153,156,159). Konopleva and colleagues have also indicated that CDDO-Me can induce the phosphorylation of p38 in U-937 leukemia cells to induce apoptosis (143,160). Therefore, both JNK and p38 play a crucial role in apoptosis in response to stress stimuli. Interestingly, CDDO has also been shown to increase $[Ca^{2+}]_{cytosol}$ in the ER in a time and dose-dependent manner in numerous

carcinoma cells including colon, breast and lung (161). The ER and mitochrondria play essential roles in intracellular calcium homeostasis, and the disruption and/or sustained elevation in $[Ca^{2+}]_{cytosol}$ can lead to apoptotic cell death by activating calcium-dependent enzymes and caspase 12, which can in turn activate other caspases in both the intrinsic and extrinsic apoptotic pathways (162,163). Therefore, Hail and his colleagues have provided yet another role for CDDO in inducing apoptosis by targeting the intracellular calcium levels. Furthermore, the triterpenoids have been shown to play a role in cell death by targeting GSK. Specifically, CDDO-Me has been shown to induce the phosphorylation of GSK3β at serine 9; thereby, inhibiting its activity. The data suggested that the inactivation of GSK3 induced by the synthetic triterpenoid could help trigger tumor cell death by reducing the apoptotic threshold and increasing the apoptotic potential of prostate cancer cells that were previously resistant to cell death (165).

In addition, synthetic triterpenoids target proteins that can modulate the transcription of target genes that are important for apoptosis. For instance, CDDO can directly inhibit IKKβ, an upstream enzyme that regulates NF-κB. NF-κB is a transcription factor that is involved in the regulation of many physiological processes including apoptosis. Yore and colleagues have shown that, CDDO-Im directly interacts with IKKβ and prevents its phosphorylation and degradation in response to TNFα. As a result, NF-κB remains inhibited, which consequently leads to decreased expression of numerous anti-apoptotic proteins including Bcl2, Bcl-X$_l$ and XIAP (85,152). In addition, numerous studies have provided convincing evidence that CDDO-Im and CDDO-Me can target signal transducer and activator of transcription3 (STAT3) to induce

apoptosis in numerous cancer cells. STAT3 is a DNA binding protein that is also involved in modulating the transcription of genes that are involved in cell differentiation, proliferation, apoptosis, angiogenesis, immune response, and tumor metastasis. The constitutive activation of STAT3 has been associated with numerous cancers including leukemia, myeloma, osteosarcoma, and cancer of the ovaries, lungs, breast, prostate and head and neck (166). More importantly, it leads to poor prognosis as it can activate genes that block apoptosis, increase proliferation and survival, as well as promote angiogenesis and metastasis while inhibiting anti-tumor immune responses (166). In numerous cancer cell culture studies, CDDO-Im and CDDO-Me have been shown to significantly reduce the level of nuclear translocation and phosphorylation of STAT3. As a result, the inhibition of STAT3 signaling pathway leads to the suppression of several anti-apoptotic STAT3 responsive genes such as Bcl-X$_l$, survivin and Myeloid cell leukemia 1 (MCL-1) in both normal cancer and multi-drug resistance cancer models. As such, CDDO-Me can also block the activation of Janus kinase (JAK), Src and Akt, all of which are upstream targets of STAT3 activation, indicating that synthetic triterpenoids can inactivate STAT3 via affecting multiple signaling pathways (167-171).

Finally, the synthetic triterpenoids have also been shown to induce autophagy, which is known as programmed cell death II. Programmed cell death II is a pathway whereby the endolysosomal system is recruited to digest intracellular components as a survival mechanism in the case of nutrient deprivation. However, it has also been implicated as another means by which cancer cells undergo cell death after a series of chemotherapeutic insults. CDDO-Me has been shown to induce autophagic cell death in

chronic myeloid leukemia cells by affecting the metabolism and function of the mitochrondria. As a result, cells undergo rapid autophagocytosis or externalization of phosphatidylserine (172).

1.9.6   Triterpenoids and tumor angiogenesis

Angiogenesis is the process whereby networks of new blood vessels are developed in order for organ growth and repair and development to occur. However, in the case of carcinogenesis, a pre-vascularized tumor can rely on simple diffusion to obtain the nutrients required to sustain its growth. However, as the tumor gets larger, the proliferation of blood vessels is crucial for supplying oxygen and nutrients in order to facilitate its further development. This growth acts as a precursor for tumor metastasis as cancer cells now have the means to travel from the original site of the tumor and disseminate to other parts in the body.

Since angiogenesis is a crucial player in tumorigenesis, studies have focused on the role of triterpenoids on angiogenesis. Recent work has shown that CDDO and its derivatives are potent and effective agents for the suppression of angiogenesis in *in vivo* models and in cell cultures studies. For instance, CDDO-Me effectively blocks angiogenesis that was induced when liquid Matrigel composed of angiogenic factors such as VEGF and TNFα was mixed with Kaposi's sarcoma cells and injected into immuno-compromised mice followed by triterpenoid treatment (173). In studies examining the role of synthetic triterpenoids on liver metastasis, Deeb and colleagues found that CDDO

effectively reduces the number of blood vessels, and hence the density of blood vessel network in prostatic cancer tissue (174). Moreover, CDDO-Me has been shown to inhibit the growth of human umbilical vein endothelial cells (hUVEC) in monolayer cultures and to suppress endothelial cell tubulogenesis in three-dimensional Matrigel cultures but at a higher concentration compared to the *in vivo* studies. Specifically in cell culture studies using hUVECs, the triterpenoids can inhibit VEGF-induced activation of the extracellular signal-regulated kinase ERK1/2 pathway (175). As mentioned previously, CDDO was also found to prevent NF-κB translocation into the nucleus by inhibiting the phosphorylation of its binding partner, IKKα; this inhibition could in turn prevent the transcription of numerous downstream angiogenesis-related genes such as COX2, VEGF, and MMP-9 (176).

1.10   TRITERPENOID INTERACTIONS WITH OTHER PROTEINS

Since cancer is composed of diseases driven by different mutations, chemotherapeutic agents are often most effective when given in combination. The rationale for combination chemotherapy stems from the fact that different signaling pathways may be altered in cancer, and a combination of drugs that target these pathways may prevent cells from developing chemo-resistance.

Triterpenoids have been shown to work synergistically with proteins or ligands present in the cell to enhance their anti-cancer effects. For example, CDDO can synergize with TGFβ and enhance TGFβ/Smad-mediated signaling by increasing TGFβ−dependent

gene expression, prolonging the activation of Smad2 and reversing the inhibitory role of Smad7, suggesting a potential role of CDDO in the treatment or prevention of diseases with aberrant TGFβ function (177). Moreover, CDDO has been shown to induce apoptosis partially *via* a PPARγ-dependent mechanism. In addition, when used in combination with TRAIL, CDDO-Me has been shown to be able to overcome the resistance to TRAIL-induced apoptosis that lung cancer cells had previously developed.

Since triterpenoids inhibit many cancer-promoting activities, research has been conducted to examine the use of these compounds in combination with other therapeutic compounds. As expected, triterpenoids have shown to have synergistic effects when used in combination with different inhibitors. For instance, FLT3-receptor tyrosine kinase mutations consisting of internal tandem duplications (ITD) can lead to the constitutive autophosphorylation of the receptor in leukemia cell lines (178). This mutation occurs frequently in patients with acute myeloid leukemia and has been associated with higher incidence of early relapse and shorter survival time compared to those without this mutation (179). Studies have shown that PKC412, a FLT3-tyrosine kinase inhibitor, can inhibit the autophosphorylation of the receptor while CDDO-Me can block the translocation of NF-κB into the nucleus, inhibit STAT3 signaling and induce caspase-3-dependent apoptosis in these cell lines (178). However, when the PKC412 inhibitor was used simultaneously with CDDO-Me, the synergistic anti-proliferative effects on cells with FLT3/ITD3 mutation were apparent (178). Therefore, even though PKC412 and CDDO-Me target different signaling pathways, they work well together to target leukemia. Similarly, CDDO-Im also produces synergistic effects in liposarcoma, a rare

class of mesenchymal tumor that is characterized by an overexpression of fatty acid synthase (FAS) and is often unresponsive to chemotherapy (180). Specifically, CDDO-Im can inhibit FAS mRNA expression, affect gene promoter activity, block FAS protein production and induce apoptosis while Cerulenin, a FAS inhibitor, works to inhibit FAS activity in liposarcoma tissues and cell lines. Interestingly, when cells were treated with both CDDO-Im and Cerulenin, a synergistic cytotoxic effect was observed whereby CDDO-Im treated cells could increase their sensitivity towards Cerulenin, indicating that triterpenoids function to enhance the efficacy of other compounds when used simultaneously (180). Consistent with these studies, the rexinoid LG100268 and CDDO-Me also exert similar synergistic effects on tumor burden in *in vivo* breast cancer models by targeting different signaling pathways (181). CDDO-Me is a powerful agent that can block constitutive phosphorylation of STAT3 and the degradation of IKBα in ER-negative breast cancer cells (181). While LG100268 also blocks IKBα degradation, it is also a potent agent that can trigger the release of IL-6 in RAW264.7 macrophage-like cells, inhibit the ability of endothelial cells to organize into networks and block angiogenesis *in vivo* (181). However, when used in combination, LG100268 and CDDO-Me are significantly more potent at preventing the formation of ER-negative breast tumors compared to LG1000268 or CDDO-Me alone (181).

Perhaps, the most interesting fact about the triterpenoids is their ability to not only work synergistically with other ligands and inhibitors to elicit a positive effect in cancer cells but also function synergistically with other inhibitors to overcome the chemoresistance that tumor cells may have acquired from conventional chemotherapy

(157). As such, CDDO-Im and PS341 can work together to overcome the cytoprotective effects that anti-apoptotic proteins may have as well as NF-κB-related drug resistance (157). This synergistic effect is observed even in bortezomib-resistant multiple myeloma cells, providing a potential means to improve the outcome of patients with this disease. From *in vivo* studies, the combination of CDDO-Im and TRAIL treatment was well tolerated and was able to effectively reduce tumor burden in an MDA-MB468 tumor xenograft model (147).

1.11   RATIONALE AND HYPOTHESIS

Cell migration is a complex process that involves many structural proteins, signaling molecules and transcriptional factors. Extensive research over the past few decades has been carried out to identify how multiple signaling pathways converge into a self-regulating network for cell migration. It is also abundantly clear that tumorigenesis and cancer metastasis are dependent on cell migration. Therefore, it is important to further our understanding of cell migration and examine how it can contribute to tumorigenesis. Although there is substantial evidence that triterpenoids can induce apoptosis and cell differentiation and exert anti-proliferative effects on tumor cells, there are very limited data that explains the role of triterpenoids on metastasis. In particular, prior to my thesis work, there were no studies that focused on how triterpenoids affect cell migration, an important precursor event to cancer metastasis.

Therefore, the overall objective of this thesis is to understand the molecular biology of triterpenoids and their role in cell migration. Specifically, I would like to:

1) Examine the role of CDDO-Im on cell migration

2) Identify proteins that interact with triterpenoids to mediate their influence on cell migration

3) Manipulate triterpenoid-binding proteins to understand their involvement in cell migration

Given that triterpenoids are multi-functional compounds that can target different cellular processes and the fact that Couch *et al*. have shown that triterpenoids can bind to β-tubulin and affect microtubule dynamics (83), we hypothesize that triterpenoids will inhibit cell migration by affecting the cytoskeletal network and the associated proteins that regulate its dynamics.

1.12 REFERENCES

1. Ridley, A. J. (2011) *Cell* **145**, 1012-1022

2. Akhmanova, A., and Steinmetz, M. O. (2008) *Nat Rev Mol Cell Biol* **9**, 309-322

3. Watanabe, T., Noritake, J., and Kaibuchi, K. (2005) *Trends Cell Biol* **15**, 76-83

4. Le Clainche, C., and Carlier, M. F. (2008) *Physiol Rev* **88**, 489-513

5. Gournier, H., Goley, E. D., Niederstrasser, H., Trinh, T., and Welch, M. D. (2001) *Mol Cell* **8**, 1041-1052

6. Mullins, R. D., Heuser, J. A., and Pollard, T. D. (1998) *Proc Natl Acad Sci U S A* **95**, 6181-6186

7. Amann, K. J., and Pollard, T. D. (2001) *Nat Cell Biol* **3**, 306-310

8. Blanchoin, L., Amann, K. J., Higgs, H. N., Marchand, J. B., Kaiser, D. A., and Pollard, T. D. (2000) *Nature* **404**, 1007-1011

9. Boujemaa-Paterski, R., Gouin, E., Hansen, G., Samarin, S., Le Clainche, C., Didry, D., Dehoux, P., Cossart, P., Kocks, C., Carlier, M. F., and Pantaloni, D. (2001) *Biochemistry* **40**, 11390-11404

10. Pantaloni, D., Boujemaa, R., Didry, D., Gounon, P., and Carlier, M. F. (2000) *Nat Cell Biol* **2**, 385-391

11. Egile, C., Rouiller, I., Xu, X. P., Volkmann, N., Li, R., and Hanein, D. (2005) *PLoS Biol* **3**, e383

12. Goode, B. L., and Eck, M. J. (2007) *Annu Rev Biochem* **76**, 593-627

13. Aranda, V., Nolan, M. E., and Muthuswamy, S. K. (2008) *Oncogene* **27**, 6878-6887

14. Assemat, E., Bazellieres, E., Pallesi-Pocachard, E., Le Bivic, A., and Massey-Harroche, D. (2008) *Biochim Biophys Acta* **1778**, 614-630

15. Iden, S., and Collard, J. G. (2008) *Nat Rev Mol Cell Biol* **9**, 846-859

16. Bose, R., and Wrana, J. L. (2006) *Curr Opin Cell Biol* **18**, 206-212

17. Lin, D., Edwards, A. S., Fawcett, J. P., Mbamalu, G., Scott, J. D., and Pawson, T. (2000) *Nat Cell Biol* **2**, 540-547

18. Ranganathan, R., and Ross, E. M. (1997) *Curr Biol* **7**, R770-773

19. Kim, S. K. (2000) *Nat Cell Biol* **2**, E143-145

20. Izumi, Y., Hirose, T., Tamai, Y., Hirai, S., Nagashima, Y., Fujimoto, T., Tabuse, Y., Kemphues, K. J., and Ohno, S. (1998) *J Cell Biol* **143**, 95-106

21. Chen, X., and Macara, I. G. (2006) *Methods Enzymol* **406**, 362-374

22. Pellettieri, J., and Seydoux, G. (2002) *Science* **298**, 1946-1950

23. Joberty, G., Petersen, C., Gao, L., and Macara, I. G. (2000) *Nat Cell Biol* **2**, 531-539

24. Suzuki, A., and Ohno, S. (2006) *J Cell Sci* **119**, 979-987

25. Etienne-Manneville, S., and Hall, A. (2003) *Nature* **421**, 753-756

26. Jiang, W., Betson, M., Mulloy, R., Foster, R., Levay, M., Ligeti, E., and Settleman, J. (2008) *J Biol Chem* **283**, 20978-20988

27. ten Dijke, P., and Hill, C. S. (2004) *Trends Biochem Sci* **29**, 265-273

28. Schmierer, B., and Hill, C. S. (2007) *Nat Rev Mol Cell Biol* **8**, 970-982

29. Le Roy, C., and Wrana, J. L. (2005) *Nature reviews* **6**, 112-126

30. Ozdamar, B., Bose, R., Barrios-Rodiles, M., Wang, H. R., Zhang, Y., and Wrana, J. L. (2005) *Science* **307**, 1603-1609

31. Wang, H. R., Zhang, Y., Ozdamar, B., Ogunjimi, A. A., Alexandrova, E., Thomsen, G. H., and Wrana, J. L. (2003) *Science* **302**, 1775-1779

32. Pegtel, D. M., Ellenbroek, S. I., Mertens, A. E., van der Kammen, R. A., de Rooij, J., and Collard, J. G. (2007) *Curr Biol* **17**, 1623-1634

33. Fukata, M., Kuroda, S., Fujii, K., Nakamura, T., Shoji, I., Matsuura, Y., Okawa, K., Iwamatsu, A., Kikuchi, A., and Kaibuchi, K. (1997) *J Biol Chem* **272**, 29579-29583

34. White, C. D., Erdemir, H. H., and Sacks, D. B. (2012) *Cell Signal* **24**, 826-34

35. Pelikan-Conchaudron, A., Le Clainche, C., Didry, D., and Carlier, M. F. (2011) *J Biol Chem* **286**, 35119-35128

36. Le Clainche, C., Schlaepfer, D., Ferrari, A., Klingauf, M., Grohmanova, K., Veligodskiy, A., Didry, D., Le, D., Egile, C., Carlier, M. F., and Kroschewski, R. (2007) *J Biol Chem* **282**, 426-435

37.   Fukata, M., Watanabe, T., Noritake, J., Nakagawa, M., Yamaga, M., Kuroda, S., Matsuura, Y., Iwamatsu, A., Perez, F., and Kaibuchi, K. (2002) *Cell* **109**, 873-885

38.   Watanabe, T., Noritake, J., Kakeno, M., Matsui, T., Harada, T., Wang, S., Itoh, N., Sato, K., Matsuzawa, K., Iwamatsu, A., Galjart, N., and Kaibuchi, K. (2009) *J Cell Sci* **122**, 2969-2979

39.   Watanabe, T., Wang, S., Noritake, J., Sato, K., Fukata, M., Takefuji, M., Nakagawa, M., Izumi, N., Akiyama, T., and Kaibuchi, K. (2004) *Dev Cell* **7**, 871-883

40.   Parsons, J. T., Horwitz, A. R., and Schwartz, M. A. (2010) *Nat Rev Mol Cell Biol* **11**, 633-643

41.   Izzard, C. S., and Lochner, L. R. (1980) *J Cell Sci* **42**, 81-116

42.   Gardel, M. L., Schneider, I. C., Aratyn-Schaus, Y., and Waterman, C. M. (2010) *Annu Rev Cell Dev Biol* **26**, 315-333

43.   Zaidel-Bar, R., Itzkovitz, S., Ma'ayan, A., Iyengar, R., and Geiger, B. (2007) *Nat Cell Biol* **9**, 858-867

44.   Ilic, D., Furuta, Y., Kanazawa, S., Takeda, N., Sobue, K., Nakatsuji, N., Nomura, S., Fujimoto, J., Okada, M., and Yamamoto, T. (1995) *Nature* **377**, 539-544

45.   Mitra, S. K., Hanson, D. A., and Schlaepfer, D. D. (2005) *Nat Rev Mol Cell Biol* **6**, 56-68

46.   Tomar, A., and Schlaepfer, D. D. (2009) *Curr Opin Cell Biol* **21**, 676-683

47.   Zhao, X., and Guan, J. L. (2011) *Adv Drug Deliv Rev* **63**, 610-615

48.   Schwock, J., Dhani, N., and Hedley, D. W. (2010) *Expert Opin Ther Targets* **14**, 77-94

49.   Deramaudt, T. B., Dujardin, D., Hamadi, A., Noulet, F., Kolli, K., De Mey, J., Takeda, K., and Ronde, P. (2011) *Mol Biol Cell* **22**, 964-975

50.   Ezratty, E. J., Partridge, M. A., and Gundersen, G. G. (2005) *Nat Cell Biol* **7**, 581-590

51.   Bianchi, M., De Lucchini, S., Marin, O., Turner, D. L., Hanks, S. K., and Villa-Moruzzi, E. (2005) *Biochem J* **391**, 359-370

52.   Woodgett, J. R. (1990) *EMBO J* **9**, 2431-2438

53.   Gillespie, J. R., Ulici, V., Dupuis, H., Higgs, A., Dimattia, A., Patel, S., Woodgett, J. R., and Beier, F. (2011) *Endocrinology* **152**, 1755-1766

54.   Hoeflich, K. P., Luo, J., Rubie, E. A., Tsao, M. S., Jin, O., and Woodgett, J. R. (2000) *Nature* **406**, 86-90

55.   Cho, J., Rameshwar, P., and Sadoshima, J. (2009) *J Biol Chem* **284**, 36647-36658

56.   Zhao, Y., Altman, B. J., Coloff, J. L., Herman, C. E., Jacobs, S. R., Wieman, H. L., Wofford, J. A., Dimascio, L. N., Ilkayeva, O., Kelekar, A., Reya, T., and Rathmell, J. C. (2007) *Mol Cell Biol* **27**, 4328-4339

57.   Ruel, L., Bourouis, M., Heitzler, P., Pantesco, V., and Simpson, P. (1993) *Nature* **362**, 557-560

58.   Markou, T., Cullingford, T. E., Giraldo, A., Weiss, S. C., Alsafi, A., Fuller, S. J., Clerk, A., and Sugden, P. H. (2008) *Cell Signal* **20**, 206-218

59.   Patel, S., Doble, B. W., MacAulay, K., Sinclair, E. M., Drucker, D. J., and Woodgett, J. R. (2008) *Mol Cell Biol* **28**, 6314-6328

60.   Doble, B. W., Patel, S., Wood, G. A., Kockeritz, L. K., and Woodgett, J. R. (2007) *Dev Cell* **12**, 957-971

61.   Matsuda, T., Zhai, P., Maejima, Y., Hong, C., Gao, S., Tian, B., Goto, K., Takagi, H., Tamamori-Adachi, M., Kitajima, S., and Sadoshima, J. (2008) *Proc Natl Acad Sci U S A* **105**, 20900-20905

62.   Liang, M. H., and Chuang, D. M. (2006) *J Biol Chem* **281**, 30479-30484

63.   Force, T., and Woodgett, J. R. (2009) *J Biol Chem* **284**, 9643-9647

64.   Ciaraldi, T. P., Oh, D. K., Christiansen, L., Nikoulina, S. E., Kong, A. P., Baxi, S., Mudaliar, S., and Henry, R. R. (2006) *Am J Physiol Endocrinol Metab* **291**, E891-898

65.   MacAulay, K., Doble, B. W., Patel, S., Hansotia, T., Sinclair, E. M., Drucker, D. J., Nagy, A., and Woodgett, J. R. (2007) *Cell Metab* **6**, 329-337

66.   Dajani, R., Fraser, E., Roe, S. M., Young, N., Good, V., Dale, T. C., and Pearl, L. H. (2001) *Cell* **105**, 721-732

67.   ter Haar, E., Coll, J. T., Austen, D. A., Hsiao, H. M., Swenson, L., and Jain, J. (2001) *Nat Struct Biol* **8**, 593-596

68.   Thomas, G. M., Frame, S., Goedert, M., Nathke, I., Polakis, P., and Cohen, P. (1999) *FEBS Lett* **458**, 247-251

69.   Sun, T., Rodriguez, M., and Kim, L. (2009) *Dev Growth Differ* **51**, 735-742

70.   Kobayashi, T., Hino, S., Oue, N., Asahara, T., Zollo, M., Yasui, W., and Kikuchi, A. (2006) *Mol Cell Biol* **26**, 898-911

71.   Cai, X., Li, M., Vrana, J., and Schaller, M. D. (2006) *Mol Cell Biol* **26**, 2857-2868

72.   Phillips, D. R., Rasbery, J. M., Bartel, B., and Matsuda, S. P. (2006) *Curr Opin Plant Biol* **9**, 305-314

73.   Singh, G. B., Singh, S., Bani, S., Gupta, B. D., and Banerjee, S. K. (1992) *J Pharm Pharmacol* **44**, 456-458

74.   Nishino, H., Nishino, A., Takayasu, J., Hasegawa, T., Iwashima, A., Hirabayashi, K., Iwata, S., and Shibata, S. (1988) *Cancer Res* **48**, 5210-5215

75.   Liu, J. (2005) *J Ethnopharmacol* **100**, 92-94

76.   Suh, N., Honda, T., Finlay, H. J., Barchowsky, A., Williams, C., Benoit, N. E., Xie, Q. W., Nathan, C., Gribble, G. W., and Sporn, M. B. (1998) *Cancer Res* **58**, 717-723

77.   Honda, T., Rounds, B. V., Bore, L., Finlay, H. J., Favaloro, F. G., Jr., Suh, N., Wang, Y., Sporn, M. B., and Gribble, G. W. (2000) *J Med Chem* **43**, 4233-4246

78.   Honda, T., Honda, Y., Favaloro, F. G., Jr., Gribble, G. W., Suh, N., Place, A. E., Rendi, M. H., and Sporn, M. B. (2002) *Bioorg Med Chem Lett* **12**, 1027-1030

79.   Liby, K. T., Yore, M. M., and Sporn, M. B. (2007) *Nat Rev Cancer* **7**, 357-369

80.   Petronelli, A., Pannitteri, G., and Testa, U. (2009) *Anticancer Drugs* **20**, 880-892

81.   Wang, Y., Porter, W. W., Suh, N., Honda, T., Gribble, G. W., Leesnitzer, L. M., Plunket, K. D., Mangelsdorf, D. J., Blanchard, S. G., Willson, T. M., and Sporn, M. B. (2000) *Mol Endocrinol* **14**, 1550-1556

82.   Dinkova-Kostova, A. T., Liby, K. T., Stephenson, K. K., Holtzclaw, W. D., Gao, X., Suh, N., Williams, C., Risingsong, R., Honda, T., Gribble, G. W., Sporn, M. B., and Talalay, P. (2005) *Proc Natl Acad Sci U S A* **102**, 4584-4589

83.   Couch, R. D., Ganem, N. J., Zhou, M., Popov, V. M., Honda, T., Veenstra, T. D., Sporn, M. B., and Anderson, A. C. (2006) *Mol Pharmacol* **69**, 1158-1165

84.   Ahmad, R., Raina, D., Meyer, C., Kharbanda, S., and Kufe, D. (2006) *J Biol Chem* **281**, 35764-35769

85.   Yore, M. M., Liby, K. T., Honda, T., Gribble, G. W., and Sporn, M. B. (2006) *Mol Cancer Ther* **5**, 3232-3239

86.   To, C., Shilton, B. H., and Di Guglielmo, G. M. (2010) *J Biol Chem* **285**, 27944-27957

87.   Yore, M. M., Kettenbach, A. N., Sporn, M. B., Gerber, S. A., and Liby, K. T. (2011) *PLoS One* **6**, e22862

88.   Yang, L., Calingasan, N. Y., Thomas, B., Chaturvedi, R. K., Kiaei, M., Wille, E. J., Liby, K. T., Williams, C., Royce, D., Risingsong, R., Musiek, E. S., Morrow, J. D., Sporn, M., and Beal, M. F. (2009) *PLoS One* **4**, e5757

89.   Tran, T. A., McCoy, M. K., Sporn, M. B., and Tansey, M. G. (2008) *J Neuroinflammation* **5**, 14

90.   Stack, C., Ho, D., Wille, E., Calingasan, N. Y., Williams, C., Liby, K., Sporn, M., Dumont, M., and Beal, M. F. (2010) *Free Radic Biol Med* **49**, 147-158

91.   Dumont, M., Wille, E., Calingasan, N. Y., Tampellini, D., Williams, C., Gouras, G. K., Liby, K., Sporn, M., Nathan, C., Flint Beal, M., and Lin, M. T. (2009) *J Neurochem* **109**, 502-512

92.   Segal, B. H., Han, W., Bushey, J. J., Joo, M., Bhatti, Z., Feminella, J., Dennis, C. G., Vethanayagam, R. R., Yull, F. E., Capitano, M., Wallace, P. K., Minderman, H., Christman, J. W., Sporn, M. B., Chan, J., Vinh, D. C., Holland, S. M., Romani, L. R., Gaffen, S. L., Freeman, M. L., and Blackwell, T. S. (2010) *PLoS One* **5**, e9631

93.   Nichols, D. P., Ziady, A. G., Shank, S. L., Eastman, J. F., and Davis, P. B. (2009) *Am J Physiol Lung Cell Mol Physiol* **297**, L828-836

94.   Ferguson, H. E., Thatcher, T. H., Olsen, K. C., Garcia-Bates, T. M., Baglole, C. J., Kottmann, R. M., Strong, E. R., Phipps, R. P., and Sime, P. J. (2009) *Am J Physiol Lung Cell Mol Physiol* **297**, L912-919

95.   Ferguson, H. E., Kulkarni, A., Lehmann, G. M., Garcia-Bates, T. M., Thatcher, T. H., Huxlin, K. R., Phipps, R. P., and Sime, P. J. (2009) *Am J Respir Cell Mol Biol* **41**, 722-730

96.   Kulkarni, A. A., Thatcher, T. H., Olsen, K. C., Maggirwar, S. B., Phipps, R. P., and Sime, P. J. (2011) *PLoS One* **6**, e15909

97.   Reddy, N. M., Suryanaraya, V., Yates, M. S., Kleeberger, S. R., Hassoun, P. M., Yamamoto, M., Liby, K. T., Sporn, M. B., Kensler, T. W., and Reddy, S. P. (2009) *Am J Respir Crit Care Med* **180**, 867-874

98.   Pitha-Rowe, I., Liby, K., Royce, D., and Sporn, M. (2009) *Invest Ophthalmol Vis Sci* **50**, 5339-5347

99.   Wei, Y., Gong, J., Yoshida, T., Eberhart, C. G., Xu, Z., Kombairaju, P., Sporn, M. B., Handa, J. T., and Duh, E. J. (2011) *Free Radic Biol Med* **51**, 216-224

100.   Sussan, T. E., Rangasamy, T., Blake, D. J., Malhotra, D., El-Haddad, H., Bedja, D., Yates, M. S., Kombairaju, P., Yamamoto, M., Liby, K. T., Sporn, M. B., Gabrielson, K. L., Champion, H. C., Tuder, R. M., Kensler, T. W., and Biswal, S. (2009) *Proc Natl Acad Sci U S A* **106**, 250-255

101.   Ichikawa, T., Li, J., Meyer, C. J., Janicki, J. S., Hannink, M., and Cui, T. (2009) *PLoS One* **4**, e8391

102.   Osburn, W. O., Yates, M. S., Dolan, P. D., Chen, S., Liby, K. T., Sporn, M. B., Taguchi, K., Yamamoto, M., and Kensler, T. W. (2008) *Toxicol Sci* **104**, 218-227

103.   Reisman, S. A., Buckley, D. B., Tanaka, Y., and Klaassen, C. D. (2009) *Toxicol Appl Pharmacol* **236**, 109-114

104.   Yates, M. S., Kwak, M. K., Egner, P. A., Groopman, J. D., Bodreddigari, S., Sutter, T. R., Baumgartner, K. J., Roebuck, B. D., Liby, K. T., Yore, M. M., Honda, T., Gribble, G. W., Sporn, M. B., and Kensler, T. W. (2006) *Cancer Res* **66**, 2488-2494

105.   Aleksunes, L. M., Goedken, M. J., Rockwell, C. E., Thomale, J., Manautou, J. E., and Klaassen, C. D. (2010) *J Pharmacol Exp Ther* **335**, 2-12

106.   Tanaka, Y., Aleksunes, L. M., Goedken, M. J., Chen, C., Reisman, S. A., Manautou, J. E., and Klaassen, C. D. (2008) *Toxicol Appl Pharmacol* **231**, 364-373

107.   Saha, P. K., Reddy, V. T., Konopleva, M., Andreeff, M., and Chan, L. (2010) *J Biol Chem* **285**, 40581-40592

108.   Shin, S., Wakabayashi, J., Yates, M. S., Wakabayashi, N., Dolan, P. M., Aja, S., Liby, K. T., Sporn, M. B., Yamamoto, M., and Kensler, T. W. (2009) *Eur J Pharmacol* **620**, 138-144

109.   Suh, N., Wang, Y., Honda, T., Gribble, G. W., Dmitrovsky, E., Hickey, W. F., Maue, R. A., Place, A. E., Porter, D. M., Spinella, M. J., Williams, C. R., Wu, G., Dannenberg, A. J., Flanders, K. C., Letterio, J. J., Mangelsdorf, D. J., Nathan, C. F., Nguyen, L., Porter, W. W., Ren, R. F., Roberts, A. B., Roche, N. S., Subbaramaiah, K., and Sporn, M. B. (1999) *Cancer Res* **59**, 336-341

110.   Konopleva, M., Tsao, T., Ruvolo, P., Stiouf, I., Estrov, Z., Leysath, C. E., Zhao, S., Harris, D., Chang, S., Jackson, C. E., Munsell, M., Suh, N., Gribble, G., Honda, T., May, W. S., Sporn, M. B., and Andreeff, M. (2002) *Blood* **99**, 326-335

111.   Ito, Y., Pandey, P., Place, A., Sporn, M. B., Gribble, G. W., Honda, T., Kharbanda, S., and Kufe, D. (2000) *Cell Growth Differ* **11**, 261-267

112.   Ito, Y., Pandey, P., Sporn, M. B., Datta, R., Kharbanda, S., and Kufe, D. (2001) *Mol Pharmacol* **59**, 1094-1099

113.   Ji, Y., Lee, H. J., Goodman, C., Uskokovic, M., Liby, K., Sporn, M., and Suh, N. (2006) *Mol Cancer Ther* **5**, 1452-1458

114.   Koschmieder, S., D'Alo, F., Radomska, H., Schoneich, C., Chang, J. S., Konopleva, M., Kobayashi, S., Levantini, E., Suh, N., Di Ruscio, A., Voso, M. T., Watt, J. C., Santhanam, R., Sargin, B., Kantarjian, H., Andreeff, M., Sporn, M. B., Perrotti, D., Berdel, W. E., Muller-Tidow, C., Serve, H., and Tenen, D. G. (2007) *Blood* **110**, 3695-3705

115.   Tullo, A., D'Erchia, A. M., and Sbisa, E. (2003) *Expert Rev Mol Diagn* **3**, 289-301

116.   Lapillonne, H., Konopleva, M., Tsao, T., Gold, D., McQueen, T., Sutherland, R. L., Madden, T., and Andreeff, M. (2003) *Cancer Res* **63**, 5926-5939

117.   Konopleva, M., Zhang, W., Shi, Y. X., McQueen, T., Tsao, T., Abdelrahim, M., Munsell, M. F., Johansen, M., Yu, D., Madden, T., Safe, S. H., Hung, M. C., and Andreeff, M. (2006) *Mol Cancer Ther* **5**, 317-328

118.   Dragnev, K. H., Pitha-Rowe, I., Ma, Y., Petty, W. J., Sekula, D., Murphy, B., Rendi, M., Suh, N., Desai, N. B., Sporn, M. B., Freemantle, S. J., and Dmitrovsky, E. (2004) *Clin Cancer Res* **10**, 2570-2577

119.   Chintharlapalli, S., Papineni, S., Konopleva, M., Andreef, M., Samudio, I., and Safe, S. (2005) *Mol Pharmacol* **68**, 119-128

120.   Place, A. E., Suh, N., Williams, C. R., Risingsong, R., Honda, T., Honda, Y., Gribble, G. W., Leesnitzer, L. M., Stimmel, J. B., Willson, T. M., Rosen, E., and Sporn, M. B. (2003) *Clin Cancer Res* **9**, 2798-2806

121.   Li, N., and Karin, M. (1999) *FASEB J* **13**, 1137-1143

122.   Balkwill, F., and Mantovani, A. (2010) *Clin Pharmacol Ther* **87**, 401-406

123.   Auletta, J. J., Alabran, J. L., Kim, B. G., Meyer, C. J., and Letterio, J. J. (2010) *J Interferon Cytokine Res* **30**, 497-508

124. Kidd, S., Caldwell, L., Dietrich, M., Samudio, I., Spaeth, E. L., Watson, K., Shi, Y., Abbruzzese, J., Konopleva, M., Andreeff, M., and Marini, F. C. (2010) *Cytotherapy* **12**, 615-625

125. Honda, T., Padegimas, E. M., David, E., Sundararajan, C., Liby, K. T., Williams, C., Sporn, M. B., and Visnick, M. (2010) *Bioorg Med Chem Lett* **20**, 2275-2278

126. Honda, T., Dinkova-Kostova, A. T., David, E., Padegimas, E. M., Sundararajan, C., Visnick, M., Bumeister, R., and Christian Wigley, W. (2011) *Bioorg Med Chem Lett* **21**, 2188-2191

127. Honda, T., Yoshizawa, H., Sundararajan, C., David, E., Lajoie, M. J., Favaloro, F. G., Jr., Janosik, T., Su, X., Honda, Y., Roebuck, B. D., and Gribble, G. W. (2011) *J Med Chem* **54**, 1762-1778

128. Liby, K., Yore, M. M., Roebuck, B. D., Baumgartner, K. J., Honda, T., Sundararajan, C., Yoshizawa, H., Gribble, G. W., Williams, C. R., Risingsong, R., Royce, D. B., Dinkova-Kostova, A. T., Stephenson, K. K., Egner, P. A., Yates, M. S., Groopman, J. D., Kensler, T. W., and Sporn, M. B. (2008) *Cancer Res* **68**, 6727-6733

129. Honda, T., Sundararajan, C., Yoshizawa, H., Su, X., Honda, Y., Liby, K. T., Sporn, M. B., and Gribble, G. W. (2007) *J Med Chem* **50**, 1731-1734

130. Honda, T., Favaloro, F. G., Jr., Janosik, T., Honda, Y., Suh, N., Sporn, M. B., and Gribble, G. W. (2003) *Org Biomol Chem* **1**, 4384-4391

131. Favaloro, F. G., Jr., Honda, T., Honda, Y., Gribble, G. W., Suh, N., Risingsong, R., and Sporn, M. B. (2002) *J Med Chem* **45**, 4801-4805

132. Baird, L., and Dinkova-Kostova, A. T. (2011) *Arch Toxicol* **85**, 241-272

133. Li, W., Khor, T. O., Xu, C., Shen, G., Jeong, W. S., Yu, S., and Kong, A. N. (2008) *Biochem Pharmacol* **76**, 1485-1489

134. Liby, K., Hock, T., Yore, M. M., Suh, N., Place, A. E., Risingsong, R., Williams, C. R., Royce, D. B., Honda, T., Honda, Y., Gribble, G. W., Hill-Kapturczak, N., Agarwal, A., and Sporn, M. B. (2005) *Cancer Res* **65**, 4789-4798

135. Thimmulappa, R. K., Scollick, C., Traore, K., Yates, M., Trush, M. A., Liby, K. T., Sporn, M. B., Yamamoto, M., Kensler, T. W., and Biswal, S. (2006) *Biochem Biophys Res Commun* **351**, 883-889

136. Thimmulappa, R. K., Fuchs, R. J., Malhotra, D., Scollick, C., Traore, K., Bream, J. H., Trush, M. A., Liby, K. T., Sporn, M. B., Kensler, T. W., and Biswal, S. (2007) *Antioxid Redox Signal* **9**, 1963-1970

137.   Yates, M. S., Tauchi, M., Katsuoka, F., Flanders, K. C., Liby, K. T., Honda, T., Gribble, G. W., Johnson, D. A., Johnson, J. A., Burton, N. C., Guilarte, T. R., Yamamoto, M., Sporn, M. B., and Kensler, T. W. (2007) *Mol Cancer Ther* **6**, 154-162

138.   Pereira, W. O., and Amarante-Mendes, G. P. (2011) *Scand J Immunol* **73**, 401-407

139.   Melet, A., Song, K., Bucur, O., Jagani, Z., Grassian, A. R., and Khosravi-Far, R. (2008) *Adv Exp Med Biol* **615**, 47-79

140.   Safa, A. R., Day, T. W., and Wu, C. H. (2008) *Curr Cancer Drug Targets* **8**, 37-46

141.   Kataoka, T. (2005) *Crit Rev Immunol* **25**, 31-58

142.   Riccioni, R., Senese, M., Diverio, D., Riti, V., Mariani, G., Boe, A., LoCoco, F., Foa, R., Peschle, C., Sporn, M., and Testa, U. (2008) *Leuk Res* **32**, 1244-1258

143.   Ikeda, T., Nakata, Y., Kimura, F., Sato, K., Anderson, K., Motoyoshi, K., Sporn, M., and Kufe, D. (2004) *Mol Cancer Ther* **3**, 39-45

144.   Pedersen, I. M., Kitada, S., Schimmer, A., Kim, Y., Zapata, J. M., Charboneau, L., Rassenti, L., Andreeff, M., Bennett, F., Sporn, M. B., Liotta, L. D., Kipps, T. J., and Reed, J. C. (2002) *Blood* **100**, 2965-2972

145.   Zou, W., Chen, S., Liu, X., Yue, P., Sporn, M. B., Khuri, F. R., and Sun, S. Y. (2007) *Cancer Biol Ther* **6**, 1614-1620

146.   Zou, W., Liu, X., Yue, P., Khuri, F. R., and Sun, S. Y. (2007) *Cancer Biol Ther* **6**, 99-106

147.   Hyer, M. L., Croxton, R., Krajewska, M., Krajewski, S., Kress, C. L., Lu, M., Suh, N., Sporn, M. B., Cryns, V. L., Zapata, J. M., and Reed, J. C. (2005) *Cancer Res* **65**, 4799-4808

148.   Hyer, M. L., Shi, R., Krajewska, M., Meyer, C., Lebedeva, I. V., Fisher, P. B., and Reed, J. C. (2008) *Cancer Res* **68**, 2927-2933

149.   Petronelli, A., Saulle, E., Pasquini, L., Petrucci, E., Mariani, G., Biffoni, M., Ferretti, G., Scambia, G., Benedetti-Panici, P., Greggi, S., Cognetti, F., Russo, M. A., Sporn, M., and Testa, U. (2009) *Cancer Lett* **282**, 214-228

150.   Zou, W., Liu, X., Yue, P., Zhou, Z., Sporn, M. B., Lotan, R., Khuri, F. R., and Sun, S. Y. (2004) *Cancer Res* **64**, 7570-7578

151. Alabran, J. L., Cheuk, A., Liby, K., Sporn, M., Khan, J., Letterio, J., and Leskov, K. S. (2008) *Cancer Biol Ther* **7**, 709-717

152. Deeb, D., Gao, X., Dulchavsky, S. A., and Gautam, S. C. (2007) *Anticancer Res* **27**, 3035-3044

153. Stadheim, T. A., Suh, N., Ganju, N., Sporn, M. B., and Eastman, A. (2002) *J Biol Chem* **277**, 16448-16455

154. Konopleva, M., Tsao, T., Estrov, Z., Lee, R. M., Wang, R. Y., Jackson, C. E., McQueen, T., Monaco, G., Munsell, M., Belmont, J., Kantarjian, H., Sporn, M. B., and Andreeff, M. (2004) *Cancer Res* **64**, 7927-7935

155. Brookes, P. S., Morse, K., Ray, D., Tompkins, A., Young, S. M., Hilchey, S., Salim, S., Konopleva, M., Andreeff, M., Phipps, R., and Bernstein, S. H. (2007) *Cancer Res* **67**, 1793-1802

156. Ikeda, T., Sporn, M., Honda, T., Gribble, G. W., and Kufe, D. (2003) *Cancer Res* **63**, 5551-5558

157. Chauhan, D., Li, G., Podar, K., Hideshima, T., Shringarpure, R., Catley, L., Mitsiades, C., Munshi, N., Tai, Y. T., Suh, N., Gribble, G. W., Honda, T., Schlossman, R., Richardson, P., Sporn, M. B., and Anderson, K. C. (2004) *Blood* **103**, 3158-3166

158. Suh, W. S., Kim, Y. S., Schimmer, A. D., Kitada, S., Minden, M., Andreeff, M., Suh, N., Sporn, M., and Reed, J. C. (2003) *Leukemia* **17**, 2122-2129

159. Zou, W., Yue, P., Khuri, F. R., and Sun, S. Y. (2008) *Cancer Res* **68**, 7484-7492

160. Konopleva, M., Contractor, R., Kurinna, S. M., Chen, W., Andreeff, M., and Ruvolo, P. P. (2005) *Leukemia* **19**, 1350-1354

161. Hail, N., Jr., Konopleva, M., Sporn, M., Lotan, R., and Andreeff, M. (2004) *J Biol Chem* **279**, 11179-11187

162. Jimbo, A., Fujita, E., Kouroku, Y., Ohnishi, J., Inohara, N., Kuida, K., Sakamaki, K., Yonehara, S., and Momoi, T. (2003) *Exp Cell Res* **283**, 156-166

163. Wang, K. K. (2000) *Trends Neurosci* **23**, 20-26

164. Rayasam, G. V., Tulasi, V. K., Sodhi, R., Davis, J. A., and Ray, A. (2009) *Br J Pharmacol* **156**, 885-898

165. Vene, R., Larghero, P., Arena, G., Sporn, M. B., Albini, A., and Tosetti, F. (2008) *Cancer Res* **68**, 6987-6996

166. Johnston, P. A., and Grandis, J. R. (2011) *Mol Interv* **11**, 18-26

167. Liby, K., Voong, N., Williams, C. R., Risingsong, R., Royce, D. B., Honda, T., Gribble, G. W., Sporn, M. B., and Letterio, J. J. (2006) *Clin Cancer Res* **12**, 4288-4293

168. Ling, X., Konopleva, M., Zeng, Z., Ruvolo, V., Stephens, L. C., Schober, W., McQueen, T., Dietrich, M., Madden, T. L., and Andreeff, M. (2007) *Cancer Res* **67**, 4210-4218

169. Ryu, K., Choy, E., Yang, C., Susa, M., Hornicek, F. J., Mankin, H., and Duan, Z. (2010) *J Orthop Res* **28**, 971-978

170. Ryu, K., Susa, M., Choy, E., Yang, C., Hornicek, F. J., Mankin, H. J., and Duan, Z. (2010) *BMC Cancer* **10**, 187

171. Duan, Z., Ames, R. Y., Ryan, M., Hornicek, F. J., Mankin, H., and Seiden, M. V. (2009) *Cancer Chemother Pharmacol* **63**, 681-689

172. Samudio, I., Kurinna, S., Ruvolo, P., Korchin, B., Kantarjian, H., Beran, M., Dunner, K., Jr., Kondo, S., Andreeff, M., and Konopleva, M. (2008) *Mol Cancer Ther* **7**, 1130-1139

173. Vannini, N., Lorusso, G., Cammarota, R., Barberis, M., Noonan, D. M., Sporn, M. B., and Albini, A. (2007) *Mol Cancer Ther* **6**, 3139-3146

174. Deeb, D., Gao, X., Liu, Y., Jiang, D., Divine, G. W., Arbab, A. S., Dulchavsky, S. A., and Gautam, S. C. (2011) *Carcinogenesis* **32**, 757-764

175. Sogno, I., Vannini, N., Lorusso, G., Cammarota, R., Noonan, D. M., Generoso, L., Sporn, M. B., and Albini, A. (2009) *Recent Results Cancer Res* **181**, 209-212

176. Shishodia, S., Sethi, G., Konopleva, M., Andreeff, M., and Aggarwal, B. B. (2006) *Clin Cancer Res* **12**, 1828-1838

177. Suh, N., Roberts, A. B., Birkey Reffey, S., Miyazono, K., Itoh, S., ten Dijke, P., Heiss, E. H., Place, A. E., Risingsong, R., Williams, C. R., Honda, T., Gribble, G. W., and Sporn, M. B. (2003) *Cancer Res* **63**, 1371-1376

178. Ahmad, R., Liu, S., Weisberg, E., Nelson, E., Galinsky, I., Meyer, C., Kufe, D., Kharbanda, S., and Stone, R. (2010) *Mol Cancer Res* **8**, 986-993

179. Govedarovic, N., and Marjanovic, G. (2011) *J BUON* **16**, 108-111

180. Hughes, D. T., Martel, P. M., Kinlaw, W. B., and Eisenberg, B. L. (2008) *Cancer Invest* **26**, 118-127

181.   Liby, K., Risingsong, R., Royce, D. B., Williams, C. R., Ma, T., Yore, M. M., and Sporn, M. B. (2009) *Cancer Prev Res (Phila)* **2**, 1050-1058

CHAPTER 2

THE SYNTHETIC TRITERPENOID CDDO-IMIDAZOLIDE ALTERS TGFβ-DEPENDENT SIGNALING AND CELL MIGRATION BY AFFECTING THE CYTOSKELETON AND THE POLARITY COMPLEX.

2   CHAPTER 2

2.1   CHAPTER SUMMARY

The anti-tumor synthetic triterpenoid CDDO-Imidazolide (CDDO-Im) ectopically activates the TGFβ-Smad pathway and extends the duration of signaling by an undefined mechanism.   Here, I showed that CDDO-Im-dependent persistence of Smad2 phosphorylation was independent of Smad2 phosphatase activity and correlates with delayed TGFβ receptor degradation and trafficking. Altered TGFβ trafficking paralleled the dispersal of EEA1-positive endosomes from the peri-nuclear region of CDDO-Im-treated cells. The effect of CDDO-Im on the EEA1 compartment led to an analysis of the cytoskeleton, and we observed that CDDO-Im altered microtubule dynamics by disrupting the microtubule-capping protein, CLIP170.   Interestingly, biotinylated triterpenoid was found to localize to the polarity complex at the leading edge of migrating cells. Furthermore, CDDO-Im disrupted the localization of IQGAP1, PKCζ, Par6 and TGFβ receptors from the leading edge of migrating cells and inhibited TGFβ-dependent cell migration. Thus, the synthetic triterpenoid CDDO-Im interferes with TGFβ receptor trafficking and turnover, and disrupts cell migration by severing the link between members of the polarity complex and the microtubule network.

2.2   INTRODUCTION

Transforming growth factor beta (TGFβ) family members regulate many cellular functions including proliferation and differentiation and TGFβ is a potent apoptotic agent in many cells including early stage epithelial tumors (1). However, in late stage epithelial tumors, TGFβ becomes a metastatic agent and stimulates epithelial to mesenchymal transition (EMT) and cell migration (2-5). Signaling by TGFβ growth factor is initiated via ligand-induced heteromeric complex formation of the Ser/Thr kinase type I (TβRI) and type II (TβRII) transmembrane receptors (6). The phosphorylation of receptor-regulated Smad proteins: R-Smad2 and R-Smad3 is facilitated by Smad anchor for receptor activation protein (SARA), which binds the receptors and recruits R-Smad to the membrane of EEA1-positive early endosomes (7). Early endosomes also contain other modulators of TGFβ receptor signaling such as hepatocyte growth factor-regulated tyrosine kinase substrate (HRS) (8) and cytoplasmic promyelocytic leukemia protein (cPML) (9).

Inactivation of the TGFβ signaling pathway is carried out by several mechanisms. Phosphorylated Smad2 is targeted by the nuclear phosphatase PPM1A (10) and the receptors are the target of inhibitory Smad7, which interacts with TβRI in lipid rafts/caveolae and recruits the E3 ligases, Smurf1 and Smurf2, which direct ubiquitin-dependent degradation of the TGFβ receptors (11-13). Perturbation of lipid rafts increases signaling and reduces the rate of receptor degradation (14-18). Thus, the signal transduction pathway initiated by cell surface TGFβ receptor complex is dependent on receptor internalization and trafficking via distinct endocytic pathways (19).

Endocytosis of cell surface proteins is dependent on the microtubule cytoskeleton (20-22). Microtubules are dynamic protein filaments that span the cell interior and provide a mechanical framework for chromosome sorting, cell polarity and organelle localization, among other functions (23-28). Microtubules grow and shrink from their plus-ends and their minus-ends are usually located at the microtubule-organizing center, but are also found at the apical domain in epithelial cells (29).

Polarized migration of cells as well as the movement of vesicles along the microtubules is dependent on molecular motors and microtubule binding proteins, such as the capping protein, CLIP170 (30,31). Furthermore, the association of microtubule-bound CLIP170 at the cell membrane with the Rac1/Cdc42 binding protein, IQGAP1, is an essential mediator between microtubules and the leading edge of migrating cells (32,33). Cdc42 also binds to the Par6-PKCζ polarity complex, which in turn links Cdc42 to APC and the microtubule network to form a focal point for directional cellular movement (26). These molecular links, in combination with the observation that Par6 associates with TGFβ receptors (34), have introduced a new area of study to the field of TGFβ-dependent signaling in cell migration and metastasis (2).

Chemotherapeutic agents that block TGFβ-dependent signaling and TGFβ-dependent metastasis have been a major focus in cancer chemotherapy (35). Recently, 2-cyano-3, 12-dioxooleana-1, 9-dien-28-oic acid (CDDO), has been shown to be a promising cancer therapeutic agent that is currently in Phase I clinical trials (36). Interestingly, both CDDO and its imidazolide derivative, CDDO-Im, have been shown to synergistically increase cellular responses to factors such as TGFβ in cell culture studies (37-39). The mechanism whereby CDDO-Im does this has yet to be elucidated. In this

study, I demonstrate that CDDO-Im alters TGFβ cell signaling, receptor trafficking and inhibits cell migration by disrupting cytoskeletal attachments to the polarity complex.

2.3   MATERIALS AND METHODS

2.3.1   Cell Lines and Antibodies

Mv1Lu cells were cultured in minimal essential medium (MEM) supplemented with 1%
non-essential amino acids (NEAA). Mv1Lu cells stably transfected with the HA-epitope
tagged TGFβ type II Receptor (HAT cells) were cultured in MEM/1% NEAA and
0.3mg/ml Hygromycin.   Cos-7, C2C12, HEK293 and Rat2 cells were cultured in
Dulbecco's modified Eagle's medium (DMEM). All media was supplemented with 10%
fetal bovine serum (FBS) unless otherwise stated. Texas Red-conjugated phalloidin, anti-
caveolin-1 (610059), anti-EEA1 (610456), anti-Rac1 (610650), anti-GM130 (610822),
anti-Smad2 (610842) and anti-LAMP1 (555798) antibodies were purchased from BD
Transduction Laboratories (Mississauga, ON, Canada).   Monoclonal anti-tubulin
(Tub2.1), anti-Flag (M2), and polyclonal anti-actin (A2668) antibodies were purchased
from Sigma (Oakville, ON, Canada). Polyclonal anti-PKCζ (C-20), anti-TGFβ type II
receptor (C-16), anti-Par6 (H-90), anti-IQGAP1 (H-109), anti-HA (Y-11), and goat anti-
lamin A/C antibodies (sc-6215) were purchased from Santa Cruz Biotechnology (Santa
Cruz, CA). Anti-phospho-Smad2 (AB3849) antibodies were purchased from Chemicon
(Temecula, CA). The polyclonal phospho-Par6 (S345) antibody was used as previously
described (34). The polyclonal anti-CLIP170 (N-terminal) antibody was a generous gift
from Dr. K. Kaibuchi (Nagoya University, Nagoya, Japan) and the polyclonal anti-
Calnexin was kindly provided by Dr. J. J. M. Bergeron and Ms. P. H. Cameron (McGill
University, Montreal, Canada). The GFP-tagged CLIP170 construct was a generous gift
from Dr. F. Perez (CNRS, Paris, France).

2.3.2   Affinity Labeling

Cells were pre-incubated in control media or media containing 1 μM CDDO-Im for 1 hour at 37°C, placed on ice and incubated with 250 pM ^{125}I-TGFβ in KRH-0.5 % BSA at 4°C for 2 hours. Following cross-linking with DSS, cells were lysed (Time 0) or incubated at 37°C for 2, 4 or 8 hours prior to lysis. Receptors were visualized by SDS-PAGE and quantified using phosphoimager analysis (Molecular Dynamics).

2.3.3   Subcellular Fractionation

2.3.3.1   *Cytoskeleton*

Fractions containing the cytoskeleton were separated from those containing detergent-solubilized membranes and cytosol by the method described by Contin and colleagues (40). Briefly, Cos-7 cells were incubated for 3 hours in control medium or media containing 10 μM nocodazole or 1 μM CDDO-Im and then rinsed with microtubule stabilization buffer (MSB; 90 mM Mes (pH 6.7), 1 mM EGTA, 1mM MgCl$_2$, 10% (v/v) glycerol) that had been pre-heated to 37°C. Cells were then lysed with MSB containing 10 μM placitaxel (Sigma; St. Louis, MO), 0.5% TX-100 and protease inhibitors for 4 minutes at 37°C. The solubilized fractions were then collected. To collect the remaining cellular structures containing the cytoskeleton, SDS-PAGE sample buffer was added to the culture dishes. Following scraping and passaging through a syringe, the fractions containing the cytoskeleton were collected.

To analyze the partitioning of cytoskeletal proteins, fractions containing the soluble proteins or the cytoskeleton were subjected to SDS-PAGE followed by immunoblotting with anti-Rac1, anti-tubulin, anti-actin, anti-IQGAP1, anti-EEA1, anti-Calnexin, anti-LAMP1, anti-GM130 or anti-CLIP170 antibodies.

2.3.3.2   *Nuclear Fractionation*

To quantify the amount of Smad2 present in the nucleus in the presence of CDDO-Im, subcellular fractionation was carried out as described by Cong and Varmus (41). Briefly, cells were incubated with 0.5 μM TGFβ for 30 minutes in the absence or presence of 1 μM CDDO-Im, washed and incubated in media containing DMSO (Control), 1 μM CDDO-Im, 10 μM SB431542 or both compounds (CDDO-Im + SB431542) at 37°C for an additional 1 or 4 hours. The cells were then scraped into ice cold PBS and collected by centrifugation at $1000xg_{av}$ for 5 minutes. The cells were then washed once again with PBS and resuspended in hypotonic buffer (10mM Hepes-KOH; 10mM NaCl; 1 mM KH_2PO_4; 5 mM $NaHCO_3$; 1mM $CaCl_2$; 0.5 mM $MgCl_2$; pH 7.4). After a 5-minute incubation on ice, cells were homogenized with 50 strokes using a Dounce homogenizer. Cells were then centrifuged at 1000 x g_{av} for 5 min. The pellets were washed twice with hypotonic buffer and resuspended in nuclear isolation buffer (10 mM Tris (pH 7.5); 300mM sucrose; 0.1% Nonidet P-40). The pellets in the nuclear isolation buffer were then further homogenized 50 times using a Dounce homogenizer and centrifuged at 1000 xg_{av} for 5 minutes. The nuclear pellet was resuspended with nuclear isolation buffer with 1 % Trition X-100 to generate the nuclear fraction. The

nuclear fractions were subjected to SDS-PAGE and immunobloted with mouse anti-Smad2 or goat anti-lamin A/C antibodies. The levels of Smad2 were quantitated using QuantityOne software (Biorad) and normalized to the amount of lamin A/C in each fraction.

2.3.4 Phospho-Smad2 Timecourse

Cells were incubated with 0.5 μM TGFβ for 30 minutes, in the absence or presence of 1 μM CDDO-Im, washed and incubated in media containing DMSO (Control), 1 μM CDDO-Im, 10 μM SB431542 (Sigma; St. Louis, MO) or both compounds (CDDO-Im + SB431542) at 37°C for an additional 1 or 4 hours prior to lysis. Cell lysates were then analyzed by SDS-PAGE and immunoblotted with mouse anti-Smad2 or rabbit anti-phospho-Smad2 antibodies. Quantitation of the amount of phosphorylated Smad2 was carried out using QuantityOne software and normalized to Smad2 levels.

2.3.5 Immunofluorescence Microscopy

2.3.5.1 Smad2 Nuclear Accumulation

Cells were incubated with 0.5 μM TGFβ for 30 minutes in the absence or presence of 1 μM CDDO-Im, washed and incubated in media containing DMSO (Control), 1 μM CDDO-Im, 10 μM SB431542 or both compounds (CDDO-Im +

SB431542) at 37°C for an additional 1, 4 or 8 hours prior to fixation and permeabilization. Cells were then immunostained with anti-Smad2/3 antibody followed by Cy2-conjugated secondary antibody. DAPI staining was used to visualize cell nuclei. To quantify the amount of Smad2 nuclear localization, nuclear vs. cytoplasmic intensity profiles were generated from individual cells using ImagePro software. The quantitation of $\geq$ 100 cells/condition from 3 experiments was graphed as the nuclear signal minus the cytoplasmic signal vs. time ($\pm$ SD).

2.3.5.2   *Receptor Traffic*

Receptor internalization studies were carried out as previously described (15). Briefly, HAT cells expressing extracellularly HA-tagged TβRII receptors were incubated with biotinylated-TGFβ for 2 hours at 4°C, washed and incubated with Cy3-streptavidin (Jackson Immunoresearch, West Grove, PA). Cells were then washed and incubated at 37°C for 1 hour with or without CDDO-Im. After the 37°C incubation, cells were fixed and incubated with mouse monoclonal anti-EEA1 antibodies and rabbit polyclonal anti-caveolin-1 antibodies. Anti-EEA1 and anti-caveolin-1 were detected using anti-mouse Cy5-conjugated antibodies and anti-rabbit Cy2-conjugated antibodies (Jackson Laboratories Inc.) respectively. Acid washing was carried out as previously described (15). Images were captured using an Olympus 1X81 inverted microscope equipped with fluorescence optics and deconvolved using ImagePro software.

2.3.5.3   *EEA1 Distribution*

To visualize the effect of CDDO-Im on EEA1-positive endosomes I assessed the staining pattern of the EEA1 compartment via immunofluorescence microscopy as described above with the exception that Cy2-labelled secondary antibodies were used. DAPI staining was used to visualize cell nuclei.

Staining observed to be localized to an area no greater than one half of the cell area and located more intensely on one side of the nucleus was scored as 'peri-nuclear-positive'. If the intensity and distribution of the stain was equal throughout the cell body, it was scored as 'dispersed'. The quantitation of $\geq$ 100 cells/condition from 3 experiments was graphed ($\pm$ SD).

2.3.5.4   *Cytoskeleton Studies*

To visualize the effect of CDDO-Im on the microtubule cytoskeleton, cells were incubated for 1 hour with or without 1 μM CDDO-Im or 10 μM nocodazole (Sigma; Oakville, Canada) at 37˚C. Following fixation and permeabilization, cells were incubated with monoclonal anti-tubulin antibody followed by FITC-conjugated secondary antibodies. To assess the effect of CDDO-Im on the actin cytoskeleton, cells were incubated with 1 μM CDDO-Im or 10 μM cytochalasin B for 1 hour prior to fixation and permeabilization. The cells were then incubated for 30 minutes with Texas Red-conjugated phalloidin. Images were collected from a Leica DMIRE inverted microscope.

2.3.6   Scratch Assays

Rat2 fibroblasts were grown to confluency and the cell monolayer was scratched with a sterile pipette tip to create a 'wound'. For brightfield or DIC microscopy, images were collected using an Olympus IX81 inverted microscope. For immunofluorescence studies, cells were fixed, permeabilized and incubated with anti-CLIP170, anti-tubulin, anti-Rac1, anti-TβRII, anti-IQGAP1, anti-Par6 or anti-PKCζ antibodies. Following fluorescently-tagged secondary antibody incubation, the nuclei of cells were stained with DAPI and cells were visualized using an Olympus IX81 microscope controlled by QED *Invivo* software (Olympus, Canada).

The quantitation of the number of cells containing proteins at the leading edge of the cell was carried out using ≥ 100 cells/condition from 3 experiments (± SD). Briefly, a cell containing a positive immunofluorescence signal only along the edge of the plasma membrane that was directly adjacent to the scratch was scored as positive for leading edge localization. If a cell contained no signal along the adjacent edge to the scratch or contained dispersed signal along the complete cell periphery, it was scored as negative for leading edge staining.

2.3.7   CLIP170 Movies

Rat2 fibroblasts were microinjected with 0.25 nM cDNA encoding GFP-tagged CLIP170 protein and incubated at 37°C for 4 hours. The cells were then incubated in

control media or media containing 0.1 μM or 1 μM CDDO-Im. Expressed GFP-tagged CLIP170 was visualized by immunofluorescence and time-lapse images were collected using a Leica DMIRE inverted microscope utilizing Openlab 3.0 software.

2.3.8 Cell Transfection

Cells were transfected with the constructs described in the figure legends using the calcium phosphate method as previously described (15).

2.3.9 Immunoprecipitation

Cells were lysed (50 mM Tris-HCl, pH 7.4, 150 mM NaCl, 1 mM EDTA, 0.5 % Triton X-100, 1 mM PMSF, and cocktail protease inhibitors) and centrifuged at 15,000 × g_{av} at 4°C for 5 minutes. Aliquots of supernatants were collected for analysis of total protein concentration. The remaining cell lysates were incubated with primary antibody followed by incubation with protein G-sepharose. The precipitates were washed 3 times with lysis buffer, eluted with Laemmli sample buffer and subjected to SDS-PAGE and immunoblot analysis.

2.3.10 CDDO-Biotin Subcellular Localization

Rat2 fibroblasts were grown to 100% confluency and scratched to create a wound. The cells were then incubated at 37°C for 6 hours to allow for the establishment of polarity. The cells were then fixed, permeabilized and incubated with Rac1 antibodies followed by Cy2-labelled secondary antibodies. The cells were then incubated with 10 μM biotin, CDDO or CDDO-biotin for 2 hours, followed by incubation with Cy3-labelled streptavidin and DAPI. Cells were visualized using an Olympus IX81 inverted microscope.

2.3.11 Protein Concentration

Protein concentrations of lysates were measured using the Lowry method (Fisher Scientific, Ottawa, ON, Canada).

2.3.12 Statistical Analyses

Results are provided as means ± SD. One-way ANOVA analysis followed by a Tukey's post-hoc test was performed using GraphPad PRISM 5 Software to assess statistical differences between experimental groups. $P<0.0001$ was considered statistically significant.

2.4   RESULTS

2.4.1   CDDO-Im extends TGFβ-dependent signaling by increasing Smad2

phosphorylation and its accumulation in the nuclei

The triterpenoid, 1-(2-cyano-3,12-dioxooleana-1,9-dien-28-oyl) imidazolide (CDDO-Im) extends TGFβ signal transduction in several cell lines (37,39), however, the mechanism(s) and functional consequences have yet to be fully elucidated.

In order to study the mechanism of how CDDO-Im extends TGFβ-dependent signaling, I first attempted to identify cell lines in which TGFβ-dependent Smad2 phosphorylation is transient. I treated various cell lines with a 30 minute-pulse of TGFβ and investigated the state of Smad2 phosphorylation by immunoblot analysis using a phospho-Smad2 specific antibody. I observed that the phosphorylation of Smad2 was transient in Rat2, Cos-7 and C2C12 cells (≤ 4.5 hours) whereas it was prolonged (> 8 hours) in HepG2 and Hela cells (Figure 2.1 and data not shown). In Rat2 and Cos-7 cells, Smad2 phosphorylation was observed 30 minutes after TGFβ stimulation and attenuated over the remainder of the time course (Figure 2.1A and B, lanes 1-4). In C2C12 cells, Smad2 phosphorylation returned to background levels within 1 hour of ligand removal from the culture medium (Figure 2.1C, lanes 1-4). Having observed transient Smad2 phosphorylation in Rat2, C2C12 and Cos-7 cells, I next assessed the effect of co-incubating cells with TGFβ and CDDO-Im. I observed that CDDO-Im increased both the extent and duration of TGFβ-dependent Smad2 phosphorylation in all of the three cell types tested (Figure 2.1, lanes 5-8).

Figure 2.1 CDDO-Im extends TGFβ-dependent Smad2 phosphorylation independently of Smad2 phosphatase activity.

Rat2 **(A)** Cos-7 **(B)** or C2C12 **(C)** cells were incubated with 0.5 µM TGFβ for 30 minutes in the absence or presence of 1 µM CDDO-Im, washed and incubated in media containing DMSO (Control), 1 µM CDDO-Im, 10 µM SB431542 or both compounds (CDDO-Im + SB431542) at 37˚C for an additional 1 or 4 hours prior to lysis. One hundred micrograms of cell lysates were then processed for SDS-PAGE and immunoblotted with anti-phosphospecific Smad2 (α-P-Smad2) or Smad2/3 (α-Smad2/3) antibodies. The bands corresponding to phosphoserine-modified Smad2 (P-Smad2) and Smad2 (Smad2) are indicated. Representative blots from 4 experiments are shown.

Figure 2-1

A

Rat2

B

Cos-7

C

C2C12
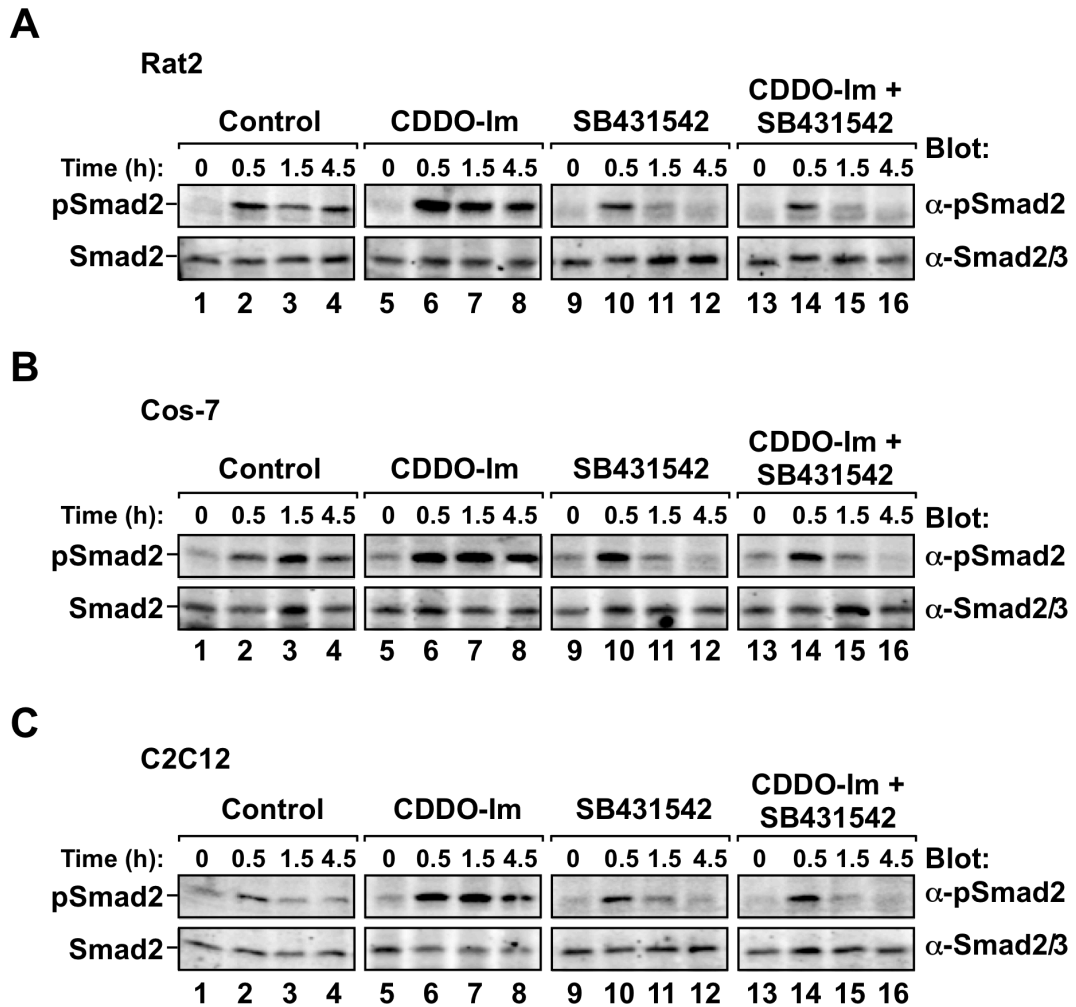
I next investigated if the effect of CDDO-Im on the duration of Smad2 phosphorylation could be due to an inhibition of Smad2 phosphatase activity. In order to test this, I employed one of the strategies used by Lin and colleagues to identify PPM1A as the nuclear Smad2 phosphatase (10). Briefly, the TGFβ type I receptor inhibitor, SB431542, was added to the cell culture media after a pre-incubation of the cells with TGFβ. The addition of the inhibitor would assess if TGFβ receptor activity would influence the effect of CDDO-Im on TGFβ-dependent Smad2 phosphorylation. In Rat2, Cos-7 and C2C12 cells, the SB431542 inhibitor greatly reduced the phosphorylation of Smad2 within 1 hour of incubation, indicating that these cell types have functional phosphatase activity (Figure 2.1, lanes 9-12). I next assessed if CDDO-Im would influence Smad2 phosphatase by co-incubating cells with SB431542 and CDDO-Im. I observed that CDDO-Im did not extend TGFβ-dependent Smad2 phosphorylation in Rat2, Cos-7 or C2C12 cells when SB431542 was present in the culture media (Figure 2.1, lanes 13-16). These results suggest that the Smad2 phosphatase was not a CDDO-Im target since CDDO-Im was unable to extend the duration of Smad2 phosphorylation after TGFβ receptor inactivation.

As a second line of investigation, I assessed TGFβ-dependent Smad2 nuclear translocation using immunofluorescence microscopy (Figure 2.2). I found that in the absence of TGFβ, Smad2 staining was observed throughout the cytoplasm of C2C12 cells (Figure 2.2A). After 1 hour of TGFβ stimulation, Smad2 staining was only observed in the nuclei of cells regardless of treatment (Figure 2.2 B-E, top panels). Eight hours after TGFβ was removed from the cell culture medium, Smad2 cytoplasmic

Figure 2.2 CDDO-Im extends TGFβ-dependent Smad2 nuclear accumulation independently of Smad2 phosphatase activity.

Unstimulated C2C12 cells **(A)** or C2C12 cells pulsed with 0.5 µM TGFβ for 30 minutes in the absence or presence of 1 µM CDDO-Im were incubated in media containing DMSO **(B)**, 1 µM CDDO-Im **(C)**, 10 µM SB431542 **(D)** or both compounds **(E)** at 37˚C for 1 or 8 hours. The cells were then processed for immunofluorescence microscopy and probed with DAPI (blue) to indicate nuclei and anti-Smad2/3 (Smad2) antibodies (green). Nuclear and cytoplasmic Smad2 from 3 experiments (±SD) were quantitated using ImagePro software and graphed as nuclear-cytoplasmic Smad2 ratio vs. time **(F)**. Bar = 10 µm.
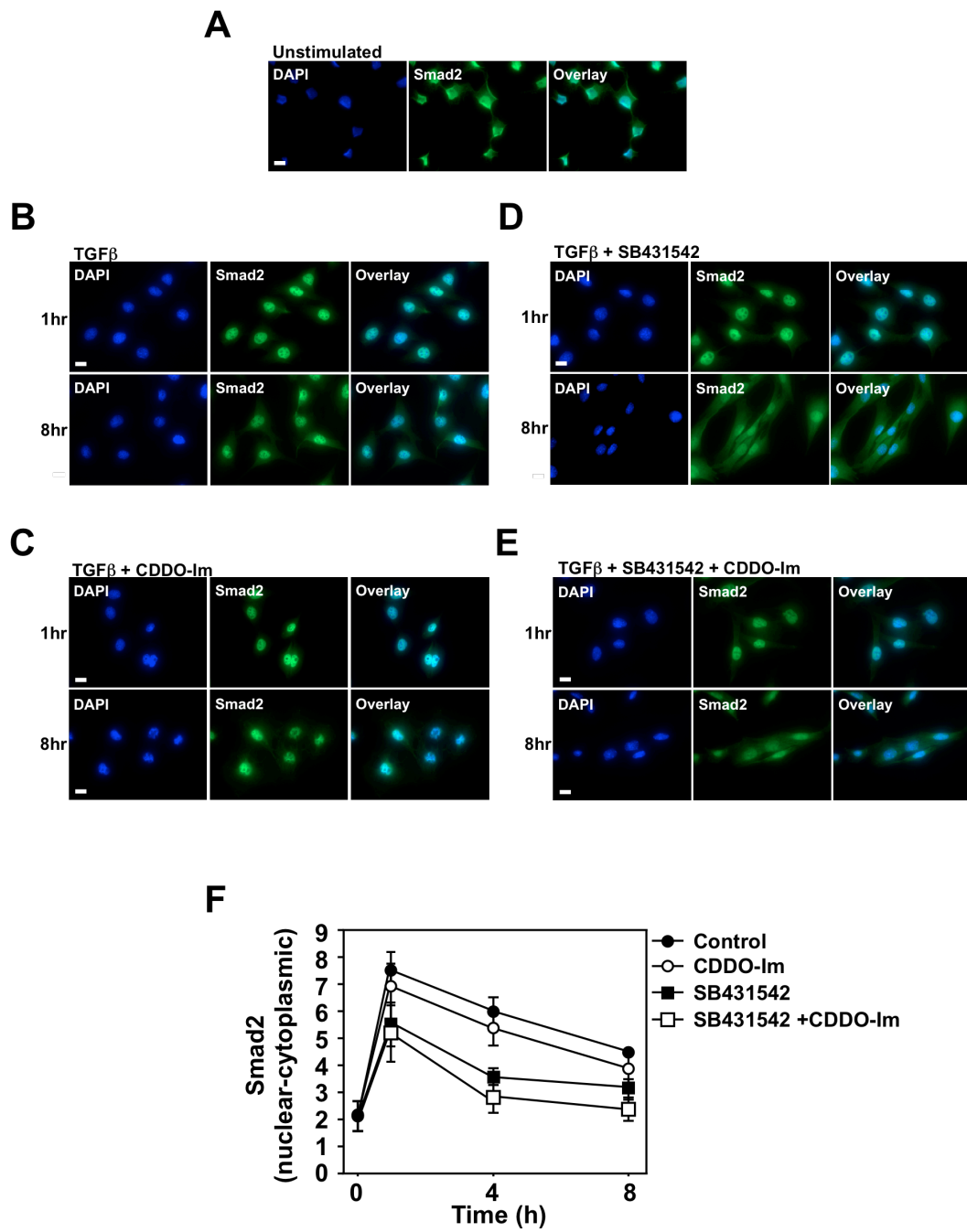
Figure 2-2

staining reappeared in both control and CDDO-Im treated cells (Figure 2.2B and C, bottom panels).

Consistent with the phospho-Smad2 time course studies, the TGFβ type I receptor inhibitor, SB431542, increased cytoplasmic Smad2 staining after 8 hours of incubation (Figure 2.2D) and this was also observed if the cells were co-incubated with SB431542 and CDDO-Im (Figure 2.2E). These results were supported by the quantitation of three experiments (Figure 2.2F) and similar results were obtained with the use of Rat2 or Cos-7 cells (data not shown).

Finally, to further evaluate TGFβ dependent nuclear accumulation of Smad2 in the presence or absence of CDDO-Im and/or SB431542, I carried out subcellular fractionation studies. I assessed TGFβ-dependent Smad2 nuclear accumulation by immunoblotting isolated nuclear fractions with anti-Smad2 antibodies (Figure 2.3). In control cells I observed Smad2 in the nuclear fractions after 0.5 hours of TGFβ stimulation and the signal attenuated after 4.5 hours of stimulation (Figure 2.3, lanes 1-3). This was accentuated if the cells were incubated CDDO-Im (Figure 2.3, lanes 4-6). I observed that the TGFβ type I receptor inhibitor, SB431542, decreased the amount of Smad2 in the nuclear fractions after 4 hours of incubation (Figure 2.3, lanes 7-9) and this was also observed if the cells were co-incubated with SB431542 and CDDO-Im (Figure 2.3, lanes 10-12).

Taken together, these results support the conclusion that CDDO-Im increases TGFβ-dependent Smad2 phosphorylation and nuclear accumulation in a process that is independent of Smad2 phosphatase activity.

.

Figure 2.3 CDDO-Im extends TGFβ-dependent Smad2 accumulation in nuclear fractions.

Rat2 cells were incubated with 0.5 μM TGFβ for 30 minutes in the absence or presence of 1 μM CDDO-Im, washed and incubated in media containing DMSO (Control), 1 μM CDDO-Im, 10 μM SB431542 or both compounds (CDDO-Im + SB431542) at 37˚C for an additional 1 or 4 hours. Following subcellular fractionation, 100 μg of nuclear fractions were processed for SDS-PAGE and immunoblotted with anti-Smad2/3 (α-Smad2/3) or lamin A/C (α-lamin A/C) antibodies. The bands corresponding to Smad2 or lamin A/C are indicated. Smad2 levels were quantitated using QuantityOne software and normalized to the levels of lamin A/C (bottom graph). Representative blots from 6 experiments are shown.

Figure 2-3
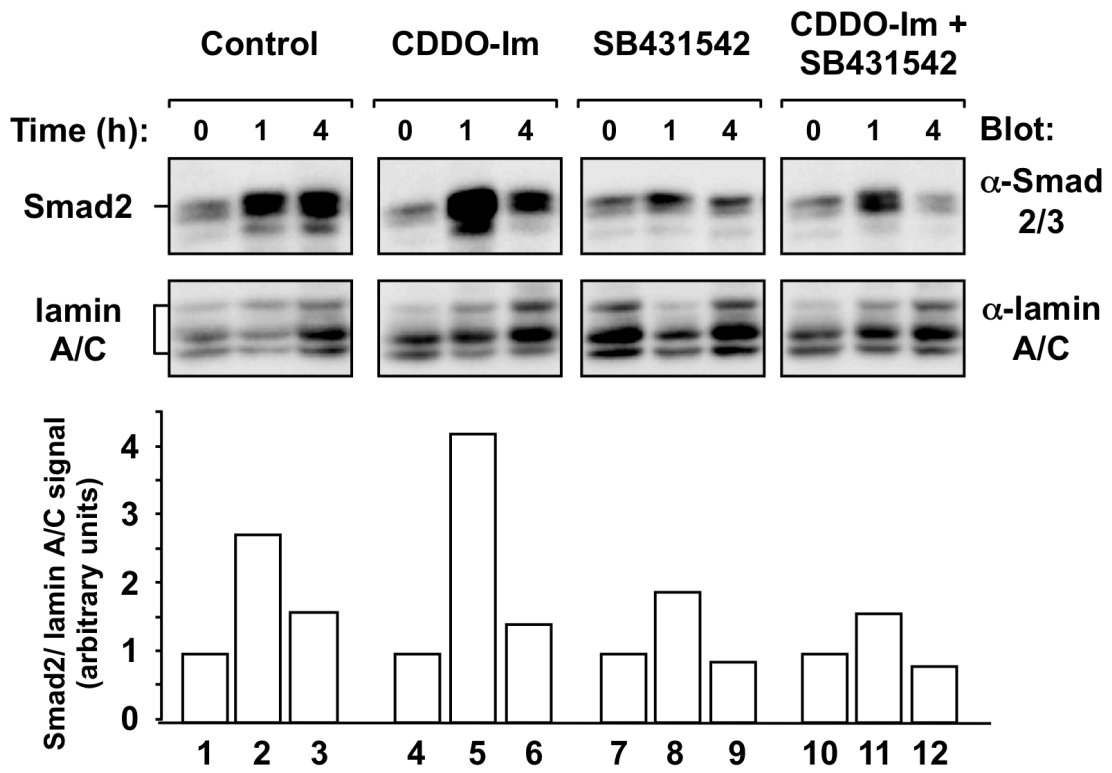
2.4.2   CDDO-Im interferes with TGFβ receptor degradation and trafficking

Efficient phosphorylation and nuclear translocation of Smad2 is dependent on the proper targeting of TGFβ receptors to the early endosomal compartment (8,9,15,42-45). Inhibition of the signal transduction pathway is dependent on Smad2 phosphatase activity (10) and on the association of TGFβ receptors with the Smad7/Smurf2 complex, which inhibits TGFβ receptor kinase activity and promotes receptor complex degradation (11,12). Since I concluded that Smad2 phosphatase activity was not targeted by CDDO-Im, I attempted to determine if CDDO-Im regulates the kinetics of Smad activation by altering TGFβ receptor degradation.   I therefore assessed TGFβ receptor turnover in C2C12 and Cos-7 cells by affinity-labeling receptors with ^{125}I-TGFβ at 4˚C followed by incubation at 37˚C, SDS-PAGE and phosphoimaging analysis.   I observed that both C2C12 and Cos-7 cells exhibited a receptor half-life of approximately 2 hours and that treating cells with CDDO-Im greatly reduced the rate of TGFβ receptor degradation (Figure 2.4A).   I also carried out TGFβ receptor degradation studies in mink lung epithelial cells, Mv1Lu cells, a cell line that has been used to study TGFβ signaling and degradation (12,13).   In Mv1Lu cells, the receptor half-life was observed to be approximately 3 hours (Figure 2.4A). Consistent with the results observed with Cos-7 and C2C12 cells, the rate of TGFβ receptor degradation was delayed to at least 8 hours in the CDDO-Im treated Mv1Lu cells.

A delay in receptor degradation might be due to receptor exclusion from the compartment where degradation occurs or to a reduction in receptor trafficking to that compartment. To clarify this, I investigated receptor internalization and co-localization

Figure 2.4 CDDO-Im delays TGFβ receptor degradation and trafficking.

A) C2C12, Cos-7, or Mv1Lu cells were affinity labeled with ^{125}I-TGFβ at 4˚C, cross-linked and lysed (0 time control) or incubated at 37˚C for 2, 4 or 8 hours prior to lysis. One hundred micrograms of cell lysates were then subjected to SDS-PAGE followed by autoradiography and phosphoimager analysis. The bands representing TGFβ type I receptors (TβRI) or type II receptors (TβRII) are indicated on the left side of each panel. Total receptor levels were quantified and graphed (right panel) as receptor levels (% of control) vs. time (n = 3 ± SD).

B) Mv1Lu cells stably expressing TβRII were incubated at 4˚C with biotinylated TGFβ (bTGFβ) followed by streptavidin Cy3 (red). The cells were then incubated at 37˚C in the absence (left panel; Control) or presence (right panel) of 1 μM CDDO-Im for 1 hour. Cells were then fixed, permeabilized and immunostained with anti-caveolin-1 (Cav-1; green) and anti-EEA1 (EEA1; blue) antibodies. Areas of interest (white boxes) are magnified for both the control and CDDO-Im treated cells and are shown underneath each panel (insets). Representative cells shown indicate the co-localization of bTGFβ with either caveolin-1 or EEA1 as described in the key and by yellow or magenta arrowheads, respectively. The contour (dotted line) of each cell was established using brightfield images and overlayed on the DAPI nuclear stain. Representative micrographs from 3 experiments are shown. Bar = 10 μm.

Figure 2-4
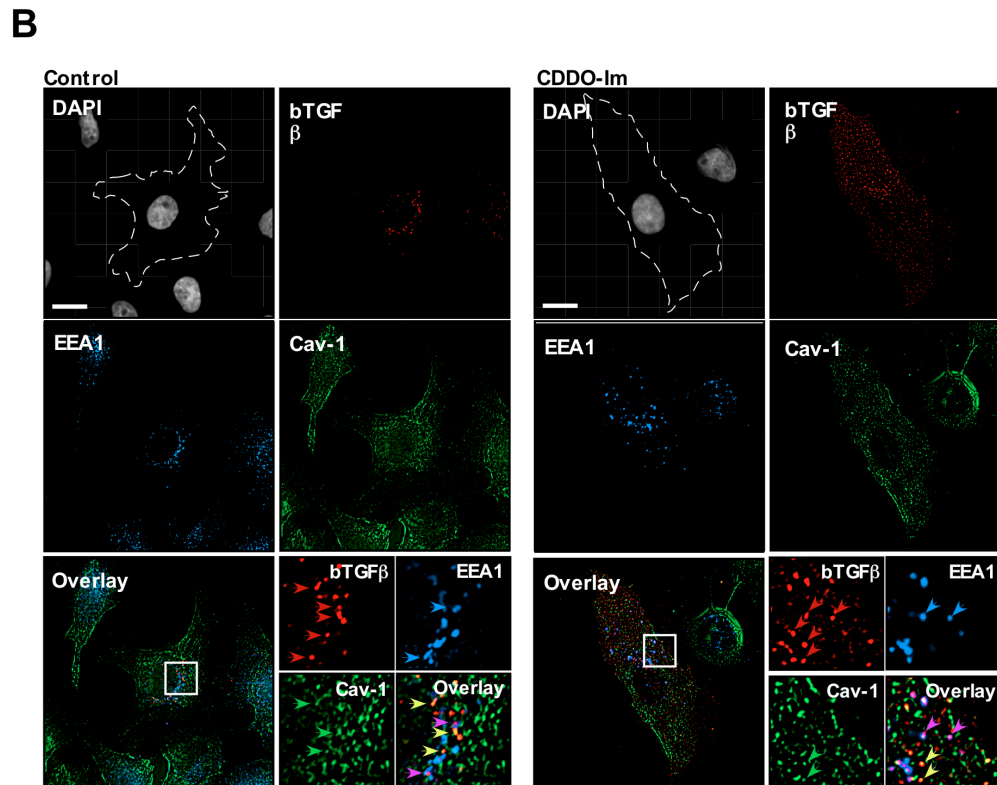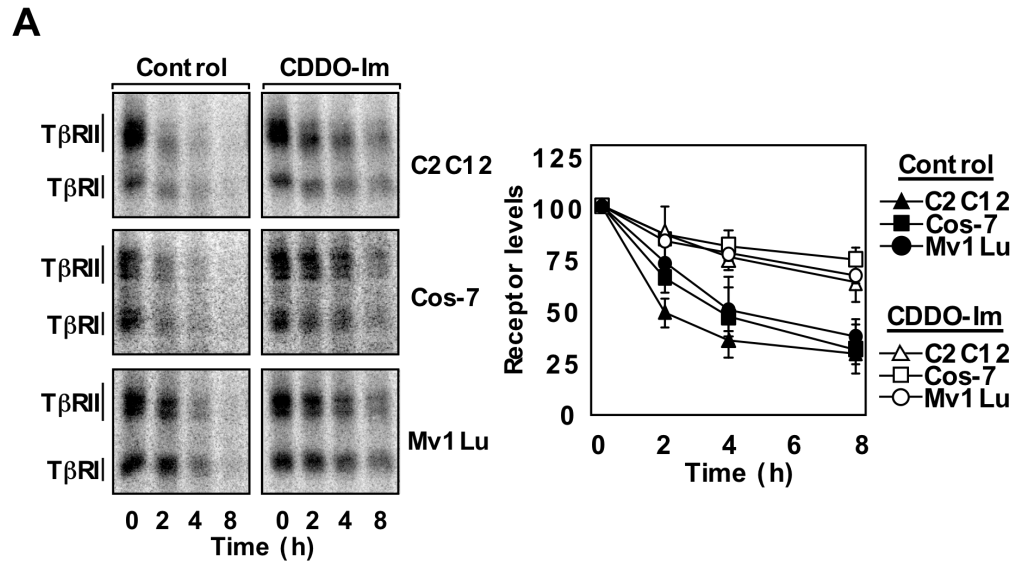
with EEA1- or caveolin-1-positive vesicles in the same cell. As previously reported, Mv1Lu cells expressing HA-tagged TβRII internalize biotinylated TGFβ into both EEA1- and caveolin-1-positive vesicles using deconvolution immunofluorescence microscopy (15) and we have confirmed this phenomenon as well (Figure 2.4B; left panel). In the presence of CDDO-Im, the amount of TGFβ receptor trafficking was reduced, as the majority of receptors after 1 hour of incubation at 37°C did not accumulate in the peri-nuclear regions of cells (Figure 2.4B; right panel). However, co-localization with EEA1 or caveolin-1-positive compartments, even in regions close to the plasma membranes of cells was still readily apparent (Figure 2.4B, inset). Although this suggested that TGFβ receptors had indeed internalized from the plasma membrane, I wanted to test this further by carrying out acid washing experiments (Figure 2.5). Briefly, Mv1Lu cells stably expressing TβRII were incubated at 4°C with biotinylated TGFβ followed by streptavidin-Cy3. The cells were then either acid washed to remove any cell surface labeling or incubated at 37°C in the absence or presence of 1 μM CDDO-Im for 1 hour prior to incubation in acidic conditions. I observed that fluorescent probes bound to cell surface receptors at 4°C were susceptible to acid washing and were removed. However, receptor-bound probes were not removed by acidic treatment after the cells had been incubated at 37°C for 1 hour either in the presence or absence of CDDO-Im (Figure 2.5). This demonstrated that although CDDO-Im altered TGFβ receptor trafficking, it did not inhibit receptor internalization from the plasma membrane.

Interestingly, I noted that caveolin-1-positive vesicles were closer to the plasma membrane in CDDO-Im-treated cells (Figure 2.4B). Moreover, co-localization of TGFβ

Figure 2.5 CDDO-Im does not inhibit TGFβ receptor internalization.

Mv1Lu cells stably expressing HA-tagged TGFβ type II receptors (TβRII) were incubated at 4˚C with biotinylated TGFβ (bTGFβ) followed by streptavidin-Cy3 (red). The cells were then acid washed or incubated at 37˚C in the absence (left panel) or presence (right panel) of 1 μM CDDO-Im for 1 hour prior to acid washing. Bar = 10 μm.

Figure 2-5

A Control

bTGFβ 0'

bTGFβ 0' + acid wash

bTGFβ 1h + acid wash

B CDDO-Im

bTGFβ 0'

bTGFβ 0' + acid wash

bTGFβ 1h + acid wash
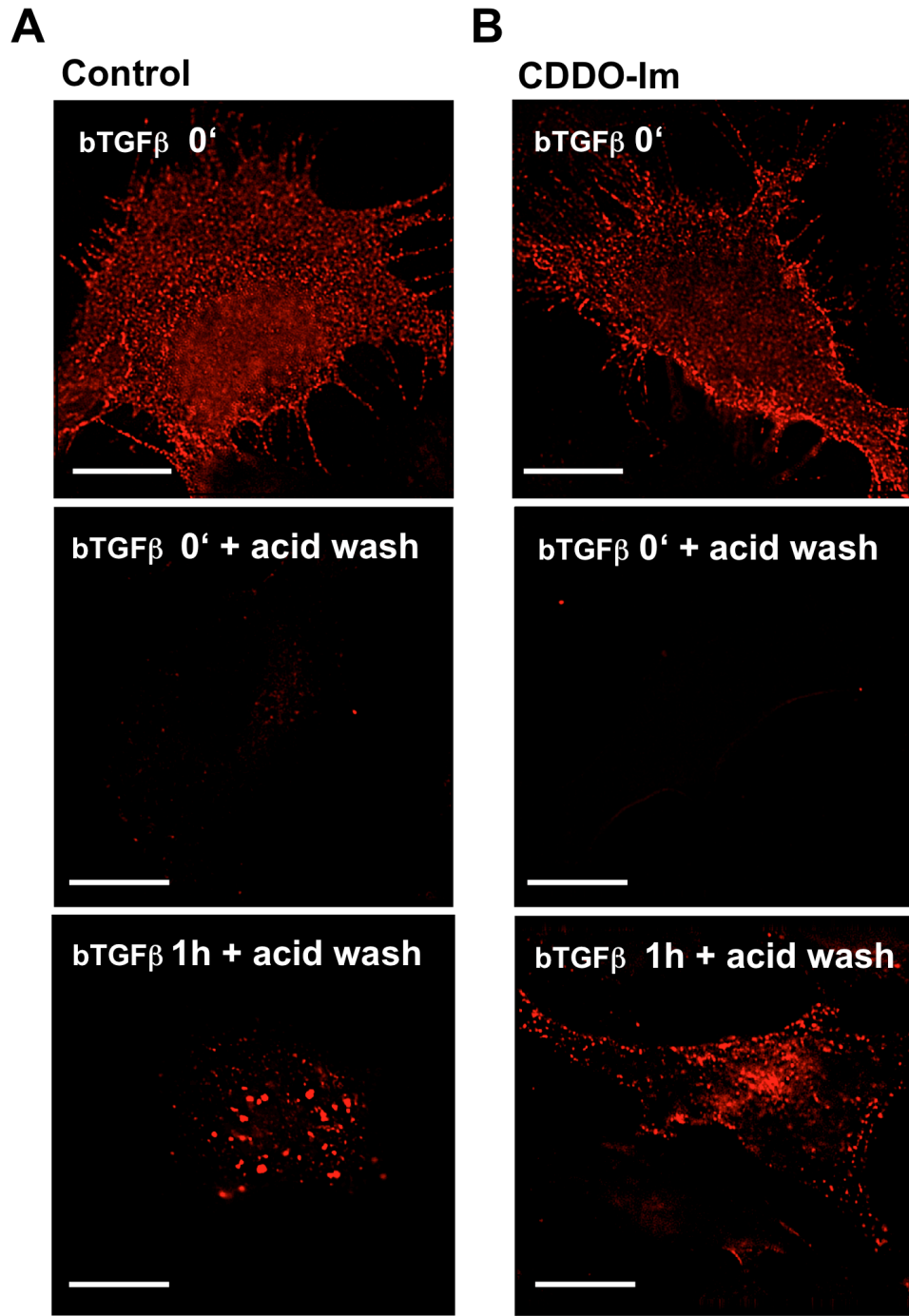
receptors with the caveolin-1-positive compartment became quite prominent. The EEA1-positive vesicles also appeared to have an altered subcellular distribution in cells treated with CDDO-Im.

To further assess the effect of CDDO-Im on the EEA1-positive endosomal compartment, I stained untreated or CDDO-Im-treated cells with anti-EEA1 antibodies and scored the number of cells that demonstrated a peri-nuclear staining pattern versus cells with a dispersed EEA1 staining pattern (Figure 2.6). In cells that were not incubated with CDDO-Im, $72 \pm 5\%$ of the cells counted displayed EEA1 in a peri-nuclear distribution, whereas CDDO-Im treated cells only had $27 \pm 4\%$ peri-nuclear staining (Figure 2.6B). These data indicate that although CDDO-Im does not affect TGFβ entrance into either the EEA1 or caveolin-1-positive compartments, it interferes with the dynamics of their trafficking.

Furthermore, CDDO-Im leads to the dispersal of the EEA1 compartment and an accumulation of caveolin-1-positive structures in close proximity to the plasma membranes of cells.

2.4.3   *CDDO-Im interferes with TGFβ-dependent cell migration*

In order to investigate a functional consequence of extending TGFβ-dependent Smad signaling by CDDO-Im, I assessed TGFβ-dependent cell migration because CDDO-Im, as well as the parental CDDO compound, exhibit potent anti-metastatic activity in animal models (36). To assess polarized cell movement I carried out 'wound

Figure 2.6 CDDO-Im disperses the EEA1-early endosomal compartment.

A) Vehicle-treated Mv1Lu cells (Control) or Mv1lu cells treated with 1 μM CDDO-Im for 1 hour at 37˚C were fixed, permeabilized and immunostained with anti-EEA1 antibodies (EEA1; green). The nuclei were visualized using DAPI staining (blue). A representative cell (inset) was magnified and shown at the bottom. Bar = 10 μm.

B) Three experiments were carried out as described in Panel A. One hundred cells from each experimental condition were analyzed, scored on the basis of peri-nuclear or dispersed staining of EEA1 protein and graphed (n = 3 ± SD).

Figure 2-6
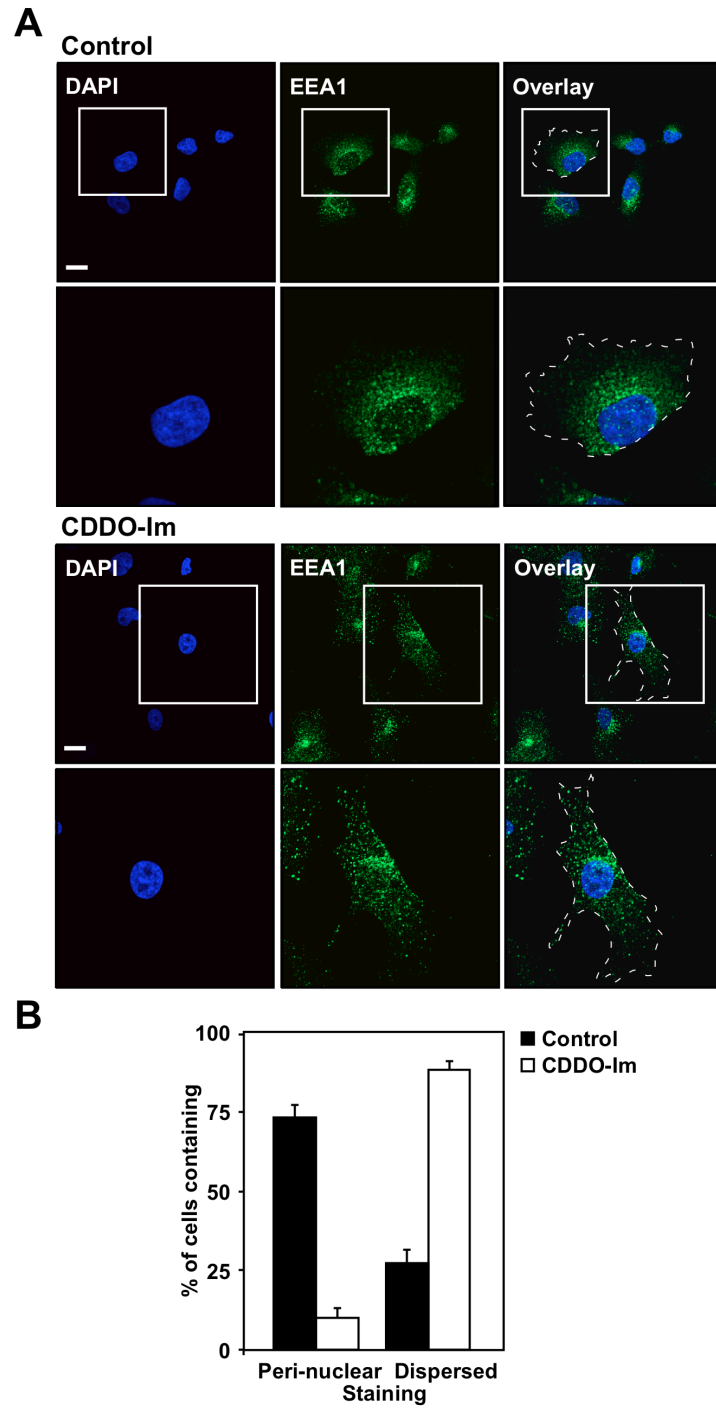
healing' assays using Rat2 fibroblasts. In this assay, regions of confluent Rat2 cells were removed and cell migration into the cell-free space was assessed (Figure 2.7A). When cells were incubated in medium containing low serum, the 'wound' was observed even after 12 hours of incubation at 37°C (Figure 2.7A; top panel). The addition of TGFβ to the media containing low serum induced the cells at the edge of the scratch to migrate perpendicularly into the cell-free space (Figure 2.7A; middle panel). Interestingly, the co-incubation of TGFβ and CDDO-Im inhibited TGFβ–dependent cell migration (Figure 2.7A; bottom panel).

One possibility for this inhibition is that it could be due to a dissociation of TGFβ receptors from the polarity complex protein Par6. This is based on the observation that the association between TGFβ receptors and Par6 is essential for epithelial to mesenchymal transition (EMT) and cell migration (2). I therefore carried out co-immunoprecipitation studies and observed that TGFβ type I and II receptors associate with Par6 in untreated or CDDO-Im treated cells (Figure 2.7B). To assess the specificity of association, I used a Par6 mutant that lacks the PB1 domain (Par6-ΔPB1). This domain was previously shown to be essential for Par6-TGFβ receptor association (34). As expected, I observed little association between the Par6-ΔPB1 mutant and TGFβ receptors (Figure 2.7B). I next assessed the phosphorylation of Par6 by the TGFβ type II receptor using a phospho-Serine 345-specific antibody. The phosphorylation of S345 by TGFβ type II receptors has been shown to be necessary for TGFβ-dependent EMT (34). As seen in the co-immunoprecipitation studies, I did not observe a change in TGFβ receptor dependent phosphorylation of Par6 in the presence of CDDO-Im (data not shown).

Figure 2.7 CDDO-Im delays TGFβ-dependent cell migration but does not disrupt the association of TGFβ Receptors with Par6 protein.

A) Confluent monolayers of Rat2 fibroblasts were scratched and incubated at 37°C for 12 hours in media supplemented with 0.2% FBS (Control; top panel), in media supplemented with 0.2% FBS + 0.5 nM TGFβ (middle panel) or media supplemented with 0.2% FBS + 0.5 nM TGFβ + 0.5 μM CDDO-Im (bottom panel). Cells were then fixed and imaged using brightfied microscopy. The dotted lines indicate the starting point of cell migration. Representative micrographs from 3 experiments are shown. Bar = 0.1 mm.

B) HEK293 cells were transiently transfected with cDNA encoding the proteins indicated and incubated in the absence or presence of 1 μM CDDO-Im for 2 hours prior to lysis and immunoprecipitation with anti-Par6 antibodies. The immunoprecipitates were then subjected to SDS-PAGE and immunoblotting with anti-HA or anti-Flag antibodies to reveal protein complexes.   One hundred micrograms of total protein lysates were immunoblotted (bottom panels) to assess protein expression. The bands corresponding to TGFβ type I receptors (TβRI), TGFβ type II receptors (TβRII), wild type Par6 (Par6 wt.), Par6 lacking the PB1 domain (Par6-ΔPB1) and IgG heavy chain (IgG HC) are indicated. Representative immunoblots from 4 experiments are shown.

Figure 2-7

A

Control

TGFβ

TGFβ + CDDO-Im

B
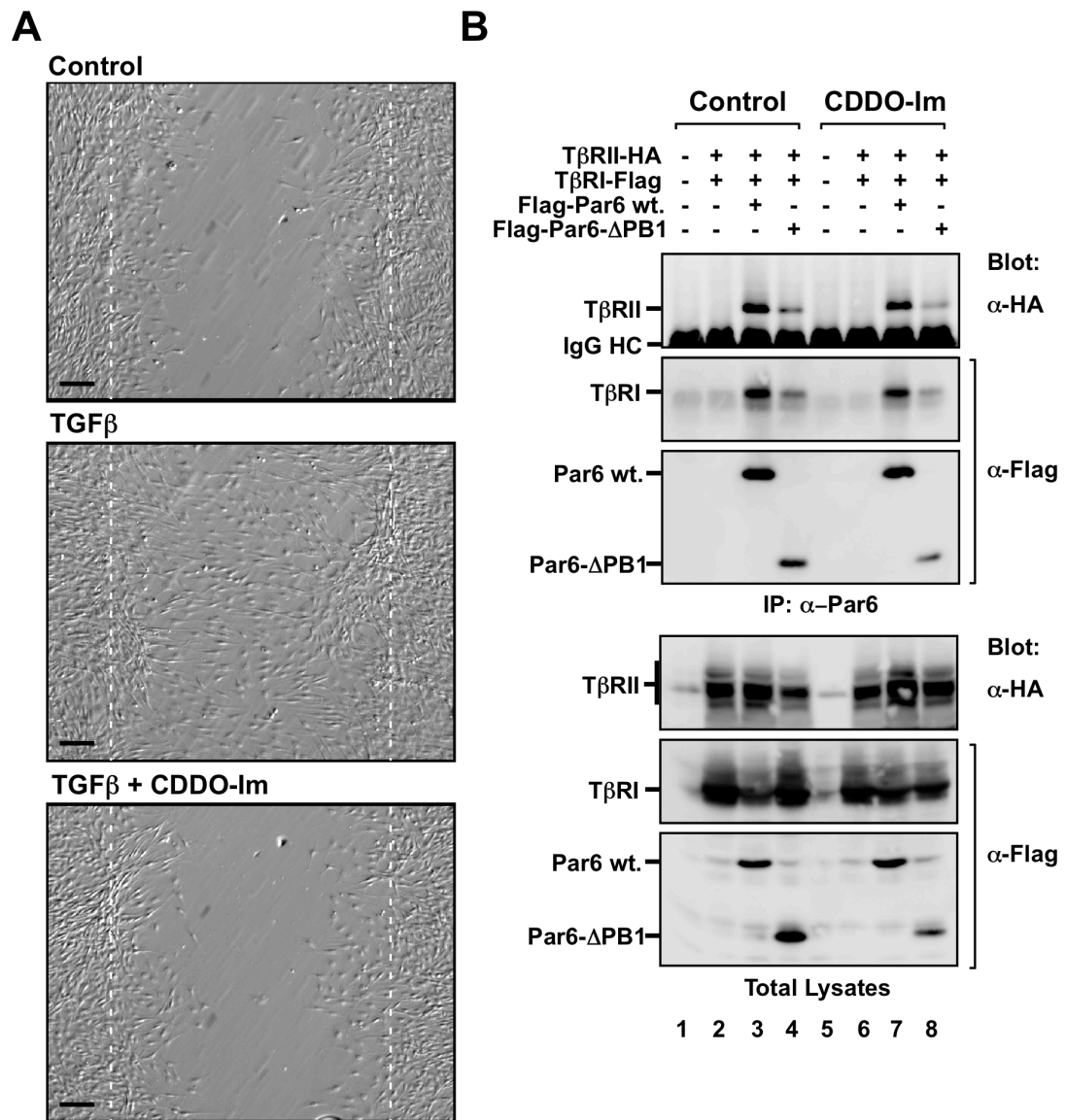
These results suggested that the inhibition of TGFβ-dependent migration by CDDO-Im was not dependent on the association of Par6 with TGFβ receptors or its phosphorylation, and that other cellular targets could be part of the underlying mechanism(s).

2.4.4   CDDO-Im alters cytoskeletal dynamics

The cellular cytoskeleton regulates subcellular position of organelles, vesicular traffic as well as cell polarity and cell migration (46,47). Since I observed that CDDO-Im affects all of these processes in various cell lines, I examined if the cytoskeletal network is a potential target for this compound. First, I evaluated the actin cytoskeleton in control and CDDO-Im-treated cells by staining for filamentous actin (F-actin) using Texas-Red-labeled phalloidin (Figure 2.8A, top and middle panels). In untreated cells, F-actin was observed as both a membrane bound network, as well as stress fibers. In CDDO-Im-treated cells, the pattern of F-actin staining was indistinguishable from control cells, suggesting that the actin cytoskeleton is not a target of CDDO-Im. As a positive control, I treated cells with cytochalasin B, which depolymerizes the actin cytoskeleton, and observed marked structural differences compared to control or CDDO-Im-treated cells (Figure 2.8A, bottom panel).

I next assessed how CDDO-Im affected the microtubule network (Figure 2.8B). Although CDDO-Im did not cause depolymerization of the microtubule network, the compound had a marked effect on the organization and orientation of microtubules. In control cells, the microtubule network radiated outward from the microtubule-organizing

Figure 2.8 CDDO-Im does not affect the actin cytoskeleton but alters the microtubule cytoskeleton.

A) Control Mv1Lu cells (top panel) or cells treated with 1μM CDDO-Im (middle panel) or 10 μM cytochalasin B (bottom panel) for 1 hour were fixed and permeabilized. To visualize the actin cytoskeleton and the nuclei, cells were incubated with Texas Red (TR)-Phalloidin (red) and DAPI stain (blue), respectively. Representative micrographs from 3 experiments are shown. Bar = 10 μm.

B) Mv1Lu cells stably expressing the HA-tagged TβRII were incubated at 4°C with biotinylated TGFβ followed by streptavidin-Cy3 (red; bTGFβ) and transferred to 37°C in the absence (Control) or presence of 1 μM CDDO-Im, 10 μM nocodazole or 10 μM cytochalasin B. The cells were fixed, permeabilized and probed with anti-β-tubulin antibodies (Tubulin; green). The nuclei were visualized using DAPI staining (blue). The micrographs of the microtubule staining for the control (i) or the CDDO-Im treated cells (ii) were magnified to demonstrate microtubule structural differences (right panels). Representative micrographs from 5 experiments are shown. Bar = 10 μm.

Figure 2-8

A

B
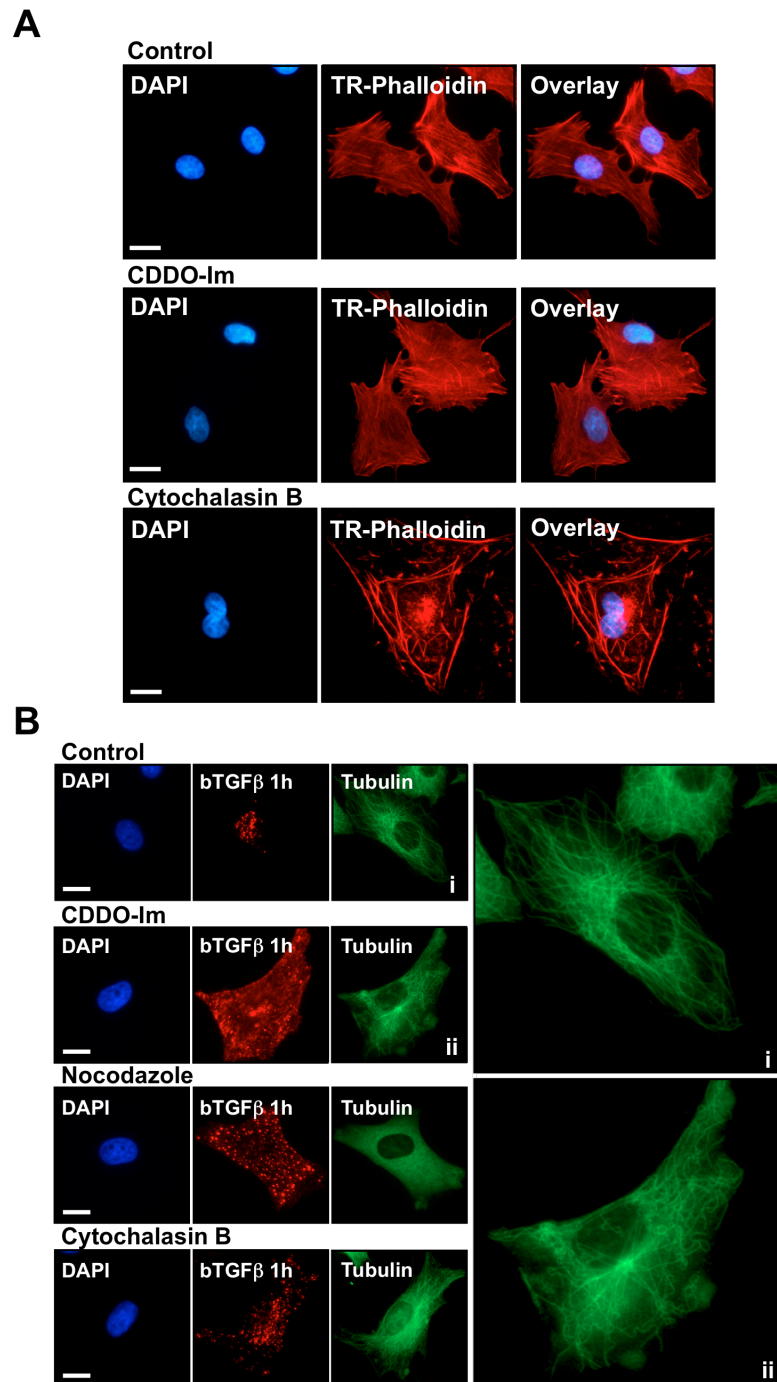
center (MTOC) towards the cell periphery (Figure 2.8B; i). However, in CDDO-Im treated cells, microtubules emanating from the MTOC clearly lacked the characteristic pattern of the microtubule network, appearing to snake through the cytoplasm in a less organized fashion (Figure 2.8B; ii). As positive and negative controls, I treated cells with nocodazole (which causes complete microtubule disruption) and cytochalasin B (which does not alter microtubule networking), respectively. As expected, nocodazole but not cytochalasin B depolymerized microtubules, and interfered with the trafficking of TGFβ receptors. I also examined TGFβ receptor localization after CDDO-Im-treatment and observed that the drug interfered with the distribution of TGFβ receptors. Thus, trafficking of TGFβ receptors to the peri-nuclear region is dependent on proper microtubule organization and polarity. Together, these data indicate that CDDO-Im alters the microtubule network in a fashion that is distinct from the microtubule depolymerizing drug, nocodazole. To further investigate the mechanism of CDDO-Im–dependent microtubule network interference, I first investigated microtubule-capping proteins, which modulate membrane association of the microtubule both at the plasma membrane and with vesicles (48). CLIP170 is a major capping protein that associates with the plus end of growing microtubules and links the microtubule to vesicles and to the plasma membrane via interactions with IQGAP1 (32). Given the meandering nature of the microtubules in CDDO-Im-treated cells, I postulated that membrane and vesicular attachment might also be affected by CDDO-Im.

To investigate the effect of CDDO-Im on CLIP170 association with microtubules, Rat2 fibroblasts was transiently transfected with GFP-tagged CLIP170 and its localization was assessed by immunofluorescence microscopy. In control cells, CLIP170

was observed to be associated with the positive end of growing microtubules (Figure 2.9A; left panel), but in CDDO-Im-treated cells, CLIP170 was redistributed to large puncta in the cytoplasm and was no longer associated with microtubules (Figure 2.9A; right panel). To further address this, I examined CLIP170 association with the cytoskeleton by biochemical fractionation. For this, I solubilized membranes and separated the soluble fraction from the insoluble cytoskeleton by centrifugation (Figure 2.9B), a method that effectively removes the majority of cellular organelles from the cytoskeleton fraction (Figure 2.10). As expected, tubulin and most of actin protein was in the cytoskeletal fraction in control cells (Figure 2.9B), whereas in nocodazole-treated cells, tubulin, but not actin, partitioned with the soluble fraction. Consistent with the immunofluorescence studies, CDDO-Im treatment of cells did not induce a solubilization and loss of tubulin from the cytoskeletal fraction. Interestingly, CLIP170 was consistently present in the cytoskeletal fraction regardless of the treatment. This was surprising because I assumed that the dissociation of CLIP170 from microtubules by either nocodazole or CDDO-Im treatment would cause the majority of the CLIP170 to be concentrated in the soluble fraction. However, CLIP170 remained in the cytoskeletal fraction suggesting that either CDDO-Im did not induce complete CLIP170 dissociation from the cytoskeleton or that CLIP170 aggregated in punctate masses in response to CDDO-Im. In order to distinguish between the two possibilities, the dynamics of CLIP170 mobility was visualized in real time by microinjecting cDNA encoding GFP-CLIP170 into Rat2 fibroblasts and carrying out time-lapse immunofluorescence microscopy. In control cells, the GFP-CLIP170 followed the growing microtubules

Figure 2.9 CDDO-Im induces CLIP170 to dissociate from microtubules.

A) Rat2 fibroblasts transiently expressing GFP-CLIP170 were incubated in the absence (left panels) or presence of 1µM CDDO-Im (right panels) for 1 hour and were then fixed, permeabilized and immunostained with anti-β-tubulin antibodies (red). The co-localization of GFP-CLIP170 (green) and microtubules (red) results in yellow staining. Bar = 10 µm.

B) Cos-7 cells were incubated in the absence (Control) or presence of 1 µM CDDO-Im or 10 µM nocodazole (Nocod.) for 1 hour and then subjected to lysis at 37˚C to separate soluble proteins (S) from the cytoskeleton (C). Following processing for SDS-PAGE, cell lysates were immunoblotted with antibodies raised against CLIP170, IQGAP1, tubulin, actin or Rac1. The relative position of each resolved protein is indicated. Representative blots from 4 experiments are shown.

C) Rat2 fibroblasts were microinjected with a GFP-CLIP170 cDNA and incubated for 4 hours at 37˚C. The movement of GFP-tagged CLIP170 in control cells (top time course) or cells incubated with 0.1 µM CDDO-Im (bottom time course) were imaged using time-lapse immunofluorescence microscopy. The starting point of movement of a representative CLIP170 cap is indicated by a red bar and the white arrow follows the movement of the CLIP170 signal along microtubules in the control cell and in large aggregates in the CDDO-Im treated cell. Representative images from 3 experiments are shown. Bar = 10 µm.
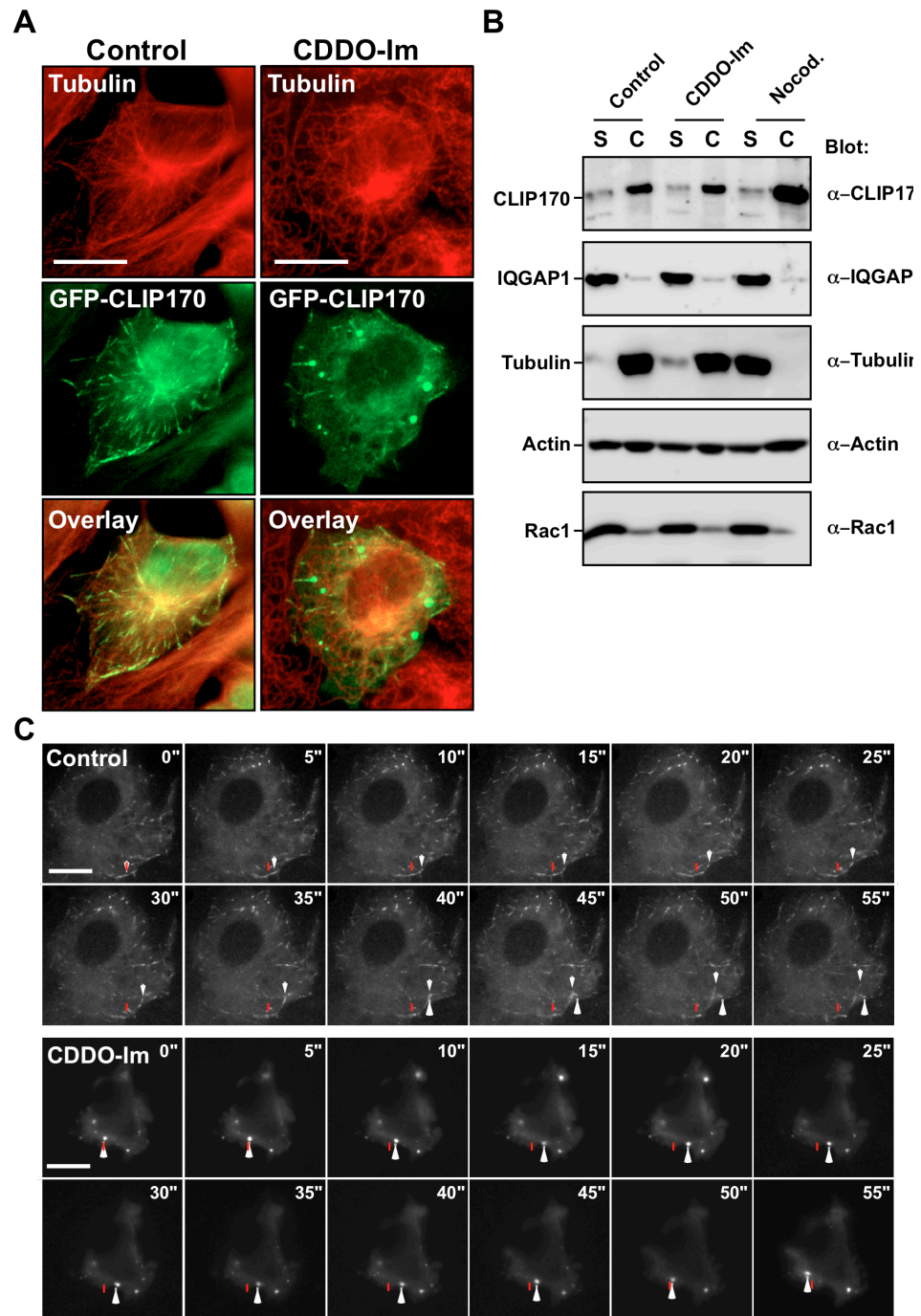
Figure 2-9

Figure 2.10 Characterization of the soluble and cytoskeletal fractions.

Cos-1 cells were lysed at 37˚C to separate soluble proteins (S) from the cytoskeleton (C). Following processing for SDS-PAGE, cell lysates were immunoblotted with antibodies raised against proteins enriched in the cytoskeleton, anti-tubulin and actin; the early and late endosome, EEA1 and LAMP-1, respectively; the endoplasmic reticulum, Calnexin; and the Golgi apparatus, GM130. The relative migration of each protein is indicated.

Figure 2-10
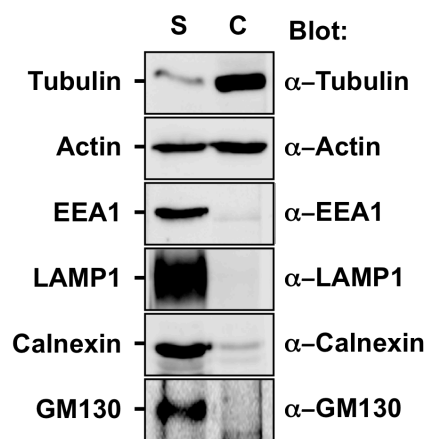
(Figure 2.9C and please see supplementary movie 1: http://www.jbc.org/content/suppl/2008/04/25/M704064200.DC1/Supp_Movie_1_clip-170_control.mov). In the CDDO-Im treated cells, the punctate aggregates that contained the GFP-CLIP170 remained mobile at lower triterpenoid concentrations (0.1 μM; Figure 2.9C and please see supplementary movie 2: http://www.jbc.org/content/suppl/2008/04/25/M704064200.DC1/Supp_Movie_2_clip-170_Im_0.1_micro.mov), but were immobilized at higher doses (1 μM; please see supplementary movie 3: http://www.jbc.org/content/suppl/2008/04/25/M704064200.DC1/Supp_Movie_3_clip-170_Im_1_micro.mov), thereby stalling the formation of a normal microtubule network. These data suggest that CDDO-Im affects the organization of the microtubular network by interfering with the function of the capping protein, CLIP170.

2.4.5   CDDO-Im targets the polarity complex

In order to evaluate the cellular target of triterpenoids, I attempted to identify the subcellular localization of triterpenoids by utilizing a biotinylated version of CDDO. The biotinylated compound elicits identical cellular responses as the CDDO-Im, albeit at higher concentrations (49) and allows for the assessment of triterpenoid subcellular localization by immunofluorescence microscopy (Figure 2.11). As controls, biotin or CDDO did not exhibit any fluorescence signal (Figure 2.11A and B). However, I observed that CDDO-biotin localized in the nuclei and at the cell membrane in patches that were consistent with the leading edge of migrating cells. To confirm this possibility,

Figure 2.11 Subcellular targeting of biotinylated CDDO.

Rat2 fibroblasts were grown to 100% confluency and scratched to create a wound. After incubation for 6 hours to allow cell polarization and migration, cells were fixed, permeabilized and incubated with monoclonal anti-Rac1 antibodies (Rac1; green) and biotin (A), CDDO (B), or biotinylated CDDO (CDDO-biotin; C) followed by Cy2-labeled anti-mouse antibody and Cy3-labeled streptavidin. The co-localization of Rac1 (green) with CDDO-biotin (red) at the leading edge of migrating cells is demonstrated in the inset (yellow arrowheads). The white arrow indicates the direction of cell movement and DIC microscopy was included to visualize the leading edge of migrating cells. Representative images from 4 experiments are shown. Bar = 10 μm.
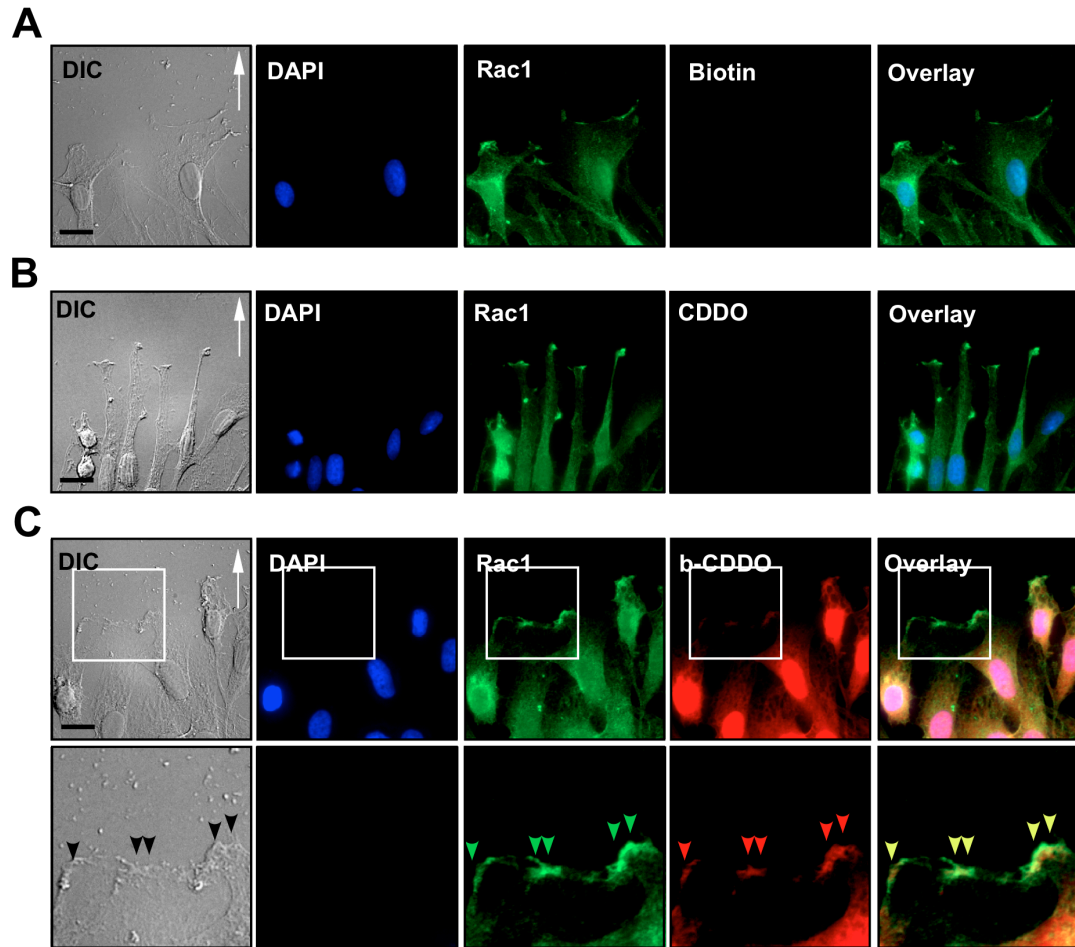
Figure 2-11

I immunostained scratched Rat2 fibroblasts using CDDO-biotin and Rac1 antibodies and observed that Rac1 co-localized with biotinylated CDDO-biotin at the leading edge of the migrating cells (Figure 2.11C).

I next examined the subcellular localization of molecules known to be involved in the leading edge of polarized cells (Figure 2.12). To carry this out I first assessed the morphology of the leading edge of migrating Rat2 cells by DIC microscopy and observed that untreated cells were elongated, and had distinct lamellipodia whereas CDDO-Im treated cells were round. In order to assess this in a dynamic fashion, I carried out a real-time study where Rat2 fibroblasts were wounded and incubated in control or CDDO-Im containing media over time. Brightfield images were collected over 13 hours and arranged in a movie (please see supplementary movie 4:http://www.jbc.org/content/suppl/2008/04/25/M704064200.DC1/Supp_Movie_4_Rat2_ migration.mov).

The positioning of CDDO-biotin at the leading edge of migrating cells (Figure 2.11C) and the CDDO-Im-dependent loss of lamellipodia (Figure 2.12A, bottom panel) prompted us to investigate the link between microtubules and the polarity complex, found at the leading edge of migrating cells (Figure 2.12B). For this line of investigation, I carried out wound-healing assays by first scratching Rat2 cells, allowing them to polarize and migrate for 6 hours and then incubate them in media containing CDDO-Im or nocodazole for an additional 2 hours. This experimental approach would allow us to study the effects of the drugs on the fate of the polarity complex after it had been pre-established for 6 hours. I therefore first assessed tubulin and CLIP170 in scratched Rat2

fibroblasts (Figure 2.12C). In addition to the cell body, control cells displayed endogenous CLIP170 decorating the leading edge of migrating cells, where tubulin extended to the plasma membrane. In contrast, CDDO-Im caused endogenous CLIP170 to disperse from the leading edge into punctate structures reminiscent of those observed after GFP-CLIP170 expression (see Figure 2.9A). I also examined the localization of tubulin and CLIP170 proteins in nocodazole-treated cells. As expected, microtubules were disrupted, but despite the accompanying alteration in cellular morphology, tubulin and CLIP170 staining remained co-localized to the leading edge in these cells (Figure 2.12C, bottom panel). This was notably different from the CDDO-Im treated cells, where there was an absence of CLIP170 staining at the leading edge. The association of microtubules to the leading edge of cells is facilitated by CLIP170, which links microtubules to IQGAP1 (32). Since CLIP170 failed to localize to the leading edge of CDDO-Im-treated cells, I examined if CDDO-Im also affects IQGAP1 targeting to the leading edge of polarized cells. In untreated cells, IQGAP1 localized to the leading edge of migrating cells and CDDO-Im-treatment abrogated this localization (Figure 2.13A). Moreover, general microtubule destabilization with nocodazole did not affect IQGAP1 localization, consistent with my observation that this drug does not affect polarity complex once it has already been established (Figure 2.13A and B). Finally, in order to determine if CDDO-Im causes a complete dissociation of proteins present in the polarity complex, I assessed the association of IQGAP1 with Rac1 (Figure 2.13C). I did not find any appreciable dissociation of Rac1 that was co-immunoprecipitated with IQGAP1 antibodies either in CDDO-Im- or nocodazole-treated cells. These data, in conjunction to the observation that CDDO-Im induced the redistribution of IQGAP1 at the plasma

Figure 2.12 CDDO-Im interferes with cell morphology and the localization of CLIP170 at the leading edge of migrating cells.

A) Rat2 fibroblasts were grown to 100% confluency and scratched to create a wound. The cells were then incubated for 4 hours at 37°C and then treated with control medium or medium containing 1 μM CDDO-Im for an additional 2 hours before being fixed and processed for DIC microscopy. The dotted lines indicate the starting point of cell migration. Representative micrographs from three experiments are shown. White arrows indicate the direction of cellular movement. Bar = 10 μm.

B) Model of microtubule association with a subset of polarity complex proteins at the leading edge of migrating cells. The microtubule capping protein, CLIP170, associates with IQGAP1. PKCζ is shown in this model as a member of the polarity complex and the white arrow indicates the direction of cellular movement.

C) Rat2 fibroblasts were grown to 100% confluency, scratched and then incubated for 6 hours at 37°C. Cells were then incubated an additional 2 hours in control medium (Control; top panels), or media containing 1 μM CDDO-Im (middle panels) or 10 μM nocodazole (bottom panels) prior to fixation, permeabilization and immunostaining with anti-CLIP170 (CLIP170) and anti-tubulin (Tubulin) antibodies. The scratches were subjected in the horizontal plane above the cells shown, and the leading edge of migrating cells containing microtubule ends and CLIP170, are indicated with green and red arrowheads, respectively. Yellow arrowheads show the co-localization of microtubule ends and CLIP170. White arrows indicate the direction of cellular movement. Bar = 10 μm.
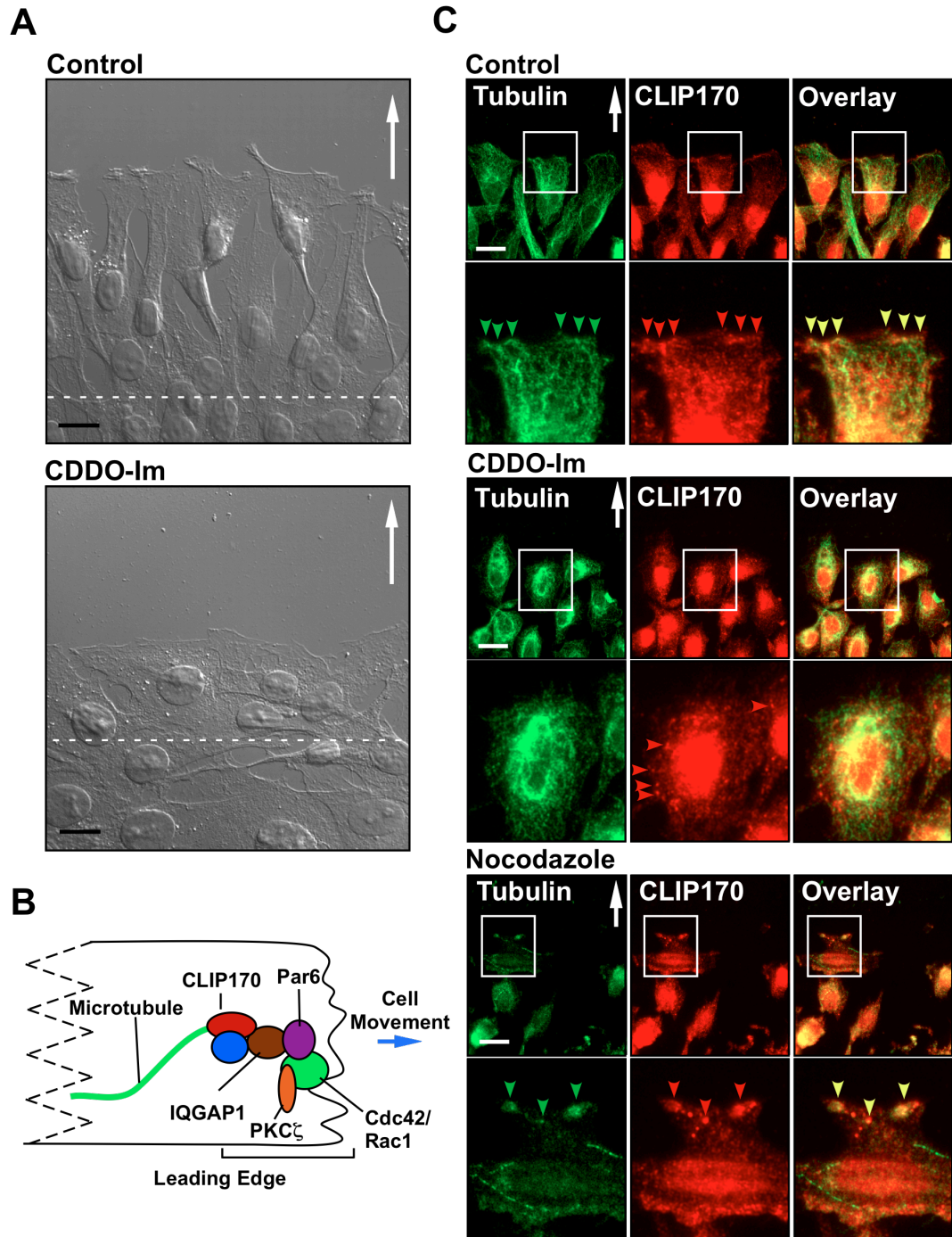
Figure 2-12

Figure 2.13 Reduction of IQGAP1 localization at the leading edge of migrating cells in response to CDDO-Im treatment.

A) Cells were scratched and allowed to migrate into the wound for 6 hours in order to establish cell polarity prior to incubation with control medium (top panels) or media containing 1μM CDDO-Im (middle panels) or 10 μM nocodazole (bottom panels) for an additional 2 hours. Cells were then fixed, permeabilized and immunostained for endogenous Rac1 (green) and IQGAP1 (red) protein. A representative area of interest (white box) from each condition was enlarged and shown (inset). Green and red arrows indicate Rac1 and IQGAP1 at the leading edge of migrating cells, respectively. The co-localization of Rac1 with IQGAP1 is indicated by yellow arrowheads. The white arrows indicate the direction of cellular movement. Bar = 10 μm.

B) Quantitation of cells containing Rac1 or IQGAP1 at the leading edge of migrating cells was carried out as described in the Experimental Procedures and graphed (n=3 ± SD). *,#: p<0.0001.

C) Untreated cells (Control) or cells incubated with either CDDO-Im or nocodazole (Nocod.) were lysed and immunoprecipitated with non-immune IgG (Non-IM IgG) or anti-IQGAP1 antibodies (α-IQGAP1) and immunoblotted (Blot) with anti-IQGAP1 or anti-Rac1 antibodies. The relative mobilities of Rac1 or IQGAP1 are indicated on the left of each panel. One hundred micrograms of total protein lysates were immunoblotted and shown on the left. Representative blots from 3 experiments are shown.

Figure 2-13

A

B

C
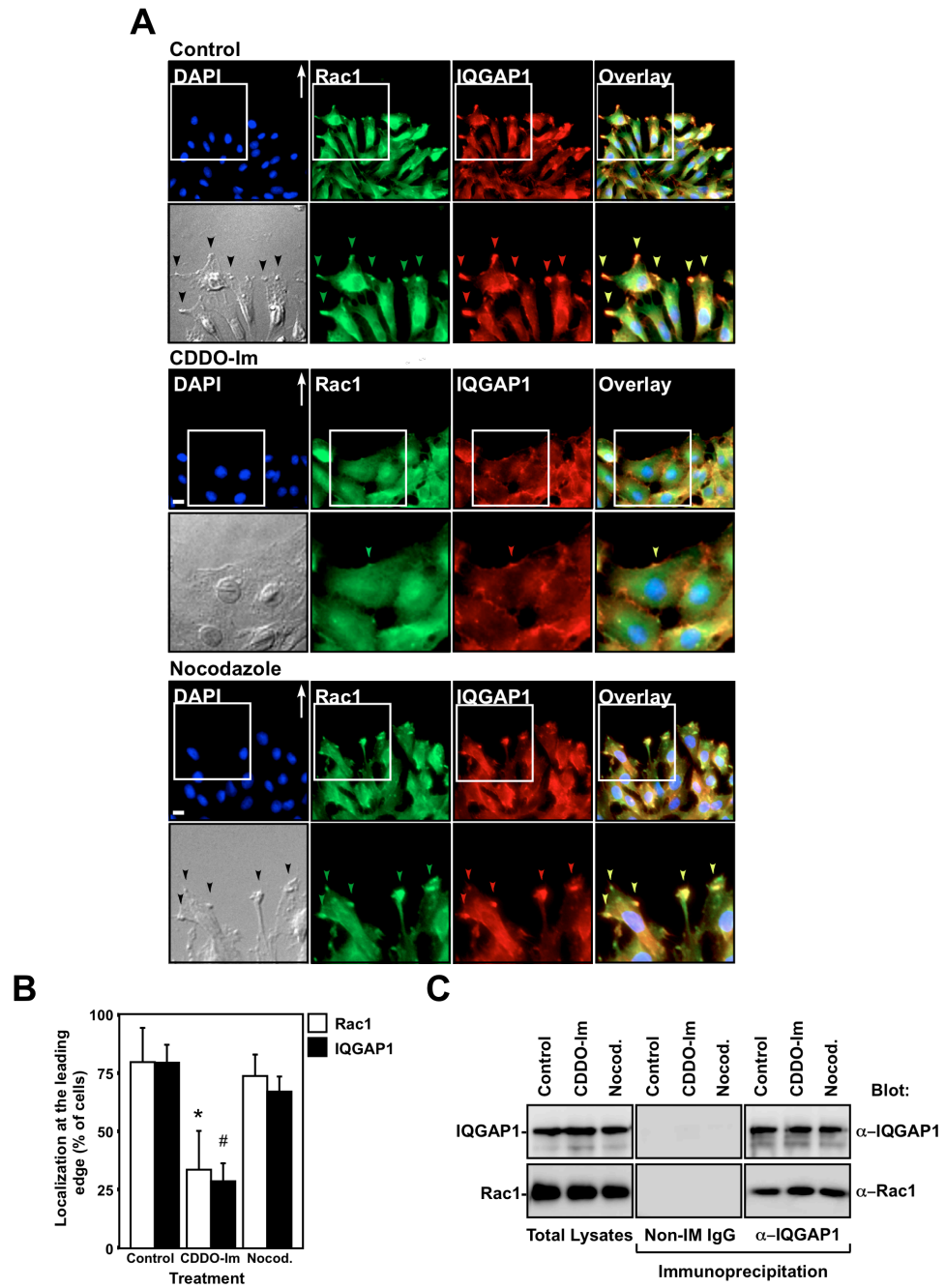
membrane, suggested that the localization of Rac1 and IQGAP1 to the leading edge might be affected by triterpenoid treatment.

To expand my analysis to other members of the polarity complex, I assessed the localization of Rac1 and PKCζ, both of which normally localize to the leading edge of cells undergoing polarized cell movement (Figure 2.14). In untreated cells, both Rac1 and PKCζ were observed to co-localize at the leading edge of migrating cells (Figure 2.14A). However in response to CDDO-Im, I observed that although Rac1 localized to the membrane, it was less organized and dispersed along the cell membrane. Furthermore, PKCζ staining was altogether absent from the cell membrane of CDDO-Im-treated cells (Figure 2.14B). Nocodazole treatment altered the morphology of leading edge cells, and Rac1 was now found in numerous protrusive structures all around the cell (Figure 2.14C). In these cells, PKCζ remained co-localized with Rac1, consistent with the lack of change in IQGAP1 or CLIP170 localization observed after nocodazole treatment. These results indicate that the function and assembly of the polarity complex is disrupted in response to CDDO-Im treatment and that this effect is not dependent on general microtubule disruption since polarity complex constituents remained associated in nocodazole-treated cells.

Based on my observations that CDDO-Im does not disrupt the association between Par6 and TGFβ receptors (Figure 2.7B) but does disrupt the localization of members of the polarity complex (Figures 2.12, 2.13, 2.14), I predicted that the localization of TGFβ receptors and Par6 at the leading edge might be reduced and/or abrogated in the presence of CDDO-Im. To test this, I assessed the localization of Par6

Figure 2.14 CDDO-Im disrupts PKCζ localization at the leading edge of polarized cells.

Rat2 fibroblast monolayers were scratched and allowed to grow into the wound for 6 hours in order to polarize before being incubated in the absence (Control; **A**), or presence of 1 µM CDDO-Im **(B)** or 10 µM nocodazole **(C)** for an additional 2 hours. Cells were then fixed, permeabilized and immunostained for endogenous Rac1 (green) or PKCζ (red) using anti-Rac1 and anti-PKCζ antibodies, respectively. A representative area of interest (white box) from each condition was enlarged and shown (inset). Green and red arrows indicate Rac1 and PKCζ at the leading edge of migrating cells, respectively. The co-localization of Rac1 with PKCζ is indicated by yellow arrowheads. The white arrows indicate the direction of movement. Representative images from 4 experiments are shown. Bar = 10 µm. *,#: $p < 0.0001$.

Figure 2-14

A

Control
DAPI | Rac1 | PKCζ | Overlay

CDDO-Im
DAPI | Rac1 | PKCζ | Overlay

Nocodazole
DAPI | Rac1 | PKCζ | Overlay

B
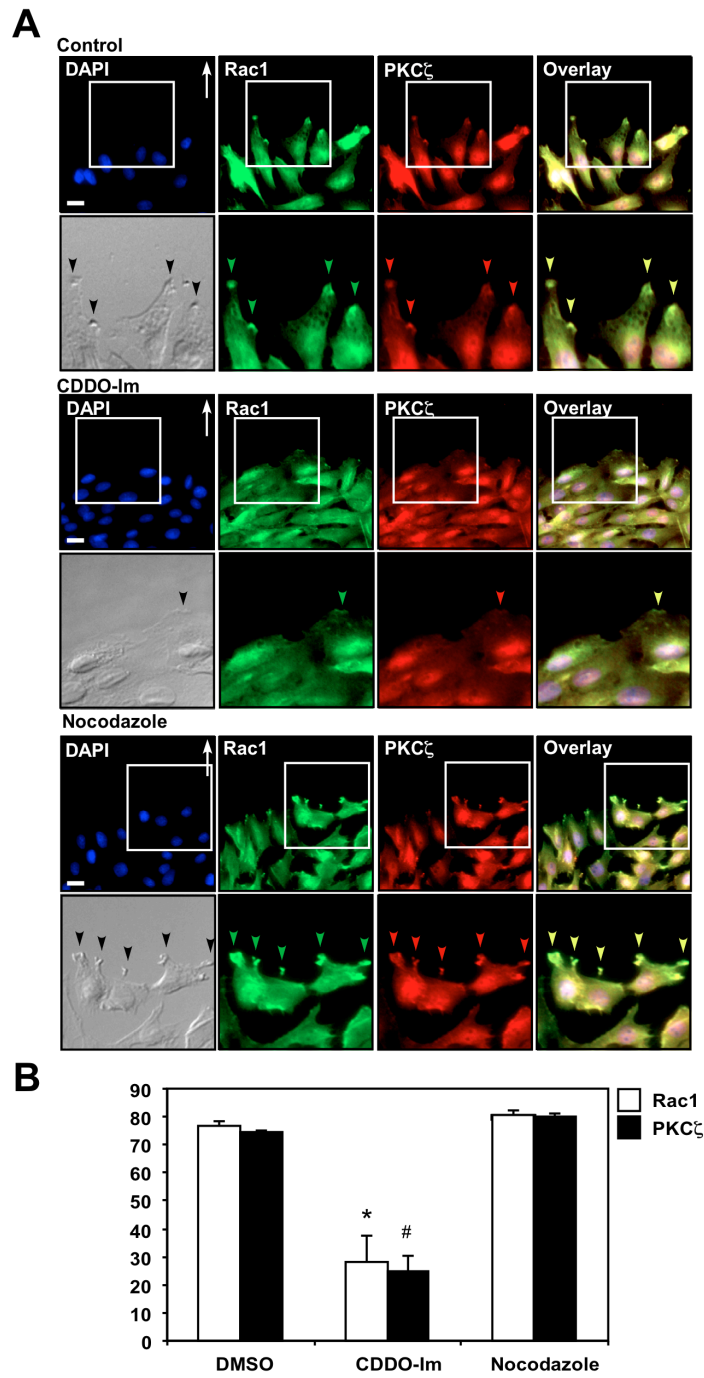
and TβRII by immunofluorescence microscopy (Figure 2.15). In untreated cells, I observed that both Par6 and TGFβ receptors were indeed present at the leading edge of migrating cells and that they both co-localized with Rac1 (Figure 2.15). However, in response to CDDO-Im treatment, the amounts of Par6 and TβRII at the leading edge of cells were markedly reduced (Figure 2.15). These results further support my observations that CDDO-Im disrupts TGFβ-dependent cell migration by disrupting the polarity complex.

Taken together, my results demonstrate that the triterpenoid CDDO-Im alters TGFβ receptor trafficking and signal transduction, microtubule-plasma membrane attachments, as well as vesicular transport. The mechanism of affecting cell polarity and migration is dependent on the disruption of CLIP170 capping of microtubules, which causes the disruption of microtubule attachments with the polarity complex. Furthermore, the co-localization of triterpenoid with Rac-1 at the leading edge of migrating cells positions it to interfere with cell polarity by disrupting the localization of IQGAP1, PKCζ, Par6 and TGFβ receptors at the leading edge of migrating cells.

Figure 2.15 CDDO-Im disrupts Par6 and TGFβ Receptor localization at the leading edge of migrating cells.

Rat2 fibroblast monolayers were scratched and allowed to grow into the wound for 6 hours before being incubated in the absence (Control), or presence of 1 μM CDDO-Im for an additional 2 hours. Cells were then fixed, permeabilized and immunostained for endogenous Rac1 (green) and Par6 (red) using anti-Rac1 and anti-Par6 antibodies **(A)** or for endogenous Rac1 (green) and TGFβ type II receptor (TβRII; red) using anti-Rac1 and anti-TβRII antibodies, respectively **(B)**. A representative area of interest (white box) from each condition was enlarged and shown (inset). Green arrowheads indicate Rac1 and red arrowheads indicate Par6 or TβRII at the leading edge of migrating cells. The co-localization of Rac1 with Par6 or TβRII is indicated by yellow arrowheads. The white arrows indicate the direction of movement. Bar = 10 μm. Cells containing Rac1, Par6 or TβRII at the leading edge were quantitated from 3 experiments carried out as described in Panels A and B (± SD) and graphed **(C)**. *,#: $p < 0.0001$.

Figure 2-15
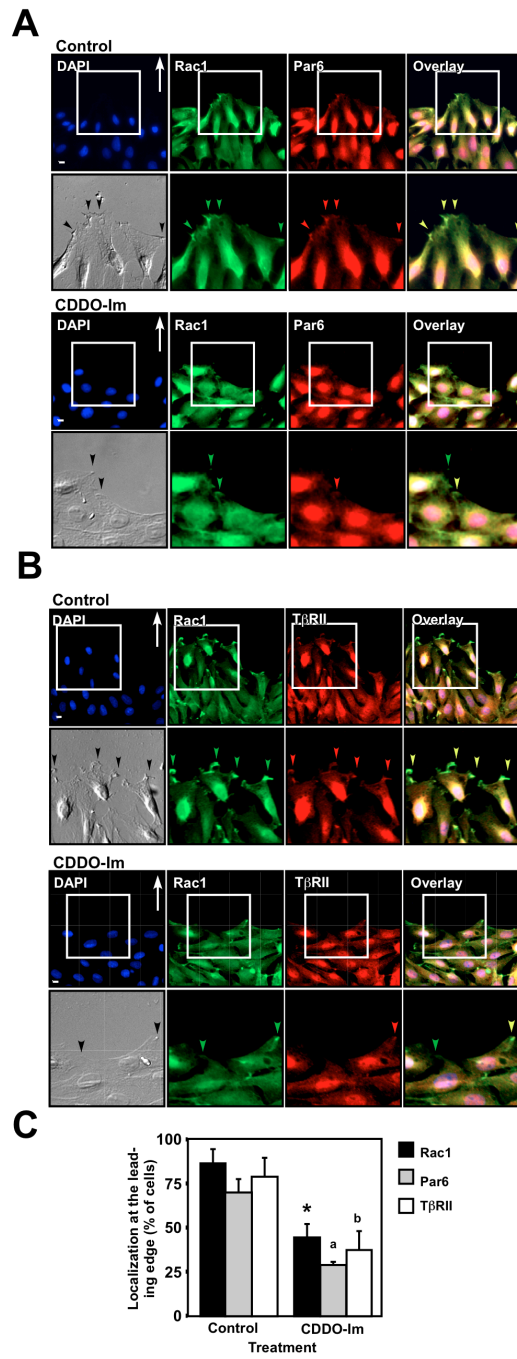
2.5   DISCUSSION

TGFβ is a growth factor that acts as a tumor suppressor or promoter depending on cellular context (4,50). TGFβ receptors propagate several signaling pathways, two of which are essential for epithelial to mesenchymal transition (EMT), the Smad pathway (51,52) and the Par6 pathway (34,53). In this study I found that CDDO-Im inhibits TGFβ-dependent cell migration. In order to identify the mechanism I first assessed its effect on TGFβ signaling. As previously described in studies using U937 and HL60 cells (37,39), I found that CDDO-Im extended the phosphorylation profile of Smad2, however, further investigation suggested that this was not due a decrease in Smad2 phosphatase activity (Figures 2.1, 2.2 and 2.3). I next assessed receptor trafficking and degradation. Previous studies indicated that by perturbing the lipid raft compartment, the distribution of internalized cell surface TGFβ receptors could be shifted from the caveolin-1-positive compartment to the EEA1-early endosomal compartment, leading to enhanced signaling and delayed receptor degradation (15). I observed that CDDO-Im did delay receptor degradation however, unlike lipid-raft destabilizing agents such as nystatin, CDDO-Im did not shift receptor equilibrium toward the caveolin-1-positive compartment. Instead, CDDO-Im delayed overall receptor traffic and induced both caveolin-1- and EEA1-positive vesicles to be localized to the peri-plasma membrane regions of cells (Figures 2.4 and 2.6). This led us to conclude that the compound was affecting a cellular structural component and quite possibly the cytoskeleton, as both the actin and microtubule cytoskeleton have been shown to be important for the trafficking of vesicles from the plasma membrane to the cell interior (21,46,54,55).

Further study revealed that although the actin cytoskeleton was not morphologically affected, the microtubule network became disorganized (Figure 2.8). The disorganization of vesicular positioning in the cell is a hallmark of microtubule catastrophe brought on by destabilizing drugs such as nocodazole (20). Indeed the microtubule network will disperse if cells are treated with high triterpenoid concentrations (56). However, in the present study I used lower concentrations of CDDO-Im, consistent with the concentrations used in animal studies (57-59), and found that CDDO-Im does not dissolve the microtubule cytoskeleton. Rather, I observed that microtubules in CDDO-Im treated cells take on a looping morphology that is reminiscent of a lack of proper attachment to the cell membrane and loss of cell polarity. I therefore tested if microtubule-capping proteins might be affected since they act as anchorage points both between microtubules and vesicles, and between microtubules and the cell membrane (26,48). The latter process involves a number of intermediate molecules, such as CLIP170, and members of the polarity complex, Cdc42/Rac1, via IQGAP1 (32,33,48).

Interestingly, CLIP170 and IQGAP1 were found to dissociate from the leading edge of cells in response to CDDO-Im. These observations explain both the loss of vesicular traffic to the cell interior as well as the loss of microtubule targeting and association with the leading edge of cells (Figure 2.9, 2.12 and 2.13). Of note, nocodazole, a drug that disrupts microtubules, was unable to affect the polarity complex after the cells were allowed to polarize in the absence of drugs. These observations indicate that the effects of CDDO-Im on CLIP170 dissociation from microtubules and the loss of concentration of molecules in the polarity complex are distinct from compounds that dissociate CLIP170 from microtubules via microtubule catastrophe. My results also

suggest that the association of different members of the polarity complex have variable stability. Indeed, I found that Rac1 remains associated with IQGAP1 regardless of the pharmacological treatment (Figure 2.13). This stable association is also reflected in the fractionation studies, as the majority of Rac1 and IQGAP1 both partitioned with the soluble fractions while CLIP170 was concentrated in the cytoskeletal fractions (Figure 2.9). However, the dissociation of CLIP170 from microtubules and the loss of PKCζ from the polarity complex were exquisitely sensitive to CDDO-Im treatment. This has implications not only for TGFβ-dependent cell migration, but migration dependent on other growth factors and receptors as well. Indeed, CDDO-Im inhibits serum-stimulated Rat2 fibroblast migration (please see supplementary movie 4:http://www.jbc.org/content/suppl/2008/04/25/M704064200.DC1/Supp_Movie_4_Rat2_ migration.mov). However, in the case of TGFβ-dependent cell migration, my results indicate that the location of Par6 and TGFβ receptors is important.

It was interesting that TGFβ receptors remained associated with Par6 even as TGFβ-dependent migration was abrogated by CDDO-Im. When I assessed the association of Par6 with TGFβ receptors, I detected no difference in the association or phosphorylation of Par6 in response to CDDO-Im treatment. Therefore this aspect of TGFβ dependent migration was not perturbed. The localization of the triterpenoid to the leading edge of migrating cells was intriguing (Figure 2.11) as it may suggest that the mechanism of CDDO-Im block could be the modulation of proteins at this locus. I reasoned that perhaps the loss of IQGAP1, PKCζ and Rac1 at the leading edge of migrating cells would be accompanied with a loss of Par6 and TGFβ receptors. This was confirmed when I assessed Par6 and TGFβ receptor localization by immunofluorescence

microscopy and found both partners to be greatly reduced at this site (Figure 2.15). Further investigation of how CDDO-Im modulates TGFβ receptor signaling will be interesting as the concentration of TGFβ receptors in various subcellular locations has been shown to be essential to stimulate Smad2 phosphorylation on endosomal membranes (8,9,15,42-45), EMT at tight junctions (34) and degradation of RhoA in lamellipodia and filopodia (60-62).

Finally, my results may also give some insight into the mechanism of the anti-metastatic and anti-proliferative effects of CDDO-Im in animal studies (57-59) and would be an interesting area of study particularly for understanding mechanisms of cell migration and metastasis in human cancer. A general class of anti-metastatic agents, microtubule destabilizing drugs, affect cell motility, migration and metastasis (63). Therefore combining anti-microtubule drugs with drugs such as CDDO-Im that target the attachment sites between microtubules and the cell membrane may be an effective therapeutic approach to metastasis.

2.6 FOOTNOTES

2.7   REFERENCES

1.   Pardali, K., and Moustakas, A. (2007) *Biochim Biophys Acta* **1775**, 21-62

2.   Bose, R., and Wrana, J. L. (2006) *Curr Opin Cell Biol* **18**, 206-212

3.   Muraoka, R. S., Dumont, N., Ritter, C. A., Dugger, T. C., Brantley, D. M., Chen, J., Easterly, E., Roebuck, L. R., Ryan, S., Gotwals, P. J., Koteliansky, V., and Arteaga, C. L. (2002) *J Clin Invest* **109**, 1551-1559

4.   Thiery, J. P. (2002) *Nat Rev Cancer* **2**, 442-454

5.   Xu, Z., Shen, M. X., Ma, D. Z., Wang, L. Y., and Zha, X. L. (2003) *Cell Res* **13**, 343-350

6.   Attisano, L., and Wrana, J. L. (2002) *Science* **296**, 1646-1647

7.   Tsukazaki, T., Chiang, T. A., Davison, A. F., Attisano, L., and Wrana, J. L. (1998) *Cell* **95**, 779-791

8.   Miura, S., Takeshita, T., Asao, H., Kimura, Y., Murata, K., Sasaki, Y., Hanai, J. I., Beppu, H., Tsukazaki, T., Wrana, J. L., Miyazono, K., and Sugamura, K. (2000) *Mol Cell Biol* **20**, 9346-9355

9.   Lin, H. K., Bergmann, S., and Pandolfi, P. P. (2004) *Nature* **431**, 205-211

10.   Lin, X., Duan, X., Liang, Y. Y., Su, Y., Wrighton, K. H., Long, J., Hu, M., Davis, C. M., Wang, J., Brunicardi, F. C., Shi, Y., Chen, Y. G., Meng, A., and Feng, X. H. (2006) *Cell* **125**, 915-928

11.   Ebisawa, T., Fukuchi, M., Murakami, G., Chiba, T., Tanaka, K., Imamura, T., and Miyazono, K. (2001) *J Biol Chem* **276**, 12477-12480

12.   Kavsak, P., Rasmussen, R. K., Causing, C. G., Bonni, S., Zhu, H., Thomsen, G. H., and Wrana, J. L. (2000) *Mol Cell* **6**, 1365-1375

13.   Ogunjimi, A. A., Briant, D. J., Pece-Barbara, N., Le Roy, C., Di Guglielmo, G. M., Kavsak, P., Rasmussen, R. K., Seet, B. T., Sicheri, F., and Wrana, J. L. (2005) *Mol Cell* **19**, 297-308

14.   Chen, C. L., Huang, S. S., and Huang, J. S. (2006) *J Biol Chem* **281**, 11506-11514

15.   Di Guglielmo, G. M., Le Roy, C., Goodfellow, A. F., and Wrana, J. L. (2003) *Nat Cell Biol* **5**, 410-421

16.   Ito, T., Williams, J. D., Fraser, D. J., and Phillips, A. O. (2004) *J Biol Chem* **279**, 25326-25332

17. Schwartz, E. A., Reaven, E., Topper, J. N., and Tsao, P. S. (2005) *Biochem J* **390**, 199-206

18. Zhang, X. L., Topley, N., Ito, T., and Phillips, A. (2005) *J Biol Chem* **280**, 12239-12245

19. Le Roy, C., and Wrana, J. L. (2005) *Nat Rev Mol Cell Biol* **6**, 112-126

20. D'Arrigo, A., Bucci, C., Toh, B. H., and Stenmark, H. (1997) *Eur J Cell Biol* **72**, 95-103

21. Pelkmans, L., Kartenbeck, J., and Helenius, A. (2001) *Nat Cell Biol* **3**, 473-483

22. Pol, A., Martin, S., Fernandez, M. A., Ferguson, C., Carozzi, A., Luetterforst, R., Enrich, C., and Parton, R. G. (2004) *Mol Biol Cell* **15**, 99-110

23. Burkhardt, J. K. (1998) *Biochim Biophys Acta* **1404**, 113-126

24. Galjart, N., and Perez, F. (2003) *Curr Opin Cell Biol* **15**, 48-53

25. Musch, A. (2004) *Traffic* **5**, 1-9

26. Raftopoulou, M., and Hall, A. (2004) *Dev Biol* **265**, 23-32

27. Siegrist, S. E., and Doe, C. Q. (2007) *Genes Dev* **21** 483-496

28. Tirnauer, J. S., and Bierer, B. E. (2000) *J Cell Biol* **149**, 761-766

29. Pearson, C. G., and Bloom, K. (2004) *Nat Rev Mol Cell Biol* **5**, 481-492

30. Goode, B. L., Drubin, D. G., and Barnes, G. (2000) *Curr Opin Cell Biol* **12**, 63-71

31. Perez, F., Diamantopoulos, G. S., Stalder, R., and Kreis, T. E. (1999) *Cell* **96**, 517-527

32. Fukata, M., Watanabe, T., Noritake, J., Nakagawa, M., Yamaga, M., Kuroda, S., Matsuura, Y., Iwamatsu, A., Perez, F., and Kaibuchi, K. (2002) *Cell* **109**, 873-885

33. Watanabe, T., Wang, S., Noritake, J., Sato, K., Fukata, M., Takefuji, M., Nakagawa, M., Izumi, N., Akiyama, T., and Kaibuchi, K. (2004) *Dev Cell* **7**, 871-883

34. Ozdamar, B., Bose, R., Barrios-Rodiles, M., Wang, H. R., Zhang, Y., and Wrana, J. L. (2005) *Science* **307**, 1603-1609

35. Yingling, J. M., Blanchard, K. L., and Sawyer, J. S. (2004) *Nat Rev Drug Discov* **3**, 1011-1022

36. Liby, K. T., Yore, M. M., and Sporn, M. B. (2007) *Nat Rev Cancer* **7**, 357-369

37. Ji, Y., Lee, H. J., Goodman, C., Uskokovic, M., Liby, K., Sporn, M., and Suh, N. (2006) *Mol Cancer Ther* **5**, 1452-1458

38. Mix, K. S., Coon, C. I., Rosen, E. D., Suh, N., Sporn, M. B., and Brinckerhoff, C. E. (2004) *Mol Pharmacol* **65**, 309-318

39. Suh, N., Roberts, A. B., Birkey Reffey, S., Miyazono, K., Itoh, S., ten Dijke, P., Heiss, E. H., Place, A. E., Risingsong, R., Williams, C. R., Honda, T., Gribble, G. W., and Sporn, M. B. (2003) *Cancer Res* **63**, 1371-1376

40. Contin, M. A., Sironi, J. J., Barra, H. S., and Arce, C. A. (1999) *Biochem J* **339**, 463-471

41. Cong, F., and Varmus, H. (2004) *Proceedings of the National Academy of Sciences of the United States of America* **101**, 2882-2887

42. Hayes, S., Chawla, A., and Corvera, S. (2002) *J Cell Biol* **158**, 1239-1249

43. Itoh, F., Divecha, N., Brocks, L., Oomen, L., Janssen, H., Calafat, J., Itoh, S., and Dijke Pt, P. (2002) *Genes Cells* **7**, 321-331

44. Panopoulou, E., Gillooly, D. J., Wrana, J. L., Zerial, M., Stenmark, H., Murphy, C., and Fotsis, T. (2002) *J Biol Chem* **277**, 18046-18052

45. Runyan, C. E., Schnaper, H. W., and Poncelet, A. C. (2005) *J Biol Chem* **280**, 8300-8308

46. Apodaca, G. (2001) *Traffic* **2**, 149-159

47. Murray, J. W., and Wolkoff, A. W. (2003) *Adv Drug Deliv Rev* **55**, 1385-1403

48. Galjart, N. (2005) *Nat Rev Mol Cell Biol* **6**, 487-498

49. Yore, M. M., Liby, K. T., Honda, T., Gribble, G. W., and Sporn, M. B. (2006) *Mol Cancer Ther* **5**, 3232-3239

50. Sporn, M. B. (2006) *Cytokine Growth Factor Rev* **17**, 3-7

51. Kang, Y., He, W., Tulley, S., Gupta, G. P., Serganova, I., Chen, C. R., Manova-Todorova, K., Blasberg, R., Gerald, W. L., and Massague, J. (2005) *Proceedings of the National Academy of Sciences of the United States of America* **102**, 13909-13914

52. Levy, L., and Hill, C. S. (2005) *Mol Cell Biol* **25**, 8108-8125

53. Barrios-Rodiles, M., Brown, K. R., Ozdamar, B., Bose, R., Liu, Z., Donovan, R. S., Shinjo, F., Liu, Y., Dembowy, J., Taylor, I. W., Luga, V., Przulj, N., Robinson, M., Suzuki, H., Hayashizaki, Y., Jurisica, I., and Wrana, J. L. (2005) *Science* **307**, 1621-1625

54. Mundy, D. I., Machleidt, T., Ying, Y. S., Anderson, R. G., and Bloom, G. S. (2002) *J Cell Sci* **115**, 4327-4339

55. Parton, R. G., Joggerst, B., and Simons, K. (1994) *J Cell Biol* **127**, 1199-1215

56. Couch, R. D., Ganem, N. J., Zhou, M., Popov, V. M., Honda, T., Veenstra, T. D., Sporn, M. B., and Anderson, A. C. (2006) *Mol Pharmacol* **69**, 1158-1165

57. Hyer, M. L., Croxton, R., Krajewska, M., Krajewski, S., Kress, C. L., Lu, M., Suh, N., Sporn, M. B., Cryns, V. L., Zapata, J. M., and Reed, J. C. (2005) *Cancer Res* **65**, 4799-4808

58. Lapillonne, H., Konopleva, M., Tsao, T., Gold, D., McQueen, T., Sutherland, R. L., Madden, T., and Andreeff, M. (2003) *Cancer Res* **63**, 5926-5939

59. Place, A. E., Suh, N., Williams, C. R., Risingsong, R., Honda, T., Honda, Y., Gribble, G. W., Leesnitzer, L. M., Stimmel, J. B., Willson, T. M., Rosen, E., and Sporn, M. B. (2003) *Clin Cancer Res* **9**, 2798-2806

60. Wang, H. R., Ogunjimi, A. A., Zhang, Y., Ozdamar, B., Bose, R., and Wrana, J. L. (2006) *Methods Enzymol* **406**, 437-447

61. Wang, H. R., Zhang, Y., Ozdamar, B., Ogunjimi, A. A., Alexandrova, E., Thomsen, G. H., and Wrana, J. L. (2003) *Science* **302**, 1775-1779

62. Zhang, Y., Wang, H. R., and Wrana, J. L. (2004) *Cell Cycle* **3**, 391-392

63. Verrills, N. M., and Kavallaris, M. (2005) *Curr Pharm Des* **11**, 1719-1733

CHAPTER 3

SYNTHETIC TRITERPENOIDS TARGET THE ARP2/3 COMPLEX AND INHIBIT BRANCHED ACTIN POLYMERIZATION

3   CHAPTER 3

3.1   CHAPTER SUMMARY

Synthetic triterpenoids are anti-tumor agents that affect numerous cellular functions including apoptosis and growth. Here, I used mass spectrometric and protein array approaches and uncovered that triterpenoids associate with proteins of the actin cytoskeleton, including Actin-related protein 3 (Arp3). Arp3, a subunit of the Arp2/3 complex, is involved in branched actin polymerization and the formation of lamellipodia. CDDO-Im and CDDO-Me were observed to 1) inhibit the localization of Arp3 and actin at the leading edge of cells, 2) abrogate cell polarity and 3) inhibit Arp2/3-dependent branched actin polymerization. I confirmed our drug effects with siRNA targeting of Arp3 and observed a decrease in Rat2 cell migration. Taken together, my data suggest that synthetic triterpenoids target Arp3 and branched actin polymerization to inhibit cell migration.

3.2   INTRODUCTION

Cell migration is crucial in many physiological processes such as embryogenesis, cell differentiation, cell renewal and immune system responses. During these processes, cells undergo highly regulated and coordinated cell migration to enable growth or repair of cells. Cell migration is also important in the metastasis of tumor cells. Indeed, it is a hallmark of the most aggressive and advanced epithelial tumors prior to entering the metastatic stage. These tumor cells often undergo epithelial to mesenchymal transition (EMT) and migrate in a deregulated manner. As a result, they invade other tissues and take over the host organism (1), causing 90% of cancer-related deaths (2).

Cell migration occurs through the coordination of numerous cellular proteins. This process includes directional sensing of cell, anchorage of cells at the leading edge and the reorganization of different components in the cell to assist in cell movement. The orientation of cell movement is largely dependent on the reorganization of the cytoskeleton, which consists of microtubules, intermediate filaments and actin cytoskeleton. Although microtubules, intermediate filaments and leading edge proteins are pivotal in the structure and organization of migrating cells, the actin cytoskeleton also plays an essential role in cell polarity and cell migration. For instance, actin is involved in the formation of the lamellipodia and filopodia, which are membrane and fingerlike projections respectively, at the leading edge of migrating cells. Both lamellipodia and filopodia are important for directional and environmental sensing even though they may be formed through two distinct actin-assembly machineries with different actin dynamic properties (3). Lamellipodia are formed by actin-related protein (Arp2/3) complexes

through branched actin nucleation whereas filopodia are formed by formin by progressive unbranched actin nucleation. Although the processes of the two are similar in that they are both activated by small Rho GTPases and a nucleation-promoting factor is required for actin polymerization, the key effectors that enable these processes are distinct. For instance, Cdc42 activates neural Wiskott-Aldrich Syndrome protein (n-WASp), which in turn promotes nucleation and branched actin polymerization, while the activation of the RhoA induces formin-dependent unbranched actin polymerization. Interestingly, Rac1, another small Rho GTPase, has been shown to be involved both indirectly and directly in branched and unbranched actin polymerization, respectively. The understanding of the two distinct actin polymerization processes is crucial in understanding how cell migration is coordinated with other key cellular processes.

Since cell migration is a precursor event of cancer metastasis, chemotherapeutic agents that block cell migration have been an important focus in the field of cancer chemotherapy. Recently, the parental synthetic oleanane triterpenoid (CDDO) and its more potent derivatives (CDDO-Im and CDDO-Me) have been suggested to be promising therapeutic agents. Specifically, CDDO and its methyl ester (CDDO-Me) and imidazolide (CDDO-Im) derivatives have been shown to inhibit tumor growth and induce apoptosis (4-18). CDDO and its derivatives also disrupt the intracellular REDOX (reduction-oxidation reaction) balance (19-24) and are potent suppressors of nitric oxide production and at least two inflammatory enzymes, iNOS and COX-2, which are implicated with enhanced carcinogenesis in many organs (25). These mechanisms have been evident in various cancers including lymphoma (26, 27-30), leukemia (12), (26), (31-35), glioblastoma (36), neuroblastoma (36), osteosarcoma (37) and in cancer cell

lines of the lung (8,38-41), breast (10), (42,43,44), ovaries (45), pancreas (46), colon (5), and prostate (6). In addition, CDDO-based compounds have been shown to sensitize resistant CLL B cells (47) and TRAIL (Tumor necrosis factor Related Apoptosis-Inducing Ligand)-resistant cancer cells to induce apoptosis (43,48). However, even though recent studies have shown that CDDO-Im is highly effective in various cancer cell lines and animal studies for inhibiting tumor growth and inducing apoptosis, the effect of the synthetic triterpenoids on cell migration and metastasis remains unclear. Thus far, CDDO-Im has been shown to target proteins at the leading edge of the cells and causes the disruption of the microtubule network through a mechanism that differs from microtubule-depolymerizing agents such as Nocodazole (49). The present study aims to explore in further detail how other derivatives of CDDO may affect general cell migration.

3.3   MATERIALS AND METHODS

3.3.1   *Cell Culture, Antibodies and Reagents*

Rat2 fibroblasts were cultured in a 37˚C incubator with 5% CO_2, and Dulbecco's Modified Eagle Medium (DMEM) with 10% Fetal Bovine Serum (FBS). Alexa Fluor 555-conjugated phalloidin (A34055) was purchased from Invitrogen Molecular Probes (Oregon, USA). Monoclonal anti-Rac1 (610650), and anti- paxillin (610051) were purchased from BD Transduction Laboratories (Mississauga, Ontario). Monoclonal anti-β-tubulin (Tub2.1), anti-Arp3 (A5979) and polyclonal anti-actin (A2668) antibodies were purchased from Sigma (Oakville, Ontario).   Monoclonal anti-cdc42 (sc8401) and polyclonal anti-RhoA (sc179) anti-n-WASp (sc-20770), and anti-GAPDH (sc-25778) antibodies were purchased from Santa Cruz Technology (Santa Cruz, CA). CDDO, CDDO-Im, CDDO-Me, biotinylated CDDO (b-CDDO) and biotinylated CDDO-Me (b-CDDO-Me) are generous gifts from Dr. M. B. Sporn (Hanover, NH).   The biotinylated form of CDDO and CDDO-Me has been previously characterized and is referred to as compound 5 and 6 respectively by Honda and colleagues (50). The Arp3 inhibitor, CK-869, and the inactive control, CK-312, were purchased from Calbiochem.

3.3.2   *Scratch Assays and Immunofluorescence Microscopy*

Rat2 fibroblasts were grown to confluency and the monolayer was scratched with a pipette tip. Cells were given 4 hours to establish polarity and leading edges before being treated with 10 µM biotin, CDDO, CDDO-biotin, CDDO-Me or CDDO-Me biotin for

subcellular localization studies or with DMSO (vehicle) or CDDO or CDDO-Im or CDDO-Me for 2 hours for cell migration studies and immunofluorescence microscopy. For biotinylated subcellular localization studies, cells were fixed and permeabilized followed by incubation with anti-Rac1 antibody to visualize the leading edge. Cy2-labelled secondary antibodies, Cy3-labelled streptavidin and DAPI were then used to visualize Rac1, biotinylated CDDO or biotinylated CDDO-Me and the nuclei of cells, respectively. Cells were visualized using an Olympus IX81 inverted microscope. For cell migration studies, DIC images were collected using an Olympus IX81 inverted microscope at the beginning of the experiment (Time 0) and after 12-16 hours. The extent of cell migration was measured by taking the width of the wound at 0 time and 16 hours six times in duplicate. The results were averaged from four different experiments ± SD. Statistical analyses were done using one-way ANOVA. For immunofluorescence microscopy studies, cells were fixed, permeabilized, and incubated with anti-Arp3, anti-n-WASp, anti-actin and anti-paxillin antibodies and phalloidin for stress fibers. Visualization was carried out using an Olympus IX81 inverted microscope. Micrograph deconvolution was carried out using ImagePro software (Media Cybernetics Inc.). Quantitative analysis for immunofluorescence studies were done as described previously (49).

3.3.3 Affinity Pull-down using Biotinylated CDDO Derivatives

Subconfluent Rat2 fibroblasts or 2.5 μg of purified Arp2/3 complex protein were incubated with vehicle (DMSO), 10 μM biotin or 10 μM biotinylated-CDDO (b-CDDO)

or 10 μM biotinylated-CDDO-Me (b-CDDO-Me) for 2 hours before lysis, followed by incubation with neutravidin-agarose beads to precipitate proteins that associated with the biotinylated form of the synthetic triterpenoids. SDS-PAGE and silver staining were performed and proteins that were uniquely stained in biotinylated-CDDO and biotinylated CDDO-Me treated samples were excised from the gel, trypsinized and analyzed by electrospray mass spectrometry (ESI-MS). This approach was repeated three times. To confirm or identify the potential synthetic triterpenoid binding proteins, lysates were processed for SDS-PAGE followed by immunoblotting with anti-tubulin, anti-actin, anti-Rac1, anti-Arp3, anti-Cdc42, or anti-RhoA antibodies.

3.3.4   Invitrogen ™ Protoarray

The identification of triterpenoid binding proteins was done by following the protocol described in the Invitrogen Protoarrray kit. Biotin or Biotinylated CDDO-Me were incubated with a protein chip with about 8,000 human proteins spotted on a nitrocellulose membrane in duplicate for 2 hours before incubating with streptavidin-Cy3. The chip was then washed and dried before being read by the Biorad VersArray ChipReader 3m system. Data were normalized against background and only signals that were at least two fold or more than the background were considered to be potential interacting candidates of the synthetic triterpenoids.

3.3.5   Rho small GTPases Activation Assays

Subconfluent Rat2 fibroblasts were serum starved overnight before treating with vehicle (DMSO) or with CDDO-Im for 2 hours. For Rac1 and Cdc42 activation assays, cells were lysed and incubated with purified GST protein, or GST-PAK for two hours before being processed for SDS-PAGE and immunoblotted for activated Rac1 and activated Cdc42 using anti-Rac1 and anti-Cdc42 antibodies respectively. For RhoA activation assays, cells were lysed and incubated with purified GST or GST-Rhotekin for 2 hours before being processed by SDS-PAGE and immunoblotted for activated RhoA using RhoA antibody. Total protein lysates were also immunoblotted and shown. Quantitative analyses were done using densitometry (BioRad VersaDoc).

3.3.6   In-vitro Actin Polymerization Assays

Purified pyrene labeled actin was resuspended and incubated in general actin buffer provided by Cytoskeleton Inc™ Actin Polymerization Kit for 1 hour on ice to depolymerize any actin oligomers followed by micro-centrifugation at 4°C for 30 min. Two μM of actin alone or 2 μM of actin, 13 nM of Arp2/3 complexes and 100 nM of VCA domain of WASp protein were incubated with DMSO (control) or different concentrations (0, 50, 100 μM) of CDDO-Im and CDDO-Me for 15 minutes on ice before pyrene actin fluorescence was measured over time.

3.3.7 Docking Experiments

AutoDock version 4.2 was used to carry out the docking experiments (51). The crystal structures of the Arp2 and Arp3 subunits (PDB-ID 3DXM; Ref. (52)) were used for the docking procedure, with the docking surface encompassing the interface between the two subunits as well as all of the internal cavities. The structure of CDDO-Me was obtained from the Cambridge Structural Database (CSD-ID UFEHOC (53)). The CDDO-Im structure was constructed by merging the CDDO-Me structure with a suitable imidazole-containing compound (CSD-ID HEWQOQ). Both CDDO-Me and CDDO-Im are mostly rigid structures. For CDDO-Me, only the C17-C28 bond (which attaches the acid ester to the triterpenoid) was allowed to rotate; for CDDO-Im, both the C17-C28 bond and the bond between C28 and the imidazole nitrogen were rotatable. All other bonds in CDDO-Me and CDDO-Im were fixed, as was the structure of the Arp2 and Arp3 complex. The rigidity of CDDO-Me and CDDO-Im aided the docking procedure and also limited the number of potential solutions

3.3.8 Competitive Binding Studies

Arp2/3 protein complex (2.5 µg) was incubated with either DMSO or increasing concentrations (10-100µM) CDDO-Me or CK-869 for 15 min at 37˚C. Following incubation with 10 µM b-CDDO-Me for an additional 15 min, 50% neutravidin-agarose beads were added and incubated at room temperature for 10 min. The beads were washed three times with TNTE buffer and subjected to SDS-PAGE and immunoblotting for Arp3.

3.3.9   *Statistical Analyses*

Results are provided as means ± SD. One-way ANOVA followed by a Tukey's post-hoc test was performed using GraphPad PRISM 5 Software to assess statistical differences between experimental groups. P<0.05 was considered statistically significant.

3.4   RESULTS

I have shown that CDDO-Im inhibits cell migration and causes the disruption of the microtubule network through a mechanism distinct from microtubule-depolymerizing agents such as Nocodazole (49). However, the molecular target(s) of this inhibition remain(s) unknown and I sought to identify them through the use of mass spectrometry and protein array analyses. For these techniques, I opted to use biotinylated synthetic triterpenoids that could be used for the purification and identification of associated proteins. Since the active nature of the Imidazolide side group of CDDO-Im complicated its biotinylation, I used the CDDO and the methyl ester derivative (CDDO-Me) in my studies.   CDDO-Me is a suitable substitute as it has been shown to be as potent as CDDO-Im in many cellular assays (7, 13, 17, 24, 54), compared to the weaker CDDO parental compound.

3.4.1   Synthetic triterpenoids inhibit cell migration and localize to the leading edge of migrating cells.

I first set out to establish the effectiveness of the CDDO-Me compound in cell migration by comparing its rate of cell migration with CDDO and CDDO-Im treated cells (Figure 3.1). Briefly, Rat2 fibroblasts were grown to confluency before a 'wound' was created by scratching the cells off of the surface of the culture dish. The cells were treated with varying concentrations of synthetic triterpenoids (Figure 3.1). Brightfield images were taken at 0 time and again after 16 hours of incubation at 37˚C to examine

Figure 3.1 CDDO-Im and CDDO-Me inhibit cell migration.

A) Confluent Rat2 fibroblasts were scratched to create a 'wound' and treated with 1 μM CDDO, CDDO-Im or CDDO-Me for 16 hours. Brightfield images (magnification 10X) were taken at the beginning of the experiment (0h) and after 16 hours (16h) of incubation at 37°C. The white dotted lines indicate the leading edge of migrating cells (top panels). Cells were treated with increasing concentrations of CDDO-Im or CDDO-Me (0-1.5 μM, as shown) and imaged. Cell migration was quantified using ImagePro software and graphed as cell migration (percentage of control) *vs.* triterpenoid concentration (n=3±SD). *p<0.05 (bottom panel).

B) Confluent Rat2 fibroblasts were scratched and incubated with DMSO (Control), 1 or 5 μM CDDO (top panels). Cells treated with increasing concentrations of CDDO (1-10 μM, as shown) and imaged. Cell migration was quantitated as described in Panel A and graphed as cell migration (percentage of control) *vs.* triterpenoid concentration (n=3±SD). *p<0.05.
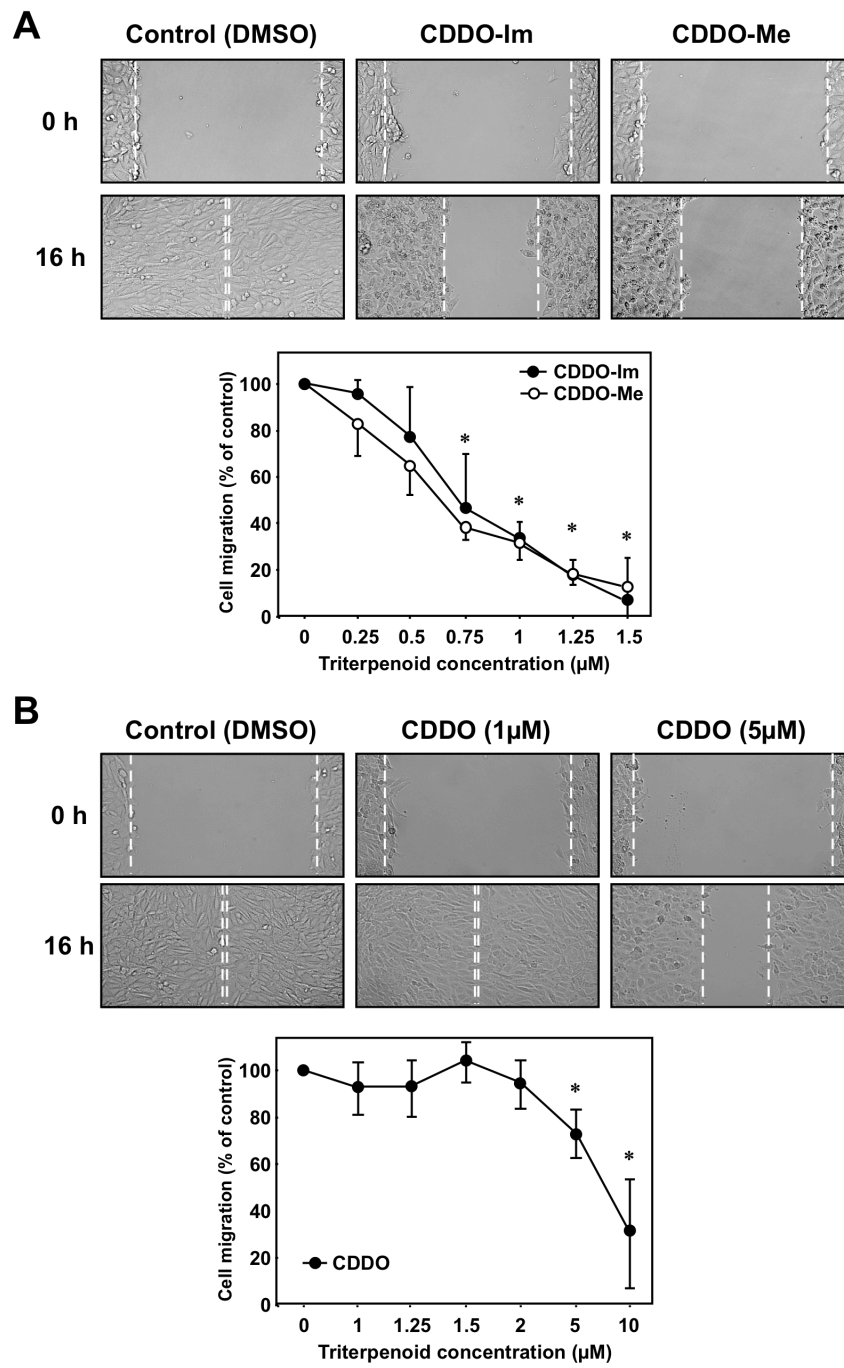
Figure 3-1

whether the rate of cell migration would be affected by CDDO, CDDO-Im and CDDO-Me (Figure 3.1A). I observed that cell migration remained relatively unaltered in the presence of 1 μM CDDO while cell migration was inhibited >50% in the presence of either 1 μM CDDO-Im or CDDO-Me (Figure 3.1). Indeed, at 1.5 μM, the rate of cell migration in CDDO-Im and CDDO-Me treated cells was reduced to 80% while the rate of migration in CDDO-treated cells did not differ from control. Compared to the imidazolide and methyl ester derivatives, the parental CDDO is inactive at 1 μM in inhibiting cell migration and was used as an inactive control in subsequent studies. To address cell toxicity, the drugs were washed out using PBS and the cells were incubated with media for an additional 24 hours. I observed that cells incubated with less than 5 μM CDDO and less than or equal to 1.25 μM of CDDO-Im and CDDO-Me migrated and filled the wound (data not shown). This further confirmed that CDDO is approximately ten times less potent than the CDDO-Im and Me derivatives. These more potent triterpenoids also acted in similar concentration ranges to reduce cell migration.

I previously demonstrated that CDDO localizes to the leading edge of migrating cells (49) and may target proteins involved in the polarity complex at this cellular locus. I therefore assessed if CDDO-Me also targets the leading edge of migrating cells using immunofluorescence microscopy. I observed that biotinylated CDDO-Me (b-CDDO-Me) localizes to the leading edge of migrating cells, similar to biotinylated CDDO (Figure 3.2). These results demonstrate that the subcellular localization of CDDO and CDDO-Me are similar.

Figure 3.2 b-CDDO and b-CDDO-Me target the leading edge of migrating cells.

Confluent Rat2 fibroblasts were scratched to create a 'wound'. After incubation for 4 hours to allow cell polarization and migration, cells were fixed, permeabilized and incubated with monoclonal anti-Rac1 antibodies (Rac1; green) and biotin, CDDO, biotinylated CDDO (b-CDDO), CDDO-Me, or biotinylated CDDO-Me (b-CDDO-Me) followed by Cy2-labeled anti-mouse antibody and Cy3-labeled streptavidin. Cell nuclei were stained with DAPI (blue). The co-localization of Rac1 (green) with b-CDDO or b-CDDO-Me (red) at the leading edge of migrating cells is indicated (yellow arrowheads). The white arrow indicates the direction of cell movement. Representative images from four experiments are shown. Bar = 10 μm.

Figure 3-2
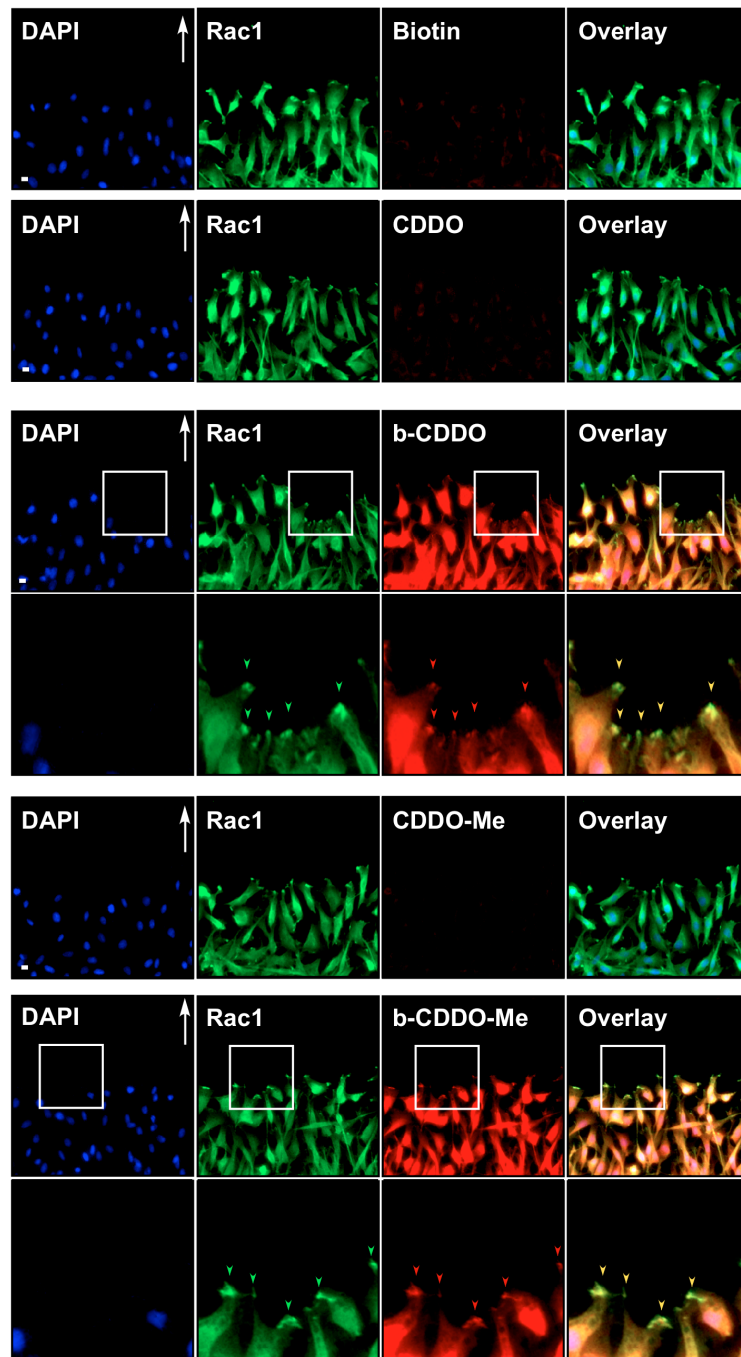
3.4.2   Several proteins involved in cytoskeletal organization and cell migration are

identified as triterpenoid-binding targets via a two-pronged proteomic approach.

Since CDDO-Im and CDDO-Me exhibited similarities in cellular localization and inhibition of cell migration, I used b-CDDO-Me to identify potential synthetic triterpenoid targets using two proteomic approaches (Figure 3.3). In the first approach, I utilized a Mass Spectrometry-based method and proteins that precipitated with b-CDDO or b-CDDO-Me were processed by SDS-PAGE followed by silver staining and trypsinization before being sent for ESI-MS analysis (Figure 3.3A). This mass spectrometry method was compared to a protein array approach which was purchased from Invitrogen. The slide, containing >8000 human purified proteins, was incubated with biotin, biotinylated CDDO or biotinylated CDDO-Me followed by Alexafluor647-labelled streptavidin. The triterpenoid-binding proteins were then visualized and proteins that bound the biotinylated-CDDO-Me ≥ 2 fold higher than biotin alone were counted as potential triterpenoid-binding targets (data not shown). Using two different proteomic approaches and by comparative analysis, several proteins involved in cytoskeletal organization and cell migration were identified (Figure 3.3B). In order to ascertain that the identified binding partners are also *bona fide* cellular interacting proteins, I incubated cells with b-CDDO or b-CDDO-Me, followed by lysis and precipitated b-CDDO or b-CDDO-Me with neutravidin beads. Precipitated samples then underwent SDS-PAGE and and was probed with antibodies against tubulin and actin (Figure 3.3B). Consistent with previous published results (55), I found that tubulin interacts with the b-CDDO-Me and

Figure 3.3 Identification of triterpenoid-binding proteins.

A) Rat2 fibroblasts were incubated with DMSO, 10 μM biotin, 10 μM biotinylated-CDDO or 10 μM biotinylated-CDDO-Me, lysed, and incubated with neutravidin-agarose beads. SDS-PAGE and silver staining were performed and proteins that were uniquely stained (dashes) in biotinylated CDDO-Me-treated samples were excised from the gel, trypsinized and analyzed by electrospray mass spectrometry.

B) Summarized table of cell migration-related proteins from mass spectrometry and protein array approaches.

C) Rat2 fibroblasts were incubated with DMSO, 10 μM biotin, 10 μM b-CDDO or 10 μM b-CDDO-Me, lysed, and incubated with neutravidin-agarose beads. Precipitated samples (left panels) were processed by SDS-PAGE and immunoblotted for cytoskeletal proteins (anti-β-tubulin and anti-actin). Fifty micrograms of total protein lysates were also immunoblotted for tubulin and actin and shown (right panel).

Figure 3-3

A
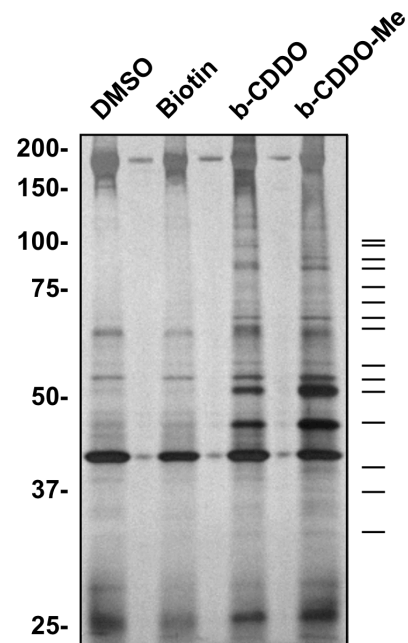
B

Mass Spectrometry	Protein Array
Actin	Actin
Tubulin	Tubulin
Actin-related protein 3 (Arp3)	Actin-related protein 2/3 (Arp2/3)
Rho GEFs	Rho GEFs
Rac GEF	Rho GDI
F-actin capping protein	Rho GDS
Microtubule crosslinking factor	Rho GAPs
Microtubule associated protein	Protein Kinase C (PKC) iota, mu, nu
Rhotekin 2	P-21 Activated Kinase (PAK)
Cdc42 binding protein kinase	

C
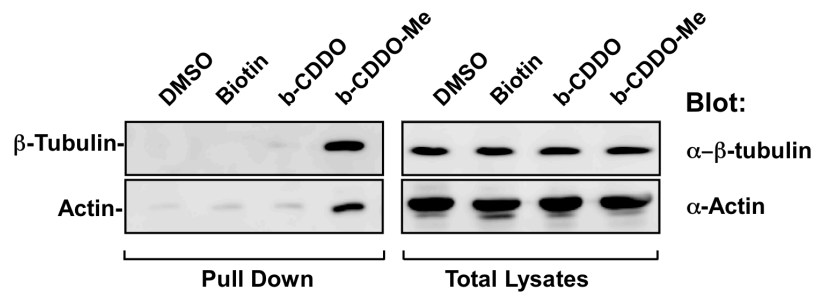
was also detected to interact with b-CDDO, albeit to a much lower extent. Interestingly, actin, a large component of the cytoskeleton, and Actin-related protein 3 (Arp3), were also found to associate with b-CDDO-Me (Figure 3.3C and 3.4A).

Another group of proteins identified in my proteomic approaches were modulators of the Rho small GTPase family (Figure 3.3B). Rho small GTPases are a group of G-proteins that are extensively involved in the establishment of cell polarity and orientation of the cytoskeletal dynamics during cell migration. They are regulated by Guanine Exchange Factors (GEFs), which promote the activation of Rho small GTPases, and by GTPase Activating Proteins (GAPs), which render the protein into its inactive state. The possibility that triterpenoids affect the activity of one or more of the numerous GEF and GAP (56) was assessed by directly examining the level of GTP-bound Rac1, RhoA or Cdc42 in the presence or absence of CDDO-Im. I observed that CDDO-Im only moderately increased Rac1 activity but was ineffective in altering Cdc42 and RhoA activities (Figure 3.5A and B). In addition, affinity pull down assays using specific antibodies against Rac1, Cdc42 and RhoA indicated that b-CDDO-Me does not bind to these Rho small GTPases (Figure 3.5C).

3.4.3   *CDDO-Im and CDDO-Me inhibit branched actin polymerization by targeting Arp3.*

I next directed my attention to molecules that are downstream of GTPases and alter the cytoskeleton and cell migration: molecules that alter the actin cytoskeleton.

Figure 3.4 Synthetic triterpenoids interact with the Arp2/3 and inhibit branched actin polymerization.

A) Purified Arp2/3 protein complex (2.5 μg) was incubated with 10 μM biotin or 10 μM biotinylated CDDO-Me (b-CDDO-Me) for 2 hours. An affinity pull down assay was performed by incubating samples with neutravidin beads for 1 hour followed by SDS-PAGE and immunoblotting with anti-Arp3 antibodies (left panel). Total input was also immunoblotted with Arp3 and shown (right panel).

B) Rat2 fibroblasts were incubated with 10 μM Biotin or biotinylated-CDDO-Me (b-CDDO-Me) for 2 hours before lysis, followed by incubation with streptavidin-agarose beads to precipitate proteins that associated with the biotinylated form of the synthetic triterpenoids. SDS-PAGE was performed followed by immunoblotting for Arp3 with anti-Arp3 antibody (top panel). Fifty μg of protein lysates was also immunoblotted for Arp3 and shown (bottom panel).

C) Subconfluent Rat2 fibroblasts were treated with DMSO (Control; C), 1 μM of CDDO-Im (Im) or 1 μM of CDDO-Me (Me) for 2 hours before lysis followed by immunoprecipitation with anti-Arp3 antibody. The immunoprecipitates (IP; left panel) were then subjected to SDS-PAGE and immunoblotting with anti-n-WASp, anti-actin and anti-Arp3 antibodies. Fifty micrograms of total lysates were also immunoblotted for n-WASp, actin and Arp3 and shown (right panel). Note that the association of Arp3 and n-WASp is not altered by triterpenoid treatment.

D) Purified Arp2/3 complex and GST-VCA domain of nWASp were incubated in the absence or presence of triterpenoids and immunoprecipitated with anti-GST antibodies. The immunoprecipitates (IP; left panel) were then subjected to SDS-PAGE and immunoblotting with anti-GST and anti-Arp3 antibodies. Fifty percent of the input was also immunoblotted for GST and Arp3 and shown (right panel). Note that the association of Arp3 and n-WASp is not altered by triterpenoid treatment.

E) Purified pyrene-labeled actin was incubated for 1 hour on ice to depolymerize actin oligomers. 2 μM of actin (Actin) or actin in the presence of 13 μM of Arp2/3 complex (Arp2/3) and 100 nM of VCA domain of n-WASp protein (VCA) were incubated with DMSO, 50 μM or 100 μM of either CDDO-Im (Im), or CDDO-Me (Me). Actin polymerization was measured by pyrene fluorescence and graphed as fluorescence intensity (arbitrary unit) *vs.* time (minutes).
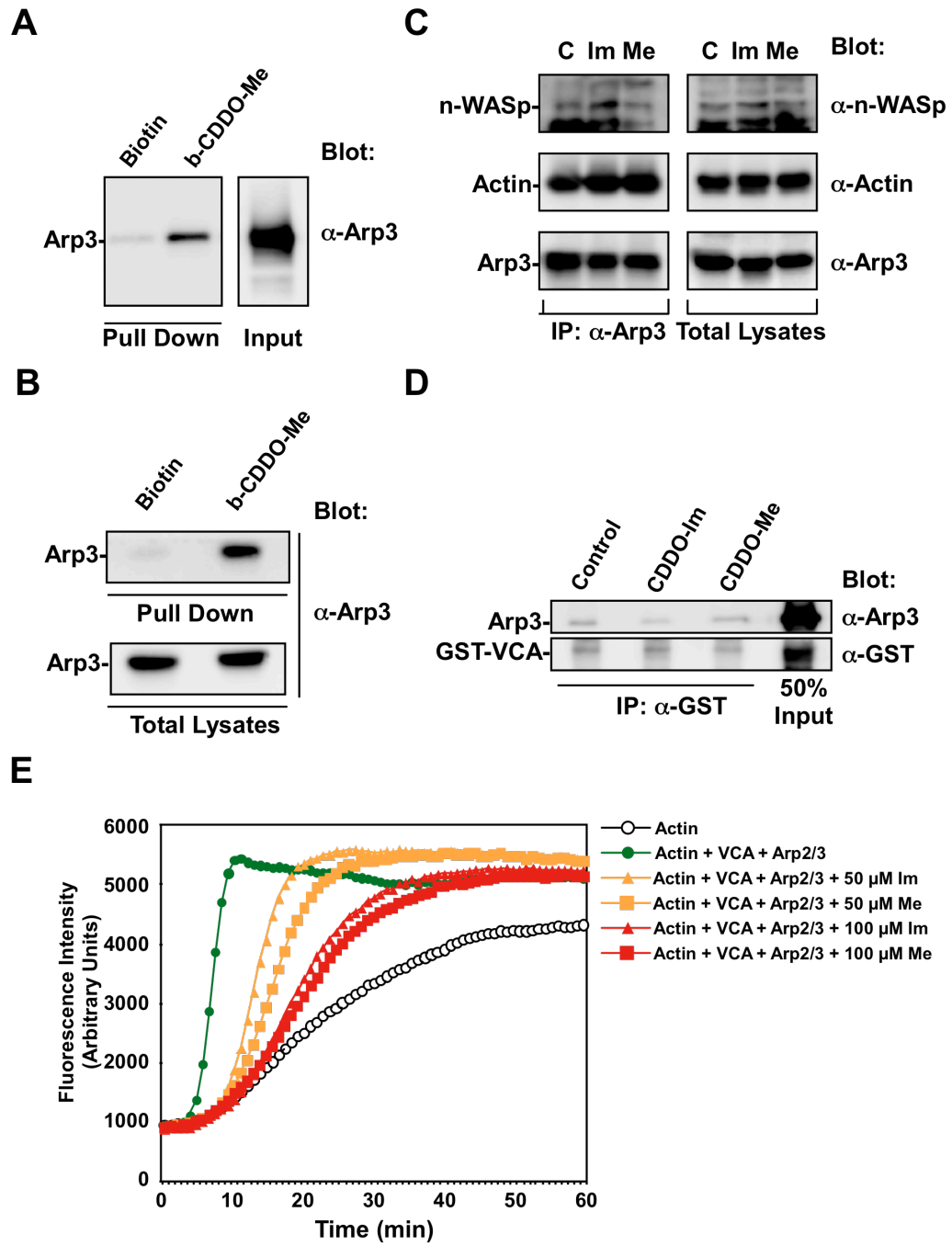
Figure 3-4

A

B

C

D

E

Figure 3.5 The effect of CDDO-Im on Rho small GTPases.

A) Rat2 fibroblasts were serum starved and treated with vehicle (DMSO) or with CDDO-Im for 2 hours. For Rac1 and Cdc42 activity assays, cells were lysed and incubated with GST-PAK and processed for SDS-PAGE and immunoblotted for the GTP-bound forms of Rac1 or Cdc42 using anti-Rac1 antibody (top panel) and anti-Cdc42 antibody (middle panel). For RhoA activity assays, cells were lysed and incubated with GST-Rhotekin beads. Samples were processed for SDS-PAGE and immunoblotted for the GTP-bound form of RhoA using anti-RhoA antibody (bottom panel). Fifty micrograms of total protein lysates were immunoblotted for Rac1, Cdc42 or RhoA and shown (right panels).

B) Densitometric quantitation of Rho small GTPase activity (Rac1, Cdc42 or RhoA) was performed and graphed as activated Rho small GTPase levels (Arbitrary units) versus treatment (n=3±SD, *p<0.05).

C) Rat2 fibroblasts were incubated with 10 µM biotin or 10 µM biotinylated-CDDO-Me for 2 hours before lysis, followed by incubation of neutravidin-agarose beads. Pull down samples (left panel) were processed by SDS-PAGE and immunoblotted for anti-RhoA, anti-Rac1 and anti-Cdc42 antibodies. Fifty micrograms of total protein lysates of RhoA, Rac1 and Cdc42 were immunoblotted and shown (right panel). Note that Rho GTPases do not associate with b-CDDO-Me.

Figure 3-5

A

CDDO-Im

| | - | + | | - | + | Blot: |

Rac1-   α-Rac1

Cdc42-   α-Cdc42

GST-PAK   Total
Pull Down   Lysates

RhoA-   α-RhoA

GST-Rhotekin   Total
Pull Down   Lysates

B

■ Rac1
□ Cdc42
▨ RhoA

Activated Rho small GTPase levels (Arbitrary units)

Control   1 μM CDDO-Im

Treatment

C

Biotin   b-CDDO-Me   Biotin   b-CDDO-Me   Blot:

RhoA-   α-RhoA

Rac1-   α-Rac1

Cdc42-   α-Cdc42

Pull Down   Total Lysates
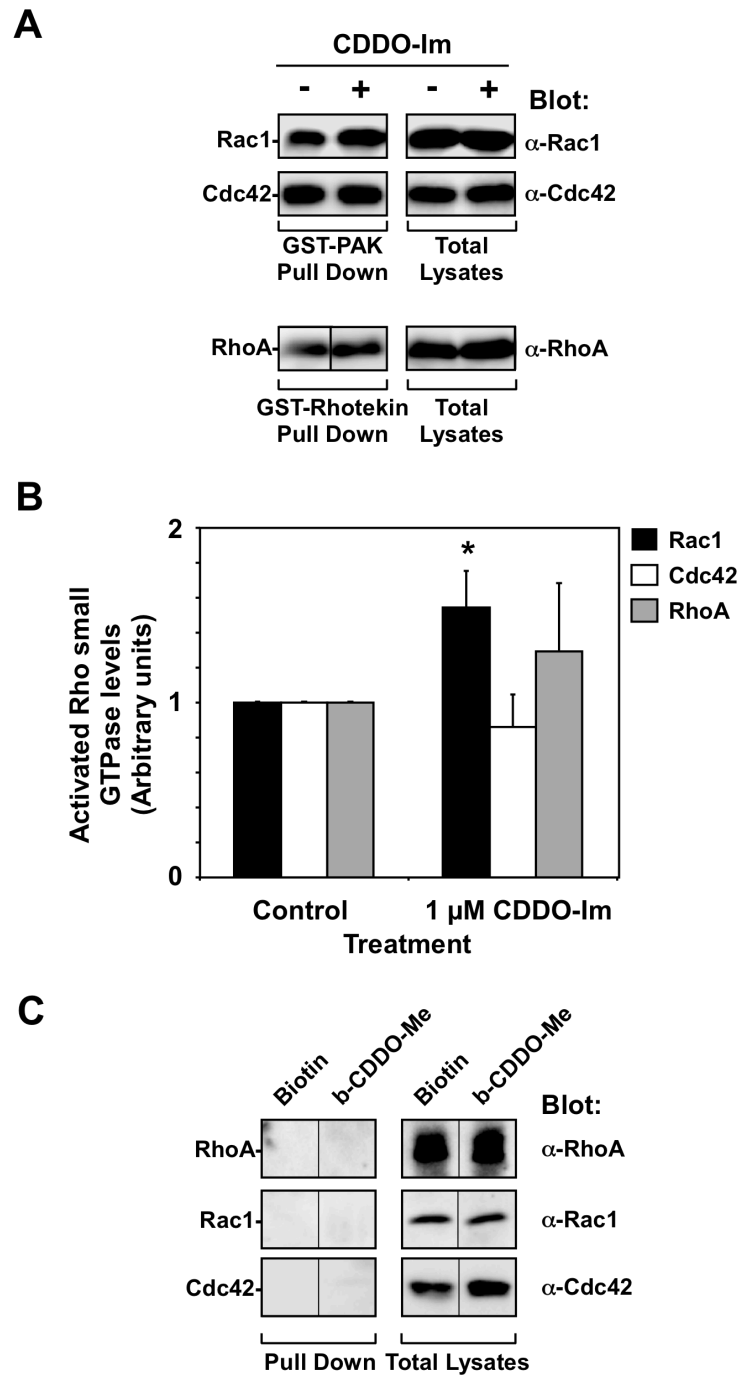
There are two different actin assembly machineries that are involved in the formation of actin with different properties in different areas of migrating cells. Arp2/3 complex is involved in the assembly of branched actin at the leading edge of migrating cells while formin is involved in the formation of unbranched actin such as stress fibers (3). I have previously observed that the actin stress fibers are largely unaffected by triterpenoid treatment (49), so I examined whether the synthetic triterpenoids have any effect on branched actin formation by studying actin and Arp2/3 complex. Arp2/3 is a stable complex that is composed of five subunits: ARPC1, ARPC2, ARPC3, ARPC4, ARPC5 and two actin-related proteins Arp2 and Arp3. In particular, studies have shown that Arp3 is involved in the nucleation process of branched actin formation (3). I first attempted to confirm whether Arp3 was a direct target of the synthetic triterpenoid through affinity pull-down assays by using both purified Arp2/3 complex protein as well as in Rat2 cells (Figure 3.4). Briefly, Arp2/3 purified protein was incubated with DMSO (control), biotin, biotinylated CDDO or biotinylated CDDO-Me for 2 hours and precipitated with neutravidin beads followed by immunoblotting with anti-Arp3 antibody. My results showed that Arp3 interacted with both CDDO and CDDO-Me *in vitro* (Figure 3.4A). To confirm this interaction in cells, I incubated Rat2 fibroblasts with b-CDDO-Me, precipitated and immunoblotted for Arp3 (Figure 3.4B). These two approaches confirmed my proteomic analyses and indicate that Arp3 associates with triterpenoids.

In order for the formation of branched actin to occur, Arp2/3 must interact and work closely with not only actin itself, but also neural-Wiskott Aldrich Syndrome protein (n-WASp). Indeed, n-WASp regulates cytoskeletal dynamics by activating Arp2/3 complexes so that it can begin the nucleation process for branched actin polymerization.

Therefore, I hypothesize that the triterpenoid may inhibit cell migration by targeting Arp3 directly and affecting the association of Arp3 with actin and/or nWASp. To assess this, co-immunoprecipitation assays were done using Rat2 fibroblasts. Cells were treated with DMSO, 1 µM CDDO-Im or CDDO-Me, immunoprecipitated with anti-Arp3 antibody and immunoblotted for actin, n-WASp, and Arp3 antibodies. Results showed that Arp3 remained associated with both n-WASp and actin upon CDDO-Im or CDDO-Me incubation (Figure 3.4C). These results suggest that the association between Arp3 and n-WASp is unaffected by the synthetic triterpenoids in cells or *in vitro* (Figure 3.4D).

The identification that subunits of the Arp2/3 complex are direct triterpenoid-binding proteins next led us to study the effect of branched actin polymerization in the presence of CDDO-Im and CDDO-Me. I examined the rate of actin polymerization in the presence of actin alone or actin and VCA domain of n-WASp and Arp2/3, in the absence or presence of different concentration of CDDO-Im (Figure 3.4E). I observed that the rate of actin polymerization was reduced by both CDDO-Me and CDDO-Im, with 50 µM of either compound effectively reducing the rate of actin polymerization by about 50%. At 100 µM, both triterpenoids were able to greatly reduce Arp2/3/VCA-dependent actin polymerization but did not alter actin polymerization in the absence of Arp2/3-VCA (Figure 3.4E and data not shown). My results suggest that triterpenoids target Arp2/3/n-WASp-mediated branched actin polymerization.
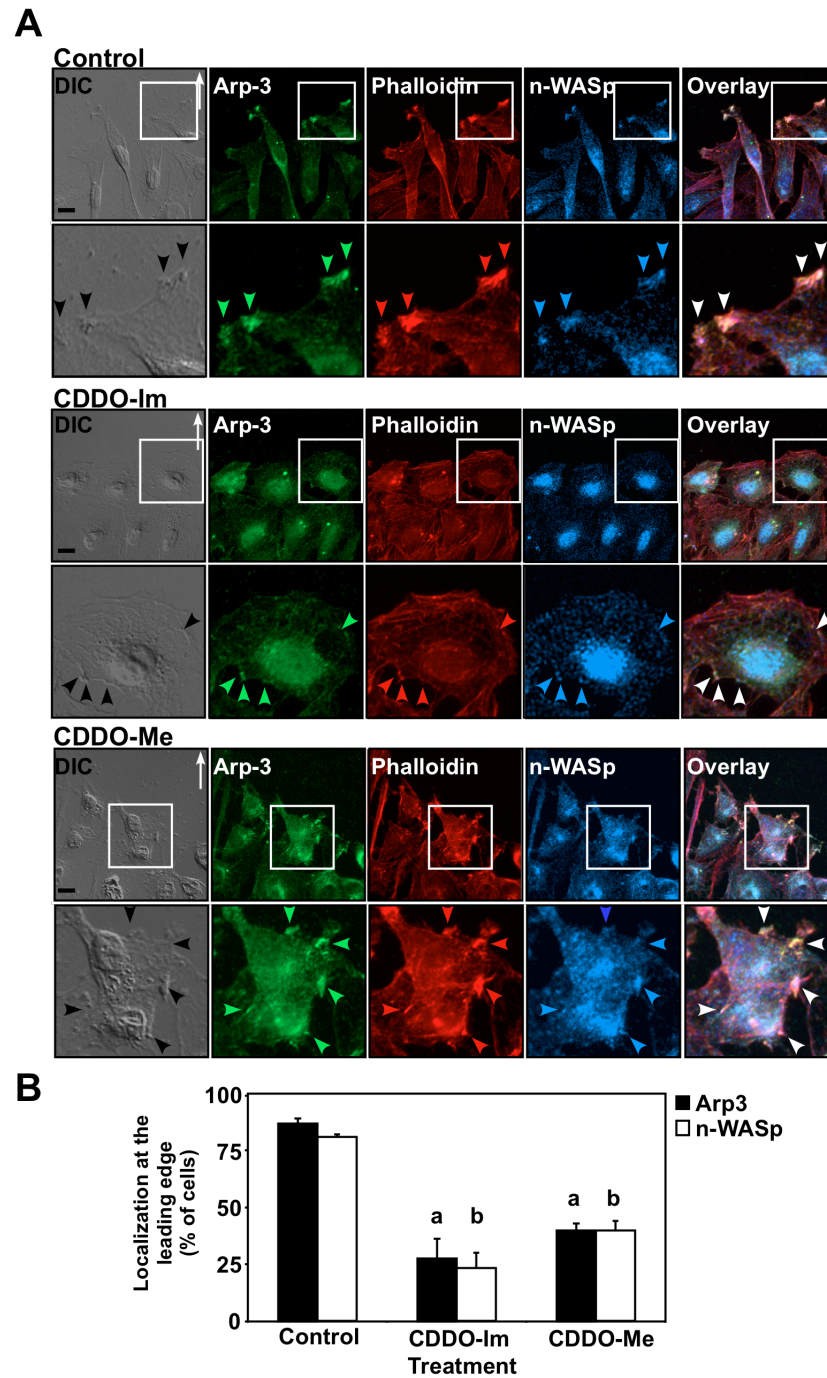
I then assessed whether the cellular localization of Arp3 was also affected by triterpenoid treatment (Figure 3.6). Confluent Rat2 fibroblasts were scratched and cells were then allowed to polarize and to establish a leading edge before being treated with DMSO, 1 µM of CDDO-Im or CDDO-Me. The cells were then fixed, permeabilized and

Figure. 3.6 Synthetic triterpenoids affect the localization of Arp3 and n-WASp at the leading edge of polarized cells.

A) Rat2 fibroblasts were scratched and incubated for 4 hours at 37°C to establish cell polarity and then treated with control medium (Control; top), 1 μM CDDO-Im (CDDO-Im; middle panel) or 1 μM CDDO-Me (CDDO-Me; bottom panel) for an additional 2 hours. The cells were then fixed, permeabilized and immunostained with anti-Arp-3 (Arp3; green), phalloidin for stress fibers (Phalloidin; red), and anti-n-WASp (n-WASp; blue) antibodies. The scratches were made in the horizontal plane above the cells. Arp-3, actin, and n-WASp proteins at the leading edge of migrating cells are indicated by green, red and blue arrowheads, respectively. The white arrowheads indicate the co-localization of all three proteins. White arrows indicate the direction of cellular movement. DIC microscopy was included to visualize the leading edge of migrating cells. Bar=10 μm.

B) Quantitation of cells containing Arp-3 or n-WASp at the leading edge of migrating cells was carried out using ImagePro software and graphed as localization at the leading edge (% of cells) *vs*. treatment (n=3±SD). a,b: $p < 0.05$ of Arp3 and nWASp, compared to respective controls.

Figure 3-6

A

B

stained for Arp3, n-WASp and F-actin (with phalloidin). I observed that Arp3 and n-WASp co-localized at the leading edge of polarized cells in the absence of CDDO-Im; however, when treated with CDDO-Im, both proteins were displaced from the leading edge and appeared diffused throughout the cytoplasm of the cell (Figure 3.6). CDDO-Me gave similar, albeit slightly reduced, effects as the CDDO-Im compound.

To confirm that the action of triterpenoids was specific to Arp3 and branched actin, I examined the effect of the synthetic triterpenoids on stress fibers and focal adhesions using immunofluorescence studies (Figure 3.7). Stress fibers are one of the most common and indicative unbranched actin structures in the cell and paxillin is a marker of focal adhesions. Confluent Rat2 cells were scratched and treated with the synthetic triterpenoids for 2 hours before fixation and permeabilization. Fluorescently tagged antibodies and phalloidin were used to stain for paxillin, stress fibers and actin respectively. I found that the structures of both stress fibers and focal adhesions were not diminished by CDDO-Im or CDDO-Me treatment (Figure 3.7). However, consistent with my *in vitro* data, branched actin staining was reduced at the leading edge of migrating cells after the incubation with triterpenoids (Figure 3.7B).

Having observed that triterpenoids inhibit Arp2/3 activity and branched actin formation, I next assessed if knockdown of Arp3 protein would inhibit Rat2 cell migration (Figure 3.8). I observed that a 65-70% silencing of Arp3 protein levels (Figure 3.8B), reduced Rat2 cell migration by approximately 35% (Figure 3.8C). These results suggest that the inhibition of Arp3 activity may be a mechanism whereby triterpenoids

Figure 3.7 CDDO-Im and CDDO-Me do not affect stress fibers or focal adhesions but reduce branched actin at the leading edge of migrating cells.

A) Rat2 fibroblasts were scratched and incubated for 4 hours at 37˚C to establish cell polarity and then treated with control medium (Control; top), 1 μM CDDO-Im (CDDO-Im; middle panel) or 1 μM CDDO-Me (CDDO-Me; bottom panel) for an additional 2 hours. The cells were then fixed, permeabilized and immunostained with anti-paxillin (paxillin; green), phalloidin for stress fibers (Phalloidin; red), and anti-actin (actin; blue) antibodies. The scratches were made in the horizontal plane above the cells shown and the leading edge of migrating cells containing paxillin, stress fibers and actin were indicated by green, red and blue arrowheads, respectively. The white arrowheads indicate co-localization and the white arrows indicate the direction of cellular movement. DIC microscopy was included to visualize the leading edges of migrating cells. Bar=10 μm.

B) Quantitation of cells containing actin at the leading edge of migrating cells was carried out using ImagePro software and graphed as localization at the leading edge (% of cells) *vs.* treatment (n=3±SD). *$p < 0.05$.

Figure 3-7
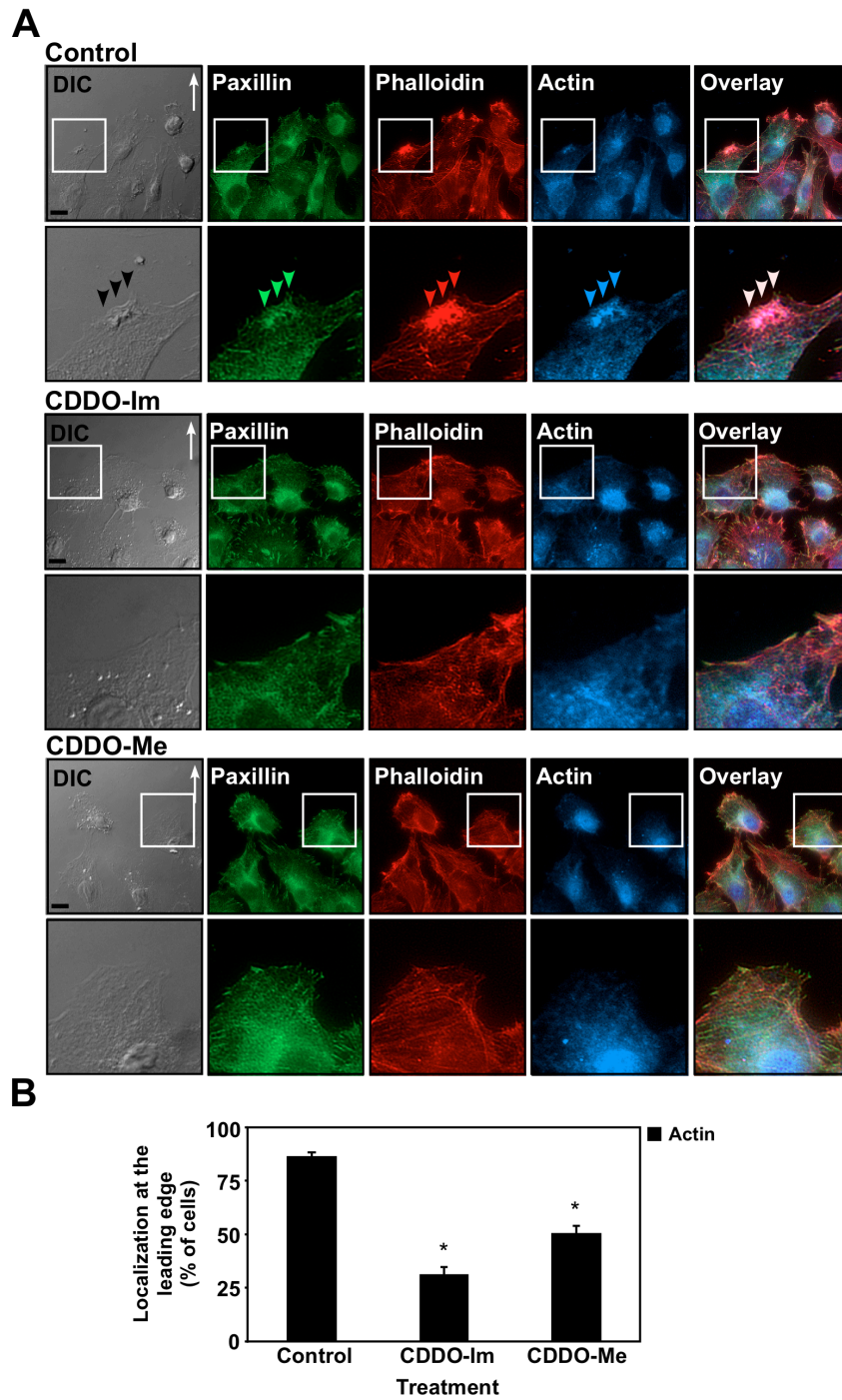
Figure. 3.8 Silencing Arp3 expression reduces cell migration.

A) Rat2 fibroblasts were transfected with control siRNA (scrambled), or two siRNA specific for Arp3 (Arp3 siRNA 1 and 2). When the cells reached confluency, they were scratched to create a 'wound'. Brightfield images (magnification 10X) were taken at the beginning of the experiment (0h) and after 12 hours (12h) of incubation at 37˚C. The white dotted lines indicate the edge of the leading edge of migrating cells.

B) Representative immunoblots of the cells described in panel A probed with Arp3 antibodies (top panel) or GAPDH (bottom panel).

C) Quantitation of cell migration described in panel A was carried out using ImagePro software and graphed as cell migration (percentage of control) *vs.* siRNA treatment (n=3±SD). *p<0.05.

Figure 3-8

A

B

C
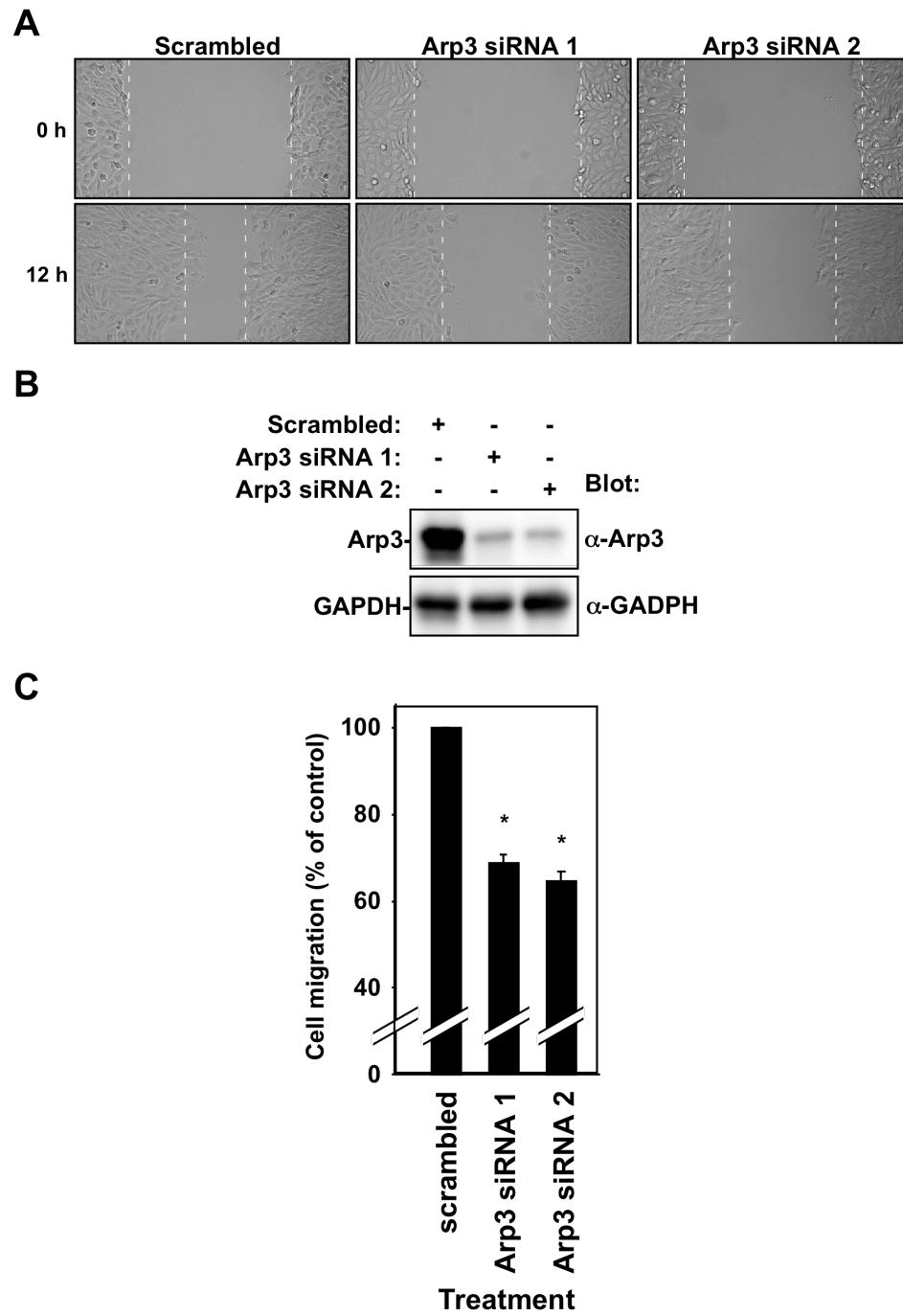
inhibit cell migration. To lend additional support for this hypothesis, I used *in silico* docking to identify potential high affinity triterpenoid binding sites in Arp3.

3.4.4 CDDO-Me binds to the hydrophobic pocket in Arp3.

To put my observations in the context of the recently characterized Arp2/3 inhibitors (52), docking experiments were carried out using the crystal structures of Arp2/3 (PDB-ID 3DXM (52)). The structure used for the docking experiments had been solved with a small molecule inhibitor, CK-548, bound to a hydrophobic pocket in Arp3. We tested the docking procedure using this inhibitor. The two top solutions corresponded to binding of CK-548 in the same hydrophobic pocket, but in two different orientations, that were the same in terms of predicted interaction energy (-8.9 kcal/mol, corresponding to a K_I of 315 nM). One of these solutions was identical to the position and conformation observed in the Arp3-CK-548 crystal structure, validating the accuracy of the docking procedure. A closely related compound, CK-869, docked to an identical position, with a slightly higher predicted K_I of 460 nM. This docked position for CK-869 corresponded very closely to the model for the Arp3-CK-869 complex proposed by Pollard and co-workers (52).

Interestingly, we observed that the triterpenoid CDDO-Me docked to Arp3 in the same hydrophobic pocket (Figure 3.9A and 3.9B). The docked position shown in Figure 3.9 has a binding energy of -13.3 kcal/mol and predicted K_I of 180 pM; this was the lowest energy solution obtained for the surface encompassing the Arp2 and Arp3

Figure 3.9 Docking of CDDO-Me to the Arp2/3 Complex.

The surface and internal cavities of the Arp2/3 complex (PDB-ID 3DXM; Ref. (52)) were used to find low energy binding sites for CDDO-Me and CDDO-Im with the program Autodock (51).

A) A hydrophobic pocket provided the lowest-energy binding site for CDDO-Me; the same pocket is predicted to bind CDDO-Im in an identical position and orientation, but with even greater affinity (not shown). The pocket is formed by a β-sheet and two α-helices, with the methyl ester moiety of CDDO-Me buried deeply in the pocket. In this situation, the site of attachment for the biotin tag (which was not included in the docking experiments) is solvent exposed and accessible. Thus, the best binding site found by *in silico* docking is consistent with the biochemical experiments. In unliganded Arp3 structures, a loop comprising residues 79 to 84 (in magenta) closes over the hydrophobic pocket, blocking access to the site. The change in conformation of this loop represents the only structural difference associated with drug binding to the hydrophobic pocket (52).

B) The internal surface of the hydrophobic pocket is outlined, with CDDO-Me in the low energy docked position. CK-869 is also shown in a docked position that is essentially identical to the position of CK-548 (not shown) in the crystal structure of the Arp2/3-CK-548 complex (52). CDDO-Me presents a greater contact surface and is much more rigid than CK-869, and its predicted affinity for Arp3 is higher.

C) A comparison of the chemical structures of the three compounds used in the docking experiments; CK-548 was also co-crystallized with Arp3 (52). In docking experiments, both CK-548 and CK-869 were predicted to bind with highest affinity to the hydrophobic pocket, in an orientation and position that is virtually identical to that observed for CK-548 in the Arp3-CK-548 crystal structure (52).

D) Competitive binding of b-CDDO-Me with CK-869. Purified Arp2/3 complex (2.5µg) was incubated with 10 µM biotinylated-CDDO-Me in the absence or presence of increasing concentrations of CDDO-Me or CK-869 (10-100 µM). The biotin-CDDO-Me-bound Arp3 was precipitated with neutravidin beads, processed for SDS-PAGE and immunoblotted with Arp3 antibodies. Fifty percent of the input was also blotted with Arp3 antibodies and shown on the right.

Figure 3-9
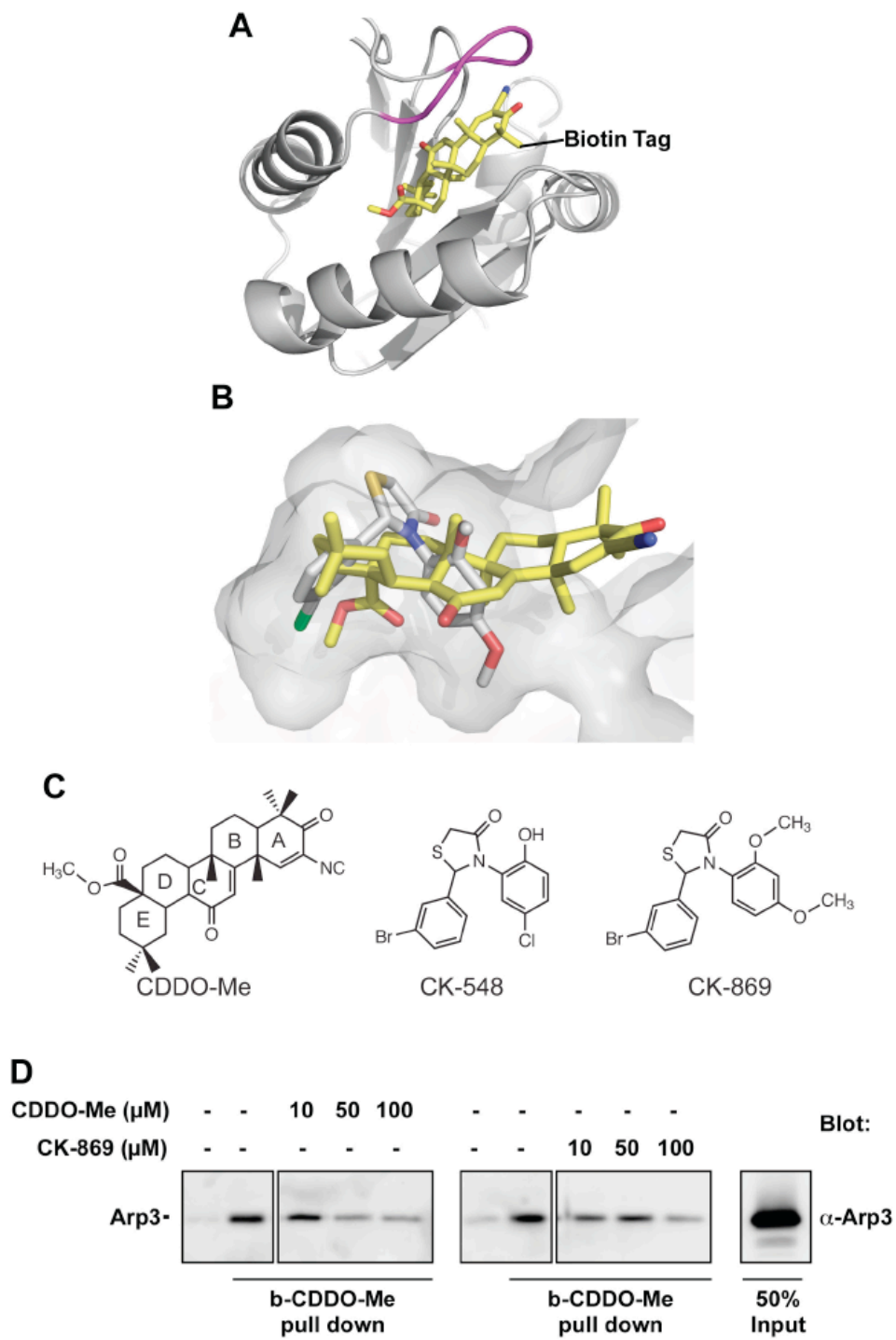
interface region, including all of the internal cavities. CDDO-Im, which has an imidazole group attached to the acid in place of the methyl in CDDO-Me, docked to the same pocket on Arp3, but with an even higher predicted affinity ($\underline{K}_I$ of 27 pM). It is noteworthy that the lowest energy docked positions for both CDDO-Me and CDDO-Im exposes C23 of the triterpenoid to the solvent: this is the site of attachment for the biotin label used for isolating the Arp2/3 complex from Rat2 fibroblasts, and therefore the lowest energy docked position is fully consistent with binding of the biotinylated CDDO-Me derivative. As can be seen in Figure 3.9B, the position that CDDO-Me is predicted to occupy matches closely to the docked position of CK-869, which in turn is virtually identical to the position of CK-548 in the actual crystal structure (52). Compared to unliganded Arp3 structures, both CDDO-Me and CDDO-Im require a localized conformation change in the loop comprising residues 79 to 84, which opens the pocket to allow binding (Figure 3.9A). The much tighter predicted binding for CDDO-Me compared to CK-869 is consistent with the lower concentrations of CDDO-Me required for biological effects.

To confirm that CDDO-Me and CK-869 bind to the same site in Arp3, binding competition assays were carried out with CK-869 and non-biotinylated CDDO-Me as a control (Fig. 3.9D). With increasing concentrations of CDDO-Me or CK-869, the amount of Arp3 that precipitated with biotinylated-CDDO-Me was reduced (Fig. 3.9D). This is consistent with our docking analysis that indicates CK-869 and CDDO-Me bind in the same hydrophobic pocket.

3.4.5   Inhibition of Arp3 attenuates cell migration and cell polarity.

To assess if the inhibition of Arp3 using CK-869 could also abrogate cell migration, I incubated cells with increasing concentrations of CK-869 (Figure 3.10). I observed that 7.5 µM CK-869 was able to inhibit cell migration by 50% (Figure 3.10B). The negative control, CK-312, which was characterized to bind to Arp3 but not inhibit its function, did not alter cell migration at the concentration range tested (Figure 3.10B). An interesting observation of the cells treated with the CK-869 Arp3 inhibitor was that the cells adopted a rounded up morphology and gave the appearance of detaching. However, over time the cells flattened (please see supplementary movie 4: http://www.jbc.org/content/suppl/2010/06/21/M110.103036.DC1/jbc.M110.103036-2.mov). This suggests that the cells may undergo cyclical rounding up and flattening in the presence of an Arp3 inhibitor.

Finally, I assessed if incubating polarized cells with CK-869 would affect branched actin polymerization in a manner similar to the triterpenoids. Rat2 fibroblasts were scratched and cells were then allowed to polarize to establish a leading edge before being treated with DMSO or 10 µM of CK-869. The cells were then fixed, permeabilized and stained for Arp3, n-WASp and phalloidin. I observed that Arp3 and n-WASp co-localized at the leading edge of polarized cells in the absence of CK-869, however, both proteins were displaced from the leading edge and appeared diffused throughout the cytoplasm of the cell (Figure 3.11). I also observed that phalloidin staining at the leading edge of polarized cells as well as actin staining were reduced in the CK-869-treated cells suggesting that the inhibition of branched actin polymerization alters cell polarity (Figure

Figure 3.10 CK-869 inhibits cell migration.

A) Confluent Rat2 fibroblasts were scratched to create a 'wound' and treated with DMSO (Control), 5 µM CK-312 (inactive control) or 5 µM CK-869 for 12 hours. Brightfield images (magnification 10X) were taken at the beginning of the experiment (0h) and after 12 hours (12 h) of incubation at 37˚C. The white dotted lines indicate the leading edge of migrating cells.

B) Cells were treated with increasing concentrations of CK-312 (inactive control) or CK-869 (1-10 µM) and imaged. Cell migration was quantified using ImagePro software and graphed as cell migration (percentage of control) *vs.* Arp3 inhibitor concentration (n=3±SD). *$p < 0.05$.

Figure 3-10

A

Control (DMSO)　　CK-312　　CK-869

0 h

12 h

B

Cell migration (% of control) vs Inhibitor concentration (µM)
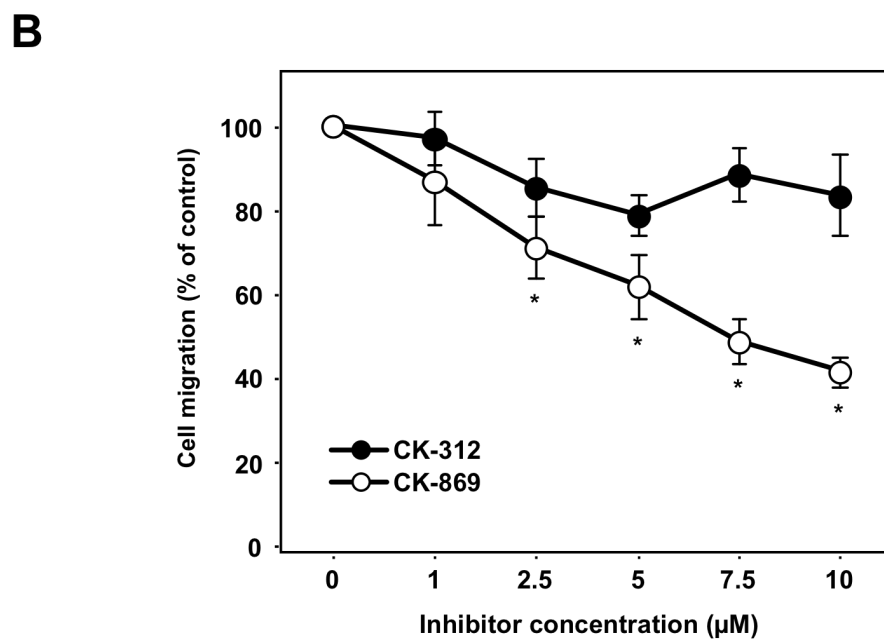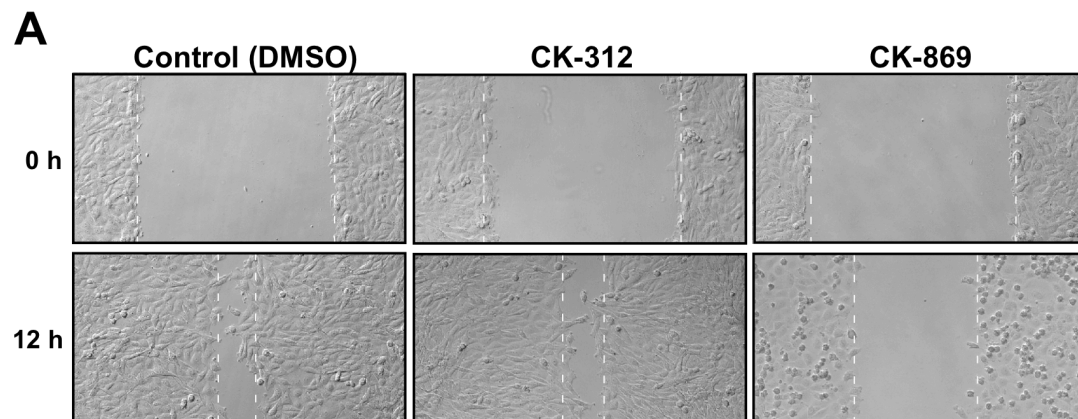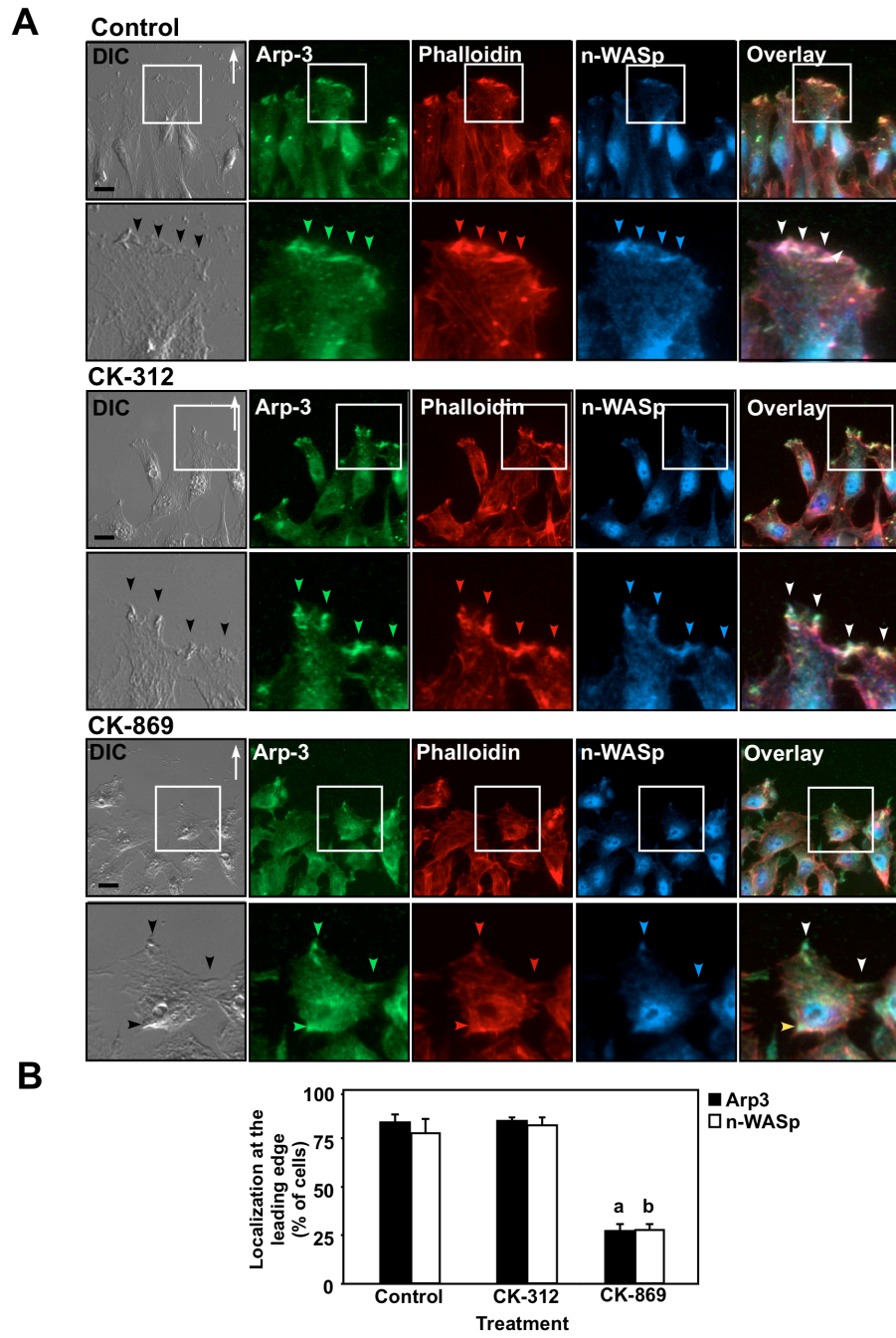
● CK-312
○ CK-869

Figure 3.11 CK-869 affects the localization of Arp3 and n-WASp at the leading edge of polarized cells.

A) Rat2 fibroblasts were scratched and incubated for 4 hours at 37˚C to establish cell polarity and then treated with control medium (Control; top), 10 μM CK-312 (middle panel) or 10 μM CK-869 (bottom panel) for an additional 2 hours. The cells were then fixed, permeabilized and immunostained with anti-Arp-3 (Arp3; green), phalloidin for stress fibers (Phalloidin; red), and anti-n-WASp (n-WASp; blue) antibodies. The scratches were made in the horizontal plane above the cells. Arp-3, actin, and n-WASp proteins at the leading edge of migrating cells are indicated by green, red and blue arrowheads, respectively. The white arrowheads indicate the co-localization of all three proteins. White arrows indicate the direction of cellular movement. DIC microscopy was included to visualize the leading edge of migrating cells. Bar=10 μm.

B) Quantitation of cells containing Arp-3 or n-WASp at the leading edge of migrating cells was carried out using ImagePro software and graphed as localization at the leading edge (% of cells) *vs*. treatment (n=3±SD). a,b: $p < 0.05$ of Arp3 and n-WASp, compared to respective controls.

Figure 3-11

A

B

3.12). Taken together, our results suggest that synthetic triterpenoids target Arp2/3-dependent actin polymerization, which contributes to the inhibition of cell migration.

Figure 3.12 CK-869 does not affect stress fibers or focal adhesions but reduces branched actin at the leading edge of migrating cells.

A) Rat2 fibroblasts were scratched and incubated for 4 hours at 37°C to establish cell polarity and then treated with control medium (Control; top), 10 μM CK-312 (middle panel) or 10 μM CK-869 (bottom panel) for an additional 2 hours. The cells were then fixed, permeabilized and immunostained with anti-Paxillin (green), phalloidin for stress fibers (Phalloidin; red), and anti-Actin (blue) antibodies. The scratches were made in the horizontal plane above the cells. Paxillin, branched actin and actin proteins at the leading edge of migrating cells are indicated by green, red and blue arrowheads, respectively. The white arrowheads indicate the co-localization of all three proteins. White arrows indicate the direction of cellular movement. DIC microscopy was included to visualize the leading edge of migrating cells. Bar=10 μm.

B) Quantitation of cells containing actin at the leading edge of migrating cells was carried out using ImagePro software and graphed as localization at the leading edge (% of cells) *vs*. treatment (n=3±SD). *p<0.05.

Figure 3-12

A

B
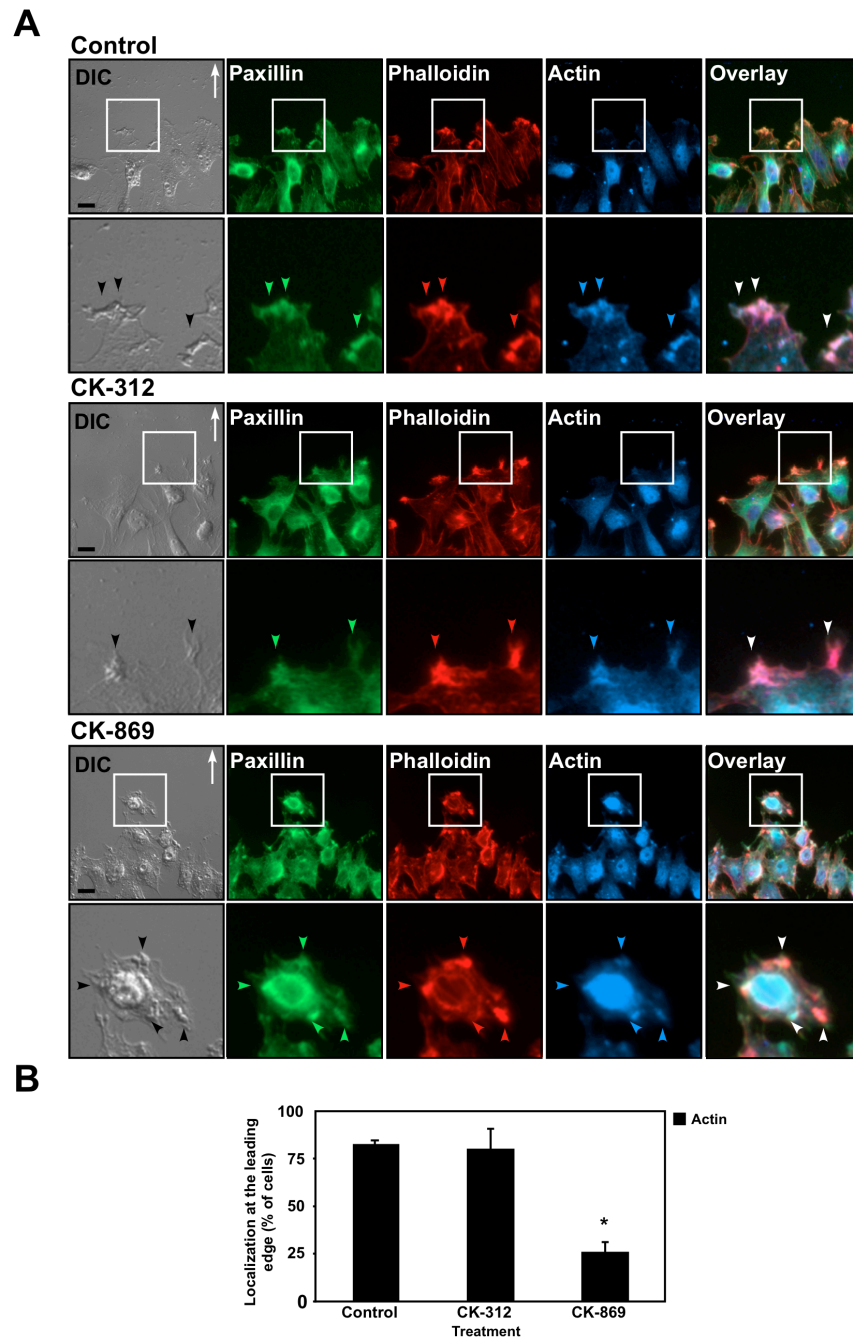
3.5   DISCUSSION

Cell migration plays an essential role in development, immune surveillance, and cellular repair. In cancer, it is the precursor event prior to most advanced cancer metastases. The diverse roles of cell migration make it difficult to understand its mechanisms of action clearly especially in the context of cancer, an illness that is made of multiple different diseases. Therefore, one of the major focuses in chemotherapy is to study the means of targeting cell migration in order to block tumor cells from migrating and invading to other parts of the body. Here we show that synthetic triterpenoids, which are effective at inducing apoptosis and modulate REDOX balance, are also effective at inhibiting cell migration. I observed that cell migration is inhibited by CDDO-Me and CDDO-Im in a dose dependent manner, with 1 μM being most effective without inducing apoptosis over 16 hours (Figure 3.1). I also found that Arp3 was a novel triterpenoid binding protein (Figure 3.3 and 3.4). Arp3 is an important subunit of the Arp2/3 complex, which is involved in the nucleation process of branched actin polymerization. Interestingly, the concentration of triterpenoids necessary to inhibit branched actin polymerization *in vitro* (50 μM) was higher than the concentration necessary to inhibit cell migration (1 μM).   This may reflect the possibility that the relative ratios of purified proteins *in vitro* rendered the inhibiting compounds less active or that there are other triterpenoid targets in the cell that have yet to be identified.   This second possibility is supported by my previous observation that the microtubule cytoskeleton is affected by CDDO-Im (49).

The knockdown of Arp2/3 using siRNA has been observed to reduce cell

migration (Figure 3.8). My studies further show that the triterpenoids target Arp3 and inhibit cell migration by specifically affecting branched actin polymerization (Figure 3.4, 3.6-3.7). Branched actin polymerization is essential for the formation of the lamellipodia at the leading edge of migrating cells, which in turn, allows for proper cell migration. Therefore, the reduction of branched actin polymerization by synthetic triterpenoids via Arp3 may provide a novel mechanism for which anti-cancer agents may be able to hinder cell migration and metastasis.

In this study, I also investigated whether the activities of small Rho GTPases would be affected by triterpenoid treatment. Although small Rho GTPases play a large role in cell migration, they do not seem to be major triterpenoid targets (Figure 3.5). Interestingly, I found that Rac1 activity was slightly elevated by CDDO-Im while the activities of the other Rho GTPases were not altered. This is contrary to what was expected with respect to the inhibition of cell migration. We reasoned that this could be due to a by-product of another triterpenoid specific phenomenon that has yet to be determined.

Recently, Arp2/3 inhibitors have been characterized by Pollard and colleagues (52). These inhibitors bind to different sites of the Arp2/3 complex, thereby, inhibiting its nucleating function. Specifically, CK-636 binds between Arp2 and Arp3; consequently, preventing Arp2 and Arp3 from forming an active complex for nucleation. CK-548 and CK-869 associate with Arp3 at its hydrophobic core, resulting in a conformation change that blocks nucleation of branched actin. This novel insight on how the binding of Arp2/3 inhibitors modulates the activation of Arp2/3 complex may possibly be transferred to the synthetic triterpenoids. Indeed, we observed that CDDO-Me docked to Arp2/3 in the

same hydrophobic pocket as CK-869 and was displaced in binding assays (Figure 3.9). This was further corroborated with functional assays where *bona fide* Arp3 inhibition blocked cell migration and polarity (Figure. 3.10-3.12). We therefore conclude that CDDO-Im and CDDO-Me inhibit Arp2/3 function in a similar manner as the Arp3 inhibitors. Taken together, this suggests that a combined inhibition of microtubule and branched actin cytoskeletal dynamics are involved in triterpenoid-mediated reduction of cell migration.

3.6   FOOTNOTES

3.7 REFERENCES

1. Ozdamar, B., Bose, R., Barrios-Rodiles, M., Wang, H. R., Zhang, Y., and Wrana, J. L. (2005) *Science* **307**, 1603-1609

2. Mehlen, P., and Puisieux, A. (2006) *Nat Rev Cancer* **6**, 449-458

3. Le Clainche, C., and Carlier, M. F. (2008) *Physiol Rev* **88**, 489-513

4. Ahmad, R., Raina, D., Meyer, C., Kharbanda, S., and Kufe, D. (2006) *J Biol Chem* **281**, 35764-35769

5. Chintharlapalli, S., Papineni, S., Konopleva, M., Andreef, M., Samudio, I., and Safe, S. (2005) *Mol Pharmacol* **68**, 119-128

6. Deeb, D., Gao, X., Dulchavsky, S. A., and Gautam, S. C. (2007) *Anticancer Res* **27**, 3035-3044

7. Gao, X., Deeb, D., Danyluk, A., Media, J., Liu, Y., Dulchavsky, S. A., and Gautam, S. C. (2008) *Immunopharmacol Immunotoxicol* **30**, 581-600

8. Liby, K., Voong, N., Williams, C. R., Risingsong, R., Royce, D. B., Honda, T., Gribble, G. W., Sporn, M. B., and Letterio, J. J. (2006) *Clin Cancer Res* **12**, 4288-4293

9. Liby, K. T., Yore, M. M., and Sporn, M. B. (2007) *Nat Rev Cancer* **7**, 357-369

10. Ling, X., Konopleva, M., Zeng, Z., Ruvolo, V., Stephens, L. C., Schober, W., McQueen, T., Dietrich, M., Madden, T. L., and Andreeff, M. (2007) *Cancer Res* **67**, 4210-4218

11. Shin, S., Wakabayashi, N., Misra, V., Biswal, S., Lee, G. H., Agoston, E. S., Yamamoto, M., and Kensler, T. W. (2007) *Mol Cell Biol* **27**, 7188-7197

12. Shishodia, S., Sethi, G., Konopleva, M., Andreeff, M., and Aggarwal, B. B. (2006) *Clin Cancer Res* **12**, 1828-1838

13. Thimmulappa, R. K., Fuchs, R. J., Malhotra, D., Scollick, C., Traore, K., Bream, J. H., Trush, M. A., Liby, K. T., Sporn, M. B., Kensler, T. W., and Biswal, S. (2007) *Antioxid Redox Signal* **9**, 1963-1970

14. Thimmulappa, R. K., Scollick, C., Traore, K., Yates, M., Trush, M. A., Liby, K. T., Sporn, M. B., Yamamoto, M., Kensler, T. W., and Biswal, S. (2006) *Biochem Biophys Res Commun* **351**, 883-889

15. Wang, Y., Porter, W. W., Suh, N., Honda, T., Gribble, G. W., Leesnitzer, L. M., Plunket, K. D., Mangelsdorf, D. J., Blanchard, S. G., Willson, T. M., and Sporn, M. B. (2000) *Mol Endocrinol* **14**, 1550-1556

16. Yates, M. S., Kwak, M. K., Egner, P. A., Groopman, J. D., Bodreddigari, S., Sutter, T. R., Baumgartner, K. J., Roebuck, B. D., Liby, K. T., Yore, M. M., Honda, T., Gribble, G. W., Sporn, M. B., and Kensler, T. W. (2006) *Cancer Res* **66**, 2488-2494

17. Yates, M. S., Tauchi, M., Katsuoka, F., Flanders, K. C., Liby, K. T., Honda, T., Gribble, G. W., Johnson, D. A., Johnson, J. A., Burton, N. C., Guilarte, T. R., Yamamoto, M., Sporn, M. B., and Kensler, T. W. (2007) *Mol Cancer Ther* **6**, 154-162

18. Yore, M. M., Liby, K. T., Honda, T., Gribble, G. W., and Sporn, M. B. (2006) *Mol Cancer Ther* **5**, 3232-3239

19. Honda, T., Honda, Y., Favaloro, F. G., Jr., Gribble, G. W., Suh, N., Place, A. E., Rendi, M. H., and Sporn, M. B. (2002) *Bioorg Med Chem Lett* **12**, 1027-1030

20. Honda, T., Rounds, B. V., Bore, L., Favaloro, F. G., Jr., Gribble, G. W., Suh, N., Wang, Y., and Spor, M. B. (1999) *Bioorg Med Chem Lett* **9**, 3429-3434

21. Honda, T., Rounds, B. V., Bore, L., Finlay, H. J., Favaloro, F. G., Jr., Suh, N., Wang, Y., Sporn, M. B., and Gribble, G. W. (2000) *J Med Chem* **43**, 4233-4246

22. Honda, T., Rounds, B. V., Gribble, G. W., Suh, N., Wang, Y., and Sporn, M. B. (1998) *Bioorg Med Chem Lett* **8**, 2711-2714

23. Ikeda, T., Nakata, Y., Kimura, F., Sato, K., Anderson, K., Motoyoshi, K., Sporn, M., and Kufe, D. (2004) *Mol Cancer Ther* **3**, 39-45

24. Ikeda, T., Sporn, M., Honda, T., Gribble, G. W., and Kufe, D. (2003) *Cancer Res* **63**, 5551-5558

25. Suh, N., Wang, Y., Honda, T., Gribble, G. W., Dmitrovsky, E., Hickey, W. F., Maue, R. A., Place, A. E., Porter, D. M., Spinella, M. J., Williams, C. R., Wu, G., Dannenberg, A. J., Flanders, K. C., Letterio, J. J., Mangelsdorf, D. J., Nathan, C. F., Nguyen, L., Porter, W. W., Ren, R. F., Roberts, A. B., Roche, N. S., Subbaramaiah, K., and Sporn, M. B. (1999) *Cancer Res* **59**, 336-341

26. Kress, C. L., Konopleva, M., Martinez-Garcia, V., Krajewska, M., Lefebvre, S., Hyer, M. L., McQueen, T., Andreeff, M., Reed, J. C., and Zapata, J. M. (2007) *PLoS ONE* **2**, e559

27. Brookes, P. S., Morse, K., Ray, D., Tompkins, A., Young, S. M., Hilchey, S., Salim, S., Konopleva, M., Andreeff, M., Phipps, R., and Bernstein, S. H. (2007) *Cancer Res* **67**, 1793-1802

28.   Han, S. S., Peng, L., Chung, S. T., DuBois, W., Maeng, S. H., Shaffer, A. L., Sporn, M. B., and Janz, S. (2006) *Mol Cancer* **5**, 22

29.   Inoue, S., Snowden, R. T., Dyer, M. J., and Cohen, G. M. (2004) *Leukemia* **18**, 948-952

30.   Ray, D. M., Morse, K. M., Hilchey, S. P., Garcia, T. M., Felgar, R. E., Maggirwar, S. B., Phipps, R. P., and Bernstein, S. H. (2006) *Exp Hematol* **34**, 1202-1211

31.   Ito, Y., Pandey, P., Place, A., Sporn, M. B., Gribble, G. W., Honda, T., Kharbanda, S., and Kufe, D. (2000) *Cell Growth Differ* **11**, 261-267

32.   Konopleva, M., Contractor, R., Kurinna, S. M., Chen, W., Andreeff, M., and Ruvolo, P. P. (2005) *Leukemia* **19**, 1350-1354

33.   Konopleva, M., Tsao, T., Estrov, Z., Lee, R. M., Wang, R. Y., Jackson, C. E., McQueen, T., Monaco, G., Munsell, M., Belmont, J., Kantarjian, H., Sporn, M. B., and Andreeff, M. (2004) *Cancer Res* **64**, 7927-7935

34.   Konopleva, M., Tsao, T., Ruvolo, P., Stiouf, I., Estrov, Z., Leysath, C. E., Zhao, S., Harris, D., Chang, S., Jackson, C. E., Munsell, M., Suh, N., Gribble, G., Honda, T., May, W. S., Sporn, M. B., and Andreeff, M. (2002) *Blood* **99**, 326-335

35.   Stadheim, T. A., Suh, N., Ganju, N., Sporn, M. B., and Eastman, A. (2002) *J Biol Chem* **277**, 16448-16455

36.   Gao, X., Deeb, D., Jiang, H., Liu, Y., Dulchavsky, S. A., and Gautam, S. C. (2007) *J Neurooncol* **84**, 147-157

37.   Ito, Y., Pandey, P., Sporn, M. B., Datta, R., Kharbanda, S., and Kufe, D. (2001) *Mol Pharmacol* **59**, 1094-1099

38.   Kim, K. B., Lotan, R., Yue, P., Sporn, M. B., Suh, N., Gribble, G. W., Honda, T., Wu, G. S., Hong, W. K., and Sun, S. Y. (2002) *Mol Cancer Ther* **1**, 177-184

39.   Liby, K., Royce, D. B., Williams, C. R., Risingsong, R., Yore, M. M., Honda, T., Gribble, G. W., Dmitrovsky, E., Sporn, T. A., and Sporn, M. B. (2007) *Cancer Res* **67**, 2414-2419

40.   Zou, W., Chen, S., Liu, X., Yue, P., Sporn, M. B., Khuri, F. R., and Sun, S. Y. (2007) *Cancer Biol Ther* **6**, 1614-1620

41.   Zou, W., Liu, X., Yue, P., Zhou, Z., Sporn, M. B., Lotan, R., Khuri, F. R., and Sun, S. Y. (2004) *Cancer Res* **64**, 7570-7578

42.   Lapillonne, H., Konopleva, M., Tsao, T., Gold, D., McQueen, T., Sutherland, R. L., Madden, T., and Andreeff, M. (2003) *Cancer Res* **63**, 5926-5939

43.	Hyer, M. L., Croxton, R., Krajewska, M., Krajewski, S., Kress, C. L., Lu, M., Suh, N., Sporn, M. B., Cryns, V. L., Zapata, J. M., and Reed, J. C. (2005) *Cancer Res* **65**, 4799-4808

44.	Konopleva, M., Zhang, W., Shi, Y. X., McQueen, T., Tsao, T., Abdelrahim, M., Munsell, M. F., Johansen, M., Yu, D., Madden, T., Safe, S. H., Hung, M. C., and Andreeff, M. (2006) *Mol Cancer Ther* **5**, 317-328

45.	Melichar, B., Konopleva, M., Hu, W., Melicharova, K., Andreeff, M., and Freedman, R. S. (2004) *Gynecol Oncol* **93**, 149-154

46.	Samudio, I., Konopleva, M., Hail, N., Jr., Shi, Y. X., McQueen, T., Hsu, T., Evans, R., Honda, T., Gribble, G. W., Sporn, M., Gilbert, H. F., Safe, S., and Andreeff, M. (2005) *J Biol Chem* **280**, 36273-36282

47.	Pedersen, I. M., Kitada, S., Schimmer, A., Kim, Y., Zapata, J. M., Charboneau, L., Rassenti, L., Andreeff, M., Bennett, F., Sporn, M. B., Liotta, L. D., Kipps, T. J., and Reed, J. C. (2002) *Blood* **100**, 2965-2972

48.	Suh, W. S., Kim, Y. S., Schimmer, A. D., Kitada, S., Minden, M., Andreeff, M., Suh, N., Sporn, M., and Reed, J. C. (2003) *Leukemia* **17**, 2122-2129

49.	To, C., Kulkarni, S., Pawson, T., Honda, T., Gribble, G. W., Sporn, M. B., Wrana, J. L., and Di Guglielmo, G. M. (2008) *J Biol Chem* **283**, 11700-11713

50.	Honda, T., Janosik, T., Honda, Y., Han, J., Liby, K. T., Williams, C. R., Couch, R. D., Anderson, A. C., Sporn, M. B., and Gribble, G. W. (2004) *J Med Chem* **47**, 4923-4932

51.	Morris, G. M., Huey, R., Lindstrom, W., Sanner, M. F., Belew, R. K., Goodsell, D. S., and Olson, A. J. (2009) *J Comput Chem* **30**, 2785-2791

52.	Nolen, B. J., Tomasevic, N., Russell, A., Pierce, D. W., Jia, Z., McCormick, C. D., Hartman, J., Sakowicz, R., and Pollard, T. D. (2009) *Nature* **460**, 1031-1034

53.	Bore, L., Honda, T., Gribble, G. W., Lork, E., and Jasinski, J. P. (2002) *Acta Crystallogr C* **58**, o199-200

54.	Sogno, I., Vannini, N., Lorusso, G., Cammarota, R., Noonan, D. M., Generoso, L., Sporn, M. B., and Albini, A. (2009) *Recent Results Cancer Res* **181**, 209-212

55.	Couch, R. D., Ganem, N. J., Zhou, M., Popov, V. M., Honda, T., Veenstra, T. D., Sporn, M. B., and Anderson, A. C. (2006) *Mol Pharmacol* **69**, 1158-1165

56.	Fukata, M., Nakagawa, M., and Kaibuchi, K. (2003) *Curr Opin Cell Biol* **15**, 590-597

CHAPTER 4

SYNTHETIC TRITERPENOIDS TARGET GSK3β AND MODULATE ITS ACTIVITY ON FOCAL ADHESION DYNAMICS TO INHIBIT CELL MIGRATION

4 CHAPTER 4

4.1 CHAPTER SUMMARY

Synthetic triterpenoids are a class of anti-cancer compounds that target cellular functions, including apoptosis, growth and inflammation in cell culture and animal models. Currently, their effect on cell migration, a precursor event to cancer metastasis, is being characterized. Previously, I showed that triterpenoids partially inhibited cell migration by interfering with Arp2/3-dependent branched actin polymerization in lamellipodia (1). My current studies revealed that Glycogen Synthase Kinase 3 beta (GSK3β), a kinase that regulates many cellular processes including cell adhesion dynamics, is a triterpenoid-binding target. Specifically, triterpenoids inhibited GSK3β activity and they appeared to increase focal adhesion size. To further examine whether these effects on focal adhesions in triterpenoid-treated cells were GSK3β-dependent, I used GSK3 inhibitors (lithium chloride and SB216763), to examine cell adhesion and morphology as well as cell migration. My studies showed that GSK3β inhibitors also altered cell adhesion sizes, inhibited cell migration and inactivated GSK3β, consistent with what we observed in triterpenoid-treated cells. Therefore, triterpenoids may affect focal adhesion dynamics as well as cell migration by targeting and altering the activity of GSK3β.

4.2   INTRODUCTION

The triterpenoids are a class of compounds biosynthesized in plants by the cyclization of squalene. Specifically, oleanolic acid is one of the 2,000 triterpenoids found in nature, and is widely used in Asia for its weak anti-inflammatory and anti-tumorigenic properties (2). The modification of oleanolic acid to the synthetic oleanolic triterpenoid, 2-cyano-3,12-dioxooleana-1,9 (11)-dien-28-oic acid (CDDO) and its methyl ester (CDDO-Me) and imidazolide (CDDO-Im) derivatives increases the biological activities of these compounds (3). In fact, CDDO and its derivatives are effective in inducing cytoprotection and apoptosis, as well as in reducing tumor proliferation, as assessed using animal models and cancer cell culture studies (4). However, very few studies have examined the effects of triterpenoids on cell adhesion and cell migration, both of which are important players in tumor metastasis.

Cell migration is the process in which a cell can initiate movement in response to stimuli such as chemo-attractants or stress in the biological system. It is a highly orchestrated process involving many different cellular components that collectively regulate cell motility. This process mainly encompasses the reorganization of the actin and microtubule cytoskeletons and cellular proteins to establish cell polarity, and the formation of a definitive leading edge. More importantly, as a cell extends its protrusions to explore its surrounding environment in preparation for cell movement, the protrusions are stabilized by adhesion structures used as traction points that allow cells to advance towards or away from the stimuli (5). These adhesion structures are composed of complexes with multiple adhesion proteins that are often characterized as focal

complexes, focal adhesions or fibrillar adhesions depending on their sizes, morphology and dynamics (6). Focal complexes are small nascent adhesions that are often observed in rapidly migrating cells and most of these structures turnover within minutes, so the cell continues to migrate (7). However, some of these nascent adhesions do mature and evolve into focal adhesions that attach to the ends of stress fibers to maintain the structure of the cell (8). Similarly, most of the focal adhesions disassemble, but at a slower rate, in order for the cell to maintain its flexibility as it moves forward. The adhesions that mature are known as fibrillar adhesions and they are involved in the remodeling of the extracellular matrix. Therefore, a delicate balance between the disassembly and the maturation of adhesions is a critical contributing factor towards regulating cell migration. In fact, the reduction of adhesion turnover has been shown to increase the size of focal adhesions and reduce cell motility (9,10).

Within these multi-protein adhesion complexes, different scaffolding and signaling molecules are recruited to regulate the dynamics of the adhesion structures. For instance, paxillin and FAK are important proteins that are commonly found at focal adhesion sites and thus, are often used as focal adhesion markers. Although it possesses no kinase activity itself, paxillin is one of the first scaffolding proteins that is recruited to the adhesion complex during focal adhesion assembly. In addition, paxillin is important for the recruitment of other signaling proteins, such as FAK, to the complex. In fact, mice deficient in paxillin die during embryogenesis due to defects in cell migration (11) and paxillin-null embryonic stem cells show defects in cell spreading (12). FAK is an important kinase that is known as a master regulator of focal adhesion turnover. It is an essential player in the regulation of numerous important intracellular signaling pathways

involving the turnover of cell contacts with the extracellular matrix and the promotion of cell migration. The loss of FAK can also lead to embryonic lethality. In addition, *Fak^{-/-}* fibroblasts show enlarged focal adhesions and reduced cell motility. Glycogen Synthase Kinase 3 Beta (GSK3β), originally identified for its role in regulating glycogen metabolism and Wnt-mediated cell proliferation, is also involved in regulating cell migration and adhesion dynamics. GSK3β is a protein that is found constitutively active in cells and has been reported to phosphorylate microtubule-associated proteins and interact with microtubule motor proteins to regulate microtubule dynamics and microtubule-dependent vesicle transport (13). In addition, GSK3β also regulates several Rho small GTPases including Rac1, RhoA and Arf6, which in turn, control membrane ruffling, cell spreading and lamellipodia formation. Interestingly, a small pool of inactive GSK3β localizes at the leading edge of migrating cells and enables APC to localize to the plus end of microtubules and stimulate microtubule growth and stability. However, global inactivity of GSK3β can inhibit cell migration (14).

In this chapter, I studied the effects of triterpenoids on the dynamics of focal adhesions, as they play a critical role in regulating cell migration (9,10).

4.3   MATERIALS AND METHODS

4.3.1   Cell Culture and Antibodies

Rat2 fibroblasts were cultured using Dulbecco's modified Eagle's medium (DMEM) with 10% fetal bovine serum (FBS) in a 37°C incubator with 5% CO_2. Anti-FAK (BD610087), anti-Rac1 (610650), and anti-paxillin (BD610051) antibodies were purchased from BD Transductions Laboratories (Mississauga, Canada). Anti-phospho-FAK Y397 (#3283), anti-phospho-FAK Y576/577 (#3281), anti-phospho-FAK Y925 (#3284), anti-GSK3β (#9315) and anti-phospho-GSK3β serine 9 (#9336) antibodies were purchased from Cell Signaling Technologies (Pickering, Canada). Anti-phospho-FAK serine 722 (sc-16662-R) and anti-IQGAP1 (sc-10792) were purchased from Santa Cruz Biotechnologies Inc. (Santa Cruz, CA). Alexa Fluor 555-conjugated phalloidin (A34055) was purchased from Invitrogen Molecular Probes (Oregon, USA). Biotinylated CDDO-Me was a generous gift from Dr. M.B. Sporn (Hanover, NH). The biotinylated form of CDDO-Me (compound 6) has been characterized and by Honda and colleagues (15). Collagen I (27666) used to coat the plates for cell adhesion assays was purchased from Sigma Aldrich (Oakville, Canada).

4.3.2   Scratch Assays and Immunofluorescence Microscopy

Rat2 fibroblasts were cultured to confluency before a scratch was made with a pipette tip. Cells were then processed for either cell migration assay studies or immunofluorescence microscopy. For cell migration studies, cells were treated with

media containing 0.1% DMSO or 50 mM NaCl (as vehicles), 1 μM CDDO-Im, 1 μM CDDO-Me, 50 μM SB216763, or 50 mM lithium chloride and brightfield images were taken over 16 hours. For immunofluorescence microscopy, cells were given 4 hours to establish polarity and a leading edge before their 2-hour drug treatment followed by fixation, permeabilization and incubation with anti-Rac1, anti-IQGAP1, anti-FAK, anti-paxillin, anti-phalloidin, and anti-GSK3β antibodies. All immunofluorescence images were taken using an Olympus IX81 microscope controlled by QED *Invivo* software or the Olympus Fluoroview Confocal microscope controlled by Fluoroview software (Olympus, Canada).

4.3.3   *Affinity Pull-Down Assay using Biotinylated CDDO-Me*

To examine the co-localization of GSK3β and CDDO-Me, Rat2 fibroblasts were grown to confluency, scratched with a pipette tip and allowed to polarize for 6 hours. Cells were then fixed, permeabilized and incubated with anti-Rac1 antibodies followed by treatment with either 0.1% DMSO, 10 μM biotin, 10 μM CDDO-Me or 10 μM biotinylated CDDO-Me. Streptavidin-Cy3 was used to visualize biotinylated CDDO-Me. Samples were stained with DAPI to visualize the nuclei. To confirm that FAK and GSK3β were triterpenoid-binding targets, cell lysates were incubated with 0.1% DMSO, 10 μM biotin, 10 μM CDDO-Me or 10 μM biotinylated CDDO-Me for two hours, followed by streptavidin beads. Samples were processed by SDS-PAGE and probed with anti-FAK and anti-GSK3β antibodies.

4.3.4   Western Blotting

Rat2 fibroblasts were incubated with 0.1% DMSO or 50 mM NaCl (as controls), 1 μM CDDO-Im, 1 μM CDDO-Me, 50 mM Lithium Chloride or 50 μM SB216763 for two hours before lysis. Samples were processed using SDS-PAGE and probed with anti-GSK3β, anti-phospho-GSK3β, anti-paxillin, anti-phospho-paxillin, anti-FAK or anti-phospho-FAK antibodies.

4.3.5   Cell Adhesion Assays

For cell adhesion stability assays, 50 000 Rat2 fibroblasts were seeded overnight on either BSA or Collagen I-coated plates followed by incubation in 0.01% DMSO, 1 μM CDDO-Im or 1 μM CDDO-Me for two hours. For cell adhesion formation assays, Rat2 fibroblasts were plated on 10 cm dishes overnight and treated the next day with 0.1% DMSO, 1 μM CDDO-Im or 1 μM CDDO-Me before being lifted off from the plate using EDTA. 100 000 cells were then re-seeded into 24-well plates that were coated with either BSA or Collagen I. After reseeding, treated cells were incubated with 0.1% DMSO, 1 μM CDDO-Im or 1 μM CDDO-Me for additional two hours. All conditions in both assays were done in quadruplicates. To quantify the adhesions, cells were washed once with PBS and four images per well were taken and at least 250 cells were counted. Cells that were still adhered to the plate were counted and graphed.

4.3.6   Statistical Analyses

Results were provided as means ± SD. One-way ANOVA with a Tukey's post-hoc test was performed to assess the statistical differences between experimental groups. $P < 0.05$ and $p < 0.01$ were considered statistical significant.

4.4   RESULTS

To assess whether the triterpenoids play a role in cell adhesion dynamics, I utilized a comprehensive proteomic database that consisted of a list of triterpenoid-binding targets I created previously (1). My results showed that various structural focal adhesion proteins were bound by the triterpenoids (Table 4.1). Therefore, I examined whether triterpenoids affected focal adhesion morphology using immunofluorescence microscopy. Briefly, Rat2 fibroblasts were scratched and allowed to polarized before they were treated with DMSO, CDDO-Im or CDDO-Me for 2 hours before they were fixed, permeabilized and stained for the focal adhesion markers, paxillin (Figure 4.1A) and FAK (Figure 4.1B). Both paxillin and FAK were present in the cell body as well as at the leading edge. In cells treated with DMSO as a control, these focal adhesion markers appeared to be thin and long especially at the leading edge of migrating cells, whereas in the cell body, the staining appeared to be fainter and with a smaller area (Figure 4.1). However, when I treated cells with the triterpenoids, I observed that both paxillin and FAK staining were enlarged.

Numerous studies have shown that focal adhesion enlargement can contribute to delayed turnover and inhibition of cell migration (16,17). Therefore, I hypothesized that the alterations observed on focal adhesions by the triterpenoids may, at least in part, inhibit cell migration. Since the size of focal adhesions can be affected by the ability of cells to either assemble or disassemble them, I next evaluated whether the formation or maturation of cell adhesions was affected by triterpenoid treatment using two different cell adhesion studies (Figure 4.2).   To examine cell adhesion stability in the presence of

Table 4-1

Triterpenoid-binding targets identified *via* mass spectrometry and/or proteoarray
Integrin alpha-6
Focal Adhesion Kinase
Glycogen Synthase Kinase Beta
Integrin Linked Kinase
PINCH
Tensin
Parvin
Actin
Alpha-actinin

Figure 4.1 Triterpenoids enlarge focal adhesions at the leading edge of migrating cells.

A) Rat2 fibroblasts were scratched and incubated for 4 hours at 37˚C to establish cell polarity and then treated with 0.01% DMSO (Control; top), 1 µM CDDO-Im (CDDO-Im; middle panel) or 1 µM CDDO-Me (CDDO-Me; bottom panel) for an additional 2 hours. The cells were then fixed, permeabilized and immunostained with anti-paxillin antibodies (Paxillin; green) and phalloidin for actin stress fibers (Phalloidin; red). A representative area (inset) is magnified and shown. Bar = 10 µm. Representative images from four individual experiments are shown.

B) Rat2 fibroblasts were scratched and incubated for 4 hours at 37˚C to establish cell polarity and then treated with 0.01% DMSO (Control; top), 1 µM CDDO-Im (CDDO-Im; middle panel) or 1 µM CDDO-Me (CDDO-Me; bottom panel) for an additional 2 hours. The cells were then fixed, permeabilized and immunostained with anti-FAK antibodies (FAK; green) and phalloidin for actin stress fibers (Phalloidin; red). A representative area (inset) is magnified and shown. Bar = 10 µm. Representative images from four individual experiments are shown.
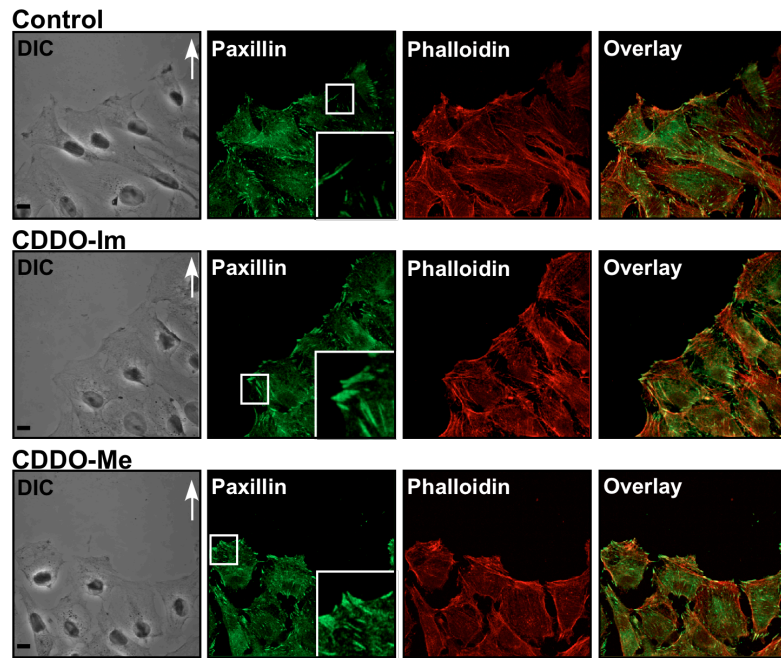
Figure 4-1

A

Control

| DIC | Paxillin | Phalloidin | Overlay |

CDDO-Im

| DIC | Paxillin | Phalloidin | Overlay |

CDDO-Me

| DIC | Paxillin | Phalloidin | Overlay |

B

Control

| DIC | FAK | Phalloidin | Overlay |

CDDO-Im

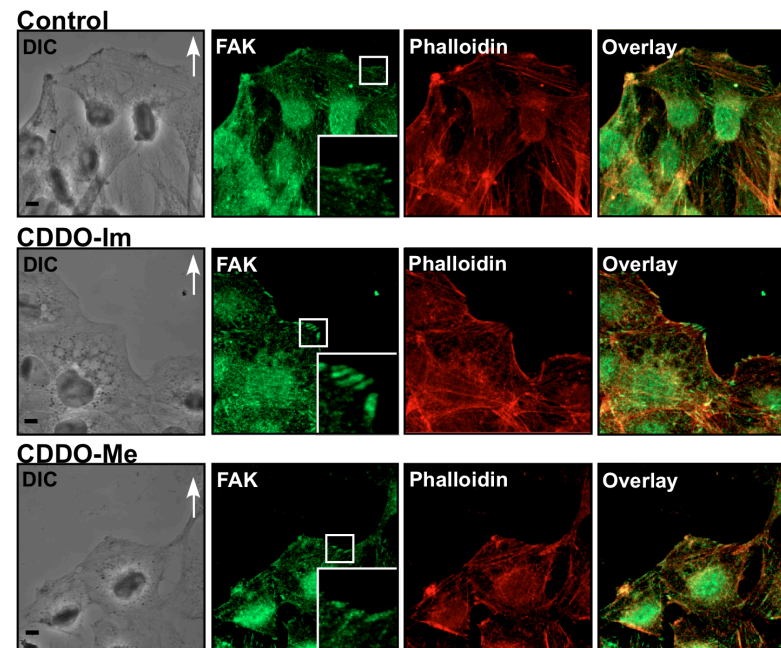| DIC | FAK | Phalloidin | Overlay |

CDDO-Me

| DIC | FAK | Phalloidin | Overlay |

Figure 4.2 Triterpenoids do not decrease the number of adhered cells but inhibit the association of detached cells to Collagen I.

 A) Rat2 fibroblasts were plated overnight on BSA or Collagen I-coated plates followed by incubation in 0.01% DMSO, 1 μM CDDO-Im or 1 μM CDDO-Me for 2 hours before cells were quantitated by counting the number of adherent cells in the DMSO, CDDO-Im or CDDO-Me (Treatment) on either BSA(-Collagen) or Collagen I-coated (+Collagen) plates.

B) Rat2 fibroblasts were plated in 10 cm dishes overnight and treated for two hours before being re-seeded on 24 well BSA or Collagen I-coated plates and treated with 0.01% DMSO, 1 μM CDDO-Im or 1 μM CDDO-Me for an additional 2 hours. Quantitation was performed as described in panel A. *$p < 0.05$.

Figure 4-2
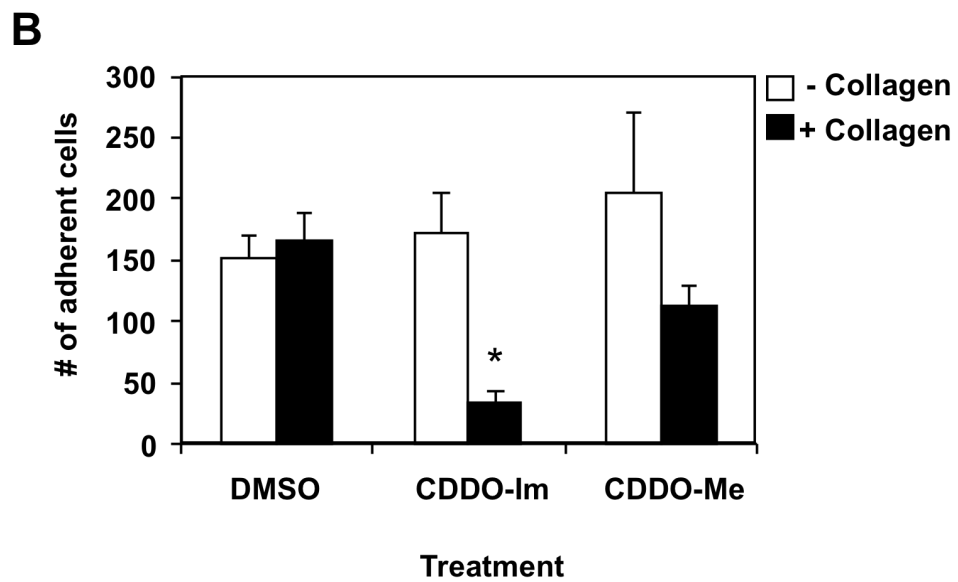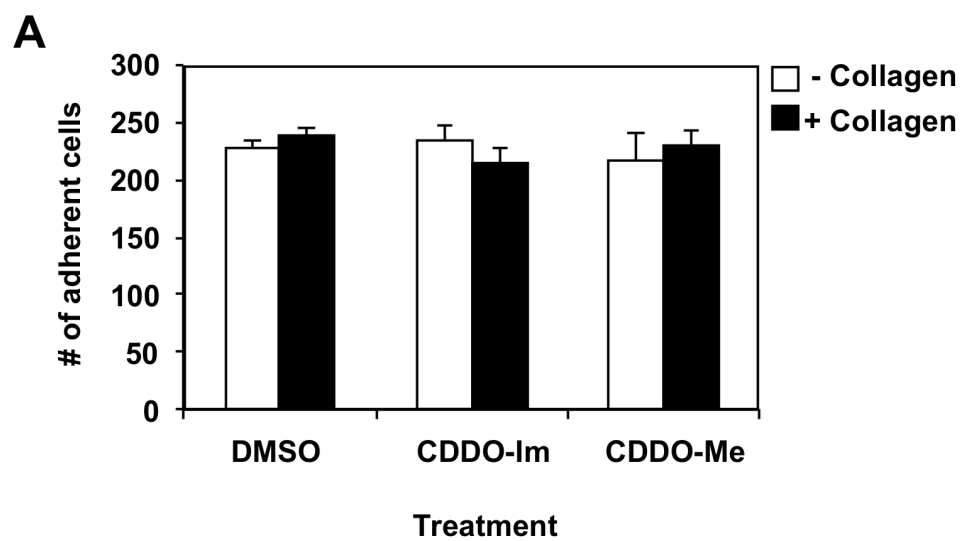
the drugs after adhesions were established, Rat2 fibroblasts were plated overnight to allow for cells to establish adhesions, followed by incubation of DMSO, CDDO-Im or CDDO-Me for 2 hours. To test whether the triterpenoids affected the ability of cells to establish new adhesions, cells were detached from plates and re-seeded, followed by treatment with DMSO, CDDO-Im or CDDO-Me for two hours. My data showed that when cell adhesions were established before drug treatments, the triterpenoids had no effect on the number of attached cells. Interestingly, when I tested the ability of cells to form new adhesions in the presence of the triterpenoids, the drugs appeared to inhibit the association of detached cells to collagen I, a common extracellular matrix protein. These results suggest that the turnover or formation kinetics of adhesions might be affected by the triterpenoids.

Having observed the alterations that triterpenoids have on the attachment of cells to Collagen I, I next re-examined the proteins that were on my list of proteomic proteins that may affect focal adhesion turnover (Table 4.1) and found focal adhesion kinase (FAK) and Glycogen Synthase Kinase Beta (GSK3β) as potential triterpenoid-binding targets. Therefore, I proceeded to confirm the associations of triterpenoids with both FAK and GSK3β by affinity pull-down assay using biotinylated CDDO-Me (Figure 4.3). Both FAK and GSKβ were confirmed as triterpenoid-binding targets. Interestingly, the association of biotinylated triterpenoid with FAK (Figure 4.3A) appeared to be weaker compared to that of GSK3β (Figure 4.3C). However as they are tritepenoid-binding targets and important kinases that regulate focal adhesion dynamics, I assessed the phosphorylation status of these proteins to examine whether their activities were affected by the triterpenoid treatment. FAK has multiple phosphorylation sites, including tyrosines

397, 576, 577, and 925, and serine 722, which are important in focal adhesion dynamics. Thus, I treated cells with either DMSO, CDDO-Im or CDDO-Me, processed them for SDS-PAGE and immunoblotted with phospho-specific FAK antibodies (Figure 4.3B). My results showed no substantial differences in the phosphorylation statuses of all of the sites that I examined (Figure 4.3B). Interestingly, when I performed similar analyses on GSK3β using Western blotting and phospho-specific GSK3β antibody, I found that triterpenoids induced the phosphorylation of GSK3β at serine 9 (Figure 4.3D). The phosphorylation (and likely inhibition) of GSK3β activity in the presence of the triterpenoids led me to examine whether GSK3β localized at the leading edge with the triterpenoids to affect cell migration. Briefly, Rat2 fibroblasts were scratched and allowed to polarize for 4 hours before they were fixed and permeabilized. Cells were then probed with DMSO or biotin or CDDO-Me or biotinylated CDDO-Me and anti-Rac1, as a leading edge marker as well as GSK3β antibodies (Figure 4.4). My studies showed that GSK3β indeed colocalized at the leading edge with Rac1 and biotinylated CDDO-Me (Figure 4.4, bottom panel).

The confirmation of GSK3β as a triterpenoid-binding target is highly significant, as recent studies have shown that GSK3β is involved in different aspects of cell migration and cell adhesion dynamics (13,18-20). Previously, I also showed that the morphology of fibroblasts was affected when cells were treated with the triterpenoids (1). Therefore, I hypothesized that triterpenoids may modulate the sizes of focal adhesions by affecting focal adhesion proteins *via* GSK3β. To examine the effects of triterpenoids on GSK3β and focal adhesion dynamics, I first examined whether focal adhesion

Figure 4.3 CDDO-Me binds to both FAK and GSK3β but affect only the activity of GSK3β.

A) Rat2 cells incubated with 0.1% DMSO, 10 μM biotin, 10 μM CDDO-Me, or 10 μM b-CDDO-Me were lysed and precipitated with neutravidin beads. Pull-down samples were then processed for SDS-PAGE and immunoblotted for FAK. Fifty micrograms of total protein lysates were also immunoblotted for FAK and shown.
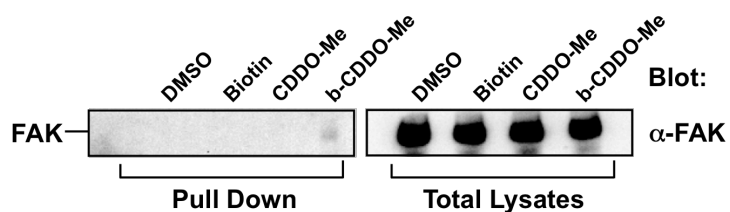
B) Rat2 fibroblasts were incubated with 0.01% DMSO, 1 μM CDDO-Im or 1 μM CDDO-Me for 2 hours. Cells were then lysed and processed by SDS-PAGE and immunoblotted with anti-FAK and specific anti-phospho-FAK antibodies against tyrosine 397, tyrosines 576/577, tyrosine 925 and serine 722.

C) Rat2 cells incubated with 0.1% DMSO, 10 μM biotin, 10 μM CDDO-Me, or 10 μM b-CDDO-Me were lysed, and precipitated with neutravidin beads. Pull down samples were then processed for SDS-PAGE and immunoblotted for GSK3β. Fifty micrograms of total protein lysates were also immunoblotted for GSK3β and shown.

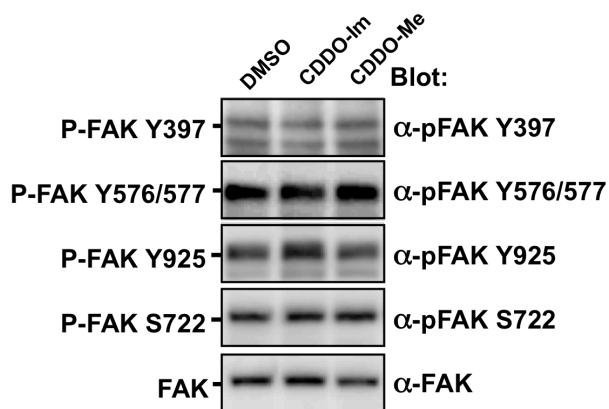**D)** Rat2 cells incubated with 0.01% DMSO (control), 1 μM CDDO-Im, or 1 μM CDDO-Me were lysed and processed for SDS-PAGE and immunoblotted with anti-GSK3β and anti-phospho-GSK3β antibodies that target serine 9 (top panel). Quantitation (bottom panel) by densitometry was carried out using the Bio-Rad VersaDoc software and graphed as arbitrary units versus treatments (n=3 +/-S.D.), *p<0.05.

Figure 4-3

A

FAK

Blot: α-FAK

DMSO Biotin CDDO-Me b-CDDO-Me DMSO Biotin CDDO-Me b-CDDO-Me

Pull Down   Total Lysates

B

DMSO CDDO-Im CDDO-Me Blot:

P-FAK Y397   α-pFAK Y397
P-FAK Y576/577   α-pFAK Y576/577
P-FAK Y925   α-pFAK Y925
P-FAK S722   α-pFAK S722
FAK   α-FAK

C

DMSO biotin CDDO-Me b-CDDO-Me DMSO biotin CDDO-Me b-CDDO-Me

GSK3β   α-GSK3β

Pull Down   Total Lysates

D

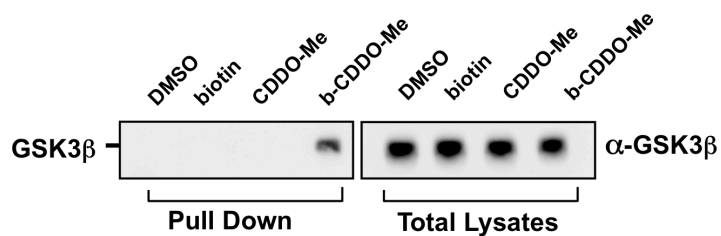DMSO CDDO-Im CDDO-Me Blot:

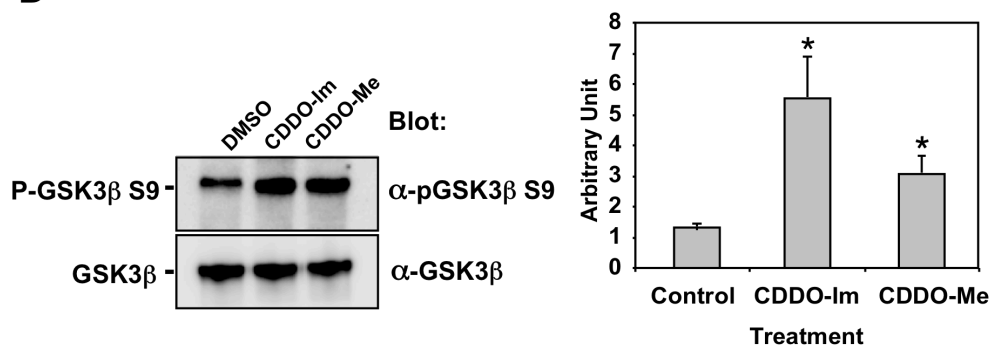P-GSK3β S9   α-pGSK3β S9
GSK3β   α-GSK3β

Figure 4.4 GSK3β co-localizes with biotinylated CDDO-Me.

Confluent Rat2 fibroblasts were scratched and allowed to polarize for 4 hours before they were fixed, permeabilized and incubated with monoclonal anti-Rac1 antibodies (Rac1; green), polyclonal anti-GSK3β antibodies (GSK3β; blue), and either DMSO, 10 μM biotin, 10 μM CDDO-Me, or 10 μM biotinylated CDDO-Me (b-CDDO-Me) followed by Cy2-labeled anti-mouse antibody, Cy5-labeled anti-rabbit and Cy3-labeled streptavidin respectively. Cell nuclei were stained with DAPI (DAPI; white). The co-localization of Rac1 (green), GSK3β (blue) with b-CDDO-Me (red) at the leading edge of migrating cells is indicated (white arrowheads). The white arrow indicates the direction of cell movement. Representative images from three experiments are shown. Bar = 10 μm.

Figure 4-4
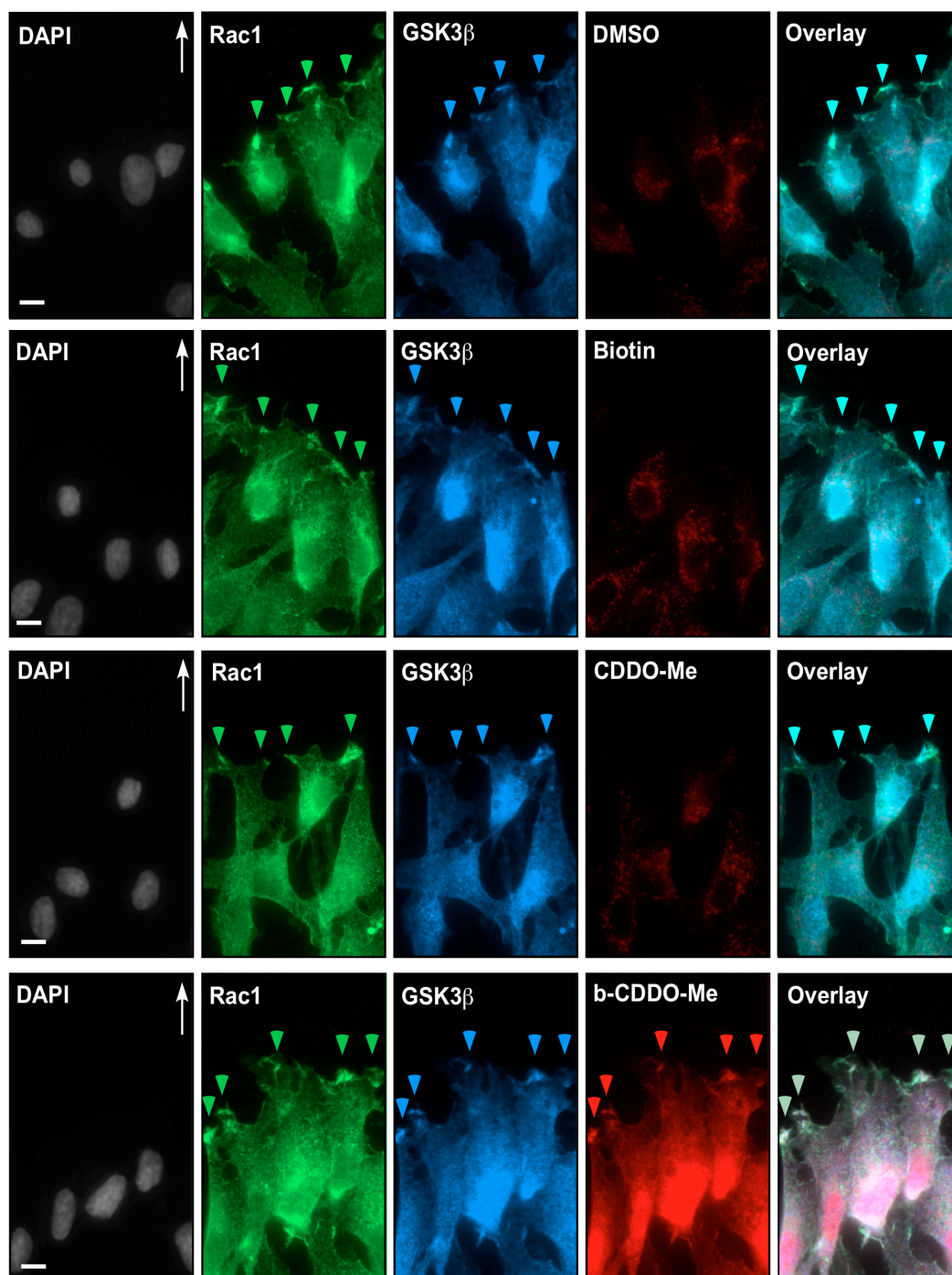
morphology was altered by the GSK3 inhibitors lithium chloride (LiCl) and SB216763 by immunofluorescence microscopy. Interestingly, LiCl and SB216763 both inhibit the activity of GSK3β, albeit *via* different modes of action. Specifically, LiCl inhibits GSK3β activity by inducing the phosphorylation of GSK3β at serine 9 whereas SB216763 elicits its inhibitory action by competitively binding to the ATP pocket of GSK3β. However, since LiCl is a less specific inhibitor, we have utilized SB216763 in parallel to our studies in order to assess whether the alteration of focal adhesions is a GSK-dependent effect. Consistent with my observations in triterpenoid-treated cells (Figure 4.1), I found that paxillin staining was also enlarged when cells were incubated with LiCl or SB216763 (Figure 4.5). In order to assess if inhibition of GSK3β would result in an inhibition of Rat2 cell migration, I performed migration studies using the GSK3 inhibitors and I observed that, similar to the triterpenoid treated cells, GSK3β inhibition led to a delay in cell migration (Figure 4.6).

Numerous studies have shown that the loss of polarity can result in the inhibition of cell migration. I have also shown in my previous studies, that the displacement of leading edge proteins and the loss of polarity by the triterpenoids is a major mechanism for inhibiting cell migration (21). Therefore, I next examined whether the inhibition of GSK3β displaces Rac1 and IQGAP1 from the leading edge of migrating cells. Cells were scratched and allowed to polarize before they were treated in the presence or absence of CDDO-Im, CDDO-Me, LiCl or SB216763. Cells were then fixed, permeabilized and immunostained with Rac1 and IQGAP1 antibodies. My results indicated that GSK3β inhibitors did indeed displace leading edge proteins. Rac1 and

Figure 4.5 GSK3 inhibitors enlarge focal adhesion size.

A) Rat2 fibroblasts were scratched and incubated for 4 hours at 37˚C to establish cell polarity and then treated with control medium (Control; top panel), 50 mM Lithium Chloride (Lithium Chloride; middle panel) or 50 µM SB216763 (SB216763; bottom panel) for an additional 2 hours. The cells were then fixed, permeabilized and immunostained with anti-paxillin antibody (Paxillin; green) and phalloidin (Phalloidin; red). The scratches were made in the horizontal plane above the cells shown. A representative area (inset) is magnified and shown. Bar = 10 µm.

B) Rat2 fibroblasts were treated with DMSO, 50 mM Sodium Chloride (NaCl), 50 mM Lithium Chloride (LiCl) or 50 µM SB216763 (SB) for 2 hours before samples were lysed and processed for SDS-PAGE followed by immunoblotting with phospho-FAK, phospho-paxillin and phospho-GSK3β antibodies. Fifty micrograms of total protein lysates were also immunoblotted for FAK, paxillin and GSK3β and shown.
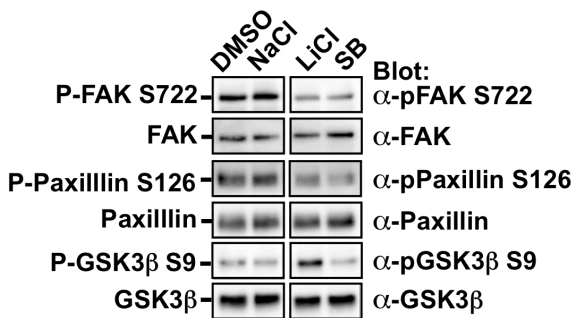
Figure 4-5

A
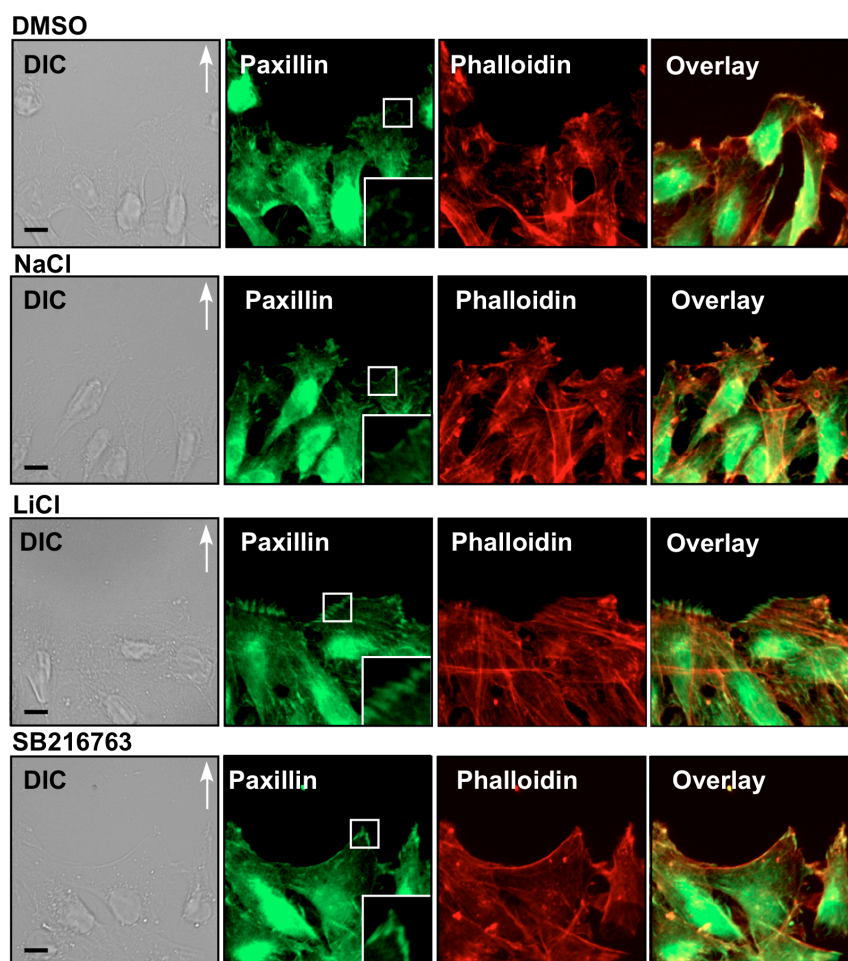
B

Figure 4.6 GSK3 inhibitors attenuate cell migration.

A) Confluent Rat2 fibroblasts were scratched and treated with vehicle (control), 50 mM LiCl or 50 µM SB216763 for 16 hours. Bright field images (magnification 10X) were taken at the beginning of the experiment (0 h) and after 16 hours (16 h) of incubation at 37˚C. The white dotted lines indicate the edge of the leading edge of migrating cells at 0 h.

B) Cells treated with increasing concentrations of LiCl or SB216763 (0 µM - 50 µM or 0 mM - 50 mM respectively, as shown) were imaged. Cell migration was quantified and graphed as cell migration (percentage of control) vs. inhibitors concentration (n=3±S.D.). *p<0.01, **p<0.05.

Figure 4-6

A
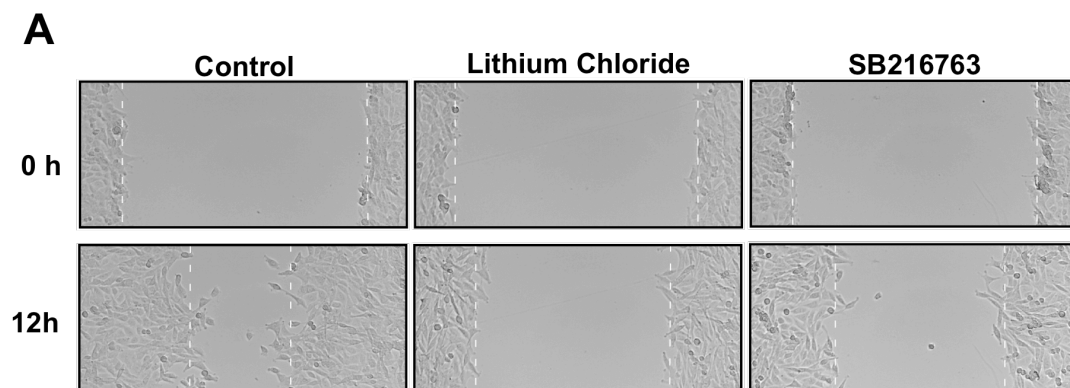
B
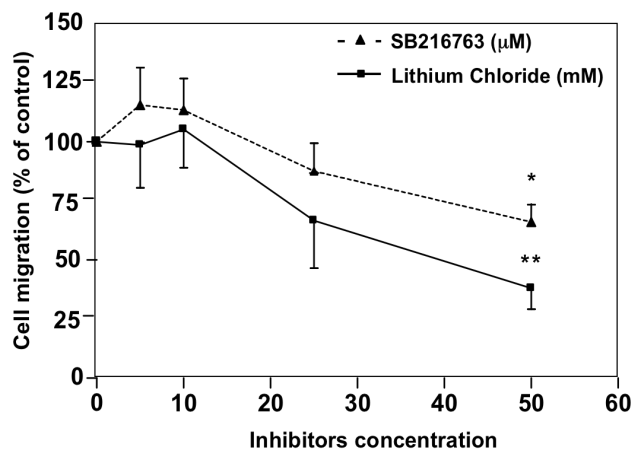
IQGAP1, and promoted the loss of polarity, consistent with what I observed in triterpenoid-treated cells (Figure 4.7). Finally, since GSK3β plays a critical role in cell polarity and GSK3 inhibitors can effectively displace important leading edge proteins, I assessed whether GSK3β at the leading edge were also displaced in the presence of triterpenoids and GSK3 inhibitors. Using the same technique as described above, I probed for GSK3β using anti-GSK3β antibodies and found that GSK3β was also displaced from the leading edge of migrating cells in GSK3 inhibitor- and triterpenoid-treated cells (Figure 4.8).

Taken together, my results suggest that triterpenoids target GSK3β activity to alter focal adhesion size and contribute to the inhibition of cell migration.

Figure 4.7 Triterpenoids and GSK3 inhibitors displace leading edge proteins, Rac1 and IQGAP1, from the leading edge of migrating cells.

A) Confluent Rat2 fibroblasts were scratched and allowed to polarize for 4 hours. Cells were then treated with DMSO, NaCl, 1 μM CDDO-Im, 1 μM CDDO-Me, 50 mM LiCl or 50 μM SB216763 for an additional 2 hours. Cells were fixed, permeabilized and incubated with anti-Rac1 antibody (Rac1; green), phalloidin (Phalloidin; red) and anti-IQGAP1 (IQGAP1; blue) antibody. The scratches were made in the horizontal plane above the cells. The staining of Rac1, phalloidin and IQGAP1 at the leading edge of migrating cells is indicated by green, red and blue arrows respectively. The white arrowheads indicate the areas of colocalization of the three proteins. White arrows indicate the direction of cellular movement. Bar = 10 μm.

B) Quantitation of cells containing Rac1 or IQGAP1 at the leading edge of migrating cells was carried out using ImagePro software and graphed as localization at the leading edge (% of cells) *vs*. treatment (n=3±SD). *,#: $p<0.05$ for staining of Rac1 and IQGAP1 compared to DMSO as control. a,b: $p<0.05$ for staining of Rac1 and IQGAP1 compared to NaCl as control.
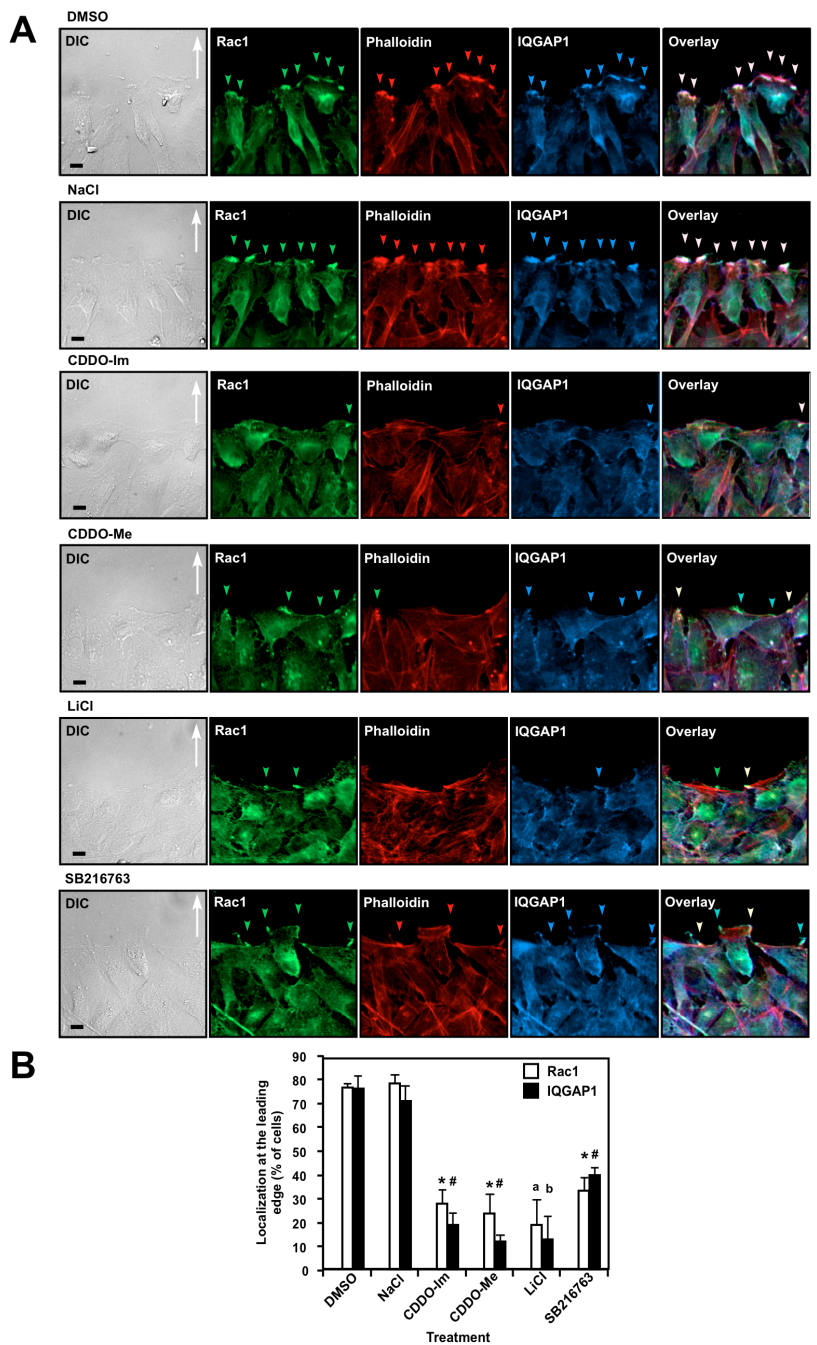
Figure 4-7

Figure 4.8 Triterpenoids displace GSK3β from the leading edge of migrating cells.

A) Confluent Rat2 fibroblasts were scratched and allowed to polarize for 4 hours. Cells were then treated with DMSO, NaCl, 1 μM CDDO-Im, 1 μM CDDO-Me , 50 mM LiCl or 50 μM SB216763 for an additional 2 hours before samples were fixed, permeabilized and incubated with anti-Rac1 (Rac1; green) antibody, phalloidin (Phalloidin; red) and anti-GSK3β (GSK3β; blue) antibody. The scratches were made in the horizontal plane above the cells. Rac1, phalloidin and GSK3β staining at the leading edge of migrating cells are indicated by green, red and blue arrows respectively. The white arrowheads indicate the areas of colocalization of all three proteins. White arrows indicate the direction of cellular movement. Bar = 10 μm.

B) Quantitations of cells containing Rac1 and GSK3β at the leading edge of migrating cells was carried out using ImagePro software and graphed as localization at the leading edge (% of cells) *vs*. treatment (n=3±SD). *,#: $p<0.05$ for staining of Rac1 and GSK3β compared to DMSO as control. a,b: $p<0.05$ for staining of Rac1 and GSK3β compared to NaCl as control.
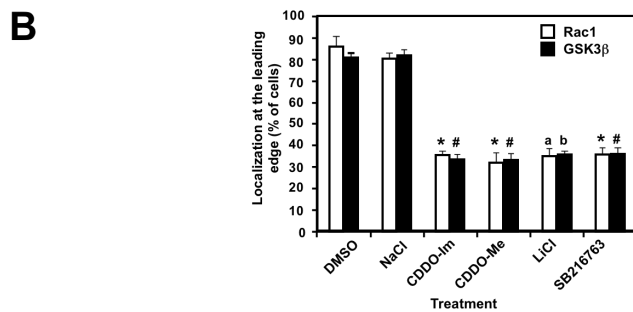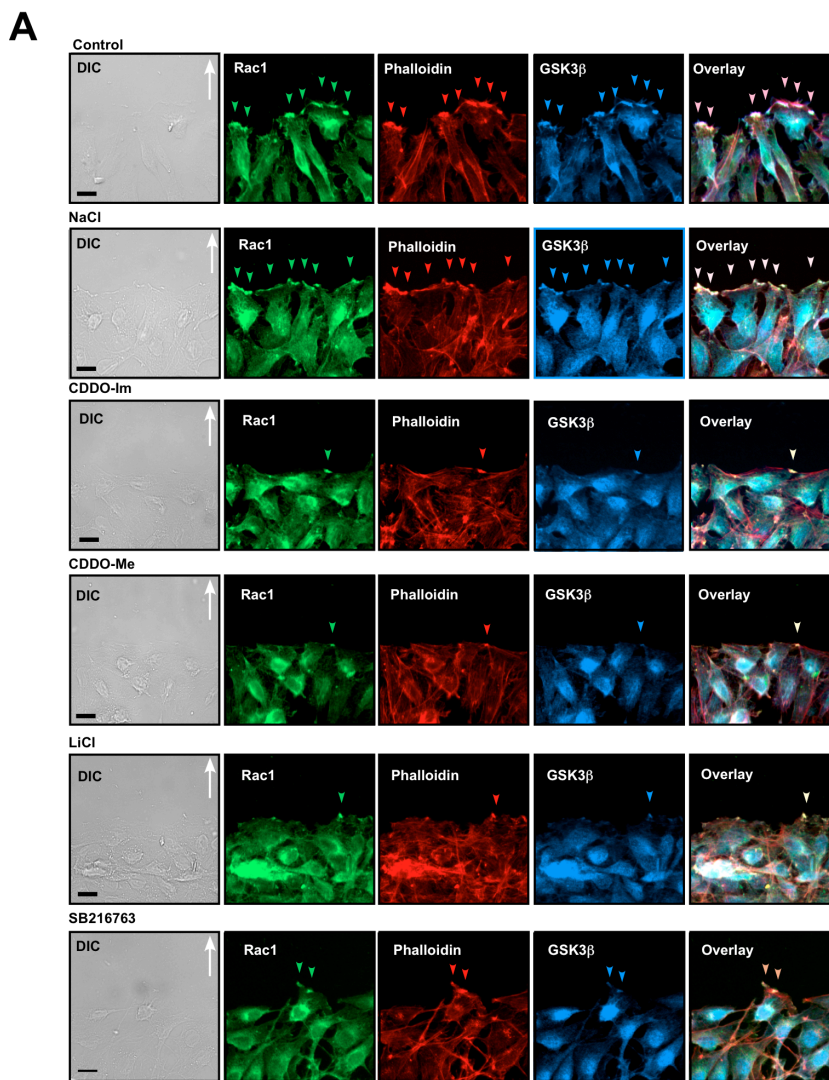
Figure 4-8

4.5   DISCUSSION

In this study, I found that the triterpenoids altered the size of focal adhesions. Knowing that the triterpenoids inhibit cell migration, the principal question that I sought to answer was whether triterpenoids could alter focal adhesions to inhibit cell migration.

To address this question, I first examined whether this enlargement of focal adhesions by triterpenoids was due to an alteration in focal adhesion turnover. Using cell adhesion assays, I found that synthetic triterpenoids targeted cell binding to collagen I, but did not induce the dissociation of adhered cells. This interesting alteration of focal adhesion dynamics by the triterpenoids led us to believe that the drug compounds may modulate kinases that regulate focal adhesion turnover to cause an alteration in the size of the focal adhesions, which ultimately lead to delayed cell migration. However, it is important to note that my adhesion binding studies were performed on Collagen I and different extracellular matrices and the variation in their concentrations can have different effects on focal adhesion dynamics. Future studies assessing different substrates will test whether this phenomenon is ECM-specific. Nonetheless, knowing that focal adhesion turnover was altered by the triterpenoids, I next sought to identify triterpenoid-binding targets that regulate focal adhesion dynamics and found FAK and GSK3β to be triterpenoid-binding proteins.

FAK and GSK3β can modulate multiple signaling pathways relating to focal adhesion turnover. Of the two kinases, FAK is a known master regulator of focal adhesion turnover. Therefore, I began my assessment with FAK by studying its activity and observed that triterpenoids did not affect the activities of FAK at various

phosphorylation sites known for its regulation in focal adhesion dynamics. However, this could be due to the fact that FAK is a weak binding triterpenoid-binding target; thus, the drugs may exert their effects *via* FAK. In addition, since FAK is involved in modulating numerous cellular processes, the phosphorylation of FAK at one specific site may lead to the activation of different signaling cascades. Therefore, it is possible that even if one signaling pathway that is responsible for the enlargement of focal adhesions is altered, it is concealed by another signaling pathway that acts through the same phosphorylation site.

Interestingly, when I examined the effect of triterpenoids on GSK3β activity, I observed an elevation in GSK3β phosphorylation on Ser 9, indicating that the GSK3β activity was inhibited. Since the triterpenoids have previously been shown to inhibit cell migration, I sought to examine the possible mechanism. Indeed, when I examined the localization of GSK3β using biotinylated CDDO-Me immunofluorescence assays, I observed that GSK3β colocalized with the biotinylated triterpenoid, b-CDDO-Me, mainly at the leading edge and in the nucleus. This result indicated to us that the alteration of GSK3β by the triterpenoids could play a possible role in cell migration. To confirm this hypothesis, I assessed the effect of GSK3β inhibition in scratch assays using GSK3 inhibitors, LiCl and SB216763. LiCl is a non-competitive inhibitor of GSK3 activity that has been used extensively to examine the functional roles of GSK3. However, LiCl is not a selective inhibitor of GSK3 and has been reported to inhibit other kinases such as casein kinase-2, p38 regulated/activated kinase and MAPK activated protein kinase 2, polyphosphate 1-phosphatase and inositol monophosphatase. Therefore, I used SB216763 in parallel with LiCl in my studies. SB216763 is a soluble, small

molecule GSK3 inhibitor that can effectively inhibit the activities of both GSK3α and GSK3β at concentration that is as low as 34 nM in *in vitro* kinase assays using purified proteins (22). In addition, SB216763 is highly specific and elicits no effect on the activity of at least 24 different serine/threonine and tyrosine protein kinases that were tested (22). My data from my scratch assays indicated that cell migration was indeed delayed when cells were treated with LiCl or SB216763. Although the concentrations of both GSK3β inhibitors that were used in my studies were at the millimolar and micromolar ranges, respectively, these concentrations are consistent with the ranges that other studies had used in their *in vitro* cell culture studies. I also observed that SB216763 was more effective in inhibiting cell migration than LiCl. This is not surprising as SB216763 was a more specific GSK3β inhibitor than LiCl, which was known to affect other signaling pathways, and hence may have potential confounding effect on cell migration. However, I found that the concentration of GSK3β inhibitors required to reduce cell migration by 40-50% was much higher than that of the triterpenoids, indicating that the triterpenoids were much more effective in inhibiting cell migration and that GSK3β inhibition alone was not the main target for cell migration inhibition. These results are consistent with my previous studies since CDDO derivatives are known to target multiple proteins in a cell (1). Therefore, I would expect that even though GSK3β is an important target, the treatment of GSK3β inhibitors alone would not be sufficient in abolishing cell migration to the same extent as the triterpenoids.

Numerous studies have shown that cell migration is inhibited when the total cellular GSK3β level is inhibited by common GSK3 inhibitors such as LiCl and SB216763 (14,23-27). However, it is important to note that other studies have found that

local inhibition of GSK3β at the leading edge can actually regulate the stability of microtubules and promote cell migration (14). , Interestingly, my data seems to support both of these existing models. Specifically, through Western blotting studies, which measures the amount of total phosphorylated GSK3β level in the cells, triterpenoids may inhibit cell migration by inactivating the overall GSK3β activity. Although SB216763 does not induce the phosphorylation of GSK3 to elicit its inhibitory effect, its subsequent effect on cell migration is still consistent to the model that inhibiting overall GSK3β can impair cell migration. In our immunofluorescence studies, we also found that GSK3β was effectively displaced in triterpenoid-treated cells. Taken together, it seems that the synthetic triterpenoids can delay overall cell migration in part by inactivating total GSK3β activity and displacing the local pool of inactive GSK3β at the leading edge. Evidently, the extent and the location in which phosphorylated GSK3β resides both play critical roles in cell migration; therefore, to further understand and confirm our results, it would be imperative to examine the extent of GSK3β phosphorylation in the cell and where this phosphorylation takes place by immunofluorescence microscopy using phospho-specific GSK3β antibodies.

With the understanding that triterpenoids can affect GSK3β activity and at least partially inhibit cell migration, I then sought to understand whether the alteration of focal adhesions plays a role in GSK3β-dependent cell migration inhibition. I propose that the inhibition of GSK3β contributes to the enlargement of focal adhesion which delays cell migration. Indeed, when I treated the cells with GSK3 inhibitors and studied the morphology of focal adhesions using paxillin as my adhesion marker, I found that cells

treated with LiCl and SB216763 possessed focal adhesions that differ from cells treated with vehicle, similar and consistent with what I observed in triterpenoid-treated cells.

Finally, previous studies have shown that the local inhibition of GSK3β at the leading edge can play a critical role in regulating cell polarity by stabilizing microtubules *via* leading edge proteins such as APC and CLASP2. With the novel understanding that global inhibition of GSK3β by triterpenoids could inhibit cell migration, I wanted to investigate whether the effect of global GSK3β inactivity on cell polarity was also similar to what I observed in triterpenoid-treated cells. My previous studies have implicated that the displacement of polarity proteins such as Par6, PKC and leading edge proteins such as Rac1 and IQGAP1 by the triterpenoids can severely reduce the rate of cell migration (21). Since Rac1 plays a critical role in membrane ruffling and the formation of leading edge whereas IQGAP1 is an important scaffolding protein that acts to coordinate multiple cytoskeletal proteins for cell migration, I examined whether global GSK3β inhibition could affect these proteins from localizing to the leading edge. My data showed that the inactivation of total GSK3β using GSK3β inhibitors could indeed cause the displacement of these important proteins, similar to my observations with triterpenoid-treated cells.

Cell motility is critical in regulating many physiological processes including growth, development and tissue homeostasis. While cell migration is a precursor event for tumor metastasis, to effectively inhibit cell migration is challenging, as it involves the convergence of different signaling pathways. Triterpenoids are promising candidates for targeting multiple signaling pathways including the cytoskeletal network and the polarity complex (Chapters 2 and 3). In the present study, I found that triterpenoids targeted

GSK3β and altered its activity, its localization as well as the localization of other leading edge proteins. As a correlate, an apparent enlargement of focal adhesions and delayed cell migration were observed. This mechanism represents yet another pathway where triterpenoids may be effective in targeting cell migration. I expect that the results obtained from these studies will provide better insight that would ultimately improve the design of future triterpenoid analogues so that they could target more specific aspects of cell migration.

4.6 FOOTNOTES

4.7 REFERENCES

1. To, C., Shilton, B. H., and Di Guglielmo, G. M. (2010) *J Biol Chem* **285**, 27944-27957

2. Prasad, S., Phromnoi, K., Yadav, V. R., Chaturvedi, M. M., and Aggarwal, B. B. (2010) *Planta Med* **76**, 1044-1063

3. Sporn, M. B., Liby, K. T., Yore, M. M., Fu, L., Lopchuk, J. M., and Gribble, G. W. (2011) *J Nat Prod* **74**, 537-545

4. Petronelli, A., Pannitteri, G., and Testa, U. (2009) *Anticancer Drugs* **20**, 880-892

5. Parsons, J. T., Horwitz, A. R., and Schwartz, M. A. (2010) *Nat Rev Mol Cell Biol* **11**, 633-643

6. Webb, D. J., Parsons, J. T., and Horwitz, A. F. (2002) *Nat Cell Biol* **4**, E97-100

7. Nobes, C. D., and Hall, A. (1995) *Cell* **81**, 53-62

8. Zaidel-Bar, R., Cohen, M., Addadi, L., and Geiger, B. (2004) *Biochem Soc Trans* **32**, 416-420

9. Tran, A. D., Marmo, T. P., Salam, A. A., Che, S., Finkelstein, E., Kabarriti, R., Xenias, H. S., Mazitschek, R., Hubbert, C., Kawaguchi, Y., Sheetz, M. P., Yao, T. P., and Bulinski, J. C. (2007) *J Cell Sci* **120**, 1469-1479

10. Rooney, C., White, G., Nazgiewicz, A., Woodcock, S. A., Anderson, K. I., Ballestrem, C., and Malliri, A. (2010) *EMBO Rep* **11**, 292-298

11. Hagel, M., George, E. L., Kim, A., Tamimi, R., Opitz, S. L., Turner, C. E., Imamoto, A., and Thomas, S. M. (2002) *Mol Cell Biol* **22**, 901-915

12. Wade, R., Bohl, J., and Vande Pol, S. (2002) *Oncogene* **21**, 96-107

13. Sun, T., Rodriguez, M., and Kim, L. (2009) *Dev Growth Differ* **51**, 735-742

14. Jope, R. S., Yuskaitis, C. J., and Beurel, E. (2007) *Neurochem Res* **32**, 577-595

15. Sporn, M. B. (2006) *Cytokine Growth Factor Rev* **17**, 3-7

16. Ilic, D., Furuta, Y., Kanazawa, S., Takeda, N., Sobue, K., Nakatsuji, N., Nomura, S., Fujimoto, J., Okada, M., and Yamamoto, T. (1995) *Nature* **377**, 539-544

17. Deramaudt, T. B., Dujardin, D., Hamadi, A., Noulet, F., Kolli, K., De Mey, J., Takeda, K., and Ronde, P. (2011) *Mol Biol Cell* **22**, 964-975

18.   Cai, X., Li, M., Vrana, J., and Schaller, M. D. (2006) *Mol Cell Biol* **26**, 2857-2868

19.   Cohen, P., and Frame, S. (2001) *Nat Rev Mol Cell Biol* **2**, 769-776

20.   Kobayashi, T., Hino, S., Oue, N., Asahara, T., Zollo, M., Yasui, W., and Kikuchi, A. (2006) *Mol Cell Biol* **26**, 898-911

21.   To, C., Kulkarni, S., Pawson, T., Honda, T., Gribble, G. W., Sporn, M. B., Wrana, J. L., and Di Guglielmo, G. M. (2008) *J Biol Chem* **283**, 11700-11713

22.   Coghlan, M. P., Culbert, A. A., Cross, D. A., Corcoran, S. L., Yates, J. W., Pearce, N. J., Rausch, O. L., Murphy, G. J., Carter, P. S., Roxbee Cox, L., Mills, D., Brown, M. J., Haigh, D., Ward, R. W., Smith, D. G., Murray, K. J., Reith, A. D., and Holder, J. C. (2000) *Chem Biol* **7**, 793-803

23.   George, B., Vollenbroker, B., Saleem, M. A., Huber, T. B., Pavenstadt, H., and Weide, T. (2011) *Am J Physiol Renal Physiol* **300**, F1152-1162

24.   Flugel, D., Gorlach, A., and Kietzmann, T. (2012) *Blood* **119**, 1292-1301

25.   Peng, J., Ramesh, G., Sun, L., and Dong, Z.(2012) *J Pharmacol Exp Ther* **340**, 176-184

26.   Vidal, F., de Araujo, W. M., Cruz, A. L., Tanaka, M. N., Viola, J. P., and Morgado-Diaz, J. A. (2011) *Int J Oncol* **38**, 1365-1373

27.   Harris, E. S., and Nelson, W. J. (2010) *Mol Biol Cell* **21**, 2611-2623

CHAPTER 5

SUMMARY AND CONCLUSIONS

5 CHAPTER 5

5.1 SUMMARY OF MAJOR FINDINGS

Synthetic triterpenoids are promising candidates that have received notable attention as anti-cancer agents in recent years for their favorable effects on specific targeted areas of cancer, including apoptosis, anti-inflammation, and anti-proliferation. However, very little work had been done on their effect on cancer metastasis. Specifically, there were virtual no data assessing how triterpenoids might affect the underlying cell motility. Therefore, the overall goal of my thesis was to characterize the effect of triterpenoids on cell migration.

The first part of this thesis asked whether one of the most potent triterpenoid derivatives, CDDO-Im, played a role in TGFβ-mediated signaling and cell migration and if so, through which molecular mechanisms. My initial studies on the triterpenoids were TGFβ–focused because aberrant TGFβ signaling pathway is an important player in tumorigenesis (1-6). In addition, Ji *et. al* had shown that the activation of the canonical Smad signaling pathway by CDDO-Im led to the monocytic differentiation of HL60 leukemia cells (7). Therefore, since CDDO-Im is shown to play a role in affecting an important aspect of cancer through delaying the activation of the Smad pathway, I predicted that the triterpenoids may also have an effect on cell migration *via* the regulation of the TGFβ signaling pathway. Understanding the underlying mechanism of action in which triterpenoids affect cell migration via TGFβ can provide useful insights in how to better utilize the drugs to target metastasis. In Chapter 2 of this thesis, I showed that the synthetic triterpenoid, CDDO-Im, played a role in delaying TGFβ-mediated

signaling by affecting the trafficking and turnover of TGFβ receptors, which explained the prolonged Smad2 activation that was observed in triterpenoid-treated cells. In addition, my findings demonstrated for the first time that CDDO-Im could impair TGFβ mediated cell migration by disrupting the microtubule network and displacing the important proteins at the leading edge that establish cell polarity (Figure 5.1).

In Chapter 3, I provided evidence that the inhibitory effects of the triterpenoids on cell migration inhibition were not limited to TGFβ. In fact, the phenomenon that we observed in TGFβ-dependent cell migration could actually be extended to general cell migration. To understand how triterpenoids inhibit cell migration, I utilized a two-pronged proteomic approach that led to the discovery of several novel triterpenoid-binding proteins involved in cell migration. Having established that microtubules were affected by the triterpenoids through my previous studies, I decided to examine whether these drugs had an effect on the actin cytoskeleton. I predicted that the triterpenoids would affect cell migration by disrupting actin cytoskeleton dynamics, since I observed the loss of the leading edge and polarity in triterpenoid-treated cells, and these processes are heavily regulated by actin polymerization. Interestingly, I found that triterpenoids affected only branched actin polymerization by targeting the Arp3 nucleation site of the novel triterpenoid-binding target, the Arp2/3 complex, while leaving stress fibers intact (Figure 5.1).

While I was conducting studies to confirm that stress fibers were indeed not triterpenoid-binding targets, I noticed that triterpenoids appear to enlarge focal adhesions, suggesting that these drugs may affect cell adhesions and consequently, inhibit cell migration. Therefore, I began to investigate the underlying mechanism in which

triterpenoids regulate cell adhesion dynamics and ultimately cell migration. Indeed, Chapter 4 shows that triterpenoids can inhibit cell migration in part by changing adhesion sizes *via* the alteration of GSK3β activity and displacing GSK3β as well as other proteins from the leading edge of migrating cells (Figure 5.1).
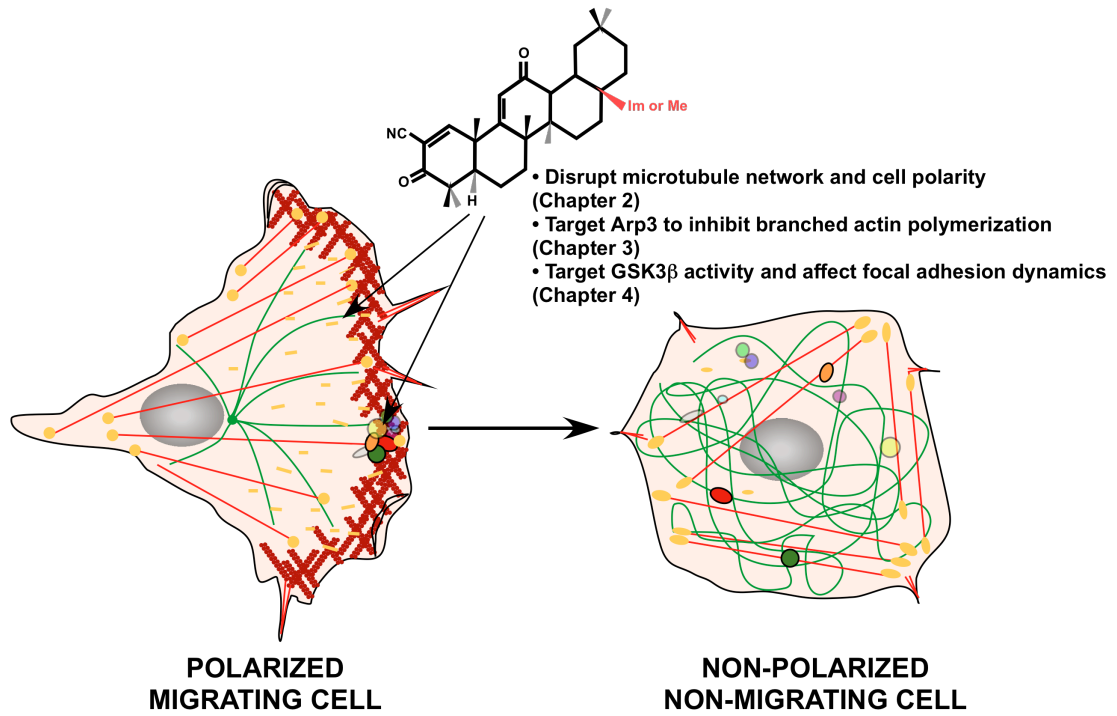
5.2   LIMITATIONS AND FUTURE STUDIES

It is important to note that all of the work presented in this thesis was done using purified proteins and cultured cell models. Since the nature of my work was heavily mechanism-based, these models offered great advantages as I attempted to characterize signaling pathways targeted by triterpenoids. Using cell culture models, I was able to understand the effects of synthetic triterpenoids on cell migration in a much simpler system with less confounding factors and where the physiochemical and physiological environments were tightly controlled.   To ensure that the triterpenoid-induced phenomena that I observed were not cell type specific, I carried out parallel studies in different cell lines. Using purified proteins, I was also able to test the direct interactions of the triterpenoids with specific proteins of interest. However, one of the limitations of using non-tumorigenic cells was that they might be less relevant in the context of a cancer cell model or *in vivo*. Therefore, now that we have a better basic understanding of how the triterpenoids act on non-transformed cell lines, future studies using tumor cells where more variables exist and animal tumor models will be useful and imperative in allowing us to extend our understanding on how triterpenoids function as potential anti-cancer agents. Normal embryonic development requires that cells migrate to specific regions

Figure 5.1 Molecular mechanisms whereby the synthetic triterpenoids inhibit cell migration.

In response to a stimulus, a cell establishes polarity, redistributes its proteins to the leading edge and rearranges the cytoskeletal network in order to prepare for movement. However, our studies have shown that the triterpenoids can disrupt the microtubule network, target proteins at the leading edge by displacing them from the leading edge, prevent branched actin polymerization by binding to Arp3 in the Arp2/3 complex and affect GSK3β activity. As a result, a migrating cell (left cell) loses its polarity; in addition, important proteins at the leading edge are displaced and focal adhesion sizes are altered. These changes collectively lead to the inhibition of cell migration (right cell).

Figure 5-1

• Disrupt microtubule network and cell polarity
(Chapter 2)
• Target Arp3 to inhibit branched actin polymerization
(Chapter 3)
• Target GSK3β activity and affect focal adhesion dynamics
(Chapter 4)

**POLARIZED
MIGRATING CELL**

**NON-POLARIZED
NON-MIGRATING CELL**

of the organism. Both cancer cells and cells involved in embryonic development are often highly migratory and express proteins that are important for cell motility. Since Rat2 fibroblasts are highly migratory, it makes them not only good models for our studies but the results that were attained from them are also likely to be translatable to future tumor cell and *in vivo* studies using rodents. Therefore, I predict that the results attained using tumor cell lines and *in vivo* models will be similar to my own observations with the Rat2 fibroblast culture model. In addition, it would be interesting to examine whether triterpenoids can affect EMT, a process which many cells undergo prior to acquiring migratory and invasive phenotypes. To conduct these studies, we can utilize cell lines such as A549 (non-small cell lung cancer cells) that are of epithelial origin and can be induced by TGFβ to undergo mesenchymal transition. Specifically, we can examine whether the treatment of triterpenoids can delay or even prevent A549 cells from becoming more invasive and migratory by immunofluorescence microscopy and invasion assays. This type of studies should provide insights on how triterpenoids may play a role in cancer metastasis.

In Chapters 2 and 3, I provided evidence that cell migration was inhibited by the triterpenoids. I also identified three different and novel underlying mechanisms of actions whereby triterpenoids inhibited cell migration. Specifically, I showed that the triterpenoids target the TGFβ signaling pathway by delaying TGFβ receptor endocytosis and trafficking. However, the importance of receptor trafficking and endocytosis is not limited to the TGFβ pathway. In fact, signaling associated with different growth factors and chemokines relies on endocytosis and trafficking of their receptors, and manipulations that compromise these processes can severely affect cell polarity and

migration. As such, studies have shown that the disruption of endocytosis impairs cell polarization and affects the distribution of important membrane proteins such as integrins, which are involved in cell adhesion (8). In addition, Arp2/3 and WASP, both of which are affected by the triterpenoids, also play an important role in these processes (9). In my previous studies, I have shown that microtubules were affected by the triterpenoids and that the network no longer spanned from the microtubule organizing center and stabilize to the edge of migrating cells. The microtubule network serves as an important function for vesicle transport. Therefore, it is possible that motor proteins along the microtubule cytoskeleton which play a critical role in endosomal movement may be affected and represents a potential mechanism of action that explains why trafficking was altered in triterpenoid-treated cells. This could also explain why some proteins are displaced from the leading edge of migrating cells, as some of these proteins may rely on vesicle transport to localize to the leading edge. Hence, it will be essential to examine how triterpenoids regulate receptor trafficking and endocytosis, and whether the drugs exert their effects through the proteins that regulate membrane trafficking and endocytosis. Particularly, dynamin as well as Rab and Arf GTPases play critical roles in controlling receptor recycling, which in turn regulate different aspects of cell migration, adhesion and cytoskeletal dynamics (8,10-16). Aside from trafficking, the loss of polarity induced by triterpenoids that we observed could be due to the possibility that triterpenoids may target the components that make up the cell migration process, which includes leading edge proteins. Leading edge proteins are important in regulating cytoskeletal dynamics, adhesions and consequently, cell motility. Therefore, it will be imperative to understand the roles that triterpenoids play on them in order to gain more insights on how triterpenoids affect cell migration. For instance, IQGAP1 would be a prime candidate for

further investigation. As mentioned before, IQGAP1 is a key scaffolding protein that serves as a hub for a large array of proteins involved in cell migration; in addition, it acts as a bridge to link and coordinate the microtubule and actin cytoskeletal network during forward cell movement. Since we saw the displacement of the leading edge proteins, Par6, PKC and Rac1, as well as IQGAP1 in the presence of the synthetic triterpenoids, it will be important to investigate whether the displacement of these leading edge proteins is a consequence of an initial displacement of IQGAP1,

In Chapter 4 of this thesis, I have offered some insights on how focal adhesions may be altered by the triterpenoids, which in turn would affect cell migration. However, some future studies must be performed in order to fully decipher the effect of the drugs on focal adhesions. For instance, I found that the re-establishment of focal adhesions on Collagen I was affected by the triterpenoids. Although the purpose of these experiments was to examine whether triterpenoids affected the general turnover of focal adhesions, the different results that we observed in the presence and absence of collagen suggested to me that cells could react differently depending on different substrates beneath them. In fact, while the extracellular matrix proteins play a key role in providing structural integrity of normal tissues, they are also important components that tumor cells can exploit to create a microenvironment that is favorable for tumorigenesis (17,18). Therefore, it would be important to understand how triterpenoids affect focal adhesions when cells are plated on different ECM proteins. In Chapter 4, I also showed that triterpenoids targeted GSK3β activity to inhibit cell adhesion, which was consistent with what was observed when cells were treated with GSK3 inhibitors, suggesting that the effect of triterpenoids on focal adhesions likely involves GSK3β. However, these inhibitors target both the

alpha and beta isoforms of GSK3. Thus, these studies did not fully address whether GSK3α, GSK3β or both isoforms are the targets of triterpenoids. GSK3α and GSK3β have overlapping as well as unique functions in different cellular processes although this has not been thoroughly examined *vis-à-vis* cell migration. Therefore, it will be of major significance to confirm that triterpenoids are indeed targeting specifically GSK3β to elicit their effects. In order to test this, siRNA studies targeting only GSK3α, GSK3β or both GSK3 isoforms followed by the examination of their activities, focal adhesion sizes and rate of cell migration should be done.

Although two novel triterpenoid binding targets that are important for cell migration have been identified in my studies, the exact binding site(s) bound by the triterpenoids are unknown. So far, reactive cysteines seem to be a favorable binding site for triterpenoids and the hydrophobic site of both β-tubulin and Arp3 of the Arp2/3 complex have been identified (19,20). But comparative analysis between proteins and biochemical studies should be performed to see whether there is a consensus amino acid sequence that triterpenoids preferably bind. Having this knowledge will be important in designing more effective derivatives of synthetic triterpenoids to specifically target cell migration and possibly other cellular processes.

5.3   SIGNIFICANCE OF RESEARCH AND CONCLUSION

Cancer is one of the leading causes of deaths in Canada. It not only affects the well being of many Canadians fighting against this disease, but it is also a tremendous financial burden on the Canadian health care system. Therefore, the development of

drugs that can treat or control cancer is one of the foremost priorities of the pharmaceutical industry. As such, a vast number of compounds are constantly developed, and some have even shown remarkable success. However, the two major caveats of all chemotherapeutic compounds are their toxic side effects and the development of resistance after chronic treatment. These issues stem from the fact that effective cancer compounds target specific signaling pathways in cancer that are also important for the regulation of normal cellular functions. Thus, the inhibition or augmentation of aberrant pathways by various compounds may slow the progression of cancer, but also cause detrimental effects in normal cellular functions. In addition, as tumors develop, they have been shown to acquire mutations that allow them to be more tolerant to anti-cancer compounds and eventually resistant to previous treatment. As a result, despite all the drugs that are on the market, there is still a constant need for drugs that can effectively treat cancer with minimal side effects.

Although triterpenoids were known to target tumor cells by inducing apoptosis, my work has determined that they may also target cell migration. Indeed, I have provided evidence that the triterpenoids can act *via* different signaling pathways that are often affected in cancer to elicit their inhibitory effects on cell migration. In fact, in the past three years, research studies have begun to examine the effects of synthetic triterpenoids on cancer metastasis and metastatic burden in *in vivo* models (21,22). In addition, I have identified two novel protein targets, Arp2/3 and GSK3β and provided the underlying molecular mechanism in which triterpenoids may govern cell migration through these proteins. Furthermore, I have presented a list of other potential

triterpenoid-binding targets that form the basis for future work towards deciphering pathways that may be important in targeting cell migration.

Collectively, the information in this thesis offers novel insights into not only how cell migration is regulated as a whole, but also how the triterpenoid compounds may be modified to specifically target tumor metastasis (Figure 5.2).

Triterpenoids are unique because they have minimal side effects and can selectively target cancer cells while generally sparing normal cells. This property renders them favorable candidates for biochemical modifications and they have a great potential to become highly effective anti-cancer agents. Although cancer may not be curable, a novel way of creating a bottleneck for invasive tumor cells by inhibiting cell migration and consequently, preventing metastasis will undoubtedly increase the survival rates and well being of cancer patients.

Figure 5.2 Triterpenoids affect different aspects of carcinogenesis.

Cancer occurs when a single cell becomes mutated due to multiple insults stemming from different genetic and/or environmental factors. As a result, the cancer cell proliferates abnormally and forms a tumor mass that can bypass the fate of terminal cell differentiation, an important regulator of cell growth. These cancer cells eventually acquire the ability to escape apoptosis and form new blood vessels, a process known as angiogenesis, in order to support the growing tumor mass. Eventually, these cells undergo epithelial-to-mesenchymal transition (EMT), in which they become more migratory and invasive. They then degrade and move through the extracellular matrix of the surrounding tissues, which allows them to enter the blood vessels and migrate (or metastasize) to other parts of the body. Upon arrival at a new site, the tumor cell begins to invade, divide, and form a new tumor. Note that cancer cells can also metastasize to other parts of the body through the lymphatic system. In early stages of cancer, cell division, differentiation, apoptosis and angiogenesis are all important aspects of tumorigenesis. Many studies have shown that triterpenoids can effectively target all of these events. In addition, triterpenoids have also displayed cytoprotective effect, which is important since inflammation is heavily associated to cancer progression. In recent years, a few studies have shown the effects of synthetic triterpenoids on cancer metastasis. Our laboratory (To *et al*.) was the first to show that the triterpenoids can effectively inhibit cell migration, which is an important precursor event to cancer metastasis.

Figure 5-2
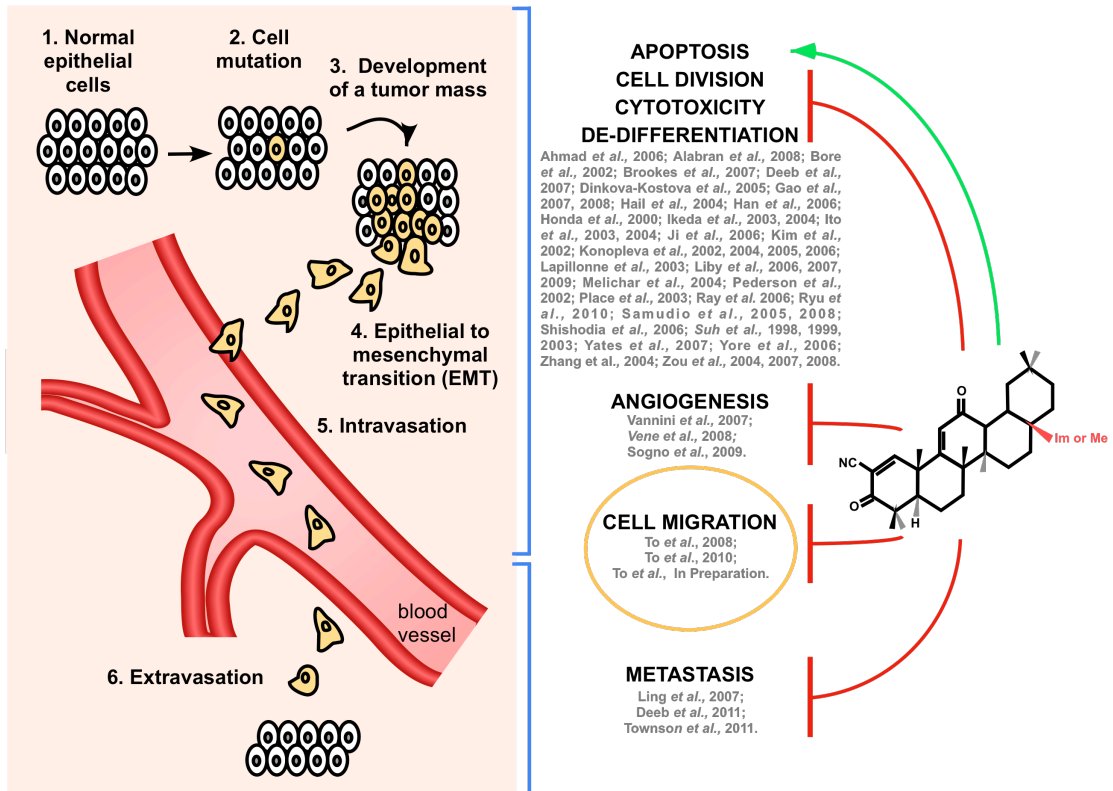
5.4   REFERENCES

1.   Lampropoulos, P., Zizi-Sermpetzoglou, A., Rizos, S., Kostakis, A., Nikiteas, N., and Papavassiliou, A. G. (2012) *Cancer Lett* **314**, 1-7

2.   Javelaud, D., Alexaki, V. I., Dennler, S., Mohammad, K. S., Guise, T. A., and Mauviel, A. (2011) *Cancer Res* **71**, 5606-5610

3.   Achyut, B. R., and Yang, L. (2011) *Gastroenterology* **141**, 1167-1178

4.   Santibanez, J. F., Quintanilla, M., and Bernabeu, (2011) C. *Clin Sci (Lond)* **121**, 233-251

5.   Drabsch, Y., and ten Dijke, P. (2011) *J Mammary Gland Biol Neoplasia* **16**, 97-108

6.   Su, E., Han, X., and Jiang, G. (2010) *Tumori* **96**, 659-666

7.   Ji, Y., Lee, H. J., Goodman, C., Uskokovic, M., Liby, K., Sporn, M., and Suh, N. (2006) *Mol Cancer Ther* **5**, 1452-1458

8.   Jones, M. C., Caswell, P. T., and Norman, J. C. (2006) *Curr Opin Cell Biol* **18**, 549-557

9.   Anitei, M., and Hoflack, B. (2011) *Nat Cell Biol* **14**, 11-19

10.   Farooqui, R., Zhu, S., and Fenteany, G. (2006) *Exp Cell Res* **312**, 1514-1525

11.   Randazzo, P. A., and Hirsch, D. S. (2004) *Cell Signal* **16**, 401-413

12.   Sabe, H. (2003) *J Biochem* **134**, 485-489

13.   Turner, C. E., West, K. A., and Brown, M. C. (2001) *Curr Opin Cell Biol* **13**, 593-599

14.   Hutagalung, A. H., and Novick, P. J. (2011) *Physiol Rev* **91**, 119-149

15.   Mohrmann, K., and van der Sluijs, P. (1999) *Mol Membr Biol* **16**, 81-87

16.   Ezratty, E. J., Partridge, M. A., and Gundersen, G. G. (2005) *Nat Cell Biol* **7**, 581-590

17.   Campbell, N. E., Kellenberger, L., Greenaway, J., Moorehead, R. A., Linnerth-Petrik, N. M., and Petrik, J. (2010) *J Oncol* **2010**, 586905

18. Friedl, P., and Alexander, S. (2011) *Cell* **147**, 992-1009

19. Couch, R. D., Ganem, N. J., Zhou, M., Popov, V. M., Honda, T., Veenstra, T. D., Sporn, M. B., and Anderson, A. C. (2006) *Mol Pharmacol* **69**, 1158-1165

20. To, C., Shilton, B. H., and Di Guglielmo, G. M. (2010) *J Biol Chem* **285**, 27944-27957

21. Townson, J. L., Macdonald, I. C., Liby, K. T., Mackenzie, L., Dales, D. W., Hedley, B. D., Foster, P. J., Sporn, M. B., and Chambers, A. F. (2011) *Clin Exp Metastasis* **28**, 309-317

22. Deeb, D., Gao, X., Liu, Y., Jiang, D., Divine, G. W., Arbab, A. S., Dulchavsky, S. A., and Gautam, S. C. (2011) *Carcinogenesis* **32**, 757-764

CURRICULUM VITAE

Name: **Ciric Chi Wing To**

Post-secondary   **University of Toronto**
Education and   Toronto, Ontario, Canada
Degrees: 2002-2006, B.Sc.

Western University
London, Ontario, Canada
2007-2012, Ph.D.

Honors and   **Western University**
Awards: *Charles W. Gowdey Research Day – Best Poster Award*
2007
Schulich Graduate Scholarship
2007-2008
Hari and Gudrun Sharma Award
2009

Canadian Cancer Society Research Institute
Senior Ph.D. Student Travel Award
2009

Western University
Western Graduate Research Scholarship
2007-2011
Graduate Programs in Physiology and Pharmacology/Toxicology
Graduate Student Travel Award
2011
Graduate Thesis Research Award
2007, 2009-2012

Ontario Ministry of Training, Colleges and Universities
Ontario Graduate Scholarship
2010-2012

Related Work   **Research Assistant**
Experience: *University of Toronto*
2005-2006

Research Assistant
Western University

2006-2007

Teaching Assistant
Western University
2008-2011

Publications:

To C, Shilton BH, Di Guglielmo GM. Synthetic triterpenoids target the Arp2/3 complex and inhibit branched actin polymerization. (2010) *J. Biol. Chem.* **285** (36): 27944-57.

To C, Kulkarni S, Pawson T, Honda T, Gribble GW, Sporn MB, Wrana JL, Di Guglielmo GM. The synthetic triterpenoid CDDO-Imidazolide alters TGFβ-dependent signaling and cell migration by affecting the cytoskeleton and the polarity complex. (2008) *J. Biol. Chem.* **283** (17):11700-11713.

Poster Presentations:

To C and Di Guglielmo GM. *The effects of synthetic triterpenoids on Glycogen Synthase Kinase 3 Beta (GSKβ) and cell adhesions*. A.C. Camargo Global Meeting of Translational Science, Sao Paulo, Brazil (2011)

To C and Di Guglielmo GM. *The effects of synthetic triterpenoids on Glycogen Synthase Kinase 3 Beta (GSKβ) and cell adhesions*. American Association for Cancer Research (AACR) Annual Meeting, Florida, CA. (2011)

To C, Shilton, BH, Di Guglielmo GM. *Synthetic triterpenoids target Actin-related protein 3 (Arp-3) and inhibit cell migration.* American Society of Cell Biology (ASCB) Annual Meeting, San Diego, CA. (2009)

To C and Di Guglielmo GM. *Synthetic triterpenoids target members of the polarity complex and inhibit cell migration.* American Society of Cell Biology (ASCB) Annual Meeting, San Francisco, CA. (2008)

To C, Kulkarni S, Pawson T, Honda T, Gribble GW, Sporn MB, Wrana JL, Di Guglielmo GM. *The synthetic triterpenoid CDDO-Imidazolide alters TGFβ-dependent signaling and cell migration by affecting the cytoskeleton and the polarity complex.* American Society of Cell Biology (ASCB) Annual Meeting, Washington, DC. (2007)

To C and Di Guglielmo GM. *The synthetic triterpenoid CDDO-Imidazolide alters TGFβ-dependent signaling and cell migration by affecting the cytoskeleton and the polarity complex.* Charles W. Gowdey Research Day, London, ON. (2007).